Kaposi sarcoma herpesvirus microRNA function in lymphatic endothelial cells

Amy Hansen BSc

University College London

Submitted for the degree of Doctor of Philosophy

2010

Declaration

I, Amy Hansen, confirm that the work presented in this thesis is my own. Where information has been derived from other sources, I confirm that this has been indicated in the thesis.

Amy Hansen
April 2010

Acknowledgements

First and foremost I would like to thank my PhD supervisor Chris Boshoff for all his encouragement and guidance, I truly appreciate all the opportunities you have provided over the last four years. I am extremely grateful and forever indebted to Dimitrios Lagos for his patience and time, thank you for showing me the joy in scientific endeavor.

I would also like to thank the rest of the CR-UK viral oncology group for their assistance throughout the course of my PhD and for creating such an open, friendly environment in which to learn. In particular, I'd like to thank Vicky Emuss for generously agreeing to proof read this thesis. Thanks to Stephen Henderson for all his bioinformatic expertise. Thanks to Juanma Funes for his help with tissue culture and the early bioenergetic assays, to Leonid Nikitenko for his help with Western blotting and immunohistochemistry and to Fiona Gratrix for her continual help from start to finish. I'd also like to thank Paul Kellam and the members of his group, especially Eve Coulter, for sharing their expertise on miRNA profiling. I would also like to acknowledge the MRC for funding my studentship.

Thanks to my wonderful friends and family for their love and support, your understanding over the last few years has been invaluable. Finally, I am grateful beyond words to George and Sylvia, thanks for always believing in me.

For David Goodwin

Abstract

Kaposi's sarcoma herpesvirus (KSHV) is the causative agent of Kaposi's sarcoma (KS), the most common AIDS-associated malignancy. KS lesions are comprised of poorly differentiated, spindle-shaped endothelial cells, the precursors of which are lymphatic endothelial cells (LEC). KSHV infection of LEC induces transcriptional reprogramming towards a phenotype more analogous to blood vessel endothelial cells BEC.

KSHV encodes 17 mature miRNAs (miRNA), 14 of which are co-expressed as a cluster. miRNAs are small non-coding RNA molecules that act post-transcriptionally to negatively regulate gene expression. It was the aim of this thesis to investigate the function of the KSHV miRNAs through identifying viral miRNA targets in LEC. miRNAs silence their target genes by either blocking translation or inducing mRNA degradation. Gene expression microarray (GEM) analysis was used to quantify changes in mRNA abundance of LEC transcripts induced by the KSHV miRNA cluster. MAF, a leucine zipper transcription factor, was significantly down-regulated in the presence of the viral miRNAs. miRNA expression analysis of KS lesions identified those KSHV miRNAs which are expressed and therefore relevant to KS pathogenesis.

In silico prediction analysis identified multiple KSHV miRNAs binding sites in the MAF 3'UTR, MAF silencing was mediated through specific interactions with these sites. In particular, KSHV miRNAs miR-K12-6 and miR-K12-11 were identified as individual miRNAs responsible for MAF down-regulation. MAF was silenced specifically by these miRNAs during primary KSHV infection of LEC. MAF has been previously characterised as a LEC-specific transcription factor, although its function and target genes were unknown. GEM profiling of LEC in which MAF was silenced by siRNA revealed an increase in expression of BEC markers.

Therefore, in LEC, MAF acts a transcriptional repressor of BEC transcripts helping to maintain lymphatic identity. Gene set enrichment analysis of three GEM data sets revealed a significant concordant increase in BEC genes during primary KSHV infection, expression of the KSHV miRNA cluster and MAF silencing. The miRNA cluster-induced up-regulation of BEC markers was shown to be by way of MAF silencing.

In this study I have identified and validated MAF as a LEC-specific KSHV miRNA target and have shown MAF to have a role in maintaining LEC identity through repression of BEC markers. Consequently, down-regulation of MAF following KSHV miRNA expression contributes to the mechanism behind the transcription reprogramming of LEC observed upon KSHV infection.

Table of Contents

Chapter 1. Introduction 22

1.1 Kaposi sarcoma herpesvirus 22

1.1.1 Kaposi sarcoma 22

1.1.1.1 Clinico-epidemiologic form 22

1.1.1.1.1 Classic KS 23

1.1.1.1.2 African or endemic KS 23

1.1.1.1.3 Post-transplant or iatrogenic KS 23

1.1.1.1.4 Acquired Immunodeficiency (AIDS-KS) 23

1.1.1.2 Disease progression 25

1.1.1.3 Clonality 25

1.1.1.4 Histogenesis 26

1.1.1.5 Epidemiology and transmission 27

1.1.1.6 Cytokines and the KS tumour microenvironment 28

1.1.2 Lymphoproliferative disorders 31

1.1.3 Related herpesviruses 32

1.1.4 KSHV genome 34

1.1.5 KSHV lifecycle 36

1.1.5.1 Virus entry 36

1.1.5.2 Latent infection 37

1.1.5.3 Latent gene expression and function 38

1.1.5.3.1 LANA 40

1.1.5.3.2 vCyclin 41

1.1.5.3.3 vFLIP 41

1.1.5.3.4 Kaposins 42

1.1.5.3.5 KSHV-encoded microRNAs (miRNAs) 43

1.1.5.4 Lytic infection 45

1.1.5.5 Lytic proteins 47

1.1.5.5.1 Viral interleukin 6 (vIL6) 47
1.1.5.5.2 Viral CC-class chemokines (vCCLs) 48
1.1.5.5.3 Viral G-protein coupled receptor (vGPCR) 48
1.1.5.5.4 Viral Interferon regulatory factors (vIRFs) 49
1.2 Lymphatic Endothelium 50
1.2.1 Organisation of the lymphatic system 50
1.2.2 Lymphatic function in health and disease 53
1.2.3 Lymphangiogenesis 54
1.2.3.1 Initiation of lymphatic endothelial phenotype 54
1.2.3.2 Plasticity of the LEC phenotype 57
1.2.3.3 Lymphatic sprouting and proliferation 58
1.2.3.4 Regulators of lymphatic vasculature development 60
1.3 MAF 62
1.3.1 Maf family identification and classification 62
1.3.2 MAF DNA binding and dimerization 65
1.3.3 MAF expression 69
1.3.4 MAF function 70
1.3.4.1 MAF regulates cellular differentiation 70
1.3.4.2 MAF as an oncogene 73
1.4 microRNAs 75
1.4.1 miRNA discovery and classification 75
1.4.2 miRNA biogenesis 76
1.4.3 miRNA target recognition 79
1.4.4 Mechanism of miRNA silencing 81
1.4.5 Different classes of small RNA molecules 84
1.4.6 miRNAs in cancer 87
1.4.6.1 miRNAs as tumour suppressors 87
1.4.6.2 miRNAs as oncogenes 88
1.4.6.3 miRNAs as therapeutic targets 89
1.4.7 Viral miRNAs 90

1.6 Thesis aims 94

Chapter 2. Materials and Methods 95

2.1 Cell culture 95

2.1.1 Lymphatic endothelial cells 95

2.1.2 Blood vessel endothelial cells 96

2.1.3 Transformed cell lines 96

2.1.4 Thawing cells 97

2.2 Transfection, virus production and infection 97

2.2.1 DNA transfections of 293T and HeLa cells 97

2.2.2 KSHV production and infection of LEC 98

2.2.3 Lentivirus production and infection of LEC 99

2.3 Molecular biology techniques 100

2.3.1 Bacterial transformation 100

2.3.2 Plasmid purification 100

2.3.3 Restriction enzyme digest 101

2.3.4 Agarose gel electrophoresis 102

2.3.5 Agarose gel extraction 102

2.3.6 Ligation 103

2.3.7 PCR cloning strategy 103

2.3.8 Site directed mutagenesis 108

2.3.9 Genomic DNA extraction 109

2.3.10 Quantitative polymerase chain reaction (qPCR) 109

2.3.11 RNA extraction 110

2.3.11.1 RNeasy Mini Kit (Qiagen) 110

2.3.11.2 miRNeasy Mini Kit (Qiagen) 111

2.3.11.3 TRIzol (Invitrogen) 112

2.3.12 cDNA synthesis 112

2.3.13 Quantitative real time reverse transcriptase polymerase chain 113

2.4	Gene expression microarray analysis	117
	2.4.1 Sample preparation	117
	2.4.2 Chip hybridization and scanning	119
	2.4.3 GEM data analysis	119
	2.4.4 Using LEC versus KLEC GEM data sets to analyze Maf family	121
	2.4.5 Using LEC versus BEC GEM data to compile a list of BEC and LEC	121
	2.4.6 Gene expression heatmaps	121
2.5	miRNA microarray profiling	122
	2.5.1 Tissue profiled	122
	2.5.2 Sample preparation	123
	2.5.3 miRNA microarray hybridization and scanning	124
	2.5.4 miRNA microarray data analysis	124
2.6	Protein analysis	125
	2.6.1 Western blotting	125
	2.6.2 Nuclear and cytoplasmic fractionation	130
	2.6.3 Immunofluorescence assay	131
	2.6.4 MAF protein immunoprecipitation	132
2.7	Luciferase reporter assays	133
2.8	siRNA transfections	136
2.9	KSHV miRNA inhibition	136
2.10	Chromatin immunoprecipitation-PCR	137
2.11	miRNA target prediction	140
2.12	Gene set enrichment analysis (GSEA)	141
2.13	Statistical analysis	142

Chapter 3. Identification of KSHV miRNA targets 143

3.1 Introduction and aims 143

3.2 KSHV miRNA expression in Kaposi sarcoma 145

3.3 Sub-cloning the KSHV miRNAs 152

3.4 KSHV miRNA activity from pSIN-K-Cluster 154

3.5 KSHV miRNA expression from pSIN-K-miR 160

3.6 KSHV miRNAs induce changes in LEC gene expression 163

3.7 KSHV miRNA target prediction 167

3.7.1 Prediction strategy 167

3.7.2 Prediction results 172

3.8 Discussion 177

Chapter 4. MAF is a KSHV miRNA target 181

4.1 Introduction and aims 181

4.2 MAF is down-regulated by the KSHV miRNA Cluster 182

4.3 MAF is down-regulated by miR-K12-11 and miR-K12-6 184

4.4 KSHV miRNAs are predicted to target the MAF 3'UTR 187

4.5 MAF silencing via KSHV miRNA binding sites in the 3'UTR 190

4.6 MAF is down-regulated during primary KSHV infection 196

4.7 KSHV miRNA expression during primary LEC infection 198

4.8 KSHV miRNA inhibition 202

4.8.1 miRIDIAN hairpin KSHV miRNA inhibitors 202

4.8.1.1 KSHV miRNA inhibition of luciferase reporter silencing 203

4.8.1.2 KSHV miRNA inhibition in LEC with miRIDIAN inhibitors 205

4.8.2 LNA-modified KSHV miRNA inhibitors 210

4.8.2.1 LNA miRNA inhibition of synthetic luciferase targets 211

4.8.2.2 LNA miRNA inhibition of KSHV induced MAF silencing 213

4.9 Does hsa-miR-155 contribute to MAF silencing? 215

4.10 MAF regulation in PEL 217

4.11 Discussion 219

Chapter 5. KSHV miRNA regulation of MAF induces endothelial 225

5.1 Introduction and aims 225

5.2 Hypothesis: MAF plays a role in LEC fate determination 226

5.3 MAF target identification in LEC 228

5.4 MAF knock-down induces up-regulation of BEC markers 234

5.5 MAF knock-down has no effect on LEC marker expression 241

5.6 MAF is a repressor of BEC identity 243

5.6.1 MAF knock-down induces increased BEC marker expression 243

5.6.2 MAF over-expression reduces BEC marker expression IN BEC 248

5.7 MAF target validation by ChIP 253

5.7.1 MAF immunoprecipitation 253

5.7.2 MAF ChIP-PCR 259

5.8 MAF auto-regulation 264

5.9 MAF and PROX1 regulate an overlapping set of target genes 268

5.10 Discussion 270

Chapter 6. Discussion and future work 278

6.1 Summary 278

6.2 Conclusions 229

6.2.1 Novel role for viral miRNAs 280

6.2.2 Mechanism underlying KSHV-induced reprogramming 282

6.2.3 MAF: a novel LEC-specifying protein 284

6.3 Future Work 285

6.3.1 KSHV miRNA target identification 285

6.3.2 MAF and PROX1 287

6.3.3 The role of MAF role during lymphangiogenesis 288

References 290

Appendix 321

List of Figures

1.1	KS lesions and incidence	24
1.2	Characteristic hallmarks of KS lesions	30
1.3	The KSHV episome	35
1.4	Organisation, promoters and transcripts of the KSHV latency region	39
1.5	Lymphatic vasculature organisation	52
1.6	MAF classification	63
1.7	MAF structure and DNA recognition sequences	67
1.8	miRNA biogenesis	78
1.9	Mechanisms of miRNA-mediated silencing	83
3.1	Skin and KS biopsies used for miRNA profiling	147
3.2	Differential expression of KSHV miRNAs in KS lesions	149
3.3	KSHV miRNAs not expressed in KS lesions.	151
3.4	Restriction enzyme digestion of pSIN-MCS constructs	153
3.5	Luciferase activity standard curve	156
3.6	KSHV miRNA-mediated reporter silencing	157
3.7	KSHV miRNAs expressed from pSIN-K-Cluster silence reporter constructs	159
3.8	LEC transduced with the KSHV miRNA Cluster.	162
3.9	Experimental overview of KSHV miRNA Cluster GEM profiling.	164
3.10	KSHV miRNA Cluster induces changes in LEC gene expression	166
3.11	Schematic describing PITA scores based on thermodynamic modelling	169
3.12	Overview of PITA KSHV miRNA target prediction analysis	171
4.1	KSHV miRNA Cluster induces MAF down-regulation	183
4.2	miR-K12-6 and miR-K-12-11 induce MAF silencing	186
4.3	Predicted KSHV miRNA bindings sites in the MAF 3’UTR	188
4.4	Schematic of the psi-MAF-UTR plasmid	192

4.5	miR-K12-6, miR-K12-1 and miR-K-12-11 target the MAF 3'UTR	195
4.6	MAF is down-regulated during primary KSHV LEC infection	197
4.7	KSHV miRNA expression during primary LEC infection	199
4.8	KSHV miR-12-6-5p and miR-K12-11 expression during primary infection	201
4.9	KSHV miRNA inhibitor optimisation in 239T cells	204
4.10	KSHV miRIDIAN miRNA inhibitor optimisation in LEC	207
4.11	KSHV miRDIAN miRNA inhibitor optimisation in KLEC	209
4.12	KSHV LNA miRNA inhibitor optimisation in 293T cells.	212
4.13	Inhibition of miR-K12-6, miR-K12-11 and miR-K12-1 attenuates MAF silencing	214
4.14	KSHV regulation of miR-155	216
4.15	MAF expression in B cell lymphoma cell lines	218
5.1	KSHV induced transcriptional reprogramming	227
5.2	siRNA-mediated MAF knock-down	230
5.3	MAF mRNA isoforms are concordantly regulated	231
5.4	MAF knock-down induces changes in gene expression	233
5.5	LEC and BEC are distinguished on the basis of their transcriptional	235
5.6	BEC markers increase upon MAF knock-down	238
5.7	BEC markers increased in the context of MAF repression	239
5.8	siRNA MAF knock-down or KSHV miRNA Cluster has no effect on LEC	242
5.9	GSEA validation	244
5.10	MAF knock-down leads to up-regulation of additional BEC markers	245
5.11	miRNA-insensitive MAF ORF rescues Cluster-mediated up-regulation	247
5.12	qRT-PCR characterisation of BEC	250
5.13	Exogenous MAF represses BEC marker expression	252
5.14	Antibody optimisation	255

5.15	MAF immunoprecipitation	258
5.16	HDAC9 promoter	260
5.17	MAF chromatin immunoprecipitation	262
5.18	MAF auto regulation	266
5.19	MAF protein in LEC	267
5.20	Reciprocal regulation of BEC markers by PROX1 and MAF	269
5.21	KSHV miRNAs contribute to LEC reprogramming	274

List of Tables

1.1	Proteins involved in lymphangiogenesis and lymphatic vasculature development	61
1.2	Experimentally validated MAF target genes	72
1.3	Differences between siRNA and miRNA	85
1.4	Experimentally validated viral miRNA targets	93
2.1	PCR cloning details	106
2.2	Plasmids used in luciferase assays	106
2.3	Primers used for mutagenesis of KSHV miRNA binding sites	107
2.4	Real-time qRT-PCR assay and primers	115
2.5	GEM and miRNA profiling data sets	120
2.6	Primary antibodies used for protein detection and quantification	129
2.7	Plasmids used in luciferase assays	135
2.8	PCR primers used to amplify chromatin immunoprecipitated DNA	139
3.1	mRNA abundance of top PITA predicted targets in the presence of the KSHV miRNA cluster	173
3.2	Testing the ability of PITA to identify experimentally validated miRNA	175
5.1	Leading core edge genes	240
5.2	ChIP target enrichment	263
A1	Top 50 probes de-regulated in the presence of the KSHV miRNA cluster	321
A2	PITA prediction results	322

Abbreviations

AIDS	Acquired immunodeficiency syndrome
ARE	AU-rich elements
BAC	Bacterial artificial chromosome
BEC	Blood vessel endothelial cells
CBP	CRB binding protein
c/c	Copies per cell
CCR	Chemokine (C-C motif) receptor
cDNA	Complementary DNA
ChIP	Chromatin immunoprecipitation
COUPTFII	Chicken ovalbumin upstream promoter transcription factor II
cRNA	Complementary RNA
CR-UK	Cancer Research UK
Ct	Threshold cycle
CXCL	Chemokine (C-X-C motif) ligand
CXCR	Chemokine (C-X-C motif) receptor
DAPI	4',6-diamidino-2-phenylindole
DMEM	Dulbecco's modified Eagle medium
DMVEC	Dermal microvascular endothelial cells
DR1/2	Direct repeat 1 and 2
dH_20	Distilled water
ddH_20	Double distilled water
EBV	Epstein-Barr virus
FADD	Fas-associated death domain
FAK	Focal adhesion kinase
FDR	False discovery rate
FLICE	Fas-associated death domain-like interleukin-1-β-converting enzyme
FLT	Fms-related tyrosine kinase
GAPDH	glyceraldehydes 3-phosphate dehydrogenase
GEM	Gene expression microarray
GFP	Green fluorescent protein
GPCR	G-protein coupled receptor
GSEA	Gene set enrichment analysis
GSK-3β	Glycogen synthase kinase 3β
GULP1	Engulfment adaptor PTB domain containing 1
HDAC	Histone deacetylase
HITS-CLIP	high-throughput sequencing of RNA isolated by crosslinking immunoprecipitation

HIV	Human immunodeficiency virus
hIL6	Human interleukin 6
HRP	Horse-radish peroxidise
Hrs	Hours
HUVEC	Human umbilical vein endothelial cells
IFA	Immunofluorescence assay
IFNγ	Interferon γ
IRF	Interferon regulatory factor
KBEC	KSHV-infected BEC
KDR	Kinase insert domain receptor
KLEC	KSHV-infected LEC
KS	Kaposi sarcoma
KSHV	Kaposi sarcoma herpesvirus
L	Liter
LANA	Latency associated nuclear antigen
LEC	Lymphatic endothelial cells
LNA	Locked nucleic acid
LTR	Long terminal repeat
LYVE1	Lymphatic vessel endothelial hyaluronan receptor 1
MCD	Multicentric Castleman's disease
MCS	Multiple cloning site
MHV68	Murine herpesvirus 68
miRNA	MicroRNA
µg	Microgram
µl	Microlitre
min	Minute
ml	Milliliter
MMVEC	Myometrium microvascular endothelial cells
mRNA	Messenger RNA
ng	Nanogram
NFκB	Nuclear factor kappa-light-chain-enhancer of activated B cells
NRCAM	Neuronal cell adhesion molecule
nts	Nucleotides
NTC	Non-targeting control
ORF	Open reading frame
PBS	Phosphate buffered saline
PCR	Polymerase chain reaction
PDPN	Podoplanin
PECAM1	Platelet/endothelial cell adhesion molecule
PEL	Primary effusion lymphoma

pg	Picogram
p.i.	Post infection
piRNA	Piwi interacting RNA
PITA	Probability of interaction by target accessibility
PROX1	Prospero homeobox 1
qPCR	quantitative PCR
qRT-PCR	quantitative reverse transcriptase-PCR
RIPA	Radioimmunoprecipitation assay
RLU	Relative light units
RNA	Ribonucleic acid
RNAi	RNA interference
RNU66	small nucleolar RNA, H/ACA box 66
RT	Room temperature
RTA	Replication and transcription activator
rRNA	Ribosomal RNA
SD	Standard deviation
SDS	Sodium dodecyl sulphate
SDS-PAGE	SDS-polyacrylamide gel electrophoresis
SIN	Self inactivating
siRNA	Short interfering RNA
SLC1A1	Solute carrier family 1, member 1
TFEC	transcription factor EC
TPA	Phorbol ester tetradecanoyl phorbol acetate
UTR	Untranslated region
vCyclin	Viral Cyclin
VEGF	Vascular endothelial growth factor
vCCL	Viral CC-class chemokine
vFLIP	Fas-associated death domain interkeukin-1β-converting enzyme inhibitory protein
vGPCR	Viral G-protein coupled receptor
vIL6	Viral interleukin 6
vIRFs	Viral interferon regulatory factor
vMIPs	Viral macrophage inflammatory proteins
VSV-G	Vesicular stomatitis virus-G
v/v	Volume/Volume
w/v	Weight/ Volume

Publications

Part of the work described in this thesis is published in the following papers:

Hansen,A., Boshoff,C., and Lagos,D. (2007). Kaposi sarcoma as a model of oncogenesis and cancer treatment. Expert. Rev. Anticancer Ther. 7, 211-220.

Hansen,A., Henderson,S., Lagos,D., Nikitenko,L., Coulter,E., Roberts,S., Gratrix,F., Plaisance,K., Renne,R., Bower,M., Kellam,P., and Boshoff,C. (2010). KSHV-encoded miRNAs target MAF to induce endothelial cell reprogramming. Genes Dev. 24, 195-205.

Lagos,D., Trotter,M.W., Vart,R.J., Wang,H.W., Matthews,N.C., **Hansen,A**., Flore,O., Gotch,F., and Boshoff,C. (2007). Kaposi sarcoma herpesvirus-encoded vFLIP and vIRF1 regulate antigen presentation in lymphatic endothelial cells. Blood 109, 1550-1558.

Chapter 1. Introduction

1.1 Kaposi sarcoma herpesvirus

In 1872 the Hungarian dermatologist Moritz Kaposi reported five cases of 'idiopathic multiple pigmented sarcomas of the skin' (Kaposi, 1872). This disease later became known as Kaposi sarcoma (KS). In 1981, increased incidences of an aggressive form of KS and Pneumocystis carinii pneumonia were reported amongst homosexual men in New York and California. These events marked the onset of HIV/AIDS epidemic and sparked a renewed interested in KS pathogenesis. The aetiological agent of KS was identified in 1994 when Yuan Chang and Patrick Moore (Chang et al., 1994) employed representational difference analysis to isolate unique DNA sequences from tumours of patients with AIDS-KS. This DNA was related to but distinct from other known herpesviruses, and represented a novel herpesvirus termed Kaposi sarcoma herpesvirus (KSHV, also called HHV-8).

1.1.1 Kaposi sarcoma

KS is a multifocal disease initially presenting as red lesions of the skin, particularly on the extremities (Fig. 1.1A). During disease progression lesions disseminate to the oral mucosa and visceral organs. KS tumours are highly vascularised and composed of proliferating spindle cells, lesions are typified by slit like vasculature and a strong inflammatory infiltrate (Fig. 1.1B) (Boshoff and Weiss, 2002).

1.1.1.1 Clinico-epidemiologic forms

There are four distinct clinico-epidemiologic forms of KS termed: classic, endemic, iatrogenic and AIDS-KS.

1.1.1.1.1 Classic KS

This was the form of KS originally described by Moritz Kaposi, it is typically an indolent disease occurring predominantly in elderly men of Mediterranean, Eastern European or Jewish ancestry (Franceschi and Geddes, 1995).

1.1.1.1.2 African or endemic KS

In the 1950s a high incidence of KS was reported in the black population of equatorial African countries (OETTLE, 1962). This endemic form of KS predominantly occurs in men and is more aggressive than other forms of KS, often involving lymph nodes and visceral organs. In addition to adults, endemic KS also affects children (Olweny, 1984).

1.1.1.1.3 Post-transplant or iatrogenic KS

This form of KS occurs in patients receiving immunosuppressive therapy, such as those undergoing organ transplants (Harwood et al., 1979). It is estimated that the incidence of KS in this risk group is 150 times higher compared with the average Western population (Penn, 1997). In addition, there is an overrepresentation of patients from Mediterranean or Jewish origin who suffer from iatrogenic KS in North America (Franceschi and Geddes, 1995).

1.1.1.1.4 Acquired Immunodeficiency Syndrome (AIDS)-KS

AIDS-KS is the most common AIDS-associated malignancy (Beral et al., 1990), it is also the most aggressive form of the disease. If left untreated the disease can progress from lesions on the skin to visceral organs such as the lungs and gut (Boshoff and Weiss, 1998). AIDS-KS predominantly affects HIV-positive homosexual men over other HIV risk groups such as intravenous drug users (Beral et al., 1990; Rabkin et al., 1990). Widespread availability of antiretroviral therapy has led to a 90% decrease in AIDS-KS incidence in the US and Europe (Fig. 1.1C) (Gates and Kaplan, 2002; Portsmouth et al., 2003), however in Sub-Saharan Africa, where such treatments are not readily available AIDS-KS remains a significant disease burden.

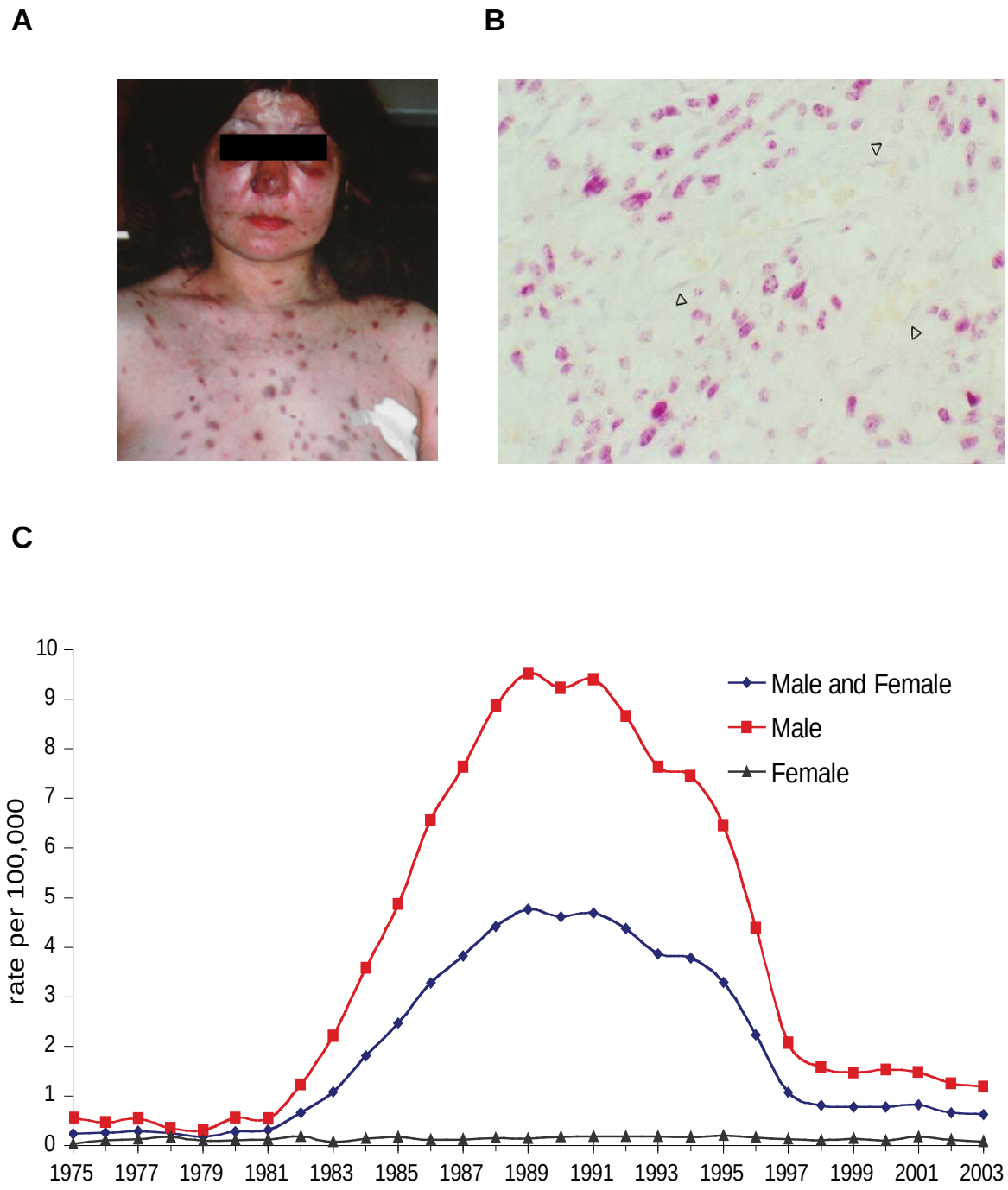

Figure 1.1 KS lesions and incidence. *A* Pigmented KS lesions of the skin, the swelling under the eyes is characteristic of KS associated oedema. *B* Tumour cells of KS lesions displaying the characteristic spindle shape. Spindle cells stain positive for KSHV as evidenced by purple staining. Arrow heads indicate blood vessels which do not stain positive for the virus. *C* Male and female incidence of KS disease from 1975 to 2003. The sharp increase in male KS in 1981 signifies the onset of the HIV-AIDS epidemic. Incidence begins to decline around 1993 with the introduction of Herpesvirus-specific therapeutics, a further decline in incidence occurs in 1997 with the introduction of the first generation of anti-retroviral therapeutics. Graph taken from WHO http://www.who.int/en/.

1.1.1.2 Disease Progression

If left untreated KS lesions will progress through three stages: patch, plaque and nodular. Early patch stage KS presents as flat red-brown lesions in the dermis, which are characterised by a high inflammatory infiltrate, including dendritic and mast cells, and an abundance of blood vessels. Lesion development is associated with neoangiogenesis and the appearance of spindle-shaped endothelial cells, which are considered to be the KS tumour cells (Ensoli et al., 2001; Gessain and Duprez, 2005). The spindle cells proliferate with disease progression to the plaque stage and neovascularisation continues along with extravasation of red blood cells which contributes to the deep red colour of the lesions (Regezi et al., 1993). Nodular KS lesions are dominated by spindle cells, although immune cells are still present. These lesions are stratified by abnormal slit-like vasculature spaces (Regezi et al., 1993).

1.1.1.3 Clonality

Malignancy results from the clonal expansion of cells that have acquired mutations which confer a selective advantage (Yao and Rubin, 1993; Chow and Rubin, 1999a; Chow and Rubin, 1999b). The manifestation of KS lesions at multiple distinct sites in the body meant that the monoclonal or oligoclonal origin of the disease was unclear. Initial studies addressed this question by analysing the paternal origin of the inactivated X chromosome in females with KS lesions (Rabkin et al., 1997; Gill et al., 1998). Rabkin et al concluded that KS lesions were clonal, since all cells contained an inactivated X chromosome from the same parent (Rabkin et al., 1997). However, Gill et al found significant evidence for both paternal and maternal inactivated X chromosomes, therefore suggesting that the lesions arose from multiple cells (Gill et al., 1998). Subsequently, Duprez et al employed a PCR-based approach to quantify the length of viral terminal repeats present in KS lesions. Since KS has a male biased incidence this technique was superior in that it was not limited to only female samples (Duprez et al., 2007). 82% of KS lesions showed heterogeneous terminal repeat lengths, indicating that multiple KSHV infected clones exist within a single lesion. Despite the majority of KS lesions being oligoclonal, clonal lesions were also detected within the same

patient (Duprez et al., 2007). Therefore, KS is a multifocal disease whereby disseminated lesions represent the expansion of distinct KSHV infected spindle cells. The mutliclonal nature of KS has led some to classify it as a reactive proliferation rather than a true malignancy (Judde et al., 2000).

1.1.1.4 Histogenesis

The spindle cells of KS lesions are the principle target of KSHV infection. In early lesions 10% of spindle cells are KSHV positive, this increases to 90% in advanced nodular lesions (Boshoff et al., 1995; Staskus et al., 1997; Dupin et al., 1999). Advanced lesions are dominated by KSHV-infected spindle cells, therefore the spindle cell has been designated the tumour compartment of KS. Spindle cells are poorly differentiated but of endothelial origin as evidenced by the expression of the pan endothelial cell marker PECAM1 (Skobe et al., 1999). The origin of these cells from lymphatic or vascular endothelia has been strongly contested.

In 1985 Beckstead et al performed immunohistochemistry on KS spindle cells testing a range of markers that distinguished between the two types of endothelium. This group was the first to show that spindle cells were phenotypically closer to lymphatic as opposed to vascular endothelial cells (Beckstead et al., 1985). Additional evidence supports a lymphatic origin for KS: the distribution of cutaneous KS lesions along the lengths of lymphatic vessels (Dorfman, 1988), the lack of KS in tissues devoid of lymphatics such as the central nervous system (Dorfman, 1988) and the paucity of KSHV staining in the vascular endothelium of KS lesions (Dupin et al., 1999). Immunohistochemical staining of KS lesions indicated the expression of the lymphangiogenic ligand, vascular endothelial growth factor-C (VEGF-C), within blood vessels and spindle cells stained positive for the associated receptors fms-related tyrosine kinase 4 (FLT4) and kinase insert domain receptor (KDR) (Skobe et al., 1999; Marchio et al., 1999). Stimulation of FLT4 by VEGF-C initiates lymphangiogenesis and these molecules are required to maintain the lymphatic endothelium (Jeltsch et al., 1997; Oh et al., 1997) In addition, KS spindle cells also stain positive for other markers of lymphatic endothelium, podoplanin (PDPN) and lymphatic vessel

endothelial hyaluronan receptor 1 (LYVE1). Furthermore, addition of VEGF-C to KS tumour cells *in vitro* stimulated proliferation (Skobe et al., 1999; Marchio et al., 1999).

More recently, gene expression microarray (GEM) profiling was performed on RNA from KS lesions, and compared to the characteristic gene expression profile associated with LEC and BEC (Wang et al., 2004). The resulting profile was closest to that of lymphatic endothelial cells (LEC) than blood vessel endothelial cells (BEC). However, KS spindle cells did not faithfully represent the LEC transcriptional profile but instead were poorly differentiated, expressing markers of both LEC and BEC endothelium (Wang et al., 2004). Wang et al also showed that, upon infection of either LEC or BEC, KSHV induces endothelial reprogramming, driving these cells away from their terminally differentiated state towards the opposing lineage (Wang et al., 2004). The resulting infected LEC or BEC are more similar to one another than their uninfected counterparts. These data were supported by findings from Hong and Carroll et al, whereby KSHV infection of BEC led to their lymphatic reprogramming, with up-regulation of the lymphatic master regulator PROX1 (Hong et al., 2004; Carroll et al., 2004). Crucially, the mechanism behind KSHV-induced reprogramming remains unknown.

1.1.1.5 Epidemiology and Transmission

There are three major patterns of KSHV seroprevalence throughout the world, high level endemic, intermediate level endemic and non-endemic. High level endemic seroprevalence is found in regions of sub-Saharan Africa, here 30-70% of adults in the general population are KSHV positive. This pattern of seroprevalence is strongly associated with HIV infection. In Mediterranean countries, which are classed as intermediate level endemic, there is a 10-25% seroprevalence. In non-endemic areas including North, Central and South America, Asia and Northern Europe there is <10% seroprevalence amongst the general adult population. However certain high risk groups in non-endemic areas exhibit increased seroprevalence akin to the high-endemic areas. These include

HIV positive and negative homosexual men. Currently, it is not known what factors, genetic or behavioural are responsible for this distribution of KSHV infection (See (Martin, 2007) and references therein).

There is strong evidence for two main routes of KSHV transmission: Sexual transmission between homosexual men, particularly in non-endemic areas (Martin et al., 1998), and horizontal non-sexual transmission between children in high-level endemic areas. In the latter cases sputum appears to be the main route of transmission. There is also evidence of transmission via infected organ transplants, sharing of infected needles amongst intravenous drug users and through transfusions of whole unprocessed blood in high-level endemic areas. However, the precise behavioural activities and mechanisms of transmission are not yet known. It is also unclear as to whether KSHV is transmitted from mother to child (Martin et al., 1998; Martin, 2007). Although there is no direct evidence for *in utero*, via placental transmission, children are more likley to test KSHV positive if their mothers are also positive, suggesting mother to child horizontal transmission (Whitby et al., 2000; Davidovici et al., 2001).

1.1.1.6 Cytokines and the KS tumour microenvironment

Angiogenesis, proliferating spindle cells and a prominent immune infiltrate are the characteristic hallmarks of KS lesions, each of these are an essential element of the tumour microenvironment (Fig. 1.2). The inflammatory cell infiltrate appears even before spindle cell formation highlighting the importance of this component to KS pathogenesis (Ensoli and Sturzl, 1998). In addition, KS has a propensity to occur at sites of local inflammation, a feature known as the Koebner phenomenon (Niedt and Prioleau, 1988). The immune infiltrate is largely comprised of CD8+ T cells and monocyte-macrophages. Dendritic cells, CD4+ T cells and B cells are also present, although not as abundant (Ensoli and Sturzl, 1998). Consequently, KS lesions are typified by high levels of inflammatory cytokines secreted by immune cells, including γIFN, TNF, IL-1, IL-6 and GMCSF. This cytokine profile influences endothelial cell activation and induces the production of angiogenic factors, leading to blood vessel formation and further recruitment of T cells and

monocytes. In addition to the cytokines produced by immune cells, KSHV infected spindle cells also secrete proangiogenic (ANG2, VEGFA and TGF-B) and proinflammatory factors (IL-1, IL-6 and GMCSF) (Di and Cesarman, 2004). This augments the cytokine profile and has a direct growth stimulatory effect on infected endothelial cells (Ensoli et al., 1989). The virus contributes directly to the proinflammatory and proangiogenic environment by encoding its own array of cytokines such as vIL-6 and the viral chemokines (v-CCL1-3) (Boshoff et al., 1997).

Due to the importance of the tumour microenvironment, KS development is often viewed as interplay between three essential components: proliferation of spindle cells, inflammation and angiogenesis. All three processes are continually active and necessary for KS progression (Fig. 1.2).

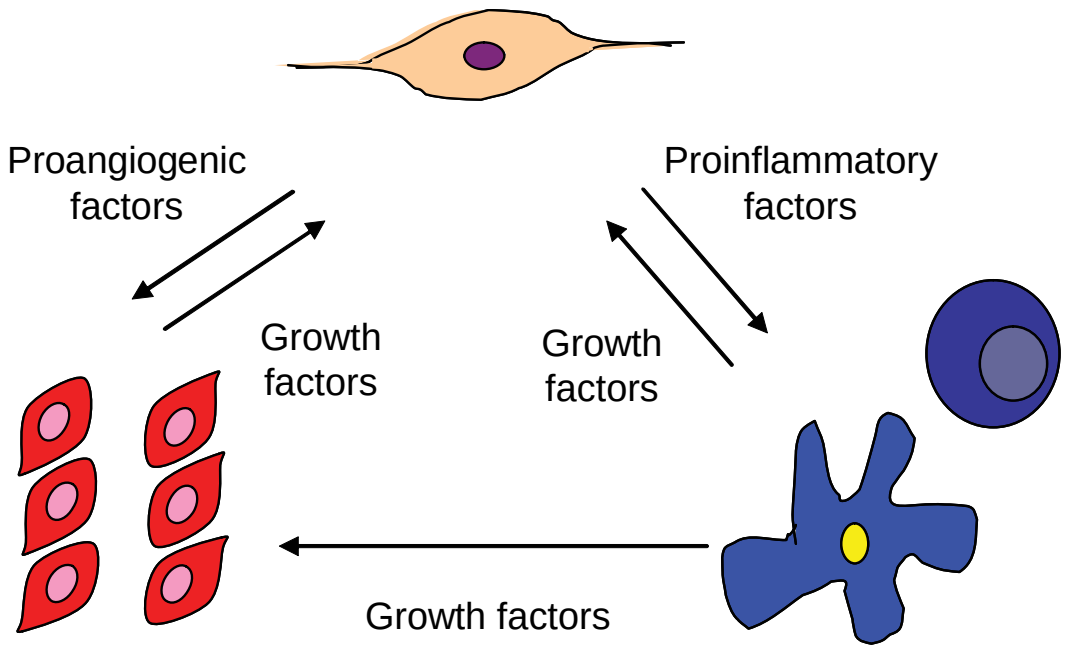

Figure 1.2 Characteristic hallmarks of KS lesions. KS development and progression is driven by the interplay of three essential components: proliferating spindle cells (Top, beige cell), inflammatory infiltrate (Right, blue cells) and angiogenesis (Left, red blood vessel endothelial cells).

1.1.2 Lymphoproliferative disorders

KSHV is also the aetiological agent of two lymphoproliferative disorders, multicentric Castleman's disease (MCD) and primary effusion lymphoma (PEL) (Cesarman et al., 1995a).

PEL is an aggressive non-Hodgkin's B cell lymphoma which lacks a distinct tumour mass and manifests as malignant effusions in the pleural, pericardial or peritoneal cavities (Jenner and Boshoff, 2002). GEM profiling of PEL and a range of B cell tumours from different stages of B cell development characterised PEL as a post-germinal centre B cell lymphoma (Jenner et al., 2003). However, PEL cells frequently lack B-cell specific markers (Boshoff et al., 1998; Cesarman et al., 1995b). Unlike KS, PEL is a clonal disease as evidenced by identical IgG rearrangements in all tumour cells. The majority of patients with PEL are HIV positive. In addition to being latently infected with KSHV, 80% of PEL cases are co-infected with EBV (Cesarman et al., 1995a; Jenner et al., 2003). Cell lines established from these lymphomas maintain the viral genome at high copy numbers and a result are widely used for experimental investigation into KSHV-mediated oncogenesis.

MCD is a polyclonal tumour with a heterogeneous pathogenesis. 50% of MCD cases in HIV-negative individuals are KSHV positive (Moore and Chang, 2003). Whereas nearly all cases of MCD in HIV positive individuals are KSHV positive (Soulier et al., 1995). It was the close association of MCD with KS in AIDS patients which prompted the discovery of the KSHV genome in these tumours (Soulier et al., 1995). The bulk of MCD tumour mass is comprised of uninfected B cells which are recruited to the site by cytokines expressed by a small population of KSHV infected cells. Human and viral interleukin 6 (IL6) are likely to play causative roles in the development of both PEL and MCD (Dupin et al., 2000). MCD plasmablasts originate from naïve B cells and unlike PEL co-infection with EBV does not occur (Du et al., 2001).

1.1.3 Related herpesviruses

Herpesviridae are a large family of viruses which were initially classified on the basis of common biological properties. Herpes virions are spherical and composed of 4 major components. The core houses a single copy of the dsDNA genome varying in length from 125-245kbp. The genome is encapsulated by an icosahedron capsid surrounded by a viral protein-containing tegument. The final layer of lipid envelope is punctuated by viral membrane glycoproteins. Recently, the herpesvirus family has been more precisely sub-classified on the basis of genomic sequence information (McGeoch et al., 2000). Herpesviruses natural host range is typically restricted to a single species. This host-specific occurrence highlights that the co-evolution of herpesviruses with their hosts and, in the majority of incidences, infection does not result in severe disease (Davison, 2002).

There are three subfamilies of herpesviridae: alphaherpesvirinae, betaherpesvirinae and gammaherpesvirinae. The prototype member of each family is simplexvirus, cytomegalovirus and Epstein-Barr virus, respectively. Each subfamily displays distinct cellular tropisms: alphaherpesvirinae infect neurons, betaherpesvirinae are restricted to the monocyte lineage, whereas gammaherpesvirinae infect lymphocytes (Davison, 2007).

The gammaherpesvirus subfamily is divided into two genera, lymphocryptoviridae and rhadinoviridae. KSHV is a rhadinovirus and was the eighth human herpesvirus to be discovered (Chang et al., 1994). KSHV is the only member of rhadinoviridae which infects humans. The most closely related human gammaherpesvirus to KSHV is the lymphocryptovirus EBV. In healthy individuals EBV establishes low level persistent infection of peripheral memory B-cells. However, especially in HIV-positive individuals EBV infection is associated with various lymphomas such as Burkitt’s lymphoma and Hodgkin’s disease (Boshoff and Weiss, 2002).

Related gammaherpesviruses that infect both Old- and New-world primates include the Rhesus monkey rhadinovirus, which is closely related to KSHV (Searles et al., 1999). These viruses provide important *in vivo* models with which to investigate gammaherpesvirus pathogenesis. Sequence analysis of the conserved herpesvirus DNA polymerase have shown that KSHV is most closely related to pan-rhadinoherpesvirus (pRHV1a) and gorilla-rhadinoherpesvirus (GorRHV1), which infect chimpanzees and gorillas, respectively (Lacoste et al., 2000). Another rhadinovirus closely related to KSHV is the murine gammaherpesvirus 68 (MHV68). MHV68 latently infects B cells in culture and causes lymphoproliferative disease in mice (Sunil-Chandra et al., 1994). Consequently, MHV68 infection is used as a mouse model to study aspects of KSHV-pathogenesis.

1.1.4 KSHV genome

Rhadinoviruses share a common genome structure. The term ‘rhadino’ derives from the ancient Greek word for fragile due to the propensity of the viral genome to dissociate into two fragments of differing density. The KSHV genome is linear dsDNA of around 160kbp, 140kb of which encode approximately 87 open reading frames (ORF) and has a low density. The coding DNA is flanked by ~800bp of multiple GC rich terminal repeats, which confer a higher density (Fig. 1.3) (Renne et al., 1996a; Russo et al., 1996).

Herpesviruses share orthologous genes, these are found in comparable genomic locations and orientation (Longnecker and Neipel, 2007). These conserved proteins have roles in essential viral processes including cleavage and packaging of the viral genome, DNA replication and virion assembly (Russo et al., 1996). Sixty-seven of the KSHV ORFs have homologues in the γ2 prototype herpesvirus saimiri (HSV) and are numbered according to HSV nomenclature. The function of many KSHV genes has been assigned purely on the basis of sequence similarity with other viral proteins. Those viral genes lacking homology and which are unique to KSHV are prefixed with a K (Fig. 1.3). Strikingly, many of these genes share significant sequence similarity to cellular genes and are likely to have been pirated by KSHV from the host cell during viral evolution (Fig. 1.3) (Moore and Chang, 1998). These genes encode proteins involved in evasion of the host immune response, nucleotide metabolism and potential regulators of cell growth (Neipel et al., 1997a). The KSHV genome encodes viral homologues of Cyclin D2 (vCyclin), vFLIP (Fas-associated death domain (FADD) interkeukin-1β-converting enzyme (FLICE) inhibitory protein), interferon regulator factors (IRFs), Bcl-2 and IL-8 receptor, IL6, CD200 and three chemokines (viral CC-class chemokine (vCCL) 1-3) (Fig. 1.3). Pirating of cellular genes is unique to KSHV and its related primate viruses; however other herpesviruses, particularly EBV, induce some of the same genes. For example EBV-encoded LMP-1 induces Cyclin D2 in B cells (Arvanitakis et al., 1995).

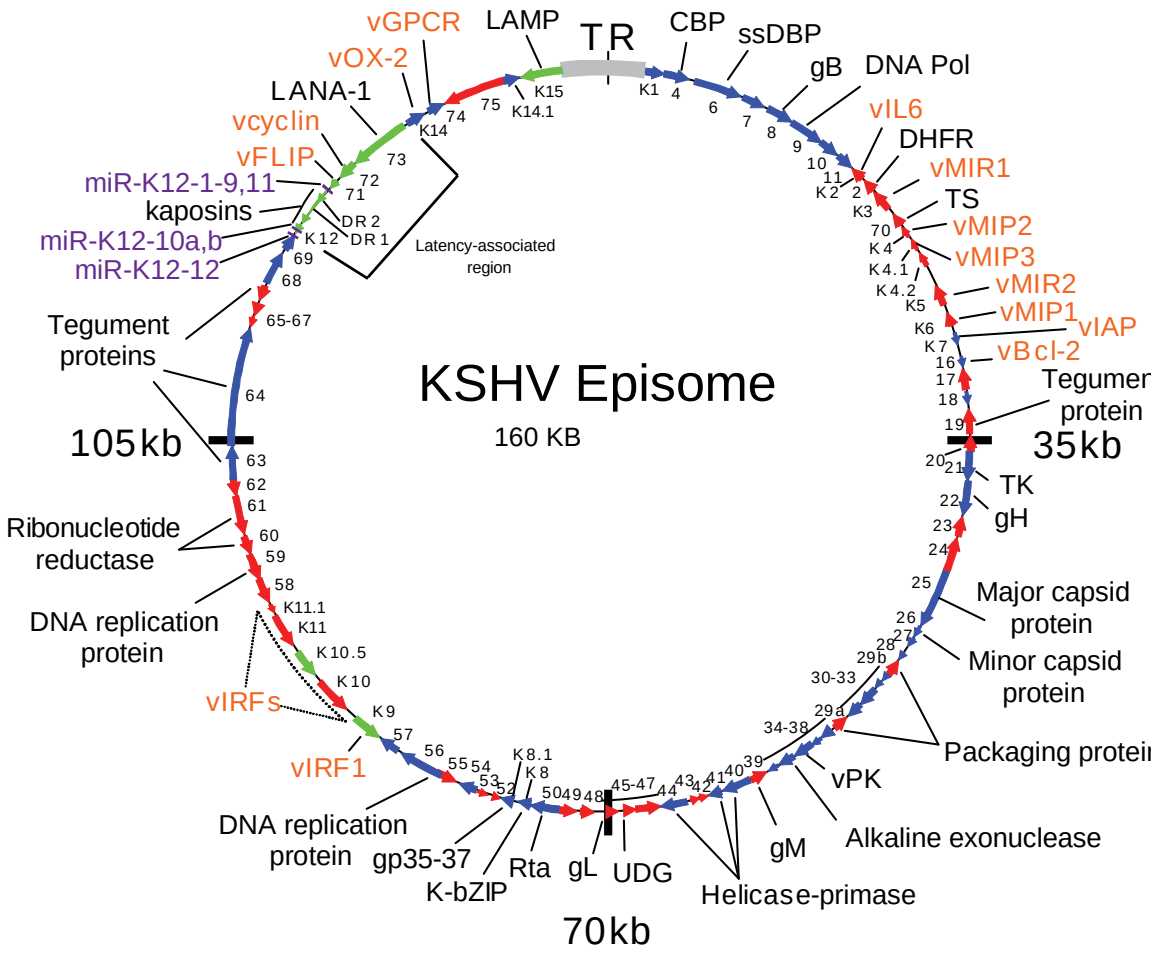

Figure 1.3 The KSHV episome. Numbers inside the episome identify the KSHV ORFs, unique ORFs are prefaced with a K. Cellular homologues are in orange and the miRNAs in purple. Green arrows indicate latent genes, blue arrows indicate ORFs encoded in a 5' to 3' positive polarity, red arrows indicate ORFs encoded in a 3' to 5' negative polarity. TR, terminal repeat; CBP, complement binding protein; ssDBP, single-stranded DNA binding protein; gB, glycoprotein B; DNA Pol, DNA polymerase; vIL6, viral interleukin-6; DHFR, dihydrofolate reductase; vMIR, viral modulators of immune responses; TS, thymidylate synthase; vMIP, viral macrophage inflammatory protein; vIAP, viral inhibitor-of-apoptosis protein; vBcl-2, viral Bcl-2; TK, thymidine kinase; gH, glycoprotein H; vPK, viral protein kinase; gM, glycoprotein M; UDG, uracil DNA glucosidase; gL, glycoprotein L; gp35-37, glycoprotein 35-37; vIRF, viral interferon regulatory factor; vFLIP, viral Fas-associated death domain interleukin-1b-converting enzyme inhibitory protein; vCyclin, viral Cyclin; LANA-1, latent nuclear antigen; vOX-2, viral OX-2; vGPCR, viral G-protein-coupled receptor; LAMP, latency-associated membrane protein. Adapted from Dr. R. Vart (Thesis).

1.1.5 KSHV lifecycle

1.1.5.1 Virus entry

In vivo KSHV genomic DNA has been detected in a number of different cell types, including B cells, endothelial cells, CD45+/CD68+ monocytes, keratinocytes and epithelial cells (Ganem, 1998; Antman and Chang, 2000). Furthermore, KSHV has been shown to have a broad range of infectivity *in vitro*, infecting a wide range of both human and animal cells (Renne et al., 1998; Moses et al., 1999; Bechtel et al., 2003; Kaleeba and Berger, 2006a). Herpesvirus entry into host cells occurs after attachment to a host cell surface receptor and then via direct fusion between virion and target cell membrane (Spear and Longnecker, 2003). Virus attachment and entry is mediated by envelope-associated glycoproteins. KSHV encodes three conserved glycoproteins, gB, gH and gL, thought to be essential for entry of all herpesvirus, as well as additional envelope associated glycoproteins, gM, gN and gpK8.1A (Akula et al., 2001a; Naranatt et al., 2002; Spear and Longnecker, 2003). Herpesviruses are capable of engaging multiple cell surface receptors, some of which serve to concentrate the virus on the host cell and others are responsible for direct fusion entry. Like other herpesviruses, KSHV utilizes heparin sulphate for cell surface binding (Akula et al., 2001b). Whereas KSHV entry is facilitated by binding to the cell surface molecule xCT (Kaleeba and Berger, 2006b). KSHV fusion permissiveness correlates with xCT expression; furthermore xCT is expressed on a wide range of cell types which accounts for the broad range of KSHV infectivity *in vitro*. Akula et al showed that viral entry can also be mediated on B cells by glycoprotein gB binding to integrin α3β1 (Akula et al., 2001a). Interestingly, xCT is not expressed on CD19+ B cells (Kaleeba and Berger, 2006b) which are peripheral blood B cells thought to be the primary reservoir for persistent KSHV infection (Antman and Chang, 2000; Dourmishev et al., 2003). The fact that inhibition of integrin α3β1 does not fully ablate KSHV entry to B cells indicates additional KSHV receptors are employed during viral penetration (Akula et al., 2002).

1.1.5.2 Latent infection

Once the virus has entered the cell, KSHV modulates the host microtubule network through induction of Rho GTPases, this facilitates trafficking of the viral DNA to the nucleus (Naranatt et al., 2005). As with other Herpesviruses, once in the nucleus KSHV can undergo two modes of infection: lytic replication, culminating in the production of new virions, or latent infection resulting in persistent host cell infection. The majority of de novo KSHV infection results in the establishment of latency (Bechtel et al., 2003) and tumour cells of both KS and PEL are latently infected (Cesarman et al., 1995a; Zhong et al., 1996). As with EBV, latency is the default mode of KSHV infection and this ability to maintain long term infection in quiescent or proliferating cells is a defining feature of the herpesvirus family. Unlike lytic replication whereby the genes involved are conserved between herpesviruses, genes required for latency are unique to each virus.

During latency the viral genome circularizes and is maintained as an extra-chromosomal episome (Renne et al., 1996a). The episome is copied by the host cell machinery during replication and is tethered to host chromatin during mitosis, thus ensuring each daughter cell receives a copy of the viral genome. Only four viral proteins and a series of microRNAs (miRNAs) are expressed and have been detected in PEL and KS spindle cells (Li et al., 2002; Pearce et al., 2005; Cai and Cullen, 2006). The restricted number of latent gene products minimizes the number of antigens for presentation and recognition by the host immune response. The KSHV latent proteins are latent nuclear antigen 1 (LANA) (ORF73), vCyclin (ORF 72), vFLIP (ORF 71) and Kaposin (K12) (Zhong et al., 1996; Dittmer, 2003). Since these are the primary proteins expressed in KSHV-associated tumours they also play a crucial role in viral-induced pathogenesis.

1.1.5.3 Latent gene expression and function

The major latency genes colocalise within 4.8kb of the viral genome referred to as the major latency locus. Within this region are genes expressing the three latent proteins (ORF71-73), followed by an array of miRNAs and then the final latent protein, Kaposin (Fig. 1.4). The latency gene products are transcribed from three differentially regulated promoters: LTc, LTi and LTd (Fig. 1.4) (Pearce et al., 2005; Sarid et al., 1999; Dittmer et al., 1998; Li et al., 2002). This creates a complex interwoven network of mono, bi and cistronic mRNAs. Transcription from LTc generates a 5.7kb transcript which encodes ORF71-73. Splicing of this long mRNA generates another shorter transcript encoding only ORF71 and ORF72 (Dittmer et al., 1998). Regardless of mRNA splicing activities all three transcripts from LTc are coterminal. Transcription of ORF71-73 is also initiated from a promoter downstream of LTc and proximal to ORF73, designated LTi. This promoter is stimulated by transcription activator (RTA/ORF50) during lytic replication (Matsumura et al., 2005). The third promoter, LTd generates a 1.5kb product encoding ORF71 and ORF72, and a 2.5kb spliced mRNA which encodes all the kaposin isoforms (Sadler et al., 1999; Liu et al., 2002). The LTd promoter is active during latency and induced upon lytic replication. In addition to the kaposins, this 2.5kb mRNA may also give rise to the KSHV miRNAs (Fig. 1.4) (Pearce et al., 2005).

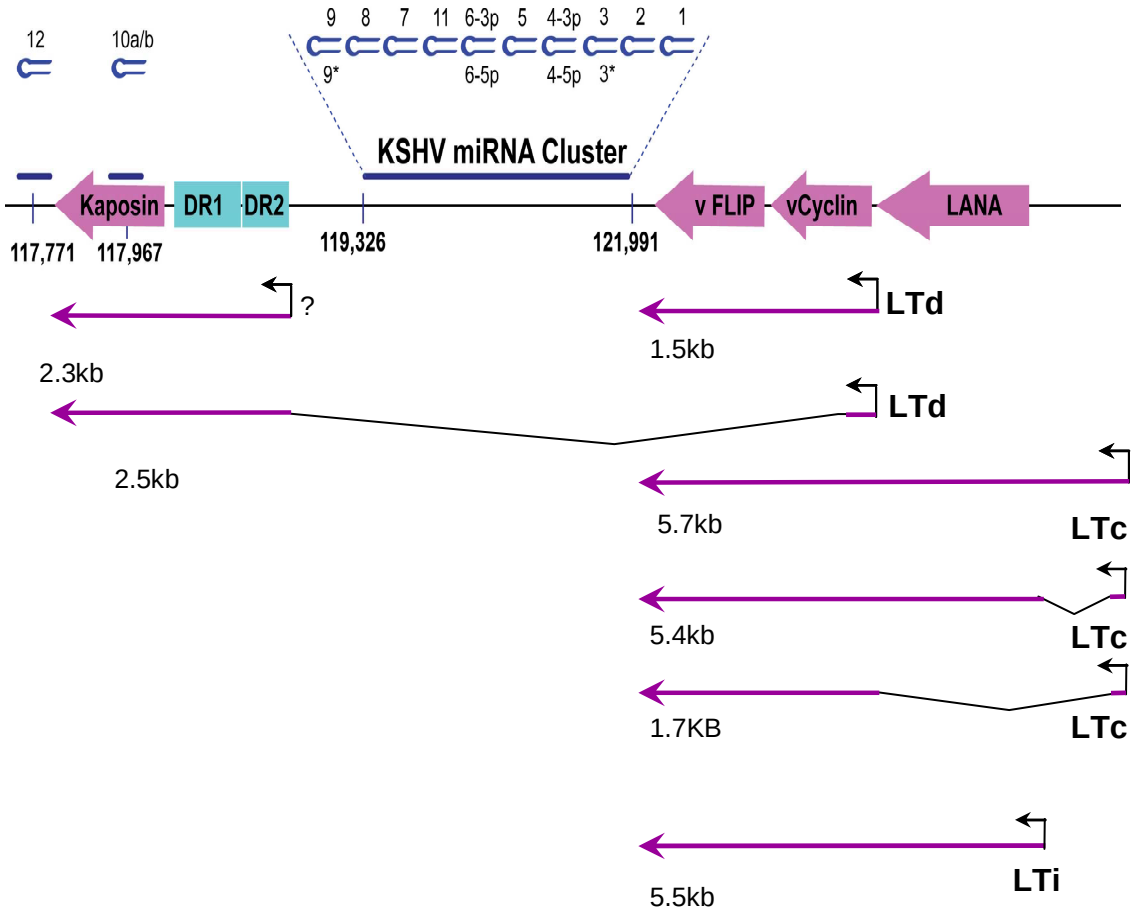

Figure 1.4 Organisation, promoters and transcripts of the KSHV latency region. Schematic representation of KSHV miRNA organization in the latency associated region of the viral genome. Viral miRNAs are indicated by horizontal blue lines with the genomic locations noted below. Individual KSHV miRNA hairpins are shown above. Protein coding open reading frames are shown in pink. The kaposin open reading frame is preceded by two sets of direct repeats (Blue rectangles, DR1 and DR2). The various promoters and transcripts encoding latency proteins and miRNAs are shown below. Black arrows correspond to promoters with purple arrows representing mRNA transcripts and black lines indicating excised RNA. The length of each transcript is noted. The miRNA cluster may be processed from a large intron spliced from the 2.5kb transcript initiated from LTd. Promoters: LTc, constitutively active latency promoter; LTi, inducible latency promoter; LTd, downstream latency promoter. ?, The promoter of this transcript identified by (Sadler et al., 1999) remains uncharacterized.

1.1.5.3.1 LANA

LANA is a large protein with central region of acidic repeats separating the N- and C-terminal domains. The C-terminus is a sequence-specific DNA binding region which recognises the viral terminal repeats (Ballestas and Kaye, 2001), the N terminus interacts with host chromatin-associated histones (Cotter and Robertson, 1999; Barbera et al., 2006). Episome tethering to host chromatin is mediated by LANA through these domains and this protein has been shown to be the sufficient for long term episomal maintenance (Ballestas et al., 1999). During mitosis LANA is bound to the viral terminal repeats and interacts with histones H1, H2A and H2B present on host cell chromatin (Cotter and Robertson, 1999; Ballestas and Kaye, 2001; Barbera et al., 2006). In addition to tethering the viral episome, LANA has a number of additional functions which contribute more directly to KSHV-oncogenesis and has led to LANA being classified as an oncogene.

LANA interacts with p53 repressing its transcriptional activity, the resulting attenuation of p53-mediated cell cycle arrest or apoptosis promotes cell survival (Friborg, Jr. et al., 1999). This correlates with the observation that expression of LANA in primary endothelial cells extends their lifespan in culture (Watanabe et al., 2003). However, PEL cells have been shown to respond to the chemotherapeutic agent doxorubicin with p53 activation and growth arrest, indicating that, at least in these cells, LANA does not completely abolish p53 activity (Petre et al., 2007). LANA also binds to pRb which inhibits its association with E2F, leaving E2F free to activate genes controlling cell cycle progression (Radkov et al., 2000). However, as with p53, LANA inhibition of pRB is only partial (Platt et al., 2002). Furthermore, LANA has been shown to bind to glycogen synthase kinase 3β (GSK-3β) relocating it to the nucleus (Fujimuro et al., 2003). This relocation prevents GSK-3β-dependent phosphorylation and subsequent proteosomal degradation of β-catenin. Consequently, β-catenin accumulates and activates transcription of c-myc, c-jun and Cyclin D. In this way LANA promotes entry to S-phase (Fujimuro et al., 2003).

1.1.5.3.2 vCyclin

Viral Cyclin (vCyclin) is an orthologue of cellular Cyclin D (Chang et al., 1996). Cyclin D proteins activate kinases which phosphorylate key cell cycle check point proteins, promoting cell cycle progression. vCyclin, like its cellular counterpart, phosphorylates cdk6 leading to inhibition of pRB (Godden-Kent et al., 1997). However, vCyclin demonstrates additional properties that distinguish it from cellular Cyclin D. vCyclin has an expanded substrate specificity leading to phosphorylation of p27, H1 and cdc25a (Godden-Kent et al., 1997; Li et al., 1997; Mann et al., 1999). In addition, vCyclin displays decreased sensitivity to inhibition by Cyclin dependant kinases, such as p27 (Ellis et al., 1999; Mann et al., 1999). Indeed the acquired ability of vCyclin to phosphorylate its inhibitor p27 targets this protein for degradation releasing vCyclin from its control. Ectopic expression of vCyclin in primary cells causes growth arrest and sensitises cells to apoptosis, these effects are p53 dependant (Verschuren et al., 2002). Therefore, only in the absence of p53 can vCyclin confer a growth advantage to cells (Verschuren et al., 2002).

1.1.5.3.3 vFLIP

vFLIP is a small protein composed of two tandem death effector domains. vFLIP is so called due to its homology to cellular FLICE-inhibitory proteins (FLIPs) (Thome et al., 1997). These proteins inhibit apoptosis by blocking recruitment of caspase 8 to the death receptor signalling complexes. Exogenous vFLIP expression in B cells has also been shown to inhibit apoptosis in this manner (Djerbi et al., 1999). In addition, vFLIP inhibits apoptosis by activating NFκB. vFLIP binds to the γ subunit of IKB kinase (IKK) which induces phosphorylation of this protein and eventual proteolysis (Liu et al., 2002; Field et al., 2003; Bagneris et al., 2008). Degradation of IKK releases NFκB subunit which moves to the nucleus and stimulates gene expression. NFκB activation results in the up-regulation of cytokines including chemokines. Therefore, the expression of vFLIP

in latently infected KS spindle cells explains in part the mechanism behind the proinflammatory microenvironment which is characteristic of KS (Xu and Ganem, 2007; Punj et al., 2009; Sakakibara et al., 2009). Through activating NFκB, vFLIP induces cytoskeletal rearrangements which produce the typical spindle shape of KSHV infected endothelial cells (Grossmann et al., 2006). PEL cells are dependant on vFLIP for their survival. Consequently, silencing of vFLIP by siRNA or inhibition of NFκB *in vitro* (Keller et al., 2000; Guasparri et al., 2004) and *in vivo* (Godfrey et al., 2005) led to B cell death. vFLIP expression in B cells led to tumour development in mice, due to inhibition of apoptosis (Djerbi et al., 1999). Therefore, vFLIP is likely to play a pivotal role in KSHV-mediated oncogenesis.

1.1.5.3.4 Kaposins

The kaposins are a set of three proteins latently expressed in PEL and KS (Staskus et al., 1997; Sturzl et al., 1997). The kaposins are transcribed on a distinct transcriptional unit from other latency proteins (Sadler et al., 1999). Transcription from the kaposin promoter encodes a small open reading frame, which is preceded by two direct repeats of GC rich sequences (DR1 and DR2). Translation of the ORF generates Kaposin A, whereas translation of the two DR gives rise to kaposin B. Translation of the DRs in frame with the ORF generates the final kaposin, kaposin C (Sadler et al., 1999).

Kaposin A is a transmembrane protein whose over-expression transformed immortalised rodent fibroblasts, clones of which generated tumours in nude mice (Muralidhar et al., 1998). The mechanism and relevance of this finding remains obscure, since spindle cells from KS tumours do not form colonies in soft agar, neither do they induce colonies in mice. Kaposin A binds the guanine exchange factor cytohesin-1, which is a regulator of integrin mediated cell adhesion. Potentially, this interaction may explain Kaposin A's transforming abilities. Alternatively, Kaposin A has also been shown to interact and inhibit septin A, which is a proapoptotic caspase 3 activator. This function may also contribute to kaposin A mediated transformation (Lin et al., 2007). Kaposin B is a small

polypeptide with no known catalytic motifs, it therefore elicits its function through interacting with other proteins (McCormick and Ganem, 2005). One such protein is mitogen-activated protein kinase-associated protein kinase 2 (MK2), binding of MK2 by kaposin B leads to MK2 activation via p38 phosphorylation (McCormick and Ganem, 2005). Activated MK2 is then free to phosphorylate its downstream targets, one of which is tristeraprolin (TTP). TTP stabilises mRNAs which contain AU-rich elements (ARE) including cytokine and growth factors (Sandler and Stoecklin, 2008). Therefore, along with vFLIP, kaposin B expression contributes to the cytokine rich tumour microenvironment of KS. To date there are no studies investigating the function of kaposin C and as a result its role in latency or pathogenesis remains obscure.

1.1.5.3.5 KSHV-encoded microRNAs (miRNAs)

In addition to the latent proteins, KSHV encodes an array of miRNAs, which are expressed primarily during latency (Pfeffer et al., 2005; Samols et al., 2005; Cai et al., 2005). miRNAs are small non-coding RNA molecules which negatively regulate gene expression (Bartel, 2004). KSHV encodes 12 pre miRNAs, 10 of which are located in a 3.6kbp intragenic gap between the Kaposin open reading frame and vFLIP; this is the longest sequence devoid of open reading frames in the unique region of the KSHV genome (Cai et al., 2005; Samols et al., 2005). The other two pre miRNAs are located upstream, one is situated within the K12 ORF and the other just proximal to the K12 coding sequence (Grundhoff et al., 2006). These 12 pre-miRNAs give rise to 17 mature effector miRNAs which are capable of regulating both host and viral gene expression. There is very little sequence variation in viral miRNAs between KSHV isolates (Marshall et al., 2007), however these miRNAs are not conserved between different herpesviruses (Schafer et al., 2007).

The role of the KSHV miRNAs in establishing infection and KS pathogenesis is still poorly understood. Thrombospondin-1 (THBS1) was the first cellular target of the KSHV miRNAs to be identified (Samols et al., 2007). THBS1 is a multifunctional protein; it is a known agonist of angiogenesis and its expression up-regulates cell adhesion molecules and promotes recruitment of monocytes to endothelial cells (Narizhneva et al., 2005). Therefore, THBS1 down-regulation by the KSHV miRNAs may contribute to the angiogenic phenotype of KS lesions and aid immune evasion of infected cells (Samols et al., 2007). Another validated miRNA target is BCLAF1, down-regulation of this protein in latently infected PEL cells led to decreased virus production following lytic induction (Ziegelbauer et al., 2009). This finding suggests the viral miRNAs may act to promote latency. Similar to protein coding viral genes, KSHV miRNA miR-K12-11 displays significant sequence similarity to the cellular miRNA miR-155 (Skalsky et al., 2007; Gottwein et al., 2007). These two miRNAs share the same seed region, which dictates miRNA target-specificity, consequently they regulate an overlapping set of genes (Skalsky et al., 2007; Gottwein et al., 2007). miR-155 is a lymphoid specific miRNA with a role in B and T cell differentiation (Thai et al., 2007; Turner and Vigorito, 2008) and T cell regulation (Lu et al., 2009). Furthermore, this miRNA is also implicated in B cell transformation and is frequently up-regulated in certain lymphomas (Eis et al., 2005; Costinean et al., 2006). Since miR155 is not expressed in PEL cells, it is tempting to speculate that miR-K12-11 mimics its function, playing an important role in PEL development (Skalsky et al., 2007). However, the role of miR-K12-11 is KS pathogenesis has not been investigated.

An investigation by Murphy et al into whether herpesvirus-encoded miRNAs regulate viral gene expression, revealed that although lacking sequence conservation miRNAs from all three herpesvirus families, including KSHV, were predicted to suppress immediate early proteins (Murphy et al., 2008). Suppression of the IE gene, IE1, was experimentally confirmed in the context of HCMV infection, and this silencing suppressed lytic reactivation (Murphy et al., 2008). These findings suggest a role for viral miRNAs in maintaining latency. The KSHV miRNAs were predicted to target the KSHV early lytic protein, RTA which is the major inducer of lytic replication (Murphy et al., 2008). Recent studies have experimentally confirmed KSHV miRNA auto-regulation of RTA, in this manner the KSHV miRNAs favour latency by down-regulating levels of the lytic transactivator (Bellare and Ganem, 2009; Lei et al., 2010; Lu et al., 2010).

1.1.5.4 Lytic infection

Latently infected cells provide a reservoir of viral genomes from which KSHV can be produced, resulting in dissemination within or between hosts. In order to do so the virus must be reactivated from latency through a programme of active gene expression and DNA replication, culminating in the synthesis of new virions and host cell death. In KS lesions 1-5% of spindle cells at any one time are undergoing lytic replication (Staskus et al., 1997; Direkze and Laman, 2004). KSHV reactivation precedes the development of KS, with viral replication increasing during disease progression (Campbell et al., 2000; Boneschi et al., 2001). Furthermore, an increase in KSHV DNA correlates with the appearance of new KS lesions (Cannon et al., 2003) and lytic gene products contribute to KS pathogenesis through paracrine effects (Direkze and Laman, 2004). These data highlight the pathogenic effect of lytic reactivation in KSHV-induced disease.

Through the *in vitro* study of lytic reactivation from latent PEL cells, a number of factors have been shown to trigger the switch from latent to lytic infection. The most potent and widely used chemical inducer is phorbol ester tetradecanoyl phorbol acetate (TPA) (Renne et al., 1996b). Other stimuli include interferon γ (IFNγ) and additional cytokines (Mercader et al., 2000), NFkB inhibitors

(Grossmann and Ganem, 2008) and expression of the transcription factor XBP-1 (Wilson et al., 2007). The mechanisms of action of these stimuli highlight multiple mechanisms by which lytic infection can be induced. Despite extensive *in vitro* characterisation, the physiological ligands which reactivate KSHV *in vivo* remain unknown. The principle site of lytic reactivation *in vivo* is the B cells of the tonsil or other lymphoid tissue in the oropharynx (Duus et al., 2004). A single viral gene known as replication and transcription activator or RTA is both necessary (Lukac et al., 1999) and sufficient (Gradoville et al., 2000) to bring about lytic replication. RTA is a sequence specific DNA binding protein (Lukac et al., 1998) that triggers the lytic cycle by activating transcription from key lytic promoters, as well as initiating viral DNA replication (Song et al., 2003). RTA also activates its own promoter, augmenting lytic protein expression and DNA replication (Gradoville et al., 2000). In those lytic promoters which lack an RTA binding motif, RTA activates transcription through protein-protein interactions with cellular transcription factors including CSL-1(Liang et al., 2002; Liang and Ganem, 2003) and CRB binding protein (CBP) (Gwack et al., 2001). In latently infected PEL cells the RTA promoter is silenced by methylation (Chen et al., 2001). In addition, LANA has been shown to negatively regulate RTA both directly (Lan et al., 2004) and indirectly through sequestering of RTA cellular cofactors (Lan et al., 2005). Therefore, KSHV employs a number of mechanisms to minimize RTA expression in order to maintain latency.

Lytic reactivation initiated by RTA is characterised by a tightly regulated temporal cascade of gene expression that culminates in the production of new viral particles. The first wave of gene expression is termed immediate early (IE), these genes are regulators of lytic gene expression. The IE genes switch on the delayed early (DE) genes which mediate viral DNA replication, immune evasion and host gene expression shutoff. Following DNA replication the late (L) genes are activated, these form the structural components of the virion. Once newly synthesized capsids exit the nucleus they acquire an envelope by budding through the cellular membrane.

1.1.5.5 Lytic proteins

Multiple lytic proteins have been shown, via paracrine effects, to contribute to the proangiogenic and proinflammatory environment of KS.

1.1.5.5.1 Viral interleukin 6 (vIL6)

vIL6 is homologous to hIL6, sharing 25% amino acid identity (Molden et al., 1997; Neipel et al., 1997b). vIL6 is expressed in approximately 5% of KS spindle and PEL cells, which corresponds to the proportion of lytic cells present in these tumours (Parravicini et al., 2000; Brousset et al., 2001). vIL6 is a functional cytokine which stimulates the proliferation of cells *in vitro* (Burger et al., 1998; Moore and Chang, 1998) and activates signalling pathways through stimulation of Jankus activated kinases (JAK)/signal transducers and activators of transcript (STAT) and the mitogen activated protein kinases (MAPK). In addition to these effects, vIL6 up-regulates proangiogenic molecules vascular endothelial growth factor (VEGF) A (Aoki et al., 1999) and angiopoietin-2 (Vart et al., 2007). hIL6 signals by binding to the IL6 receptor which consists of the gp80 binding subunit and the signal transducing subunit, gp130. hIL6 signalling is regulated by the limited distribution of gp80. However, vIL6 signals solely through gp130 and therefore has wider ranging effects (Molden et al., 1997). KS tumours are rich in hIL6 (Miles et al., 1990) with vIL6 augmenting the expression of its cellular counterpart (Mori et al., 2000), highlighting the importance of IL6 as an inflammatory molecule in KS development.

1.1.5.5.2 Viral CC-class chemokines (vCCLs)

KSHV encodes three chemokine homologues, known as vCCL1 (K6) vCCL2 (K4) and vCCL3 (K4.1), (also referred to as viral macrophage inhibitory proteins, vMIP1-3) (Moore et al., 1996; Nicholas et al., 1997) all of which are expressed during lytic replication. These chemokines interact with the chemokine (C-C motif) receptors (CCR) 3, 4 and 8, each showing distinct receptor specificity (Boshoff et al., 1997; Sozzani et al., 1998; Stine et al., 2000). The vCCLs attract inflammatory cells to the site of KS lesions including eosinophils and TH2 cells (Nicholas, 2005), thereby contributing to the proinflammatory environment of KS lesions. Interestingly, unlike their cellular homologues the vCCLs are angiogenic in the chick chorioallantoic (CAM) assay (Boshoff et al., 1997; Stine et al., 2000).

1.1.5.5.3 Viral G-protein coupled receptor (vGPCR)

Another one of KSHVs pirated cellular genes is viral G protein-coupled receptor (vGPCR), a constitutively active transmembrane signalling molecule (Cesarman et al., 1996; Arvanitakis et al., 1997). vGPCR is related to the cellular IL8 receptors CXCR1 and CXCR2 (Cesarman et al., 1996). vGPCR induces the angiogenic molecules VEGFA (Bais et al., 1998), angiogenin (Sadagopan et al., 2009) and angiopoietin-2 (Vart et al., 2007), as well as proinflammatory factors IL6, IL4 and IL8 (Shepard et al., 2001). vGPCR also activates a number of signalling pathways including the mitogenic p38 MAPK, MEK and JNK pathways (Smit et al., 2002), the antiapoptotic AKT pathway (Montaner et al., 2001) and NF-κB (Shepard et al., 2001). Transgenic mice expressing vGPCR form vascular tumours which are morphogenically similar to KS lesions (Guo et al., 2003) and its expression transforms mouse NIH3T3 cells (Bais et al., 1998). Therefore, despite the fact that only 5% of KS spindle cells express vGPCR, its upregulation of angiogenic and inflammatory cytokines could be pivotal in the development of KS.

1.1.5.5.4 Viral Interferon regulatory factors (vIRFs)

KSHV encodes four genes with sequence similarity to human interferon regulatory factors (IRFs): vIRF1, vIRF2, vIRF3 (also known as LANA-2) and K10.5/10.7. Phylogenetic analysis revealed vIRF1 is likely derived from a host IRF and subsequent gene duplication gave rise to the other three vIRFs (Jenner and Boshoff, 2002). The cellular IRFs are a family of transcription factors which in response to interferon signalling, mediate the host antiviral and antibacterial immune response (Paun and Pitha, 2007). The programme of vIRF gene expression is not as well defined as other KSHV genes. vIRF is latently expressed in PEL cell lines and in KS, however it is also induced upon lytic replication (Dittmer, 2003; Pozharskaya et al., 2004). vIRF3 shows latent expression in both PEL and MCD, although is not detected in KS (Rivas et al., 2001). Therefore, the vIRFs may be relevant to both lytic and latent lifecycles with their expression varying between KSHV-associated malignancies.

vIRF1 is the most extensively characterised, it plays an important role in regulating the host immune response to KSHV by inhibiting IFN signalling within infected cells. vIRF1 has been shown to inhibit both INFα and INFβ stimulated transcription (Zimring et al., 1998; Li et al., 1998; Lin et al., 2001). vIRF1 can bind directly to DNA through its DNA binding domain (Park et al., 2007), thereby inhibiting expression of genes involved in the immune response. However, vIRF1 also binds to and sequesters transcriptional coactivators CREB and CBP, thus preventing them from activating transcription of antiviral cytokines (Li et al., 1998; Seo et al., 2000; Lin et al., 2001). Binding of vIRF1 to p300 represses this protein's histone acetylase activity, further inhibiting gene activation (Li et al., 2000). vIRF2 acts in a similar manner to vIRF1, inhibiting the interferon response by binding to cellular IRFs and p300. In this way vIRF2 inhibits IRF1 and IRF3 mediated transcriptional activation of the IFNα promoter (Burysek et al., 1999).

1.2 Lymphatic Endothelium

The primary function of the lymphatic vasculature is to collect and drain protein rich fluid (lymph) from extracellular spaces within most organs, and return this interstitial fluid to the cardiovascular system to maintain normal tissue fluid balance and interstitial pressure (Oliver and Alitalo, 2005; Karpanen and Makinen, 2006; Cueni and Detmar, 2008). The lymphatic system developed in higher organisms in response to an additional need to clear tissues of substances not absorbed by the blood vasculature (Yoeffry and Courtice, 1970). First described as “milky veins” in 1627 by Gasparo Asellius (Asellius, 1627) the lymphatic vasculature has gone largely un-investigated until recent years when molecular biology techniques facilitated the identification and characterisation of lymphatic-specific molecules and the role they play in lymphangiogenesis (growth of new lymphatic vessels from pre-existing lymphatic vessels) (Alitalo and Carmeliet, 2002).

1.2.1 Organisation of the lymphatic system

Unlike the blood vasculature which is circulatory, the lymphatic system is unidirectional. Lymph fluid is collected from tissues by lymph capillaries and returned to the venous arteries through a series of larger collecting lymphatic vessels (Fig. 1.5) (Witte et al., 2001). Lymphatic capillaries responsible for absorbing lymph fluid are distinct from blood capillaries, in that they are blind ended structures which lack a continual basal lamina (Oliver and Alitalo, 2005) . Lymph capillaries are composed of a single layer of endothelial cells which, unlike blood vessels, lack intercellular continuous VE-cadherin linked tight junctions. Instead, lymphatic endothelial cells (LEC) form discontinuous button-like intercellular junctions generating small inter-endothelial pores (Leak, 1976; Dejana, 2004; Baluk et al., 2007). LEC are anchored by filaments to this discontinuous basement membrane (Gerli et al., 2000). These features render lymphatic capillaries highly permeable to lymph fluid as well as pathogens and migrating cells, free movement of which are required for lymphatic functioning (Dejana, 2004; Oliver and Alitalo, 2005). Lymphatic capillaries also lack

supporting pericytes which in blood vessel capillaries act to reduce leakage and prevent haemorrhaging (Oliver and Alitalo, 2005; Baluk et al., 2007). Small lymphatic capillaries feed into larger lymphatic vessels, which are lined with smooth muscle cells to facilitate fluid transport and contain flap-like valves to prevent lymph backflow (Fig. 1.5). The lymphatic vessels collect at the thoracic duct and right lymphatic duct where lymph fluid is returned to the blood circulatory system via large veins at the base of the neck (Fig. 1.5) (Oliver and Alitalo, 2005). The lymphatic system lacks a central pump such as the heart. Instead, fluid is moved by the combined actions of skeletal muscle, respiratory movement and peristaltic contractions of the smooth muscle cells lining the lymphatic vessels (Cueni and Detmar, 2008).

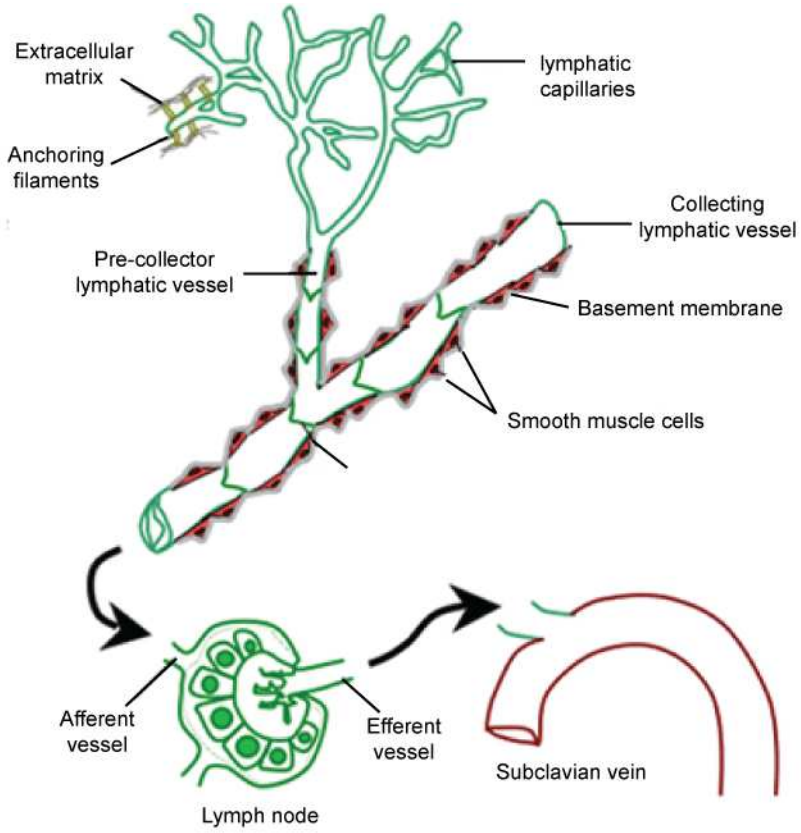

Figure 1.5 Lymphatic vasculature organisation. Lymph fluid is collected from tissues by permeating blunt-ended lymphatic capillaries. These capillaries are tethered to the extra cellular matrix by anchoring filaments. The lymphatic capillaries drain into the pre-collector lymphatic vessels, which in turn empty into larger collecting lymphatic vessels. Large lymphatic vessels are lined with smooth muscle cells to facilitate fluid transport and flap-like valves which aid directional flow and prevent lymph back flow. The lymphatic vessels converge at the thoracic duct and return lymph to the blood circulatory system via the subclavian vein. Picture taken from Maby-EL and Petrova (Maby-El and Petrova, 2008).

In addition to lymphatic vessels, the lymphatic system includes the lymphoid organs; these are the lymph nodes, tonsils, peyers patches, spleen and the thymus, all of which are involved in the immune response. Lymphatic vessels are not found in the brain and retina, as well as avascular tissues such as the epidermis, hair, nails, cartilage and cornea.

1.2.2 Lymphatic function in health and disease

In addition to collecting and redistributing tissue fluid, the lymph system has an important role in immune surveillance. Upon antigen recognition, stimulated dendritic cells exit tissues and enter the lymphatic vasculature, from here they migrate to lymph nodes and other lymphoid organs where immune responses are mounted (Johnson and Jackson, 2008). In the intestine the lymphatic system also plays a role in fat absorption, here specialised lymph vessels called lacteals absorb dietary fat and transport it via the lymphatic vasculature back to the circulatory system (Cueni and Detmar, 2006). Acquired or congenital defects in the lymphatic system lead to lymphoedema, an accumulation of lymph fluid in the tissues, which results in swelling of the extremities and can often involve inflammatory reactions and fibrosis (Witte et al., 2001; Cueni and Detmar, 2008). During oncogenesis the lymphatic vasculature provides migrating tumour cells an access route to secondary sites within the body, thereby facilitating metastasis (Skobe et al., 2001). The loosely connected lymphatic endothelium and discontinuous basement membrane facilitates tumour cell egress and dissemination to regional lymph nodes (Alitalo and Carmeliet, 2002). In breast cancer the degree of tumour-associated lymphangiogenesis correlates with secondary metastasis to the lymph nodes and lung (Skobe et al., 2001). Importantly, tumour cell metastasis to lymph nodes is used as a prognostic indicator in the assessment of cancer patients and can influence the adopted therapeutic regime. An additional role for the lymphatic system in cancer was highlighted by studies suggesting the lymphatic origin of KS tumour cells (Jussila et al., 1998; Skobe et al., 1999; Hong et al., 2004; Wang et al., 2004).

1.2.3 Lymphangiogenesis

In mice the lymphatic vasculature develops at embryonic day 5 (E5), after the formation of a functional blood vasculature (Oliver and Detmar, 2002) . Through ink injection experiments in developing pigs, Florence Sabin observed that primitive lymph sacs in the jugular region originated from endothelial cells budding off from pre-existing veins (Sabin, 1902). This observation led Sabin to propose the centrifugal theory of lymphatic development, stating that lymphatic endothelial cells were derived from venous endothelium (Sabin, 1902). The primitive lymph sacs formed after endothelial budding are present one month after the development of the first blood vessels in six week old mice (van der Putte, 1975). After the establishment of lymph sacs, cells sprout towards the periphery where they form capillaries which permeate tissues and organs (Sabin, 1902; van der Putte, 1975). The recent discovery of lymphatic-specific markers has furthered research into the process of lymphangiogenesis and the molecules which regulate it. Observing the sequential acquisition of LEC markers during embryogenesis, Oliver and Harvey formulated a step wise model of lymphatic development (Oliver and Harvey, 2002). The four main steps are LEC competence, LEC bias and LEC specification culminating in lymphatic vessel differentiation and maturation (Oliver and Harvey, 2002; Oliver, 2004)

1.2.3.1 Initiation of lymphatic endothelial phenotype

Lymphatic vasculature development begins with a subset of venous endothelial cells in the anterior cardinal vein responding to lymphangiogenic signals. Although these inducing signals are not yet known, the expression of lymphatic endothelial hyaluronan receptor-1 (LYVE1) at E9 in developing mice is the first indication of lymphatic commitment (Banerji et al., 1999; Prevo et al., 2001). Expression of LYVE1 indicates that venous endothelial cells are primed for lymphatic development and ready to receive additional inductive signals for LEC specification (Wigle et al., 2002). However, the absence of lymphatic vasculature defects in LYVE-1 knock-out mice suggests the existence of additional molecules

and pathways involved in initiating lymphatic development (Gale et al., 2007). LYVE1 is a hyaluronan transporter which aids leukocyte migration across the lymph vessel wall (Jackson, 2004). In adults, LYVE1 expression is down-regulated in collecting lymph vessels but up-regulated in lymphatic capillaries (Makinen et al., 2005).

A few hours after LYVE1 expression at E9.5, PROX1 (prospero homeobox 1) is detected in developing mice (Wigle and Oliver, 1999). In contrast to LYVE1 expression which is uniform, PROX1 is expressed in a small sub-population of endothelial cells located at one side of the cardinal vein (Wigle and Oliver, 1999). Polarized expression of PROX1 gives rise to the entirety of the lymphatic system, with cells budding and migrating in a directional manner from the site of PROX1 expression, eventually giving rise to the primary lymph sacs (Maby-El and Petrova, 2008). The venous origin of the lymphatic system was conclusively proven by lineage tracing experiments, whereby LEC were shown to sprout from venous derived lymph sacs which then proliferated and migrated to give rise to the lymphatic vasculature (Srinivasan et al., 2007). PROX1 is an evolutionary conserved homeobox-containing transcription factor, it is the most specific marker of lymphatic endothelium, identified so far. PROX1 knock-out mice are embryonic lethal and completely lack a lymphatic vasculature which is attributed to failure in LEC specification. In contrast, the blood vasculature develops as normal in these mice (Wigle and Oliver, 1999; Wigle et al., 2002). Several lines of evidence have led to the classification of PROX1 as the master regulator of lymphatic differentiation: In the absence of PROX1 venous endothelial cells fail to begin lymphatic specification, those cells which bud from the cardinal vein lack LEC marker expression, instead they continue to express blood vessel endothelial cell (BEC) markers; ectopic expression of PROX1 in cultured BEC suppresses BEC identity and induces expression of LEC specific genes (Hong et al., 2002; Petrova et al., 2002; Wigle et al., 2002). Therefore, PROX1 is both required and sufficient to confer the LEC phenotype. These findings led Wigle et al to propose that the default ground state of LEC was that of venous endothelium and only after expression of PROX1 will these cells enter the path of lymphatic differentiation

(Wigle et al., 2002; Oliver and Detmar, 2002). PROX1 is expressed in a range of other tissues, such as the retina, brain and kidney where it also plays a role in tissue specification and development, however it is not expressed in blood vessels endothelial cells (Wigle and Oliver, 1999; Wigle et al., 2002). PROX1 can function both as an enhancer or repressor of transcription.

Despite the well characterised role for PROX1 in lymphatic development, the signals which trigger its own expression and the expression of downstream target genes are poorly understood (Maby-El and Petrova, 2008). Interleukin 3 and 7 have both been shown to induce PROX1 expression in cultured BEC, however validation of these as PROX1 initiating signals *in vivo* has yet to be been confirmed (Al-Rawi et al., 2005; Groger et al., 2004). Groger et al showed that LEC, but not BEC, constitutively expressed IL3 which regulated expression of PROX1 and podoplanin (PDPN), another LEC distinguishing protein (Groger et al., 2004). Furthermore, when IL3 was inhibited in LEC, this abolished PROX1 and PDPN expression. Therefore, *in vitro* at least, IL3 is required to maintain LEC differentiation status (Groger et al., 2004). In cultured LEC, PROX1 was shown to initiate expression of key regulators of lymphatic development, including VEGRF3 (Petrova et al., 2002; Saharinen and Petrova, 2004; Wigle et al., 2002) and integrin α9 (Mishima et al., 2007).

1.2.3.2 Plasticity of the LEC phenotype

Cellular differentiation occurs at specific points during development and is coordinated by cascades in gene expression initiated by master regulator transcription factors, which are themselves regulated by signals from the local tissue environment. The classical viewpoint of differentiation is that of a unidirectional, terminal and irreversible process (Weissman, 2000). The specialisation of blood and lymphatic vessels in this manner is reflected by distinct gene expression profiles and signalling pathways in the corresponding endothelial cells (Seo et al., 2006; Adams and Alitalo, 2007). For example, arterial endothelial cells express a distinguishing array of genes which are absent from venous or lymphatic endothelial cells (Adams and Alitalo, 2007).

However, there is mounting evidence in support of developmental plasticity, whereby transcription factors can re-programme fully differentiated cells. Takahashi et al induced pluripotent stems cells from somatic cells by transduction of four specific transcription factors (Takahashi and Yamanaka, 2006). Plasticity of lymphocytes was demonstrated when mature B cells were reprogrammed into functional T cells through inhibition of PAX5 (Cobaleda et al., 2007; Cobaleda and Busslinger, 2008). Disruption or forced expression of notch signalling reprogrammed arterio-venous identity, demonstrating the plasticity of blood vessel endothelial cells (You et al., 2005; Roca and Adams, 2007).

In LEC, PROX1 is expressed in post-natal LEC and lymphatic vessels throughout adult life. Down-regulation of PROX1 was observed in defective lymphatics of mutant mouse models (Wilting et al., 2002; Odaka et al., 2006; Backhed et al., 2007; Baluk and McDonald, 2008). LEC identity is acquired upon expression of PROX1 in BEC and siRNA knock down of PROX1 in LEC leads to upregulation of BEC markers and down-regulation of LEC specific genes (Petrova et al., 2002; Hong et al., 2002). These findings argue against terminal differentiation, instead they provide evidence for LEC plasticity. The majority of PROX1 heterozygous knockout mice die shortly after birth, those which survive have mis-patterned and leaky lymphatic vasculature suggesting lymphatic functioning is sensitive to

PROX1 dosage (Harvey et al., 2005). Johnson et al elegantly proved the plasticity of LEC identity through the use of time specific conditional PROX1 knockout mice (Johnson et al., 2008). When PROX1 was silenced in either the embryonic, post-natal or adult mouse, severe defects in the lymphatic vasculature were observed (Johnson et al., 2008). Therefore, PROX1 is required not only for the initiation of LEC identify but also the maintenance of LEC phenotype throughout adult life. Interestingly, adult PROX1 mutant lymphatic vessels became morphologically akin to blood vessels: supporting pericytes were identified, LEC specific button junctions were lost and connections to the blood circulation initiated with red blood cells appearing in the lumen of mutant vessels. COUPTFII (Chicken ovalbumin upstream promoter transcription factor II) is expressed exclusively in venous endothelial cells and genetic loss of this transcriptional co-regulator results in a switch from venous to arterial identity (You et al., 2005). Recently, COUPTFII was identified as a coactivator of PROX1(Lee et al., 2009). COUPTFII physically interacts with PROX1 (Lee et al., 2009; Yamazaki et al., 2009) GEM profiling of LEC lacking either or both proteins confirmed that COUPTFII augments PROX1 activation of certain LEC specific genes (Lee et al., 2009). These data suggest COUPTFII may be an important cofactor in establishment of LEC fate (Lee et al., 2009). There were a number of LEC specific genes differentially regulated by the two factors, suggesting there are other important regulators of LEC fate yet to be identified.

1.2.3.3 Lymphatic sprouting and proliferation: VEGFR3 and VEGFC

Following specification in the cardinal vein, LEC undergo directional proliferation and sprouting resulting in the formation of primary lymph sacs at a defined location. This polarized migration is regulated through expression of a lymphatic-specific receptor signalling system (Oliver, 2004). VEGF receptor 3 (VEGFR3) was identified as one of the first markers associated with lymphatic development (Kaipainen et al., 1995). Missense mutations in VEGFR3 in patients with hereditary lymphoedema highlight the importance of this gene in lymphatic development (Karkkainen et al., 2004). VEGFR3 is expressed early during mouse embryonic development and is widely expressed in both the lymphatic and blood

vasculature, including the anterior cardinal vein (Kaipainen et al., 1995; Dumont et al., 1998). VEGFR3 is expressed in all endothelial cells and plays an important role in blood vasculature remodelling during embryogenesis (Kaipainen et al., 1995; Dumont et al., 1998). Consequently, VEGFR3 null mice are embryonic lethal, dying at E9.5 due to defective remodelling of the primary vascular plexus, and prior to the onset of lymphangiogenesis (Dumont et al., 1998). Later in development and into adulthood VEGFR3 expression is subsequently down-regulated in the blood vasculature and restricted to lymphatic endothelial cells (Kaipainen et al., 1995; Wigle et al., 2002).

Vascular endothelial growth factor C (VEGFC) is the main ligand for VEGFR3 and the primary lymphangiogenic growth factor (Joukov et al., 1996; Kukk et al., 1996). VEGFC is expressed by mesenchymal cells surrounding the cardinal vein, where signalling in PROX1-expressing LEC is essential for sprouting and migration as well as promoting LEC proliferation and survival (Oh et al., 1997; Saaristo et al., 2002; Karkkainen et al., 2004). VEGFC null mice are embryonic lethal highlighting the importance of VEGFC in lymphatic development. LEC specification occurs as normal in these mutant mice, however they fail to form primary lymph sacs and completely lack a lymphatic vasculature as LEC do not migrate from the cardinal vein (Karkkainen et al., 2004). Blood vessels are unaffected in VEGFC knock-out mice. Post-embryonic development, VEGFC is down-regulated in the majority of tissues, but its expression remains high in LEC and lymph nodes (Lymboussaki et al., 1999). In addition to VEGFC, VEGFD also signals via VEGFR3, thereby stimulating lymphangiogenesis (Byzova et al., 2002; Rissanen et al., 2003). However, VEGFD is dispensable for lymphatic development as null mice display only mild hyperplasia of the pulmonary vasculature (Baldwin et al., 2005). Although VEGFC is the primary lymphangiogenic growth factor, exogenous VEGFD expression is capable of rescuing defective vessel sprouting in VEGFC null mice (Karkkainen et al., 2004; Baldwin et al., 2005). Both growth factors are produced as precursor proteins which are activated by proteolytic cleavage, certain processed forms can also interact with VEGFR2 (Joukov et al., 1996; Tammela et al., 2005).

1.2.3.4 Regulators of lymphatic vasculature development

Major progress has been made during the last few years to characterise the key molecular pathways governing lymphangiogenesis (Tammela and Alitalo, 2010). In addition to the proteins discussed above, Table 1.1 details proteins which play important role in lymphatic endothelial biology. Despite these recent advances, there is still a lot to be deciphered regarding lymphangiogenesis. The initiating signal that governs lymphatic endothelial cell fate choice is unknown, as is the role of circulating lymphangioblasts as a potential source of lymphatic progenitors (Oliver and Alitalo, 2005; Ny et al., 2005; Wilting et al., 2006).

Gene	Protein	Function	Expression	Reference
LYVE1	Type I integral membrane glycoprotein	Receptor for hyaluronon in LEC, mediates cell migration during embryogenesis. Specific marker of lymphatic endothelium	Mouse anterior cardinal vein at E9.5, cell surface receptor	(Knudson and Knudson, 1993; Banerji et al., 1999; Prevo et al., 2001)
PDPN	Type I integral membrane glycoprotein	Precise function unknown, may contribute to LEC adhesion and migration. Distinguishing marker of lymphatic endothelial cells	Mouse E11, expressed in budding embryonic and adult LEC	(Oliver, 2004; Breiteneder-Geleff et al., 1999)
ANGPT2	Ligand for Tie2 receptor tyrosine kinase	Required for normal LEC development and patterning. Null mice display disorganised and leaky lymphatic vasculature	Restricted to sites of vascular remodelling	(Veikkola and Alitalo, 2002; Maisonpierre et al., 1997; Gale et al., 2002)
NRP2	Non-receptor tyrosine kinase	Selective role in the development of small lymphatic vessels. Binds VEGFC	Anterior cardinal vein and budding LEC	(Yuan et al., 2002; Oliver, 2004)
FOXC2	Forkhead transcription factor	Essential for morphogenesis of lymph valves. Cooperates with VEGRF3 during lymphatic vasculature patterning	Cardinal veins, jugular lymph sacs, lymph capillaries	(Dagenais et al., 2004; Petrova et al., 2004)
EFNB2	Transmembrane ligand for Eph tyrosine kinase	Essential regulator of lymphatic development. Required for remodelling of primary lymphatic plexus	Collecting lymph vessels	(Makinen et al., 2005)
SYK/ LCP2	spleen tyrosine kinase /lymphocyte cytosolic protein 2	Both proteins mediate the separation of blood and lymphatic vasculature. Precise mechanism unknown	Circulating haematopoietic cells	(Abtahian et al., 2003)

Table 1.1 Proteins involved in lymphangiogenesis and lymphatic vasculature development. Gene name, protein function and expression during lymphatic development are shown. Information was obtained from the listed references.

1.3 MAF

1.3.1 Maf family identification and classification

In 1910 Peyton Rous first described the existence of a transmissible avian tumour virus, this discovery led to the identification and classification of transforming proteins known as oncogenes (ROUS, 1910). Since this seminal discovery, numerous cellular oncogenes have been identified, many through the prior identification of a viral homologue. One such example is vMAF (viral-Musculo-Aponeurotic-Fibrosarcoma), isolated from the oncogenic avian retrovirus AVS05, which induces musculo-aponeurotic-fibrosarcoma in chickens (Nishizawa et al., 1989; Kawai et al., 1992). Using a probe containing vMAF sequences, the cellular counterpart, MAF (v-maf musculoaponeurotic fibrosarcoma oncogene homolog (avian), also referred to as c-maf) was cloned in a number of vertebrate genomes (Nishizawa et al., 1989). MAF is the archetypal transcription factor of the Maf family, which are basic leucine zipper (bZIP) transcription factors belonging to the AP1 superfamily (Fig. 1.6). According to nomenclature, the family of proteins is referred to as Maf and in humans the individual proteins are represented by capitals e.g. MAF or MAFB (Eychene et al., 2008). This API superfamily also includes the FOS, Jun, CREB and ATP families (Fig. 1.6) (Eychene et al., 2008).

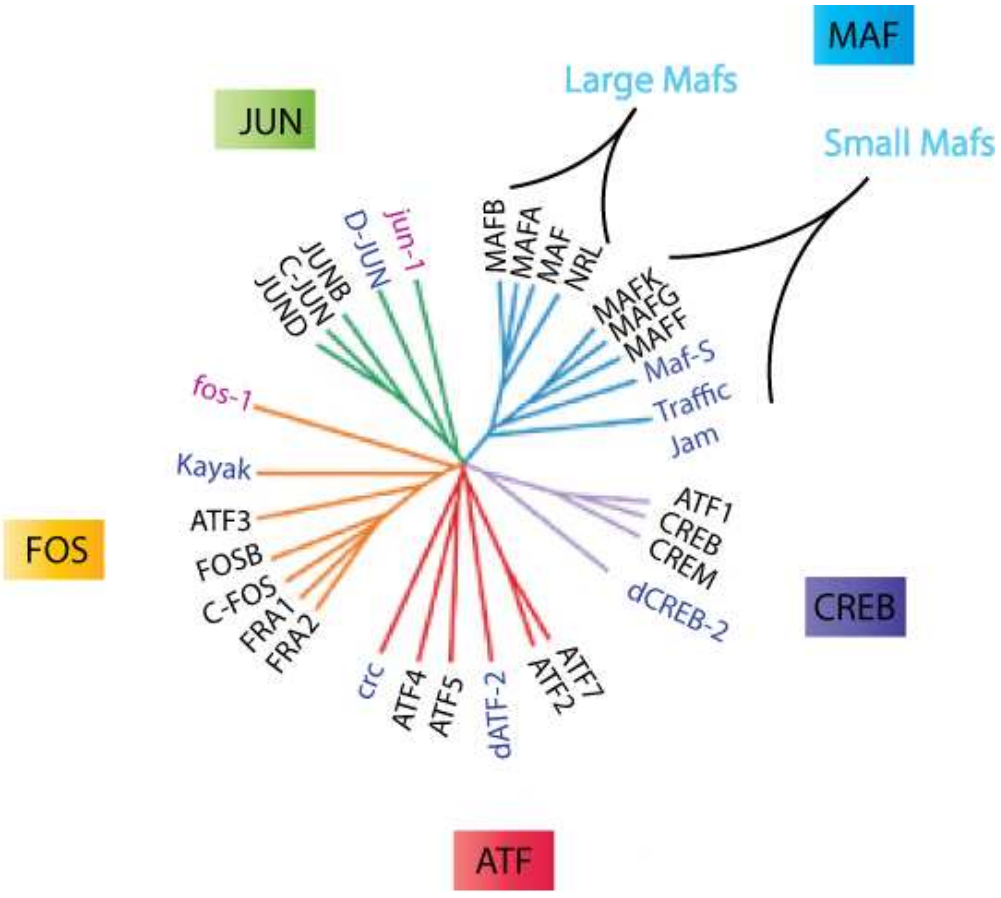

Figure 1.6 MAF classification. An unrooted phylogenic tree of the AP1 family of proteins. MAF Is a member of the API super family of bZIP transcription factors. The Maf family is sub-divided into large Mafs, of which MAF is a member, and the small Mafs. The two sub-groups are classified on the basis of structure and function. Proteins written in blue text represent Maf orthologues in D. melanogaster, those in pink correspond to C. elegans orthologues. Picture adapted from (Eychene et al., 2008).

Jun is the paradigm for transforming bZIP transcription factors and was identified in viral oncogenic form during the same period as vMAF (Maki et al., 1987). All AP1 transcription factors possess a bZIP domain: a region rich in basic residues followed by heptad repeats of hydrophobic residues forming the leucine zipper (Blank and Andrews, 1997). There are 53 genes in the human genome possessing a bZIP domain (Vinson et al., 2002). The leucine zipper domain facilitates the formation of homo or heterodimers between other bZIP possessing proteins, a feature characteristic of this class of transcription factors and a prerequisite for DNA binding (Yang and Cvekl, 2007). DNA binding is mediated directly by the adjacent basic region (Yang and Cvekl, 2007) that, as a homodimer, recognises palendromic sequences in the promoters of target genes (Eychene et al., 2008). The AP1 superfamily recognises a common DNA motif with either a TRE (TPA-responsive element) or CRE (cAMP responsive element) at its core (Shaulian and Karin, 2002; Eferl and Wagner, 2003).

There are seven Maf family members, classified by the presence of an extended homology region (EHR) (Blank and Andrews, 1997), located adjacent to the basic DNA binding region. Maf proteins are highly conserved throughout evolution with orthologues in mammals, birds, frogs and fish, as well as invertebrates including drosophila (Coolen et al., 2005). The Maf family is subdivided into four large (MAFA, MAFB, MAF and NRL) and three small Mafs (MAFF, MAFK and MAFG), classified based on structure and function (Fig. 1.6) (Blank and Andrews, 1997). Once MAF had been discovered additional family members (MAFB, MAFF, MAFK and MAFG) were identified using a MAF probe and low stringency hybridisation conditions (Fujiwara et al., 1993; Kataoka et al., 1994b; Kataoka et al., 1994a; Kataoka et al., 1995) MAFA was later discovered in quail retina (Benkhelifa et al., 1998) and chicken lens (Ogino and Yasuda, 1998) libraries. Small mafs lack a transactivation domain at their amino terminus, consequently these proteins were presumed to act as transcriptional repressors due to their inability to recruit transcriptional cooactivators (Blank and Andrews, 1997; Kusunoki et al., 2002). However, when small Mafs heterodimerise with Cap'n'coller or Bach family bZIP transcription factors they have been shown to both repress and activate

transcription (Motohashi et al., 2002). This finding highlights the importance of the dimerization partner in determining transcription factor activity. Conversely, large Mafs activate transcription via their transactivation domain by recruiting co-activators including p300, CBP (Chen et al., 2002), P/CFF (Rocques et al., 2007) and TBP (Friedman et al., 2004). Phylogenetic analysis of 38 large Maf genomic sequences revealed a single origin of a large Maf precursor which, via gene duplication gave rise to additional family members (Coolen et al., 2005).

1.3.2 MAF DNA binding and dimerization

The EHR region of Maf proteins distinguishes the family from other API members, the EHR cooperates with the adjacent basic region to mediate DNA binding (Fig. 1.5A) (Yang and Cvekl, 2007). Consequently, Maf proteins recognise longer sequences, termed Maf recognition elements (MARE), than other API transcription factors (Fig. 1.7A) (Dlakic et al., 2001; Kerppola and Curran, 1994; Kusunoki et al., 2002). At the core of a MARE is the common TRE/CRE element which is flanked by unique TGCs contacted by the EHR. While the core element is important for DNA binding it is also more degenerate, the flanking GCs however are indispensible for MAF function (Eychene et al., 2008). MAREs with TRE core are referred to as T-MAREs, where as C-MARE denotes those with a CRE core (Fig. 1.7B) (Kerppola and Curran, 1994; Kataoka et al., 1994b). In addition to these consensus sites, MAF can also bind to a 10bp antioxidant response element (ARE), which contains half a MARE site at the 5' end (Fig. 1.7B). Sequence analysis of validated MAF target genes including crystallin and rhodopsin revealed that MAF target sequences can be comprised of only half a palindromic site, referred to as a half MARE (Yoshida et al., 2005). This is suggestive of heterodimer regulation; however, MAF homodimers were also shown to regulate these sites. Furthermore, MAF binding sites lacking an internal TRE/CRE site have also been identified (Kerppola and Curran, 1994). In binding numerous different sites MAF is unique among the bZIP transcription factors, this complexity makes it difficult to predict MAF target genes. Consequently, genome-

wide identification of MAF target genes *in vivo* has thus far proved unsuccessful (Kataoka, 2007).

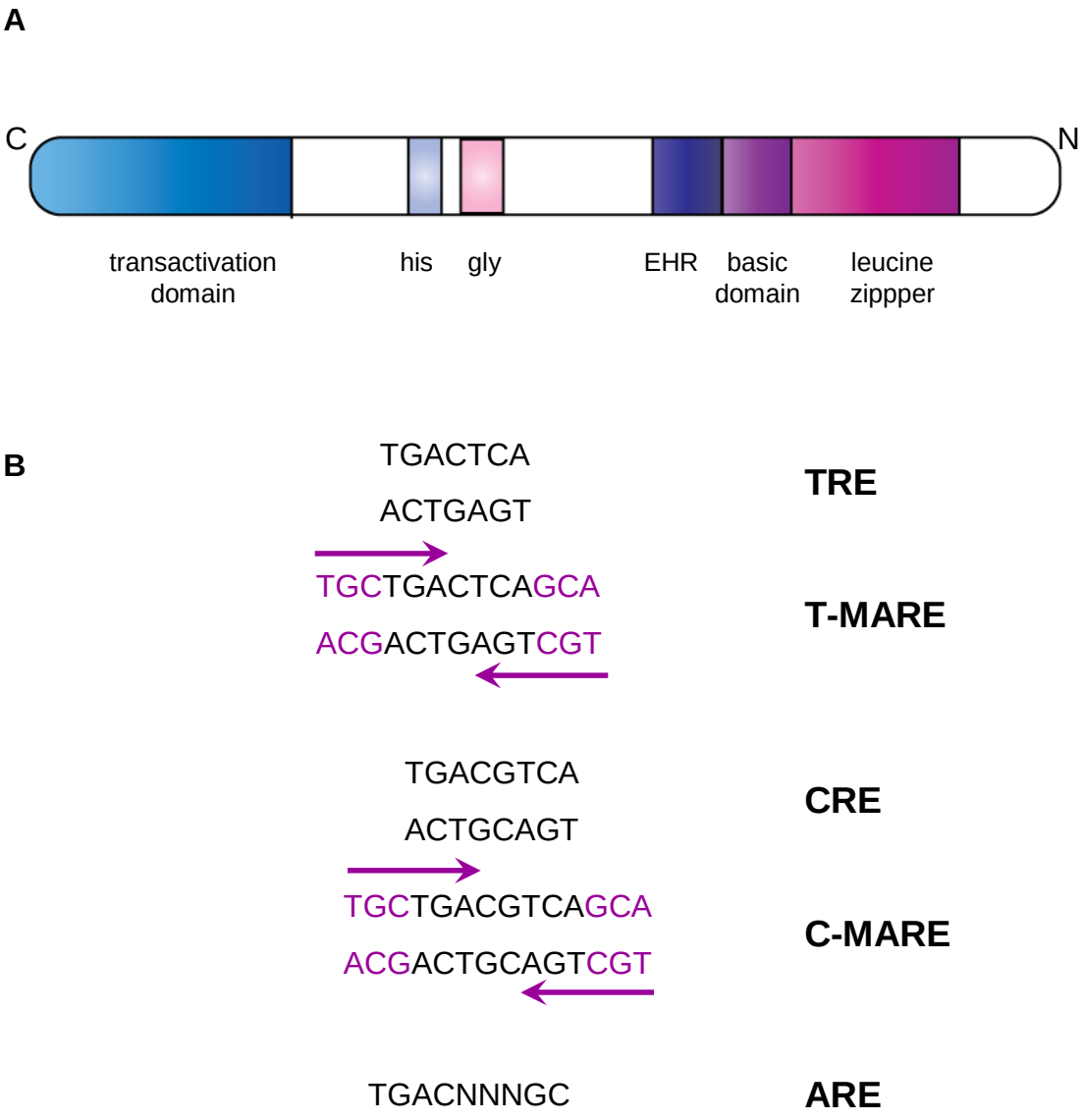

Figure 1.7 MAF structure and DNA recognition sequences. *A* Diagrammatic representation of MAF protein domains. His and gly, represent histidine and glycine rich regions, respectively. HER: extended homology region. *B* Palindromic MAF DNA recognition elements are shown. Purple residues indicate bases contacted by the extended homology region, arrows highlight sequence bound by a MAF monomer. TRE: TPA responsive element, CRE: cAMP responsive element, MARE: MAF recognition element, ARE: antioxidant response element.

Like all bZIP transcription factors MAF can from homo or heterodimers, dimerization occurs by way of the leucine coiled-coil domain (Kerppola and Curran, 1994; Motohashi et al., 2002). Large Mafs have been shown to dimerise with each other, but never to small Mafs (Yang and Cvekl, 2007). Vinson et al analysed the binding properties of all 53 human bZIP-containing proteins. Four critical amino acids were identified, the properties of the amino acids located at these key positions influenced dimer partner selectivity (Vinson et al., 2002). Analysis of MAF amino acid sequence classified MAF as a transcription factor prone to forming heterodimers (Vinson et al., 2002). Experimental analysis has confirmed these predictions, *in vitro* assays demonstrated MAF heterodimerisation with cFOS and cJUN (Kerppola and Curran, 1994). In addition, large scale analysis of 49^2 pairings of the coiled coil strands from human bZIP proteins characterised the binding partners and relative strength of bZIP heterodimer interactions (Newman and Keating, 2003). This analysis confirmed and identified novel, potential dimerization partners for MAF, including the large MAFs, MAFB and NRL; Fos transcription factors FOS, FOSB, FRA2; ATF4 and the cap'n'collar transcription factor BACH1 (Newman and Keating, 2003). However, it must be noted that *in vivo* confirmation of these interactions is still lacking.

MAF mRNA undergoes RNA processing to generate two isoforms: a long species which encodes a short single exon-encoded protein (MAF-S) or a shorter isoform which is alternatively spliced to give a longer, double-exon protein (MAF-L) (Chesi et al., 1998). MAF-S is an intronless 4.4kb long mRNA which is translated into 373 amino acids with 86% amino homology to the avian and 95% identity to the mouse MAF homologue (Chesi et al., 1998). MAF-L is identical to MAF-S from the 5'UTR to amino acid 373, where there is an alternative splice site; splicing removes a ~4kb intron which corresponds to the MAF-S '3UTR. The resulting spliced mRNA has an additional exon of 220bp, encoding 30 amino acids, generating a longer protein of 403 amino acids (Chesi et al., 1998). Both isoforms were detected via Northern blotting in a range of different tissues, although MAF-S was more abundant than MAF-L (Chesi et al., 1998). The additional amino

acids of MAF-L may affect sub-cellular localisation and Valanciute et al reported a significant increase in MAF-S, but not MAF-L, during relapse of the kidney disorder minimal change nephritic syndrome (MCNS), However, the functional difference between these two isoforms was not investigated (Valanciute et al., 2004). Sequence analysis identified no known structural motifs or functional domains in the extra exon, therefore its function remains unclear (Chesi et al., 1998).

1.3.3 MAF expression

Unlike the API transcription factors FOS and JUN, MAF transcription is not stimulated by extracellular growth signals, instead expression of the Maf family is tightly regulated in a spatio-temporal manner (Eychene et al., 2008). Expression studies in developing Xenopus tropicialis (Coolen et al., 2005) and the chick embryo (Lecoin et al., 2004) revealed distinct expression patterns at specific developmental stages for each large Maf protein. This is exemplified in the developing lens, where there is a cascade of large Maf gene expression during development (Reza and Yasuda, 2004). Here there is spatial confinement, with MAF expressed in the lens fibre and MAFB in the lens epithelia (Kawauchi et al., 1999). MAF is capable of self-regulation through the presence of a MARE in its promoter, Sakai et al reported marked activation of the rat MAF gene through this element (Sakai et al., 2001). Further to the reported auto-regulation, there may be a degree of co-operation in the regulation of gene expression by different large Maf proteins (Sakai et al., 2001). MAF is highly expressed in the developing lens, with MAF mRNA detectable at E9 in the mouse lens placode (Kawauchi et al., 1999). MAF expression is then sustained in the lens vesicle and further up-regulated in the primary lens fibre cells (Ring et al., 2000).

MAF expression has also been observed in a wide range of other tissues. Saki et al confirmed expression of rat MAF in adult muscle, spleen, lung and kidney (Sakai et al., 1997); Lecoin et al demonstrated expression in the chick embryonic neuroretina, notochord and endothelium of extra-embryonic blood vessels (Lecoin et al., 2004).

1.3.4 MAF function

1.3.4.1 MAF regulates cellular differentiation

Although initially characterised as a transforming oncogene, MAF plays a role in tissue specification and terminal differentiation. This is contrary to the function of most oncogenes which tend to mediate proliferation or apoptosis (Eychene et al., 2008). Due to the difficulty in predicting MAF binding sites, the number of validated MAF target genes is relatively few. However, experimentally defined targets from a range of cell types indicate that MAF target genes are highly cell type specific (Table 1.2).

Homozygous MAF knockout mice die shortly after birth, the major reported phenotype of these mice is inhibited lens development (Kim et al., 1999; Kawauchi et al., 1999; Ring et al., 2000). A significant lack of α, β and γ crystallins in the mutant mouse lens induces microphthalmia (Ring et al., 2000). Promoter studies have confrimed that MAF is responsible for the activation of αA, αB, αB2 and γF crystallins in the lens (Chauhan et al., 2004; Yang et al., 2004). A naturally occuring MAF point mutation in the basic domain generates mild pulverulent cataracts in humans (Jamieson et al., 2003) and mutations in the mouse MAF gene lead to the disorder opaque flecks in lens (OFL) (Lyon et al., 2003). In MAF knock-out mice, the expression of lens lineage-specifiying factors such as PAX6 and the SOX proteins was unaffected (Yang and Cvekl, 2007). Therefore, despite its pivitol role in lens development, MAF is not a master regulator of cell fate in this tissue. Outside of the lens MAF has also been shown to play a role in T helper cell differentation. MAF activates IL4 expression, thus promoting the development of the Th2 lineage (Ho et al., 1996; Ho et al., 1998). Reavaluation of

MAF homozygous knockout mice revealed endochondral bone abnormalities, identifying a role for MAF in chondrocyte differentiation (MacLean et al., 2003; Huang et al., 2002). MAF is also reported to influence myeloid differenitation (Table 1.2) (Hegde et al., 1999).

Although more commonly an activator, MAF can also function as a transcriptional repressor. Interestingly, MAF activation or repression is often mediated through cooperation with an additional transcription factor (Table 1.2) (Kataoka, 2007). This synergism is exemplified in the lens where MAF and the master regulator PAX6 cooperate to activate crystallin gene expression. Similarly, MAF and SOX9 synergise to active the COL2A1 gene during chondrocyte differentiation (MacLean et al., 2003). Binding sites of MAF and the cooperating transcription factor are often found in close proximity to each other within the enhancer region of the promoter (Kataoka, 2007). However, the exact mechanism underlying synergy has not been elucidated. A point mutation in the EHR domain which led to cataracts in mice was shown not to affect DNA binding, but instead impaired synergy between SOX and MAF, thus highlighting the importance of synergy in MAF gene regulation (Rajaram and Kerppola, 2004).

Target Gene	Cell type	Activator/ repressor	Function	Cooperating factor	Reference
PCP2	Purkinjie	activator	Unclear	NRL	(Kurschner and Morgan, 1995)
IL4	T helper 2	activator	Promotes Th2 differentiation, skewing immune response towards a Th2 pathway	NF-ATp	(Ho et al., 1996; Ho et al., 1998)
ANPEP (CD13)	HUVEC	activator	Endothelial invasion on tumour vasculature	Unknown	(Mahoney et al., 2007)
ANPEP (CD13)	Myeoblastic cells	repressor	Influence myeloid differentiation	c-MYB	(Hegde et al., 1999)
p53	NIH3T3	activator	Potentially induce p53-mediated cell death	cFOS, cJUN	(Hale et al., 2000)
Col2a1	chondrocytes	activator	Chondrocyte terminal differentiation	SOX9	(Huang et al., 2002; MacLean et al., 2003)
NADPH NQO1 GSTYa	Human Hepatoblastoma (Hep-G2)	repressor	Detoxifying enzyme expression and induction in response to anti-oxidants	Unknown	(Dhakshinamoorthy and Jaiswal, 2002)
CRYAB CRYA2 CRYA4	lens fibre	activator	Lens fibre cell differentiation	PAX6	(Kawauchi et al., 1999; Ring et al., 2000; Chauhan et al., 2004; Yang et al., 2004)
Crygf	αTN4 lens epithelial cells	activator	Lens development	Sox1-3	(Kim et al., 1999; Rajaram and Kerppola, 2004)

Table 1.2 Experimentally validated MAF target genes. Cell type, mode of regulation, function and cooperating transcription factors for MAF target genes are listed. Information was obtained from listed references.

1.3.4.2 MAF as an oncogene

Similar to vMAF which induces tumours in chickens (Nishizawa et al., 1989), MAF is implicated in the development of human tumours. MAF is over-expressed in 50% of multiple myeloma cases (Hurt et al., 2004) and 60% of angioimmunoblastic T cell lymphomas (Murakami et al., 2007; Morito et al., 2006). Likewise, over-expression of MAF in the lymphoid compartment of mice induced T cell lymphoma (Morito et al., 2006). However, MAFs transforming abilities are not universal, but depend on cell context. MAF over-expression transformed primary chicken embryo fibroblasts, but in neuroretinal cells where MAF is known to play a role in differentiation, increased MAF protein had no effect on transformation (Pouponnot et al., 2006). On the contrary, in this cell type MAF expression was anti-tumourigenic, counteracting transformation induced by the RAS/RAF/MEK/ERK pathway. These findings suggest a dual role for MAF in oncogenesis (Pouponnot et al., 2006), whereby in certain cellular contexts MAF acts as an oncogene and in others a tumour suppressor.

Interestingly, no activating mutations have been found within MAF in human cancers, instead MAF-mediated transformation appears to be dependent on its elevated expression (Eychene et al., 2008). Accordingly, only those mice with high MAF copy number develop T cell lymphoma (Morito et al., 2006). In 5% of multiple myeloma cases, MAF over-expression is induced by a chromosomal translocation that juxtaposes MAF with the IgG enhancer locus. This translocation was shown to be the oncogenic event driving multiple myeloma development (Chesi et al., 1998). Although MAF over-expression is detected in almost half of multiple myeloma cases, the exact proportion of cases where this is the causal event has yet to be experimentally determined (Eychene et al., 2008). MAFs transforming capacity is dependent on its role as a transcription factor due to increased expression of target genes as a consequence of elevated MAF protein (Zhan et al., 2006). However, transformation is not mediated through up-regulation of the target genes listed in Table 1.2 as none of these genes are de-

regulated in MAF transformed cells (Eychene et al., 2008). Instead, additional cancer-associated MAF targets including Cyclin D2, integrin β7 and ARK5 have been identified (Zhan et al., 2006; Hurt et al., 2004; Suzuki et al., 2005). Through activating Cyclin D2 MAF promoted cell cycle progression; upregulation of integrin β7 increased stromal interaction thereby enhancing adhesion and proliferation. Morito et al observed differences in MAF tumour promotion, whereby MAF activation in the thymus led to peripheral T-cell cancers, as opposed to T-cell acute lymphoblastic leukaemia which is observed after activation of most proto-oncogenes (Morito et al., 2006). The authors hypothesised that this may be due to relatively weak oncogenic activity of MAF and that over-expression may not be sufficient for transformation (Morito et al., 2006). Therefore, in addition to increased expression, MAF-mediated transformation may also be dependent on the myriad of other bZIP transcription factors and accessory transcription factors present in a particular cell type or on post-translational modifications acquired at specific times. These findings would help to explain MAFs cell context dependant behaviour during oncogenesis.

1.4 microRNAs

miRNAs are short, 21-23nt, non-coding RNA molecules which act post-transcriptionally to negatively regulate gene expression (Bartel, 2004). Ubiquitous throughout nature, miRNAs have been identified in all metazoan eukaryotes. To date over 700 human miRNAs have been identified (Griffiths-Jones et al., 2006), which are predicted to regulate up to 30% of the genome (Farh et al., 2005).

1.4.1 miRNA discovery and classification

miRNAs were first described in C. elgans by Lee and colleagues in 1993 (Lee et al., 1993). Characterisation of loss of function mutations which caused developmental timing defects, led to the identification of lin-4. The authors showed that, rather than encoding for a protein, the lin-4 gene gave rise to a 22 nucleotide RNA molecule (Lee et al., 1993). Antisense sites complimentary for lin-4 were identified in the 3'UTR of the protein coding gene lin-14 (Lee et al., 1993; Wightman et al., 1993). Wightman et al demonstrated that lin-4 acted via these sites to reduce protein output without any effect on mRNA levels (Wightman et al., 1993). Together these findings provided the first model of endogenous small RNA regulation leading to decreased protein output of the target mRNA. Consequently, lin-4 is regarded as the founding member of the class of small RNAs, known as miRNAs (Bartel, 2004). The discovery of a second miRNA, let-7, which also controlled developmental timing of C. elegans (Reinhart et al., 2000; Slack et al., 2000) and identification of homologous RNAs in drosophila and a wide range of animal species (Pasquinelli et al., 2000) indicated that miRNAs were not specific to C. elegans, but a widely distributed class of regulatory molecules. Small RNA cloning by several laboratories expanded the number of known miRNAs, identifying 60 additional C. elegans miRNAs and 20 miRNAs in drosophila, (Lee and Ambros, 2001; Lau et al., 2001), as well characterising the first human miRNAs (Lagos-Quintana et al., 2001). Since these discoveries, miRNAs have been found throughout the animal kingdom as well as in plants, green algae and viruses (Griffiths-Jones et al., 2008). The registry miRBase was established to

record all newly identified miRNAs, at its latest release there were 10883 entries (mirbase.org/) (Griffiths-Jones, 2004).

miRNAs have been implicated in regulation of almost every cellular process investigated so far, including differentiation, immunity, and metabolism, as well as pathological conditions such as cancer (Chen et al., 2004; Lu et al., 2005; Croce, 2009). Large-scale investigations into the effects of miRNAs on their target proteins show they act as rheostats rather than an on-off switch (Baek et al., 2008; Selbach et al., 2008) miRNA expression serves to fine-tune protein output, maintaining a delicate balance of target proteins. Despite their modest effects on protein output, miRNAs can be indispensible for cellular functions, especially in lineage specification (Xiao et al., 2007; Thum et al., 2007).

1.4.2 miRNA biogenesis

miRNAs are located within the introns of protein coding genes or at sites distant from annotated genes; the majority are solitary and expressed under the control of their own promoter (Ambros, 2004). However, miRNA coding regions can also be arranged in clusters, the individual miRNAs of which are transcriptionally co-regulated (Lagos-Quintana et al., 2001; Ambros, 2004). Those miRNAs located in protein coding introns in the same orientation as the mRNA, are processed from the intron rather than transcribed from their own promoters (Bartel, 2004).

miRNA biogenesis begins with RNA polymerase II-mediated transcription of a primary transcript ranging from hundreds to thousands of nucleotides in length (Fig. 1.8) (Lee et al., 2004). This transcript, termed the primary miRNA (pri-miRNA), is capped at the 5’ end and polyadenylated at the 3’ end. Pri-miRNAs contain an imperfect ~60nt hairpin structure which is excised in the nucleus by Drosha, a nuclease RNase III enzyme (Lee et al., 2003). Drosha mediates cleavage with the aid of DGCR8, together these proteins form the essential components of the microprocessor complex. DGCR8 acts as a molecular anchor facilitating microprocessor recognition of the pri-miRNA (Du and Zamore, 2005).

After Drocha cleavage the resulting hairpin structure, known as the precursor-miRNA (pre-miRNA), is exported to the cytoplasm by Exportin-5 for further processing (Lund et al., 2004; Yi et al., 2003). Once in the cytoplasm Dicer, another RNase III enzyme, cleaves the hairpin releasing a 22nt long, double stranded molecule known as the mature miRNA (Bernstein et al., 2001). One strand of this imperfectly paired duplex, referred to as the guide strand, is incorporated into a large ribonucleoprotein complex, known as the RNA induced silencing complex (RISC) (Fig. 1.8). The other passenger strand of the mature miRNA is not involved in silencing and therefore gets degraded. The decision between which strand is the guide and which the passenger, is governed by 5' end stability. The strand with the lowest base-paring stability is preferentially selected for RISC incorporation (Schwarz et al., 2003). At the core of the RISC, are the highly conserved Argonaute proteins (Hammond et al., 2000; Elbashir et al., 2001; Martinez et al., 2002). Argonaute binds to the guide strand which directs the RISC complex to homologous sequences located in the 3'UTR. In addition to the Argonaute proteins, the RISC complex includes proteins which function as assembly and regulatory factors, as well as those which mediate silencing (Filipowicz et al., 2008).

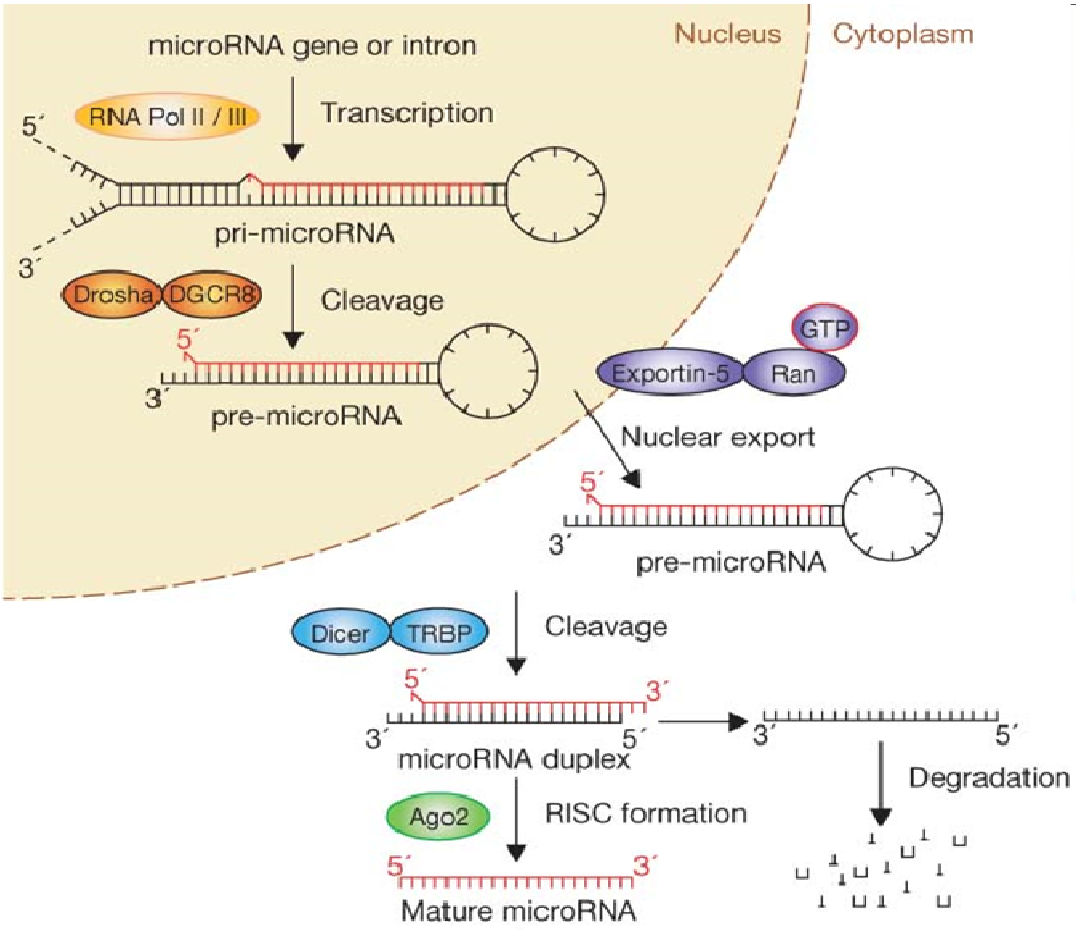

Figure 1.8 miRNA biogenesis. Schematic representation of the canonical miRNA biogenesis pathway. The first step is RNA POL II mediated transcription of the primary miRNA transcript (pri-miRNA), the hairpin containing precursor miRNA (pre-miRNA) is then excised by the microprocessor complex Drosha–DGCR8. The pre-miRNA is then exported to the cytoplasm by Exportin5. In the cytoplasm, Dicer in complex with the double stranded RNA-binding protein TRBP, excises the double stranded mature miRNA duplex. The guide strand (red) is then loaded into the RNA induced silencing complex (RISC) which contains the central component Argonaute (Ago2). The passenger strand (black) of the mature miRNA is degraded. The guide strand then directs the RISC complex to target sites located in 3'UTR. Picture from (Winter et al., 2009).

1.4.3 miRNA target recognition

In plants, miRNAs bind to their targets with near perfect sequence complementation, this triggers mRNA degradation through endonucleolytic cleavage initiated at the centre of the miRNA-mRNA duplex (Filipowicz et al., 2008). This method of silencing can also occur in vertebrates and from viral encoded miRNAs, however it is relatively rare (Bartel, 2009). Instead, the major mechanism of silencing in vertebrates is via translation inhibition with minimal effect on mRNA levels. At least 1000 miRNAs are predicted in humans, and identifying the target genes of these regulatory RNAs has been facilitated by a set of experimentally and bioinformatically defined rules (Doench and Sharp, 2004; Brennecke et al., 2005; Lewis et al., 2005; Grimson et al., 2007; Nilsen, 2007). Various combinations of these rules have been incorporated into a number of miRNA target prediction algorithms, which are reviewed along with a detailed analysis of miRNA-target recognition by Bartel (Bartel, 2009).

Instrumental to miRNA target recognition is conserved Watson and Crick base pairing across nucleotides 2-7 of the miRNA, which is referred to as the seed region (Krek et al., 2005; Brennecke et al., 2005; Lewis et al., 2005). Base pairing across this region greatly increases prediction reliability; accordingly it is this 5' region of the miRNA which is most conserved across metazoan miRNAs (Lewis et al., 2005; Lim et al., 2005). G:U base pairings or mismatches across the seed region can significantly impair target repression (Filipowicz et al., 2008). In addition, an adenosine residue at position one and an adenosine or uracil at position nine have been shown to improve site efficiency, but do not necessarily have to be paired with the miRNA. Complementarity outside the seed region is not essential for target recognition, as a result mismatches and bulges are common. However, base pairing especially at nucleotides 13-16 can improve miRNA recognition, particularly if complementation is sub-optimal across the seed (Brennecke et al., 2005). Other factors known to improve site efficacy are high A/U density surrounding the target site and location of site within the UTR, with the extremes being favoured over the middle region (Grimson et al., 2007; Nilsen, 2007). In addition, accessibility of the RISC complex to the target site has been

shown to influence silencing (Kertesz et al., 2007). Whereby target sites embedded in secondary RNA structures are less favoured over those in relative accessible regions of the UTR (Kertesz et al., 2007). Since many miRNAs are conserved throughout evolution, identifying a potential miRNA target site in multiple genomes of different species through alignment of orthologous 3'UTRs, greatly improves predictability (Karolchik et al., 2008). The number of false positives in prediction analysis can be reduced by stipulating a perfect 8bp seed match as well as multiple miRNA binding sites within a single target. However, experimentally validated targets often only possess one 7nt binding site. Although useful there are many deviations to the aforementioned target prediction rules found in bone fide miRNA targets (Bartel, 2009).

1.4.4 Mechanism of miRNA silencing

The mature miRNA sequence directs RISC to homologous sequences primarily located within the 3'UTR of the mRNA to be silenced (Schwarz et al., 2003). The ensuing method of protein inhibition is governed by the degree of sequence complementation between the miRNA seed and target site. Perfect complementation promotes mRNA degradation, most likely by Argonaute RNase-H induced cleavage (Yekta et al., 2004; Davis et al., 2005) this method of silencing is termed slicing. Argonaute 2 is the only human Argonaute to possess nuclease activity. Central mismatches in the seed region lead to bulges in the RNA duplex which can hinder Argonaute accessibility, thereby preventing nuclease activity. In the case of poorly matched targets, silencing is instead mediated via translation inhibition with no effect on mRNA abundance (Fig. 1.9) (Wu and Belasco, 2008). However, there are exceptions to the above rules whereby targets with perfect complementation are inhibited at the translational level (Umbach et al., 2008). Therefore, it is incorrect to assume mRNA degradation will always ensue upon perfect sequence complementation (Filipowicz et al., 2008). Likewise, mRNA degradation has also been observed in targets which have imperfect base pairing (Eulalio et al., 2008). miRNA binding sites found in close proximity (less than 40bp apart) to one another have been shown to cooperatively silence their targets (Doench and Sharp, 2004; Grimson et al., 2007). Similarly silencing complexes have been shown to function cooperatively, whereby increased number of RISC complexes per transcript correlates with increased repression (Doench et al., 2003; Doench and Sharp, 2004).

miRNAs have been shown to repress protein synthesis in four main ways (Fig. 1.9) (Eulalio et al., 2008; Filipowicz et al., 2008). Firstly, miRNAs can block translation initiation, here silencing occurs at the early stages of translation prior to elongation of the polypeptide (Pillai et al., 2005; Humphreys et al., 2005). Translation initiation can be blocked by Argonaute proteins competing directly with the translation initiation factor eIF4E for cap binding (Kiriakidou et al., 2007) or by interacting with eIF6, thereby preventing the association of the large and small ribosomal subunits (Chendrimada et al., 2007). Alternatively, miRNAs can interfere after initiation, during the peptide elongation phase; this is mediated either by premature ribosome drop off or slowed elongation (Maroney et al., 2006; Petersen et al., 2006; Nottrott et al., 2006). Evidence showing repressed mRNAs associated with actively translating polyribosomes supports the model whereby miRNAs act post translation initiation (Maroney et al., 2006; Petersen et al., 2006; Nottrott et al., 2006); equally there is a lot of evidence of inhibition of translation initiation. This is a highly controversial field with many questions still to be answered. Another cotranslational method of miRNA inhibition is continual degradation of the nascent polypeptide as it is being synthesised (Nottrott et al., 2006). The final mechanism is miRNA-mediated mRNA decay which is initiated by deadenylation and decapping, followed by mRNA degradation (Wu et al., 2006; Behm-Ansmant et al., 2006; Giraldez et al., 2006). The latter can be an independent mechanism of silencing or as a consequence of translational inhibition (Eulalio et al., 2008). It is still not known whether there is a predominant mechanism of translation inhibition or whether multiple models operate in succession at various stages during translation (Filipowicz et al., 2008). Overall it seems that the main mechanism involves mRNA destabilisation in some form, such as deadenylation, rather than a form of pure translational repression such as ribosome drop-off.

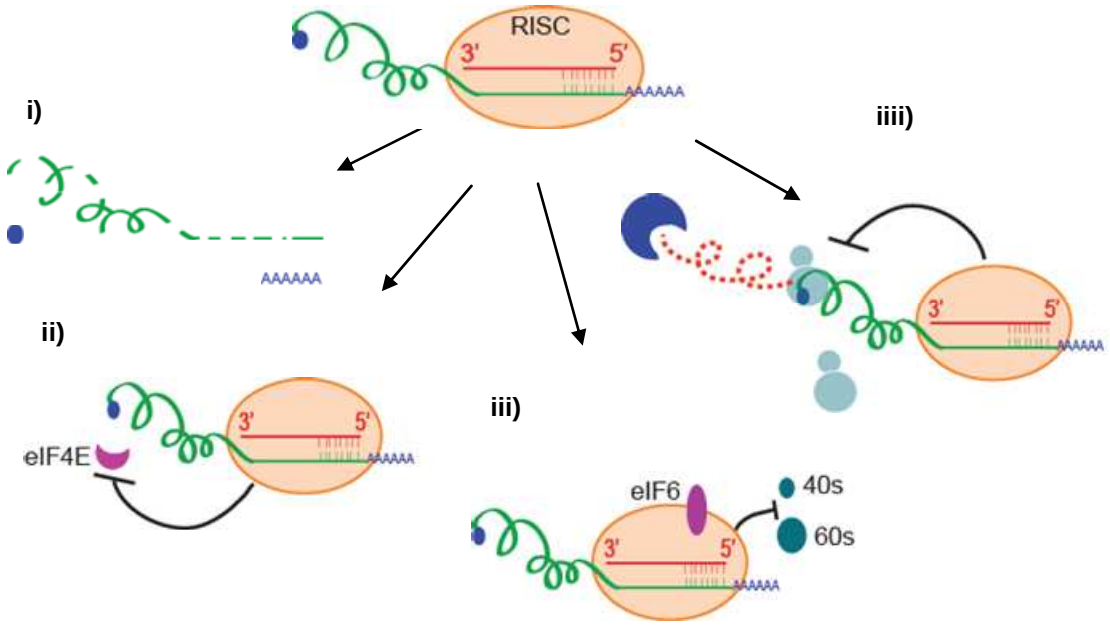

Figure 1.9 Mechanisms of miRNA-mediated silencing. miRNA bound RISC is represented by the beige circle and red line corresponds to the mature miRNA. The mRNA target is depicted in green, with the 5' cap as a blue circle and the polyA tail as a sequence of blue As. Silencing is mediated by one of a number of mechanisms, i) mRNA decay which is initiated by deadenylation and decapping. Inhibiting translation initiation by ii) Argonaute competing with eiF4E (purple semi-circle) for cap binding or iii) Argonaute binding eIF6 (purple ellipse) thereby preventing association of the small and large ribsomal subunits (teal circles). iiii) Cotranslational inhibition by either premature ribosome (light blue circles) drop of, slowed elongation or continual digestion of the nascent polypeptide (red dots).

1.4.5 Different classes of small RNA molecules

Small RNA silencing pathways, with the exception of budding yeast, are conserved throughout eukaryotes, indicating an ancient evolutionary origin (Moazed, 2009). In addition to miRNAs, there are other abundant small regulatory RNA molecules, including short interfering RNAs (siRNAs) and piwi interacting RNAs (piRNAs) (Moazed, 2009). The Argonaute family of proteins is key to all known RNA silencing pathways. There are two main phylogenetic branches of Argonaute proteins, the AGO and PIWI clades which associate with miRNA and siRNA or piRNA, respectively (Carmell et al., 2002). siRNAs are the most widely conserved small RNA family, in addition to animals they are also found in plants, fungi and ciliates. piRNAs are restricted to animals, whereas miRNAs are found in both animals and plants (Moazed, 2009).

In 1998 RNAi was first described in C. elegans by Fire et al as the silencing of homologous sequences by exogenously induced dsRNA molecules (Fire et al., 1998). It is now known that miRNAs and siRNA are generated by core biogenesis machinery and are identical both in chemical composition and in mechanism of action (Ambros et al., 2003). Both duplexes are generated by Drosha cleavage of long precursor molecules and processed by Dicer before being loaded onto RISC complexes to silence homologous sequences in the genome (Bartel, 2004). However, differences in the origin, evolutionary conservation, and types of genes regulated permit distinction and classification of siRNA and miRNA. These distinguishing features are detailed in Table 1.3 (Bartel and Bartel, 2003; Bartel, 2004).

	siRNA	miRNA
Source	mRNA, transposons, heterchromatin, viruses	Intergenic regions, introns, viruses
Evolutionary conservation	Endogenous siRNAs are rarely conserved	High degree of sequence conservation between distantly related organisms
Precursor	Long dsRNA with near perfect complementarity	Imperfectly paired dsRNA containing a hairpin
No. of effectors from a single precursor	Multiple siRNA duplexes synthesised continually from a single precursor	One miRNA duplex per pre-miRNA
Effector strand selection	Both strands of siRNA duplex utilised	Typically one strand favoured as the guide strand
Target gene	Same loci, auto-silencing	Distinct loci, hetero-silencing
Mechanism	mRNA degradation	Primarily translation inhibition, to a lesser extent mRNA degradation

Table 1.3 Differences between siRNA and miRNA. Information taken from (Bartel and Bartel, 2003; Bartel, 2004).

piRNAs are the most recently discovered class of regulatory RNA molecules (Lau et al., 2006). They are generated from a diversity of sequences, in particular repetitive elements and transposons. The mechanisms of piRNA biogenesis are not yet fully understood, but it is thought to be distinct from the miRNA/siRNA pathway. piRNA-mediated silencing utilises the nuclease activity of the PIWI proteins, in a similar fashion to the RNase-H like piwi domain of Argonaute-2 (Choudhuri, 2009). piRNAs have been classed as the ‘guardian of the germline genome’ due to their silencing of endogenous genetic elements such as retrotransposons and repetitive sequences in germline cells particularly those of the testes. Consequently, they are most abundant in germline cells with piwi mutant animals displaying defects in germ cell development (Aravin et al., 2007). For an extensive review of recent data on piRNAs see Thomson and Lin (Thomson and Lin, 2009).

1.4.6 miRNAs in cancer

miRNAs regulate a diverse range of cellular processes including cell cycle progression and apoptosis, and are predicted to target ~30% of human genes (Bartel, 2004). Unsurprisingly then, miRNAs are strongly implicated in oncogenesis both as promoting and inhibitory agents (Garzon et al., 2009). Accordingly, miRNA-encoding regions of the genome are both amplified and deleted in multiple different human tumours, depending on whether the miRNA functions as an oncogene or a tumour suppressor (Calin et al., 2002).

1.4.6.1 miRNAs as tumour suppressors

miRNAs acting as tumour suppressors are lost during tumourogenesis by deletions, mutations, epigenetic silencing or processing mutations (Calin et al., 2002). Calin et al cloned two miRNAs miR-15a and miR-16-1 to a region on chromosome 13 which was deleted in 50% of cases of chronic lymphocytic leukaemia, previously attempts to identify protein coding tumour suppressor genes in this region had failed (Calin et al., 2002). These miRNAs target Bcl-2 and wt-1 to promote apoptosis, consequently reduced expression of these miRNAs was shown to increase tumourogenicity (Cimmino et al., 2005; Linsley et al., 2007). Calin et al extended their study on chromosome 13 and found a common pattern whereby miRNA genes are frequently located at fragile sites as well as sites of minimal amplification (Calin et al., 2004), these data are supportive of a tumour suppressor function for miRNAs. Another set of miRNAs commonly down regulated in human tumours and located at fragile genomic locations is the let-7 family (Yanaihara et al., 2006; Iorio et al., 2005). These miRNAs function as tumour suppressors by silencing multiple oncogenes including RAS, HMGA2 and c-MYC (Johnson et al., 2005; Lee and Dutta, 2007; Sampson et al., 2007). Recently, p53 was shown to mediate some of its antiapoptotic tumour suppressor functions through the miRNA family miR-34 (Raver-Shapira et al., 2007; Chang et al., 2007). p53 expression correlated with that of the miRNAs and chromatin immunoprecipitation assays confirmed p53 presence on the miR-34 promoter.

There is correlative evidence that many other miRNAs can function as tumour suppressors, however this needs further experimental validation (Garzon et al., 2009).

1.4.6.2 miRNAs as oncogenes

miR-155 was one of the first miRNAs to be describe as an oncogene (Metzler et al., 2004; Kluiver et al., 2005). miR-155 is essential for normal B cell development and differentiation. miR-155 is up-regulated in many lymphomas including Burkitt's lymphoma, Hodgkin's disease as well as in acute myeloid leukaemia where it has been shown to play a role in early leukaemogenesis (Metzler et al., 2004; Garzon et al., 2008). Transgenic mice with targeted B cell miR-155 over-expression developed aggressive B cell malignancies, confirming a causal role for this miRNA in oncogenesis (Costinean et al., 2006). However, the mechanism of miR-155 regulation and over-expression is human cancer is still poorly understood (Garzon et al., 2009). miR-155 mediates some of its oncogenic effects through cooperation with c-Myc; a screen for additional miRNAs which synergise with onocogenes during transformation identified miR-372 and miR-373 as potential oncomirs (Voorhoeve et al., 2006). miR-372 and miR-373 cooperated with RAS to neutralise p53, thereby increasing proliferation and tumourogenesis (Voorhoeve et al., 2006). The miR-17-92 cluster encodes 6 miRNAs and is located at 13q31.3, a chromosomal region frequently amplified in follicular lymphoma and diffuse large B cell lymphoma. The cluster is essential for B cell proliferation; over expression of these miRNAs in mouse B cells is sufficient to induce lymphoproliferative disorders (Ventura et al., 2008; Xiao et al., 2008). Increased expression of miR-17-92 is observed in a range of solid tumours as well as haematological malignancies (Mendell, 2008). These miRNAs drive tumourogenesis by promoting proliferation through regulation of E2F (O'Donnell et al., 2005), inhibiting apoptosis via silencing pro-apoptotic proteins BIM, PTEN and p21 (Ventura et al., 2008; Xiao et al., 2008), as well as inducing tumour angiogenesis (Mendell, 2008).

1.4.6.3 miRNAs as therapeutic targets

In conjunction with their role as both tumour suppressors and oncogenes, miRNA expression profiling has been used to predict patient survival and miRNAs are currently being investigated as potential anticancer therapeutic targets (Garzon et al., 2009). Expression of a sub-group of six miRNAs was used to distinguish long-term survivors of pancreatic cancer from those who died within 24 months (Bloomston et al., 2007). Increased miR-21 expression correlated with short overall survival of colon cancer patients (Schetter et al., 2008). Further studies will determine whether miRNAs could be employed to stratify patients for cancer treatment (Garzon et al., 2009). miRNAs represent attractive therapeutic targets for several reasons. A single miRNA regulates multiple targets many of which could be involved in different oncogenic pathways, therefore targeting one miRNA may have multiple anticancer effects (Croce, 2009). A small group of miRNAs are consistently de-regulated in a large number of diverse malignancies. Therefore, silencing of oncomirs or re-introducing tumour suppressor miRNAs could affect multiple different groups of cancer patients. Re-introduction of tumour suppressor miRNAs miR-221 and miR-222 suppressed growth of erythroleukemic cells in which these miRNAs had been down-regulated (Felli et al., 2005). Furthermore, exogenous expression of miR-29 suppressed the tumourogenicity of lung cancer cells (Fabbri et al., 2007). miRNAs which act as oncogenes are silenced using complimentary RNA molecules known as antagomirs (Krutzfeldt et al., 2005). In a proof of principle experiment, Elmen et al delivered locked nucleic acid (LNA) modified antagomirs against miR-122, a liver specific miRNA, to primates. This led to effective miRNA depletion without any evidence of toxicity (Elmen et al., 2008).

1.4.7 Viral miRNAs

Viral miRNAs were first reported in EBV in 2004 after small RNA profiling of infected cells (Pfeffer et al., 2004). Since this discovery miRNAs have been identified in all herpesviruses examined to date (Cullen, 2009). Including herpesviruses which infect species other than humans such as mouse, chicken and monkey (Cullen, 2009). Viral miRNAs are largely confined, although not exclusive to herpesviruses. In addition to herpesviruses, miRNAs have been identified in human adenovirus and several members of the polyomavirus family, including SV40 (Sullivan et al., 2005; Xu et al., 2007). miRNAs provide an excellent means of regulating both host and viral gene expression thereby creating a permissive cellular environment in which to establish infection. Viral miRNAs are transcribed and processed using the cellular miRNA machinery (Cullen, 2009). Notably miRNAs are only found in nuclear DNA viruses which favour long term, persistent infection. Viruses which replicate exclusively in the cytoplasm, including RNA viruses, will not have access to core miRNA biogenesis machinery which is localised to the nucleus. Furthermore, miRNA regulation is not an instantaneous process; the existing pool of proteins must decay before a miRNA induced phenotype is observed. Therefore, for viruses with short lifecycles requiring quick entry and exit from the cell, miRNAs do not present a useful means of regulation. These factors explain why miRNAs are consistently found in herpesviruses, which establish persistent latent infection, but in only a few other virus families. miRNAs are an attractive means of gene regulation for several reasons. They are encoded by a relatively small amount of DNA (<200bp) which is advantageous due to the tight space constraints of viral genomes. miRNAs are non-immunogenic and therefore go undetected by immune surveillance (Pfeffer et al., 2004). Finally, one miRNA can regulate multiple target genes; in this manner a single molecule has the power to modulate many distinct cellular pathways which may affect the outcome of infection (Umbach and Cullen, 2009). Deep sequencing of KSHV infected PEL cell lines showed that viral miRNAs constituted 92% of the total miRNA content (Umbach and Cullen, 2010). These data suggest

that viral miRNAs dominate cellular miRNAs and in some way are preferentially processed by the miRNA biogenesis machinery (Umbach and Cullen, 2010).

Despite being identified six years ago the function of viral miRNAs is largely unknown and only a small number of targets have been identified. Experimentally validated targets are detailed in Table 1.4. The array of validated targets shows that viral miRNAs can perform autoregulation, whereby they silence expression of viral-encoded proteins. In this manner viral miRNAs have been shown to down-regulate immediate early proteins thus helping to ensure the correct temporal mode of gene expression. Targeting immediate early genes causes a reduction in viral immunogenic proteins and can facilitate the transition between lytic and latent infection (Umbach et al., 2008; Murphy et al., 2008; Grey et al., 2007; Bellare and Ganem, 2009). Autoregulating miRNAs can be transcribed antisense to their target mRNA as is the case with SV40 miR-S1 and EBV miR-BART2 (Sullivan et al., 2005) or they can target miRNAs at a distinct locus (Samols et al., 2007). Viral miRNA targets are in theory easier to identity than their cellular counterparts, due to the perfect sequence complementation of autoregulating targets and the small size of the viral genome in which to search for targets.

There are a number of validated cellular viral miRNA targets (Table 1.4), these tend to fall into three categories: apoptosis regulators, immunomodulators and latency regulation (Umbach and Cullen, 2009). In this manner viral miRNA regulation prolongs survival of the infected cell, maximising replication potential and sustaining infection. Two examples of apoptosis regulators include the EBV encoded miRNA BART5 which down-regulates the proapoptotic protein PUMA (Choy et al., 2008) and a subset of KSHV miRNAs which silence BCLAF1 (Ziegelbauer et al., 2009). miRNA silencing of cellular antiviral targets represents a novel mechanism of immune evasion. This is highlighted in HCMV, where miR-UL112-1 was shown to silence the natural killer cell ligand MICB (Stern-Ginossar et al., 2007). Down-regulation of MICB may protect infected cells from natural killer cells, which is one of the first lines of antiviral immune defence. In addition to regulating MICB, miR-UL112-1 performs autoregulation (Stern-Ginossar et al.,

2007). This is the first example of a viral miRNA targeting both viral and host transcripts. EBV encoded miRNAs have also been shown to modulate the host immune response, whereby BHRF1 down-regulates the potent T cell chemoattractant CXCL11 (Xia et al., 2008). Recently a number of studies have shown that in addition to targeting lytic proteins, viral miRNAs also control the lytic-latency balance through silencing cellular proteins (Lei et al., 2010; Lu et al., 2010). Deletion of the KSHV miRNA Cluster from the viral genome led to increased lytic gene expression and viral replication (Lei et al., 2010; Lu et al., 2010). Through silencing the NFκB inhibitor, IκBα, miR-K12-1 expression activated the NFκB pathway thereby inhibiting viral replication and favouring latent infection (Lei et al., 2010). Lu et al reported marked loss of both viral and cellular DNA methylation, due to miR-K12-4-5p induced silencing of the DNA methylatransferase inhibitor RBL2; it was proposed that his global epigenetic reprogramming helped to maintain the latent state of the KSHV genome (Lu et al., 2010).

Virus	miRNA	Target	Protein	Outcome of miRNA Regulation	Reference
SV40	miR-S1	Viral	T antigen	Reduce detection of immediate early gene, SV40 antigen by cytotoxic T cells	(Sullivan et al., 2005)
KSHV	miR9*		RTA	Prevent inappropriate entry to lytic cycle through fine-tuning expression of lytic reactivator	(Bellare and Ganem, 2009)
EBV	miR-BART2		BALF5	Down-regulation of DNA polymerase is proposed to inhibit the transition from latent to lytic replication	(Barth et al., 2008)
	miR-BART1-5p; BART16; BART17-5p		LMP-1	Modulating expression levels of oncogenic signalling molecule to balance the contradictory growth promoting and inhibitory functions of LMP1	(Lo et al., 2007)
HCMV	miR-UL112-1		IE1	Removal of immediate early transcription factor at later stages of viral life cycle.	(Murphy et al., 2008; Grey et al., 2007)
HSV-1	miR-H2-3p		ICP0	Silencing immediate early protein facilitates the establishment and maintenance of latency	(Umbach et al., 2008)
	miR-H6		IC4		
HSV-2	miR-H3 miR-H4		ICP34.5	Reducing levels of this pathogenicity factor may protect neurons from neurovirulent effects during virus reactivation	(Tang et al., 2008; Tang et al., 2009)
HvAV	miR-1		ORF1	Silencing DNA polymerase may inhibit lytic replication and promote latency	(Xu et al., 2007)
EBV	miR-BART5	Cellular	PUMA	Protect infected cells from apoptosis by down-regulating pro-apoptotic factor	(Choy et al., 2008)
	miR-BHRF1-3		CXCL11	Down-regulating of T cell chemoattractant may protect infected cells from immune detection	(Xia et al., 2008)
HCMV	miR-UL112-1		MICB	Silencing may offer protection from NK immune surveillance	(Stern-Ginossar et al., 2007)
KSHV	miR-K12-1; K12-3; K12-6-3p; K12-11		THBSD1	Silencing may promote survival, angiogenesis and inhibit detection by immune surveillance	(Samols et al., 2007)
	miR-K12-11		BACH1	Silencing the transcriptional repressor BACH1 up-regulates xCT on macrophages and endothelial cells. This increases permissiveness to KSHV infection and protects against oxidative stress	(Skalsky et al., 2007; Gottwein et al., 2007; Qin et al., 2010)
	miR-K12-5; K12-9; K12-10		BCLAF1	Reduction of BCLAF1 may stabilise latency through an as yet unknown mechanism	(Ziegelbauer et al., 2009)
	miR-K12-4-5p		RBL2	Silencing of RBL2, a repressor of DNA methylation, reduces viral and cellular DNA mutilation levels helping to maintain latency	(Lu et al., 2010)
	miR-K12-1		IκBα	Viral replication is inhibited, favouring latency, through silencing the NFκB inhibitor and activating the NFκB pathway	(Lei et al., 2010)

Table 1.4 Experimentally validated viral miRNA targets. Both viral and cellular miRNA targets are shown. miRNA, target and consequence of silencing is shown, information was obtained from listed references.

1.6 Thesis Aims

The aim of this thesis was to investigate the role of the KSHV-encoded miRNAs in infected lymphatic endothelial cells. Specifically, the KSHV miRNA Cluster was expressed in isolation in lymphatic endothelial cells to identify cellular targets de-regulated at the mRNA level. Regulation by the KSHV miRNAs of the transcription factor MAF was studied along with an investigation into the biological significance of MAF silencing during KSHV infection of LEC.

Chapter 2. Materials and Methods

2.1 Cell culture

All cells were cultured at 37^{o}C, 5% CO_2 in a humid environment.

2.1.1 Lymphatic endothelial cells

Lymphatic endothelial cells (LEC) were purchased from TCS Cellworks (Buckingham, U.K). The LEC identity of these cells was confirmed by qRT-PCR analysis and staining for lymphatic-specific markers including PDPN, LYVE1 and PROX1. Prior to culturing flasks or wells were coated with 1-5 µg/cm^2 of fibronectin diluted in phosphate buffered saline (PBS) for 30 min at 37^{o}C, after which fibronectin was removed and the plasticware rinsed with PBS. LEC were cultured in endothelial-cell growth medium MV (PromoCell) supplemented with 10 ng/mL VEGF-C (R&D Systems), media was changed every 24-48 hrs. LEC were purchased at passage 0, expanded and used for experiments at passage 2-8.

Sub-confluent LEC (70-80%) were split 1:3. Cells were washed with PBS and then incubated for 5 min at 37^{o}C with trypsin-EDTA (Invitrogen) diluted 1:5 in PBS. After the majority of cells had detached the trypsin-EDTA was quenched with an equal volume of LEC media, cells were collected and pelleted by spinning for 5 min at 1200rpm. LEC were re-suspended in LEC media, cells were then seeded at a density of ~5x10^5 per T75 flask.

2.1.2 Blood vessel endothelial cells

Microvascular myometrium endothelial cells were isolated by Dr. L. Nikitenko (CR-UK Viral Oncology group, UCL) as previously described (Nikitenko et al., 2006). The blood vessel endothelial (BEC) identity of these cells was confirmed by qRT-PCR analysis and staining for blood vessel specific markers including EDGN, CD34 and VEGRF1. Prior to seeding flasks were coated for 30 min at room temperature with attachment factor (TCS Cellworks). Cells were seeded at a density of 5×10^5 cells/cm^2. BEC were cultured in endothelial-cell growth medium MV2 (PromoCell), media was changed every 24-48hrs. Cells were passaged at 1:3 when 80% confluent. Media was removed and BEC were washed with PBS, cells were then incubated for 5 min at 37^{o}C in trypsin for endothelial cell cultures (Sigma). After the majority of cells had detached, cells were collected and pelleted by spinning for 5 min at 1200rpm.

2.1.3 Transformed cell lines

293T and HeLa cells were cultured in Dulbecco modified Eagle medium (DMEM) (Gibco, Invitrogen), supplemented with 10% FCS (Sigma) and 10% 100units/ml penicillin G and 100µg/ml streptomycin (Gibco, Invitrogen). 293 cell lines stably transfected with the KSHV miRNA Cluster or empty pcDNA vector (Samols et al., 2007) were cultured as above but with 100µg/ml Geneticin (Gibco, Invitrogen) selection. Cells were split 1:10 every 3 days at a density of ~$1x10^6$ per T75 flask.

BCLB-1 cells latently infected with recombinant GFP-KSHV (Vieira et al., 2001) were grown in suspension in RPMI 1640 (Invitrogen) supplemented with 10% FCS and 400ng/ml Geneticin (Invitrogen). Cells were grown at a density of ~4-$6x10^5$ cells/ml. Cells were split 1:10 every 3 days by transferring 10% of the culture to a new flask of media.

2.1.4 Thawing cells

Frozen cells were stored in 1:10 DMSO-FBS in cryovials in liquid nitrogen tanks. Cells were thawed by heating in 37^{o}C water bath. The thawed suspension was added to 3mls of the appropriate media and spun at 1200rpm for 5 min to pellet the cells and remove DMSO. The cell pellet was resuspended in 1ml of media and added to a flask or dish containing 9mls of pre-heated media.

2.2 Transfection, virus production and infection

2.2.1 DNA transfections of 293T and HeLa cells

Cells were seeded the day before, density of seeding varied according to the experiment, as specificed in text. Transfection of 293T and HeLa cells was performed using FuGENE (Roche) according to manufacturer's instructions. FuGENE is a non-liposomal, lipid-based transfection reagent, which facilitates DNA uptake by eukaryotic cells. Prior to transfection, media from all wells or plates to be transfected was removed and cells were washed with pre-warmed 1x PBS, serum free OPTI-MEM (Invitrogen) was then added. 1ml or 8ml of OPTI-MEM was added to a 6-well, 12-well or a 10cm plate, respectively. Standard transfection procedure was adopted regardless of the number of cells being transfected: 3x the volume of FuGENE was added to the concentration of DNA in µg. DNA to be transfected was suspended in double distilled water (ddH20), and made up to 50µl with OPTI-MEM in a 1.5ml Eppendorf tube. In a separate 1.5ml Eppendorf tube, FuGENE was added to OPTI-MEM giving a final volume of 50µl. Both tubes were incubated at room temperature (RT) for 5 min. The FuGENE-OPTI-MEM mix was then added to the DNA mix giving a final volume of 100µl, the DNA-FuGENE mix was incubated for 15-30 min at RT. 100µl was then added dropwise to the 6, 12-well or 10cm plate; 5 or 16hours (overnight) after DNA addition the transfection media was removed and fresh media added. Cells were harvested 24, 48 or 72hrs post-transfection. Master mixes of DNA or FuGENE were prepared when more than one well or plate was to be transfected.

2.2.2 KSHV production and infection of LEC

KSHV was produced from BCLB-1 cells latently infected with recombinant GFP-expressing KSHV (Vieira et al., 2001). For KSHV production BCLB-1 cultures were expanded to ~2.5L which yielded one batch of ~11ml of concentrated virus, during expansion Geneticin selection was removed. Lytic replication was induced in BCLB-1 cultures at a density of ~$1.2x10^5$ cells/ml by the addition of tetradecanoyl phorbol acetate (TPA) (Sigma) at 20 ng/mL final concentration. 3-4 days post induction, virus was harvested and concentrated through a two step centrifugation using a Beckman JLA-10.500 rotor. The first spin at 400 x g for 15 min pelleted the majority of cellular debris. The supernatant was then transferred to fresh clean tubes and the virus concentrated by spinning at 12500 x g for 3hrs. The supernatant was poured off and discarded, the virus-containing pellet was re-suspended in 12mls of endothelial-cell growth medium MV. Re-suspended virus was filtered through a 45µm filter to remove all traces of cellular debris, virus was then aliquoted and stored at -80^oC.

To test the infectivity of viral preparations, 500µl of virus was added to $1x10^5$ 293T cells seeded in 6 well plates at a total volume of 2ml per well whilst cells were still in suspension. 72hrs post infection, cells were detached from the plate and re-suspended in 1ml of PBS and subjected to flow cytometry using a FACSCaliber flow cytometer (BD Biosciences). Provided more than 20% of 293T cells were GFP positive, KSHV preparations were then used to infect LEC.

$1x10^5$ LEC were seeded in 1ml of LEC media in a 6 well the day prior to infection. Once the cells had adhered, 1ml of KSHV preparation was added per well and the cells spun at 2500rpm in an Eppendorf desktop centrifuge at room temperature for 30 min. Cells were incubated with the virus overnight, the media was then changed. Infections were scaled up or down according to the number of cells being infected. Infection typically resulted in 15-40% of LEC expressing GFP 72hrs post-infection (p.i.), this was assessed both visually using an Axiovert 100 fluorescent microscope (Carl Zeiss) and by flow cytometry using a FACSCaliber

flow cytometer. The number of viral genomes per cell was also assessed by quantitative PCR (see Section 2.3.10), infection typically resulted in 100-150 viral copies/cell. In situations where 100% KSHV positive cells were desired, cells were detached from the well and passed through the cell sorter MoFlow (DAKO), only GFP positive cells were retained for further experiments.

2.2.3 Lentivirus production and infection of LEC

Lentivirus was produced as previously described (Vart et al., 2007). Vesicular stomatitis virus-G (VSV-G) envelope-pseudotyped lentivirus virions were produced by co-transfecting 1.5µg of VSV-G plasmid with 2µg of lentiviral construct containing the gene of interest (pSIN-MCS), and 1.5µg of the packaging plasmid p8.91. 5µg of plasmid DNA was transfected into a 70% confluent 10cm plate of 293T cells using the FuGENE protocol. Five hours post transfection, the OPTI-MEM media was removed and fresh DMEM added. Virus containing supernatants were harvested 48hrs post transfection, filtered through a 45µM filter and then stored at -80℃. For those lentiviral preparations with low infectivity, the virus containing supernatant was concentrated 10x by spinning for 5hrs at 48000g using a JA-25.50 rotor. After centrifugation the supernatant was poured off and the virus containing pellet was re-suspended in LEC media at a ratio of 1ml of LEC media to one 10cm plate of 293T cells, supernatant was then stored at -80^{o}C.

Lentiviral infections were performed by incubating the desired amount of virus with LEC in culture, typically 2ml of concentrated lentivirus was added to 5x10^{4} cells. The virus was removed either 5 or 16hrs post infection and fresh LEC media added. Infected LEC were typically harvested 72hrs post infection. Infectivity of lentiviral preparations was assessed by performing qPCR 72hrs post transfection quantifying the levels of lentiviral packaging signal. Expression of the lentiviral constructs was determined by quantitative reverse transcriptase-PCR (qRT-PCR) for the gene of interest cloned into the lentiviral backbone.

2.3 Molecular biology techniques

2.3.1 Bacterial transformation

Plasmid DNA was amplified through chemical transformation and expansion of bacterial cultures. One vial of 50µl One Shot TOP10 chemically competent E.coli (Invitrogen) was transformed with 1-5µl of ligation reaction or plasmid DNA (~100ng). Bacteria were incubated on ice for a minimum of 5 mins and then heat shocked at 42^{o}C for 30 seconds, after which they were placed on ice. 250µl of room temperature SOC media (Invitrogen) was added to each vial of bacteria and incubated at 37^{o}C for 1 hour with shaking. If bacteria were transformed with ligation mixture, after shaking 200µl was streaked on ampicilin containing LB agar plates [LB agar (Sigma) with 100 µg/ml ampicilin (Sigma)]. Plates were incubated overnight at 37^{o}C, successfully transformed bacteria contained an ampicilin resistant cassette, and therefore survived ampicilin selection growing to form visible colonies, which were then picked for subsequent expansion. Alternatively, if bacteria were transformed with a pure solution of plasmid DNA, SOC media was expanded directly to 5mls with LB^{amp}. This feeder culture was grown for 3-4hours at 37^{o}C with shaking, and then expanded to 100mls with LB^{amp}, which was grown overnight.

2.3.2 Plasmid purification

Plasmid DNA was extracted from transformed bacterial cultures using Qiagen miniprep or maxiprep kits according to manufacturer's instructions. Minipreps were performed on 5ml of bacterial cultures typically transformed with ligation reactions during the cloning process in order to test for the presence of a DNA insert. Minipreps yielded approximately 20µg of plasmid DNA.

For minipreps, a single bacterial colony was picked and placed into 5mls of LB^{amp}, which was grown overnight at 37^{o}C with shaking. Bacteria were pelleted by spinning at 3000rpm for 15min in an Eppendorf desktop centrifuge. The bacterial pellet was re-suspended, lysed and neutralized through an alkaline lysis method according to manufacturer's instructions (Qiagen). Cellular debris and genomic

DNA were pelted by spinning at 13000 rpm in a desktop centrifuge. The resulting clear solution containing the plasmid DNA was passed through a mini-prep column by spinning at 13000rpm in a desktop centrifuge for 1 min. Wash steps were performed according to manufacturers protocol and clean plasmid DNA solution was eluted in 50µl of ddH_20.

Maxipreps were performed on 100ml of bacterial culture from which bacteria were pelleted through spinning at 3500rpm for 15 min at 4^oC. The pellet was re-suspended, lysed and neutralised according to manufacturer's instructions. Genomic DNA was pelleted through centrifuging the solution at 3500rpm for 30 min at 4^oC. Subsequent wash steps and elution were performed according to manufacturer's instructions. Eluted DNA was precipitated with isopropanol and washed with 70% ethanol. Precipitated DNA was them resuspended in 500µl of ddH_20. Maxipreps typically yielded ~1µg/µl of plasmid DNA.

Plasmid DNA concentration and purity was quantified by measuring the absorbance at 260nm/230nm and the absorbance at 260nm/280nm respectively using a NanoDrop UV spectrophotometer.

2.3.3 Restriction enzyme digest

Restriction enzyme digestion was performed either on plasmid DNA to confirm the presence of a cloned insert or on PCR amplified products which were to be subsequently ligated into plasmid DNA. All restriction enzyme digests were performed for 1-2hrs at 37^oC with 5-10 units of each enzyme in a total volume of 15-25µl. Included in the restriction enzyme mix was 10x restriction enzyme buffer and ~1µg of DNA. The appropriate buffer was selected by consulting Promega's enzyme buffer compatibility chart and determining in which buffer the two enzymes had maximum activity. After restriction enzyme digestion, 6x DNA loading buffer (Fermentas) was added and the product resolved by electrophoresis on an agarose gel, the product was then excised and cleaned up

using QIAquick Gel Extraction Kit (Qiagen). Alternatively, digested PCR products were purified directly using the QIAquick Gel Extraction Kit.

2.3.4 Agarose gel electrophoresis

Gel electrophoresis was performed to visualise DNA and or for gel purification. Typically 1% weight/volume (w/v) agarose (Sigma) in TAE buffer (Tris-acetate 0.4M, ethylene diamino tetraacetic acid (EDTA) 0.01M) gels were used to resolve DNA fragments > 200bp. For resolution of DNA <200bp 2-4% agarose gels were used. DNA was visualised through the addition of 0.04mg/ml of ethidium bromide (Sigma). Agarose gels were electrophoresed in TAE buffer at a voltage of 100V. DNA bands in the gel were visualised using the G:Box gel documentation system (Syngene). DNA ladders (Fermentas) of the appropriate size range were separated alongside experimental samples to estimate the size of DNA molecules.

2.3.5 Agarose gel extraction

Agarose gel extraction was performed on PCR products or digested plasmids to be used for subsequent ligation or sequencing. Gel extraction was performed using the QIAquick Gel Extraction Kit (Qiagen). Excised DNA-containing gel pieces were weighed and three times the volume of QG buffer added. Gel was dissolved in QG buffer by incubating at 50^{o}C until all gel was in solution. Then one volume of isopropanol was added and samples loaded onto the QIAquick spin column and processed according to manufacturer's protocol. DNA was eluted from the column in 30µl of dd$H_2$0. The QIAquick kit was also used to clean up PCR products which had been restriction digested, these products were not run on a gel as digesting the product had little effect on size and therefore electrophoresis was unnecessary. After restriction digest, 300µl of QG buffer was added to the DNA, followed by 100µl of isopropanol. The sample was then loaded onto the column and processed according to the manufacturer's instructions. DNA was eluted in 30µl of dd$H_2$0.

2.3.6 Ligation

Ligation reactions were performed in a total volume of 20µl using 20 units (1µl) of T4 DNA ligase and 2µl of 10x T4 DNA ligase buffer (New England Biolabs). Varying ratios of insert to plasmid DNA were used in ligation reactions, always keeping the insert at higher concentration to the plasmid DNA to encourage ligation and prevent vector re-ligation. Two different restriction enzymes were used in the cloning process, this aided cloning of the fragment in the correct orientation and minimised vector re-ligation. In addition, prior to ligation 200-1000ng of gel purified restriction digested vector was incubated with 2µl (2 units) of shrimp alkaline phosphatase (Promega) as well as 10x enzyme buffer (Promega). The enzyme-DNA mixture was incubated at 37^{o}C for 15 min after which the alkaline phosphatase was inactivated by heating to 65^{o}C for 15 min. Alkaline phosphatase treatment is another measure designed to minimise vector re-ligation, promoting the uptake of cloned insert. Typically, the highest ratio of insert to vector was used depending on the DNA concentration of the insert. Ligation reactions were carried out at 16^{o}C overnight.

2.3.7 PCR cloning strategy

The MAF ORF and 3'UTR fragment were cloned using a PCR cloning strategy. The first step was to design 5' and 3' PCR primers containing different restriction enzymes. There were two criteria used to select restriction enzymes for cloning. Firstly, there had to be no restriction sites present within the region to be cloned. The DNA sequence to be cloned was obtained from the NCBI GenBank depository of sequenced DNA, this was then entered into pDRAW32 (acaclone.com). This program identified all user specified restriction enzyme sites present within the sequence; enzymes which did not cut the DNA could then be selected. The second criterion in selecting restriction enzymes was the presence of the restriction site within the multiple cloning site (MCS) of the vector. These were restriction enzyme sites included into a defined region of the vector during vector design to facilitate the cloning process.

Primers complimentary to the beginning and end of the sequence to be cloned were designed using Primer3 v0.4.0 software (frodo.wi.mit.edu/primer3/). The DNA sequence to be cloned was entered into the program; variables including primer length, C/G composition, product length and primer melting temperature were then specified. Once complimentary primers had been designed and the appropriate restriction enzymes selected, a random sequence of junk DNA was added to the ends of both primers, this facilitated restriction enzymes digestion.

PCR was performed with 2µl of 10µM forward and reverse primers, 1µl of 10mM dNTPs (Invitrogen), 5µl PfuTurbo 10x reaction buffer (Stratagene) or 10µl of HotStart HiFidelity 5x PCR Buffer (Qiagen), 1µl of PfuTurbo DNA polymerase (2.5 units) (Stratagene) or 1µl of HotStart HiFidelity DNA polymerase (2.5 units) (Qiagen) and 100-1000ng of template DNA made up to a final volume of 50µl with ddH_20. PCR conditions were as specified by the manufacturer's instructions, typically the polymerase was activated and DNA denatured by incubating at 95^oC for 2-5min. Followed by 20-40 cycles of 95^oC for 1 min, 55^oC for 1 min, 72^oC for 1 min; during which double stranded DNA is denatured, primers anneal and polymerase mediated elongation of PCR produced occurs. The final step was 1 hold of 7 min at 72^oC, this ensured any remaining single stranded DNA was fully extended. Variables in the PCR program were cycle number, extension time and primer annealing temperature. Extension time was dictated by the length of the product, with 1min/1kb of DNA, primer annealing temperature was governed by the base composition and length of primers. The melting temperature of primers was calculated using the formula 2(A/T) + 4(G/C). However, to experimentally determine the optimum primer annealing temperature, a temperature gradient PCR was performed. In this program the annealing temperature increases in defined increments across the PCR block, the products were then run on a gel and the temperature yielding the maximum PCR product was used for subsequent cloning.

Non-template controls, whereby all reactions minus template DNA were run to confirm reagents were uncontaminated. Amplification of the PCR product of the correct size was confirmed by resolving the product on an agarose gel, the correct sequence was then confirmed through sequencing.

The KSHV miRNAs cloned into the pcDNA vector were supplied by Dr. R. Renne (University of Florida) (Samols et al., 2007). Therefore, the miRNAs did not need to be PCR amplified, instead they were subcloned from this vector into the lentivirual vector (pSIN-MCS). First of all the miRNAs were digested out of the pcDNA vector using restriction sites flanking the inserts, then they were ligated into digested pSIN-MCS vector. The presence of the inserts was confirmed by agarose gel electrophoresis and sequencing. The sequence of all PCR primers and conditions used are detailed in Table 2.1, additional plasmid used throughout experiments are detailed in Table 2.2.

Target	Vector	Plasmid name	Restriction enzymes	Template	Forward primer	Reverse primer	PCR conditions
MAF	pSIN-MCS	pSIN-MAF	BamH1/ Nde1	LEC cDNA	cgcggatc cgcagga gaatggca tcag	ggaattcc atatgtatc agggtggc tagctgga	30 cycles of 95°C for 1' 54°C for 1' 72°C for 1.5'
MAF 3'UTR	psi-check2	psi-MAF-UTR	XhoI/ NotI	LEC cDNA	ccgctcga gtgccaatc tgaaattct cca	ataagaat gcggccgc tccactgga gaaaagg atgc	40 cycles of 95°C for 1' 64°C for 1' 72°C for 2.25'

Table 2.1 PCR cloning details. The pSIN-MCS vector was supplied by Dr. R. Vart (CR-UK Viral Oncology group, UCL), psi-Check2 was purchased from Promega. Red: junk DNA, blue: restriction enzyme site used for cloning, black: sequence complimentary to DNA.

Vector	Insert	Plasmid name
pSIN-MCS	KSHV miRNA Cluster	pSIN-K-Cluster
pSIN-MCS	Individual KSHV miRNAs	pSIN-K-miR-X
pGL3 Control	2 synthetic KSHV miRNA target sites	pGL3-T-miR-X

Table 2.2 Plasmids used in luciferase assays. The cloning vector, insert and resulting plasmid name are indicated.

miRNA	Forward primer	Reverse primer
KSHV-miR-K12-1	cagttgtattgtggtgcagaactggatttt**agt**taacttaaaaaaaaatccacagttttaaagg	cctttaaaactgtggatttttttttaagtta**act**aaaatccagttctgcaccacaatacaactg
KSHV-miR-K12-6-3p	caccctcactccttctcaacc**agc**ctcttccgagatgaaagaaaa	ttttctttcatctcggaagag**gct**ggttgagaaggagtgagggtg
KSHV-miR-K12-11	cactgactgtattgaaaacca**gc**gtatta**g**gaggggaaacgcccctg	gtgactgacataacttttggt**cg**cataat**c**ctccccttgcggggac

Table 2.3 Primers used for mutagenesis of KSHV miRNA binding sites. Red: mutated bases to be incorporated into the psi-MAF-UTR vector.

2.3.8 Site directed mutagenesis

Site directed mutagenesis was performed using the QuikChange XL Site-Directed mutagenesis kit (Stratagene) to mutate KSHV miRNA binding sites identified in the MAF 3'UTR. Mutagenic primers were designed according to protocol guidelines and are detailed in Table 2.3. The primers are complementary to opposite strands of the UTR, located in the centre are the altered bases to be incorporated (red bases in Table 2.3). The first step was to incorporate the altered bases through PCR with the mutagenic primers. PfuTubro enzyme was used according to manufacturer's instructions; this is a non-strand displacing DNA polymerase and therefore generates single strand nicks in the plasmid DNA. PCR was performed with 125ng of forward and reverse primers and 50ng of psi-MAF-UTR vector, containing the first 2kb of the MAF UTR. PCR conditions were as follows: one hold of 95^{o}C for 1 min, 18 cycles of 95^{o}C for 50 seconds, 60^{o}C for 50 seconds, 68^{o}C for 2.5 min and concluded with one hold at 68^{o}C for 7 min. A distinct mutated UTR was made for miR-K12-6-3p, miR-K12-11 and miR-K12-1.

Parental psi-MAF-UTR plasmid containing wild type miRNA binding sites was isolated from E. coli which dam methylates all DNA. Therefore, all un-mutated parental DNA was removed by treatment with DpnI endonuclease which is specific for methylated DNA. 1µl DpnI (10 units) was incubated with the PCR mixture for 1 hour at 37^{o}C. After DpnI digestion, 5µl of the reaction was used to chemically transform XL10-Gold*** Ultracompetent Cells (Stragene) according to manufacturer's instructions. The next day bacterial colonies were picked and minipreps performed to isolate plasmid DNA which was sent for sequencing to confirm the presence of mutated sites.

2.3.9 Genomic DNA extraction

Genomic DNA was extracted from cultured cells using the QIAmp DNA Mini Kit (Qiagen). Cells were detached with trypsin and pelleted by spinning at 13000rpm in a table top centrifuge. Cells were then lysed and genomic DNA released by treatment with 20µl of Protease K, 200µl of buffer AK was added to the cells and mixed by pulse-vortexing. Samples were incubated at 56^{o}C for 10 min, after which 200µl of 100% ethanol was added and mixed by pulse-vortexing. Samples were passed through a QIAmp spin column by spinning at 13000rpm in a table top centrifuge for 1 min. Columns were then washed according to manufacturers protocol and cleaned genomic DNA was eluted in 50µl of dd$H_2$0. The concentration and purity of the DNA was determined by measuring absorbance at 260nm (A260) and 280nm (A280) with a NanoDrop spectrophotometer. An A260/A280 ratio of 1.8-2.0, indicating DNA free of contaminants, was obtained for all samples. DNA was stored at -20^{o}C until use.

2.3.10 Quantitative polymerase chain reaction (qPCR)

In order to determine the number of lentiviral copies per infected cell (c/c) qPCR was performed for glyceraldehydes 3-phosphate dehydrogenase (GAPDH) and the lentiviral packaging signal. Genomic DNA was extracted 72hrs post lentiviral infection as described in Section 2.3.9. GAPDH primers and probes used for qPCR were as previously described (Bourboulia et al., 2004). Primers were used at a concentration of 0.7µM and probes at 0.15µM. GAPDH forward primer: 5'-GGAGTCAACGGATTTGGTCGTA-3' and reverse primer: 5'-GGCAACAATATCCACTTTACCAGAGT-3'; GAPDH TaqMan probe: 5'-FAM-GGCAACAATATCCACTTTACCAGAGT-3'TAMRA. Primers and probe for the lentiviral packaging signal were used as previously described (Vart et al., 2007). Lentiviral forward primer: 5'-GCACGGCAAGAGGCGA-3', reverse primer: 5'-CGCACCCATCTCTCTCCTTCTA-3' and TaqMan probe: 5'-FAM-CGGCGACTCTCTCCTTCTA-3'. Reactions were performed in a total volume of 50µl using the Absolute QPCR ROX and dUTP mix (ABgene) and 0.01 units/µl AmpErase (Applied Biosystems). 10µl of genomic DNA at a concentration of 50-

100 ng/µl was added to the reactions. The q-PCR conditions used were as follows: 50℃ for 2 min followed by 95℃ for 15 min and 40 cycles of 95℃ for 15 sec and 60℃ for 1 min. Reactions were run in Optic al 96-Well Thermal Cycling Plates (Applied Biosystems) on an Eppendorf PCR machine. DNA mixtures containing linearized pSIN-MCS plasmid (Vart et al., 2007) and pcDNA3.1/V5-His-TOPO-GAPDH plasmid (Bourboulia et al., 2004) at known copy numbers were used as standards. The number of c/c was determined by adjusting the number of lentiviral constructs present to the number of cells analyzed, using GAPDH. For each sample a neat and 1/10 dilution of genomic DNA was run, a negative control of dd$H_2$0 was performed for all PCRs.

2.3.11 RNA extraction

Prior to working with RNA all surfaces and pipettes were cleaned with RNaseZAP (Ambion) to remove any traces of RNase enzymes which could contaminate samples and lead to RNA degradation. In addition, a dedicated set of pipette tips were used for RNA extraction. The amount and purity of the RNA was determined by measuring absorbance at 260nm (A260) and 280nm (A280) with a NanoDrop spectrophotometer. An A260/A280 ratio of 1.8-2.0, indicating RNA free of contaminants, was obtained for all samples. RNA was stored at -80^{o}C until use.

2.3.11.1 RNeasy Mini Kit (Qiagen)

Total RNA was extracted from cultured cells using the RNeasy mini kit according to manufacturer's protocol. Cells in culture were washed with PBS and then lysed directly in the well by addition of 350µl of buffer RLT, 350µl of ethanol was added and the mixture passed through an RNeasy mini-column to isolate RNA. The sample was then washed according to manufacturer's instructions. To remove any traces of genomic DNA contamination, DNase I digestion was performed by adding 4µl of 10x DNase I reaction buffer and 2µl of DNase I (2 units) to the column and incubating at room temperature for 15 min. RNA was then eluted from the column in 30µl of dd$H_2$0.

2.3.11.2 miRNeasy Mini Kit (Qiagen)

The RNeasy kit extracts total RNA longer than 200bp, anything smaller is removed during extraction. Therefore, in order to extract total RNA including the small RNA fraction which contains amongst other species miRNAs, the miRNeasy kit was used. This protocol was used both on cultured cells and human tissue. Cultured cells were washed with PBS, then 700µl of QIAzol added to lyse and homogenize the sample, this mixture was transferred to a 1.5 ml Eppendorf tube and incubated at room temperature for 5 min to promote the dissociation of nucleoprotein complexes. 140µl of chloroform was added to the homogenate, after incubating at room temperature for 2-3 min the sample was spun at 13000 rpm for 15 min at 4^{o}C. Addition of chloroform promotes the separation of the sample into three distinct phases: RNA molecules longer than 18 nucleotides are located in the upper clear aqueous phase, whereas DNA separates to the interphase and proteins to the lower, organic phase. The upper, RNA containing layer was transferred to a 1.5ml Eppendorf tube, after which 1.5 volume (typically 525µl) of ethanol was added. This mixture was then passed through an RNeasy Mini spin column to isolate total RNA. Phenol and other contaminants were washed off according to manufacturer's protocol. On-column DNase digestion was performed to remove any contaminating DNA. RNA was eluted in 30µl of sterile RNase free ddH20. A similar protocol was adopted for total RNA extraction from human tissue. Tissue was removed from storage in liquid nitrogen, samples were weighed and no more than 50mg of tissue was processed at one time. Prior to thawing 700µl of QIAzol was added and tissue shredded using a scalpel. This mixture was homogenized using a Tissue-Tearor (Biospec Products). The homogenate was then processed as above.

2.3.11.3 TRIzol (Invitrogen)

TRIzol extraction and subsequent purification using the RNeasy mini column (Qiagen) was performed when RNA was to be used for gene expression microarray analysis. Cultured cells were washed once with PBS and then lysed directly in the well by addition of 1ml of TRIzol reagent, lysed cells were removed from the well by scraping with a cell scraper. This mixture was transferred to a 1.5ml Eppendorf tube, RNA was then extracted according to manufacturer's instructions. Briefly, chloroform was added to the sample, which was then mixed and centrifuged. After centrifugation the sample had separated into three phases, the upper, aqueous RNA-containing phase was transferred to a 1.5ml Eppendorf and precipitated by addition of isopropanol. The sample was centrifuged, pelleted RNA washed with 75% ethanol and re-suspended in 34µl of sterile RNase free dd$H_2$0 (Ambion). RNA clean up was then performed using the RNeasy mini column clean up protocol. RNA was brought up to 100µl total volume with RNase free dd$H_2$0, to which 350µl of buffer RLT was added. After addition of 350µl of ethanol the sample was passed through RNeasy spin column to isolate RNA. RNA was then washed according to manufacturer's instructions to remove all traces of phenol and other contaminants. RNA was eluted in 30µl of sterile RNase free dd$H_2$0.

2.3.12 cDNA synthesis

Between 100-5000ng of RNA isolated by one of the above methods was used for complimentary DNA (cDNA) synthesis. cDNA was synthesized using SuperScript II reverse transcriptase (Invitrogen). Firstly, RNA was incubated at 70^{o}C for 6 min with 1µl of 5µM oligo(dT) and 1µl of 10µM dNTP mix at a total volume of 12µl made up with dd$H_2$0. After incubation the mix was cooled on ice, the following mixture was then added: 4µl of 5x first-Strand buffer (Invitrogen), 2µl of 0.1 M DTT (Invitrogen), 1µl of RNaseOUT (200units, Invitrogen) and 1µl of Superscript II reverse transcriptase (200 units, Invitrogen). Samples were incubated for 1 hr at 40^{o}C and then heated to 70^{o}C to inactivate SuperScript II. cDNA was stored at -

20^{o}C until required, it was then either used neat or diluted 1/100 depending on abundance of the transcript.

cDNA synthesis for qRT-PCR quantification of miRNAs was performed using the TaqMan® miRNA Reverse Transcription Kit (Applied Biosystems), according to manufacturer's instructions. RNA was extracted from cells or tissue using the miRNeasy total RNA extraction kit (Qiagen). 5ng of total RNA at 1ng/µl was used per 15µl reaction. Reverse transcription was performed using 3µl of custom designed miRNA specific primers from TaqMan® miRNA Assays (Applied biosystems). A reverse transcription master mix of the following was prepared: 1µl MultiScribe™ reverse transcriptase (50units/µl), 0.15µl of 100mM dNTPs, 1.5µl l0x reverse transcription buffer, 0.19µl of RNase Inhibitor (20units/µL), 4.16µl nuclease-free water. The reaction conditions were as follows: 16^{o}C for 30 min, 42^{o}C for 30 min, 85^{o}C for 5 min, samples were then cooled to 4^{o}C.

2.3.13 Quantitative real time reverse transcriptase polymerase chain reaction (qRT-PCR)

Real-time qRT-PCR was performed using Sybr Green (Applied Biosystems) for a range of genes, the primers of which are detailed in Table 2.4, primers were designed using Primer Express software (Applied Biosystems). GAPDH primers were designed as previously described (Bourboulia et al., 2004). All primers were used at a concentration of 0.3µM. qRT-PCRs were performed in a total volume of 25µl using Sybr Green PCR master mix (Applied Biosystems), 1µl of neat or diluted cDNA, and 0.75µl of forward and reverse primers. qRT-PCRs were performed in Optical 96-Well Thermal Cycling (Applied Biosystems), sealed with optical adhesion film (Applied Biosystems) and run on an Eppendorf Mastercycler ep Realplex PCR machine. Reaction conditions were as follows: 50^{o}C for 2 min, 95^{o}C for 10 min to activate the DNA polymerase, followed by 40 cycles of 95^{o}C for 15 sec and 60^{o}C for 1 min. Relative expression of the gene of interest was quantified using the comparative C_T method with GAPDH used as a housekeeping gene.

Real-time qRT-PCR was performed using TaqMan Gene Expression Assays (Applied Biosystems) according to the manufacturer's instructions, genes are detailed in Table 2.4. Reactions were performed in a total volume of 25µl using the TaqMan universal PCR master mix and 20x TaqMan probe and primer mix, to this 1µl of neat or diluted cDNA was added. Reactions were performed and analysed as described above.

Gene Symbol	Assay	Forward primer	Reverse primer
GAPDH	Sybr Green	GGAGTCAACGGATTTGGTCGTA	GGCAACAATATCCACTTTACCAGAGT
HDAC9		CAGCAACGAAAGACACTCCAACTA	CCGTGTACCAGAGCTTGGGAT
FLT1		CTTCTCCTTAGGTGGGTCTCCATAC	GTACTCAGGAGCTCTCATCCTCATG
FLT4		ACGGCCTGGTGAGTGGC	CGTTTGACTCCTCCGTGATG
LYVE1		CCCTGTCTGGATCCTATCCTCC	GGATATTATTAGGACATAGCCAGGCTAG
PDPN		AGCCTCCTGAGTAGCTGGGACT	AAACCCCATCTCTACTAAAAATACAAAAATT
CXCR4		GCATGACGGACAAGTACAGGC	CAGAAGGGAAGCGTGATGACA
CXCL12		CATGCCGATTCTTCGAAAGC	CAGTTTGGAGTGTTGAGAATTTTGAG
ITGB3		GTTTACCACTGATGCCAAGACTCATA	CCGTCATTAGGCTGGACAATG
MAF-S		TTTACTTTTAGAGCTTGCTGTGTTGC	CTCGGAAGAGATGGGTGGAGAA
MAF-L		CCTCTCCCGAGTTTTTCATAACTG	CGTCCTCTCCCGAGTTTTTCA
MAF	Taq Man	N/A	N/A
NRCAM		N/A	N/A
TFEC		N/A	N/A
SLC1A1		N/A	N/A
GULP1		N/A	N/A

Table 2.4 Real-time qRT-PCR assay and primers. N/A: not applicable, TaqMan Gene Expression assays purchased contained primers and probe.

Quantification of KSHV miRNA expression and the human small nucleolar RNA, RNU66 (small nucleolar RNA, H/ACA box 66) was performed using TaqMan® miRNA Assays (Applied Biosystems, Warrington, U.K). Custom designed assays were used for the KSHV miRNAs, these were designed against the mature miRNA sequences which were obtained from version 11.0 of miRBase (http://microrna.sanger.ac.U.K/sequences/). RNU66 was quantified using an inventoried product from Applied Biosystems. Real-time qRT-PCR reactions were composed of the following: 1µl of 20x TaqMan MicroRNA Assay, 1.33µl of miRNA specific cDNA, 10µ of 2x TaqMan Universal PCR Master Mix, no AmpErase UNG, 7.67µl of Nuclease-free water, at a final volume of 20µl. Reactions were run in Optical 96-Well Thermal Cycling Plates (Applied Biosytems) on an Eppendorf Mastercycler ep Realplex PCR machine. PCR conditions were as follows: 10 min hold at 95^{o}C, followed by 40 cycles of 95^{o}C for 15 sec and 60^{o}C for 1 min.

miRNA qRT-PCR expression data was expressed as delta Ct values, whereby the difference in threshold detection cycle between viral miRNA and loading control RNU66 is plotted. Low expression levels correspond to a high delta Ct, whereas highly expressed miRNAs have low delta Cts. In some cases where miRNA expression is extremely high, such as the viral miRNAs, these were detected before the loading control and therefore have negative delta Ct values.

2.4 Gene expression microarray analysis

The transcriptional profile of samples was determined using the Human Genome U133 Plus 2.0 Array (Affymetrix), this platform quantified the relative mRNA abundance of over 47,000 transcripts covering the entire human genome. The high density arrays contain 1,300,000 oligonucleotide features which corresponded to 11 probe pairs per transcript. Multiple independent measurements per transcript, as well as inbuilt controls provide robust mRNA quantification. Each chip contains sequences controlling for hybridization efficiency, a set of probes for normalization and housekeeping control genes.

Sequences for probe design were obtained from GenBank, dbEST and RefSeq, probes correspond to the 600 bases proximal to the 3' end of each transcript.

2.4.1 Sample preparation

The GEM profile of LEC expressing the KSHV miRNA Cluster was compared with that of cells infected with empty lentiviral vector. Three distinct infections per condition were profiled. Passage four LEC were removed from liquid nitrogen storage and grown until confluent, cells were then plated at a density of 10^5 cells per well on 6 well plates. The day after plating LEC were transduced with KSHV miRNA Cluster or empty lentiviral vector at a copy number of ~12.7 c/c as confirmed by q-PCR. 72hrs post-infection media was removed, cells washed with PBS and 1ml of TRIzol added to one well. Cells were removed by scrapping and the TRIzol-Cell mix transferred to the next well, in this manner all 6 wells of one plate were pulled together. RNA was then extracted and cleaned up and quantified as described in Section 2.3.11.3.

The GEM profile of LEC transfected with MAF siRNA (siMAF) or a non-targeting control (siCON) was obtained. $5x10^4$ cells were plated per 6-well, cells were transfected with 100nM siMAF or siCON and harvested 48hrs post transfection as described above. Three samples per condition were profiled.

All RNA samples had an absorption 260/230nm ratio of ~2 which indicated RNA was devoid of salt and other organic contamination and a ratio of ~2 for absorption at 260nm/280nm indicating samples were free of protein contamination. The RNA was therefore of suitable quality for further processing.

Total RNA was then subjected to RiboMinus™ (Invitrogen) treatment to remove 18s and 28s ribosomal RNA (rRNA), thereby enriching the sample for mRNA molecules prior to GEM analysis. According to manufacturer's instructions 2-10µg of RNA in a volume less than 20µl was hybridized to biotin labeled locked nucleic acid (LNA) probes specific to rRNA. 8µl of 100 pmol/µl RiboMinus Probe and

300µl of hybridization buffer were added to total RNA. Samples were heated to 70^{o}C for 5 min to denature the RNA and then cooled over a period of 30 min to 37^{o}C. The RiboMinus™ magnetic beads (Invitrogen) were prepared and re-suspended in hybridization buffer according to manufacturer's instructions. rRNA was removed by incubating the sample with RiboMinus magnetic beads at 37℃ for 15 min and allowing the rRNA to bind to the LNA probes. Samples were left to stand on a magnetic stand which collected the rRNA-bound beads, supernatant containing the RiboMinus RNA fraction was then transferred to a 1.5ml Eppendorf tube. 528µl of supernatant was cleaned and concentrated by ethanol precipitation according to manufacturer's instructions. RNA was re-suspended in 10µl of RNase free water (Ambion).

2µg of RNA per chip of LEC-Cluster or LEC-pSIN, 1µg of LEC-siMAF or LEC-siCON was subject to one-cycle target labeling assay according to manufacturer's protocol (Affymetrix). Briefly, first strand cDNA synthesis was primed by T7-Oligo(dT) and performed with Superscript II. Second strand reactions were then prepared with: 91 µL of RNase-free Water, 30 µL of 5X 2nd Strand Reaction Mix, 3 µL of 10mM dNTP, 1µl of E. coli DNA ligase, 1.4µl of E. coli DNA Polymerase and 1µl of RNase H. This master mix was added to cDNA and incubated at 16^{0}C for 2hrs. Double stranded cDNA was subsequently cleaned with the GeneChip Sample Cleanup Module (Affymetrix) according to manufacturer's instructions. The purified cDNA served as a template for *in vitro* transcription (IVT) reaction. IVT was performed overnight at 16oC by T7 RNA polymerase in the presence of biotinylated nucleotide analog/RNA mix generating biotin labeled complimentary RNA (cRNA). Amplification of cRNA at this stage generates sufficient RNA for chip hybridization. The biotinylated cRNA targets were purified using the Sample Cleanup Module, 20µg of clean cRNA was then fragmented using fragmentation buffer (Affymetrix) according to manufacturer's instructions.

2.4.2 Chip hybridization and scanning

Fragmented, labeled cRNA was supplied to the Cancer Institute Scientific Support Services Facility (http://www.ucl.ac.uk/cancer/core-facilities/index.htm) who carried out target hybridization, washing, staining and array scanning.

2.4.3 GEM data analysis

The raw GEM data in the format of Affymetrix CEL files was provided after array processing by the Cancer Institute Scientific Support Services. Bioinformatician Dr. S. Henderson (CR-UK Viral Oncology group, UCL) performed the initial processing of raw microarray data as previously described (Lagos et al., 2007), generating the microarray log expression values, as well as the statistical p and q values. In summary, the Bioconductor (http://www.bioconductor.org/) 'affy' package written in the R statistical programming language (http://www.r-project.org/) was used to normalize the raw array data and determine the microarray log expression values (Gautier et al., 2004). All analysis was performed at the probe level, internal chip controls including the mismatch probes were used to determine whether the experimental procedure was successful. To assess the significance of difference between two experimental conditions a moderated t-statistic was applied to microarray log expression values (Smyth, 2004). p values were corrected for multiple comparisons and false discovery rate (FDR) to obtain q-values (Storey and Tibshirani, 2003). Statistical selection of differentially expressed transcripts was performed using the 'limma' package (Smyth, 2004). Values are standardized Z-scores indicating how many standard deviations a particular probe is from the mean of log2 expression values across all samples.

The raw and background corrected data for GEM data used within this thesis can be accessed using the following links (Table 2.5).

Data set	Geo accession number	URL
LEC Cluster vs pSIN-MCS	GSE16355	http://www.ncbi.nlm.nih.gov/geo/query/acc.cgi?acc=GSE16355
LEC siMAF vs siCON	GSE16356	http://www.ncbi.nlm.nih.gov/geo/query/acc.cgi?acc=GSE16356
miRNA profile KLEC vs LEC	GSE17016	http://www.ncbi.nlm.nih.gov/geo/query/acc.cgi?acc=GSE17016
miRNA profile KS lesions and skin	GSE16353	http://www.ncbi.nlm.nih.gov/geo/query/acc.cgi?acc=GSE16353

Table 2.5. GEM and miRNA profiling data sets. Raw and background corrected microarray data are deposited in the Gene Expression Omnibus (GEO) site http://www.ncbi.nlm.nih.gov/geo/. GEO accession numbers and links for individual data sets are listed.

2.4.4 Using LEC versus KLEC GEM data sets to analyze Maf family mRNA changes upon KHSV infection

GEM data from six LEC and KLEC (72hrs post infection at a minimum of 50% GFP positivity) hybridized to Affymetrix Human Genome U133 plus 2 GeneChips were obtained from Dr. D. Lagos (CR-UK Viral Oncology group, UCL) (Lagos et al., 2007). GEM data for the seven Maf family transcription factors was extracted from all GEM data of LEC vs KLEC. Those probes with expression levels above 4.5 and a q-value of <0.05 (FDR threshold of 0.5%) were selected and expression data represented in the heatmap shown in Figure 4.6A.

2.4.5 Using LEC versus BEC GEM data to compile a list of BEC and LEC specific genes

Previously in the laboratory Dr. D. Lagos (CR-UK Viral Oncology group, UCL) performed GEM profiling using the Affymetrix Human Genome U133 plus 2 GeneChips of six cultured BEC (Unpublished data). Using the 'affy' statistical analysis package the gene expression profile of these BEC were compared with LEC. A List of differentially expressed genes distinguishing the two endothelial cell types was generated, a heatmap of which is shown in Figure 5.5.

2.4.6 Gene expression heatmaps

Heatmaps representing differentially expressed probes were generated using R software with the help of Dr. S. Henderson (CR-UK Viral Oncology group, UCL). Values used in heatmaps were standardized Z-scores, expression of each probe set in units of standard deviation across all samples is shown. The scale located at the bottom of each heatmap represents the relationship between colour and its intensity and the microarray probe log expression value's amount of standard deviation from the mean.

2.5 miRNA microarray profiling

miRNA profiling of KS biopsies and normal skin samples was performed using the Human miRNA microarray V2 (Agilent). This microarray quantifies 723 human miRNAs and 76 human viral miRNAs by ~15,000 probes. miRNA probe sequences were sourced from miRBase (http://www.mirbase.org/). Each miRNA is quantified by 20 randomly distributed probes; 5 sequence variations per miRNA are repeated 4 times at different locations across the chip. Probes were designed to distinguish miRNAs from the same family which differ by no more than one nucleotide.

2.5.1 Tissue profiled

Two nodular KS lesions and three normal skin biopsies were obtained from Dr. M. Bower (Chelsea and Westminster Hospital, Imperial College London). Normal skin sections were from the same individuals as the KS biopsies, but taken from sites devoid of KS lesions. Absence of KSHV from these samples was confirmed by qRT-PCR for multiple viral-encoded genes. Three additional nodular KS biopsies were provided by the ACIR, NIH. All participants were male, with AIDS-KS and were undergoing anti-retroviral therapy at the time of sectioning. Participants were from a range of ethnic backgrounds and aged 25-57. All biopsies were harvested and fresh frozen in liquid nitrogen until use.

2.5.2 Sample preparation

Tissue was disrupted and homogenised using the Tissue-Tearor (Biospec Products). RNA was extracted using the miRNeasy mini kit as described in Section 2.3.11.2. Prior to further processing for microarray analysis, the abundance and quality of small RNA fraction was assessed using the Agilent small RNA Kit, according to manufacturer's instructions. 1-20ng of total RNA was loaded in 1µl onto the small RNA chip, nucleic acid fragments were separated electrophorectically according to size. 11 samples were analysed per chip, a small RNA ladder was run alongside to determine the size of each fraction. Samples plus the small RNA ladder were denatured before use by heating to 70^{o}C for 2 min, then stored on ice. The electrophoretic gel and sample dye were prepared and loaded onto the chip according to manufacturer's instructions. RNA between 6 and 150nts was visualised using the Agilent 2100 Bioanalyzer (Agilent). The miRNA fraction was assessed by the size of the peak at 10-40nt on the electrophoregram, only those samples with a sufficient miRNA content were used for miRNA microarray analysis.

100ng of total RNA was incubated with 0.7µl Calf Intestine Alkaline phosphatise (25 unit/µl, TaKaRa) at 37^{o}C for 30 min to dephosphorylate the sample according to manufacturer's instructions. Dephosphorylated RNA was then denatured by treatment with 5µL of 100% DMSO and heating to 100^{o}C for 7.5 min, samples were then placed on ice. Fluorescent miRNA was generated by labelling the RNA with Cyanine 3-pCp at the 3'end according to manufacturer's instructions. Briefly, ligation master mix was prepared with the following: 2µl 10x T4 RNA ligase buffer (New England Biolabs), 2µ RNAse-Free Water, 3µ pCp-Cy3 (Agilent), 1µl NEB T4 RNA ligase (20units/µl, New England Biolabs) giving a total volume of 8µ per sample. The ligation mixture was added to the sample and incubated at 16^{o}C for 2hrs. Labelled RNA was made up to a total volume of 50µl with dd$H_2$0, then purified by passing the sample through Micro Bio-spin 6 columns (BioRad), according to manufacturer's instructions. These columns contain Bio-Gel P which

desalts samples and removes unincorporated dye, smaller RNA fragments are retained while larger molecules are excluded.

2.5.3 miRNA microarray hybridization and scanning

Clean, labelled miRNA samples were then prepared for hybridisation following manufacturer's protocol. Briefly, 10x blocking agent (GE Healthcare) was reconstituted with 125µL of nuclease-free water. Labelled samples were dried using a speed-vac, spinning at 45^{o}C for 1 hour. RNA was re-suspended in 18µl of DNase/RNase-free water and 4.5µL of the 10X GE Blocking Agent added to each sample. 22.5µL of 2x Hi-RPM Hybridization buffer was added and samples incubated for 5 min at 100^{o}C. Labelled miRNA was then hybridized to miRNA microarrays and scanned following manufacturer's protocol with the assistance of Dr. E. Coulter (Division of Infection Immunity, UCL). The hybridisation mixture was added to a clean gasket slide and loaded into the Agilent SureHyb chamber base. Samples were rotated and hybridized at 55℃ for a minimum of 20hrs. After which, chips were washed with Gene Expression wash buffer (Agilent) containing Triton X-102 according to manufacturer's protocol. Washed chips were scanned using the Agilent microarray scanner and data extracted with the Agilent Feature Extraction Software.

2.5.4 miRNA microarray data analysis

A quality control (QC) report was generated and assessed after scanning to confirm that the experimental procedure was successful. Agilent miRNA arrays were analyzed by Dr. S. Henderson (CR-UK Viral Oncology group, UCL) using the 'limma' package for the R programming language and additional custom methods. Background subtraction was undertaken for all probes, negative values were given a small positive value. Sets of probes for each gene were converted to $\log_2$ and a summary calculated from the median. Differential expression between summary probe set values was then calculated using the 'limma' methodology.

2.6 Protein analysis

2.6.1 Western blotting

Protein was extracted from cells using radioimmunoprecipitation assay (RIPA) buffer plus protease inhibitor and phosphatase inhibitor cocktails (Sigma). The composition of lysis buffer is detailed below:

Lysis buffer:

150 mM NaCl

50 mM Tris-HCL pH 7.5

1% [volume/volume (v/v)] NP40

0.5% (w/v) Deoxycholic acid

0.1% (w/v) Sodium dodecyl sulphate (SDS)

1/100 Protease inhibitor cocktail

1/100 Phosphatase inhibitor cocktail I

1/100 Phosphatase inhibitor cocktail II

20-100µl lysis buffer was added either to cell pellets ($1x10^5$ - $1x10^6$ cells) in 1.5ml Eppendorf tubes and mixed by pipetting or directly to a well or 10cm dish of confluent cells. If added directly to cells, media was removed and cells washed with PBS, cells were then placed on ice to prevent evaporation and lysis buffer added. Cells were retrieved with a cell scrapper and collected in a 1.5ml Eppendorf tube. Lysates were then incubated on ice for 30 min and the centrifuged at 13000 rpm for a minimum of 20 min at 4^oC to pellet cellular debris. Supernatant was removed and protein stored at -20^oC until required.

Protein concentration was measured using the Bradford assay (Bio-Rad). 2µl of protein lysate was diluted to 500µl with distilled water (dH_20) to which 500µl of Bradford assay reagent was added. 200µl of each sample was added in duplicate to a 96-well and the absorption at 595nm was measured with the FluroSkan Ascent (Thermo Fisher). To obtain the protein concentration of lysates, absorption

of samples were compared with those of a standard curve, which was produced with dilutions of bovine serum albumin (BSA) solution (10mg/ml) (Promega).

5-30µg of protein was mixed with 4x SDS-polyacrylamide gel electrophoresis (SDS-PAGE) sample loading buffer, the composition of which is listed below. All samples were made to the same volume with PBS. In addition, 10µl per sample of Rainbow colour protein molecular weight ladder (Bio-Rad) was mixed with 4x SDS-PAGE buffer and made up to equal volume with PBS. Prior to loading, protein was denatured by heating to 100^{o}C for 5 min and allowed to cool.

4x SDS-PAGE sample loading buffer

250nM Tris-HCL pH 6.8
8% (w/v) SDS
10% (v/v) Glycerol
5% (v/v) β-mecaptoethanol
0.05% (w/v) Bromophenol blue

Denatured protein lysates were run on 12% polyacrylamide gels which were composed of a 1.5mm thick stacking gel and a 12% resolving gel. The composition of each gel is listed:

Stacking gel

1.4ml dH_20

0.33ml 30% (w/v) acrylamide

0.25ml 1.0M Tris pH 6.8

0.02ml 10% (w/v) SDS

0.02ml 10% (w/v) ammonium persulfate

0.002ml TEMED

12% Resolving gel

4ml dH_20

3.3ml 30% (w/v) acrylamide

2.5ml 1.5M Tris pH 6.8

0.1ml 10% (w/v) SDS

0.1ml 10% (w/v) ammonium persulfate

0.004ml TEMED

Lysates and ladder were loaded on polyacrylamide gels, to empty lanes equal volume of PBS-4x-SDS-PAGE loading buffer was added. Proteins were fractionated by electrophoresis at 100V in SDS-PAGE running buffer (National Diagnostics) until the bromophenol blue marker ran off the gel. Protein was transferred onto immobilon P membranes (Millipore) at 20 V for 1 hour using semi-dry transfer apparatus (Bio-Rad) and transfer buffer (National Diagnostics). Prior to transfer the membrane was activated by soaking in methanol for 5 min and equilibrated in transfer buffer. Membranes were then blocked in blocking solution [5% (w/v) milk, 0.05% (v/v) Tween20 (sigma) in PBS] for 1 hour at room temperature. After blocking membranes were incubated with primary antibody diluted in blocking solution, overnight at 4^oC with rotation. Primary antibodies used are listed in Table 2.6. After primary antibody incubation membranes were washed three times for 15 min with rocking in PBS -Tween [5% (w/v) milk, 0.05% (v/v) Tween20 (sigma) in PBS] at room temperature and then incubated for one hour at room temperature with the appropriate horse-radish peroxidase (HRP)

conjugated secondary antibody, also diluted in blocking solution. After incubation unbound antibody was washed off with 3 x 15 min washes in PBS-Tween at room temperature with rocking. Bound antibody was then visualized using ECL (GE Healthcare) according to manufacturer's instructions. The resulting chemi-luminescence signal was detected with Hyperfilm (GE Healthcare). After development membranes were washed three times with PBS and incubated with Restore Western blot stripping buffer (Themo Scientific) for 10 min at 37^{o}C with shaking, stripping agent was then removed by washing 2x with PBS. Membranes were wrapped in foil and stored at -20^{o}C.

Antibody	Supplier	Protein	Dilution/Amount	Technique
N15	Santa Cruz	MAF	1/100	Western Blotting
IMG-6076	Imgenex	MAF	1/200	
RGM2	Advanced ImmunoChemical	GAPDH	1/10000	
CP01-1EA	Calbiochem	ACTB	1/10000	
SC-126	Santa Cruz	P53	1/5000	
IMG-6076	Imgenex	MAF	1/200	Immunofluorescence
SC-2027	Santa Cruz	rabbit IgG	1/200	
M153	Santa Cruz	MAF	0.28µg	Immunoprecipitation
SC-2027	Santa Cruz	rabbit IgG	2µg	
M153	Santa Cruz	MAF	20µg	Chromatin Immunoprecipitation
SC-900	Santa Cruz	RNA POL II	10µg	
SC-2027	Santa Cruz	rabbit IgG	10µg	

Table 2.6. Primary antibodies used for protein detection and quantification. Antibody, supplier, technique and dilution factor or total amount is listed.

2.6.2 Nuclear and cytoplasmic fractionation

The nuclear and cytoplasmic protein fractions were extracted from LEC and 293T cells using the NE-PER Nuclear and Cytoplasmic Extraction Kit (Peirce, Thermo Scientific) according to manufacturer's instructions. This method of protein extraction was used to enrich for nuclear proteins such as the MAF transcription factor for use in downstream immunoprecipitation assays. Briefly, the packed cell volume of pelleted cells was estimated and 10x the volume of ice cold CERI buffer was added. Samples were vortexed and 55% of the packed cell volume of CER II was added, after vortexing and centrifugation the cytoplasmic fraction was transferred to a new 1.5ml Eppendorf. The remaining nuclei were then lysed by the addition of 5x the packed cell volume of NER, after 40 min incubation on ice with repeated vortexing, debris was pelleted by centrifugation and the nuclear extract transferred to a new 1.5ml Eppendorf tube. Protein concentration was quantified using the Bradford assay (Bio-Rad); successful fractionation was confirmed by the absence of nuclear or cytoplasmic proteins in the cytoplasmic or nuclear fraction, respectively.

2.6.3 Immunofluorescence assay

Cells to be analyzed by Immunofluorescence assay (IFA) were grown on fibronectin-coated chamber slides (Lab-Tek, Nunc), $7.5x10^3$ cells were plated per well. Cells were either grown for 48hrs, infected with KSHV, MAF or pSIN-MCS lentivirus and processed for IFA 72hrs p.i. Media was removed and cells washed with 500µl of cold PBS, never letting the cells dry out. Cells were then fixed by incubation at room temperature for 7 min with 400ul of 4% paraformaldehyde (Sigma). After fixation cells were washed 2x with PBS, then permeabilized and blocked with 300µl of blocking solution (10% serum-PBS-0.01% TritonX-100) incubating at room temperature for a minimum of 30 min. After blocking cells were washed 2x with PBS and incubated at 4^oC overnight with either 200µl of control or primary antibody re-suspended in PBS with 2% serum and Triton-X100 to reduce background signal. After primary antibody incubation samples were washed 3 x for 5 min with PBS/0.001% Triton-X100 and then incubated for 1 hour at room temperature with the appropriate FITC-conjugated secondary antibody re-suspended in PBS with 2% serum. Secondary antibody incubation was performed in the dark to protect the flurochrome from bleaching. Prior to mounting, cells were washed 3x with PBS/0.001% Triton-X100, after all liquid was removed the chambers were detached and one drop of VECTASHIELD mounting medium with 4',6-diamidino-2-phenylindole (DAPI) (Vector) was added to each well, one cover-slip was used per slide. Visualization was performed using the Zeiss AxioImager A1 fluorescent microscope. The serum used in washes matched the species of origin (Goat, horse or rabbit) of the secondary antibody.

2.6.4 MAF protein immunoprecipitation

500µg of total protein or nuclear extract from 293T or LEC was immunuoprecipitated for MAF using 2µl of M153 antibody (200µg/ml) (Santa Cruz), as a control samples were also precipitated with 10µl of rabbit IgG (200µg/ml) (Vector). These antibody concentrations had previously been experimentally defined to give equal concentration of IgG's. Protein lysates were made up to 1ml in RIPA+PI, 50µl of which was aliquoted and stored at -20^{o}C for subsequent Western blot analysis. Samples were pre-cleared with species and isotype matched IgG; 1µg of IgG per 500µg lysate and 20µl of protein A/G agarose beads (Invitrogen) were incubated at 4^{o}C with rotation for 30 min. A/G agarose beads were pelleted by spinning in a table top centrifuge at 2500rpm at 4^{o}C for 5 min, pre-cleared lysate was then transferred to a new 1.5ml Eppendorf tube, 20-50µl of which was aliquoted and stored at -20^{o}C. Pre-cleared lysate at a total volume of 1ml was incubated with either M153 or IgG antibody for a minimum of 1 hour at 4^{o}C with rotation, 20µl of protein A/G agarose beads were then added and incubated at 4^{o}C overnight with rotation. After precipitation, samples beads were pelleted by spinning in a table top centrifuge at 2500rpm at 4^{o}C for 5 min, the depleted supernatant was then removed and stored at -20^{o}C. Protein-bound beads were washed 4x in 1ml of RIPA buffer, spinning and pelleting the beads between each wash. Finally, beads were resuspended in 40µl of RIPA+PI, 10-25µl of which was resolved by Western blotting along with the other previously collected fractions which had been stored at -20^{o}C during the immunoprecipitation protocol.

2.7 Luciferase reporter assays

Luciferase assays were performed to assess miRNA activity from pSIN-K-Cluster in 293T cells and to quantify miRNA repression of the MAF 3'UTR in HeLa. Plasmids used in luciferase assays are detailed in Table 2.7.

For the miRNA activity 10^5 293T cells were seeded per 6-well, 24hours later increasing concentrations of pSIN-K-Cluster or empty pSIN-MCS vector were co-transfected using FuGENE (Roche) along with the 100ng of individual miRNA sensor vectors (pGL3-K-miR). miRNA sensor vectors were provided by Dr. R. Renne (University of Florida) (Samols et al., 2007), they contained two synthetic miRNA target sites inserted in tandem downstream of the firefly luciferase gene. For 3'UTR repression assays, the first 2.3kb of the MAF 3'UTR was cloned into the psiCheck-2 renilla reporter. 100ng of reporter plasmid (either wild type or mutated psi-MAF UTR) was co-transfected with 500ng of the KSHV miRNAs or empty lentiviral vector in $2.5x10^4$ HeLa cells.

DNA concentration was kept constant in all wells using the non-coding pGL3 basic vector (Promega). Cells were harvested 48hrs post transfection, luciferase activity was measured using the Dual-Luciferase Reporter Assay System (Promega) based on manufacturer's protocol. Cells were washed with PBS and lysed in 500µl or 250µl Passive Lysis Buffer per well of a 6-well or 12-well plate respectively, cells were incubated with shaking for 15 min at room temperature. 10µl of each sample was assayed in duplicate on a 96-well white non-transparent plate (Thermo Fisher Scientific). Plates were read using a Fluoroskan Ascent FL luminometer (Thermo Fisher Scientific), following the addition of 50µl firefly luciferase substrate after a 10 second lag. Subsequently, 50µl of Renilla luciferase substrate was dispensed into each well and luminescence measured. Luminescence was recorded as relative light units (RLU).

For the miRNA reporter assays luminescence was normalized to total protein as determined by Bradford assay based on manufacturer's protocol. This method of normalisation has been previously performed (Cannon et al., 2003). Firefly luciferase was normalized to total protein to account for any difference between samples due to differences in cell number or pipetting error. In the case of psi-MAF-UTR experiments, the psi-Check2 plasmid contained an internal firefly luciferase gene which was used to normalise renilla values, controlling for variations in transfection efficiencies as well as pipetting errors.

Plasmid	Reporter	Promoter	Supplier
pSIN-K-Cluster	n/a	SFFV promoter	n/a
pSIN-K-miR-X	n/a	SFFV promoter	n/a
pSIN-MCS	n/a	SFFV promoter	n/a
pGL3-T-miR-X	Firefly luciferase	SV40 promoter	n/a
psi-MAF-UTR	Firefly & renilla luciferase	Firefly – HSV-TK promoter Renilla – T7 promoter	Promega
pGL3 control	Firefly luciferase	SV40 promoter	Promega
pGL3-basic	Firefly luciferase	No promoter	Promega

Table 2.7 Plasmids used in luciferase assays. Promoters identified drive expression of either luciferase reporter or gene of interest. HSV-TK, herpes simplex virus-thymidine kinase. n/a not applicable.

2.8 siRNA transfections

LEC were seeded at a density of $5x10^4$ per 6-well 16hrs prior to transfection. 100nM of either MAF On-Target Plus SMARTpool or the On-Target plus Non-targeting Pool (Thermo Fisher Scientific) siRNA per well was transfected in 1ml of OPTI-MEM (Invitrogen) using Oligofectamine™ (Invitrogen), according to manufacturer's instructions. Four hours post transfection 1.5ml of LEC media was added per well, the media was then changed 24hrs post transfection. Cells were harvested 48, 72 or 96hrs post transfection and MAF mRNA levels assessed by qRT-PCR.

2.9 KSHV miRNA inhibition

KSHV miRNAs were inhibited using miRIDIAN microRNA Hairpin Inhibitor (Dharmacon) or LNA™ modified oligonucleotides (Exiqon).

$10^{\wedge 5}$ 293T cells were transfected in OPTI-MEM using oligofectamine™ with 0.4nM or 0.8nM miRIDIAN microRNA Hairpin Inhibitors designed against the mature miRNA sequence of miR-K12-11 or miR-K12-6-5p. Control cells were mock transfected with an equal volume of oligofectamine™ only. The day after transfection 50ng of luciferase sensor vector pGL3-T-miR11 and 500ng of lentiviral plasmid pSIN-K-miR11 or pSIN-MCS were cotransfected using oligofectamine™. Samples were harvested and luciferase activity quantified 48hrs post inhibitor transfection.

A similar protocol was adopted for the LNA-modified miRNA inhibitors, whereby $10^{\wedge 5}$ 293T cells were transfected in OPTI-MEM using oligofectamine™ with 10nM or 50nM of three different inhibitor designs against miR-K12-11. Control cells were mock transfected with oligofectamine™ only. The cells were then treated as described above.

$2x10^4$ LEC were infected with 1.5ml pSIN-MCS, pSIN-K-miR-6 or pSIN-K-miR-11, then 24hrs later transfected in OPTI-MEM using oligofectamine™ with 400nM miRIDIAN microRNA Hairpin Inhibitors designed against the mature miRNA sequence of miR-K12-6-5p and miR-K12-11 or a non-targeting control. Cells were incubated for 5hrs in the transfection mixture, 1ml of LEC media was then added per well. Alternatively, LEC were transfected with the inhibitors 24hrs prior to KSHV infection of LEC. All samples were harvested 48hrs post inhibitor transfection.

For the LNA inhibitors, $2x10^4$ LEC were transfected in OPTI-MEM using oligofectamine™, with 50nM of inhibitors designed against the mature miRNA sequence of miR-K12-6-3p, miR-K12-6-5p, miR-K12-8, miR-K12-11 or a non-targeting control. Three different inhibitor designs were tested per KSHV miRNA. Cells were incubated for 5hrs in the transfection mixture, 1ml of LEC media was then added per well. 24hrs post transfection, cells were washed and media changed. 48hrs post transfection LEC were infected with 1ml of KSHV, 24hrs post infection cells were harvested and MAF mRNA levels assessed by qRT-PCR.

2.10 Chromatin immunoprecipitation-PCR

ChIP was performed as previously described (Boyer et al., 2005), with the assistance of Dr. R. Jenner (Division of Infection and Immunity, UCL). $6.7x10^7$ 293T cells per ChIP were chemically crosslinked in 1ml of fresh 11% formaldehyde solution, per 10cm plate, for 15 min at room temperature. Cells were rinsed twice with PBS, harvested with a cell scraper and flash frozen in liquid nitrogen where they were stored until use. The fixed cell pellets were resuspended and lysed in lysis buffer plus protease inhibitor. DNA was then sonnicated to solubilise and shear crosslinked DNA. All pellets were processed

together in a single tube using the Misonix Sonicator 3000. Samples were sonnicated for a total of 5min at 24 Watts, for 30sec pulses with intermittent breaks of 1min at 4℃, samples were immersed in an ice bath during sonnnication. 100µl of cell lysate from each sample was aliquoted as input whole cell extract (WCE) and stored at -20^{o}C.

The remaining whole cell extract was incubated overnight at 4℃ with 100 µl of Dynal protein G magnetic beads per ChIP. The beads had been pre-incubated for 6-8hrs at 4^{o}C with 10µg of Rabbit IgG or RNA POL II or 20µg of M153 antibody. Antibody-bound beads were isolated out of solution using a magnet, washing three times with PBS/BSA in between bead isolation. The beads were then added to sonicated cell lysate and immunoprecipitated on a disc rotator overnight 4℃. Bound complexes were isolated using a magnet, the beads were then washed and complexes eluted from the beads by heating at 65℃ for one hour, vortexing every 10min. The beads were spun down and the supernatant transferred into a new tube, and incubated at 65^{o}C for 6-7hrs to reverse the DNA-protein crosslinking, whole-cell extract DNA was also treated for crosslink reversal.

Samples were then treated with RNaseA and proteinase K to destroy any RNA and protein and purify DNA. The DNA was then ethanol-precipitated overnight at -20^{o}C. DNA pellets were washed and air dried before being resuspended in 10mM Tris (pH8). The DNA concentration was determined using a NanoDrop UV spectrophotometer, WCE samples were normalised to 100ng/µl with 10mM Tris (pH8). Approximately 5ng/µl of DNA per ChIP was obtained and ~250ng/µl of WCE DNA.

Five fold serial dilutions of WCE DNA from 100ng/µl to 0.16ng/µl were qPCR amplified with each primer pair (Table 2.8), generating a linear standard curve whereby the threshold detection cycle directly corresponded to the amount of DNA in ng/µl. PCR primers were also used to amplify DNA precipitated in each of the three ChIPs. Using the threshold detection cycle, ng/µl of precipitated DNA

was extrapolated from the standard curve generated by the WCE. Fold enrichment was calculated by comparing ng/µl of precipitated DNA from the test antibody (RNA POL II or MAF) with that precipitated by the control Rabbit IgG antibody.

Target	Forward primer	Reverse primer
HDAC9 upstream	CACCCTCACAACCTTCCTGT	AGCAGGAGCGTTAGGTTTCA
HDAC9 928	TGTTCTATTTCTGTGCCTGTGG	CTAAAGCGAGTGATAATCCATTTG
HDAC9 1476	GAGCAGTGATGAATGTTTCATG	CCACCCCATCTGAGGAAA
HDAC9 1546	CGAGAGTGACTCCTGTTTTTCC	TGAGCTGATCATACTGTGCATTC
CD13	CTGTTGGAGCCCTGGTTAAT	CGGGCTTATATCCCCAAAG
Cyclin D2	GGGAGAGGCGAGACCAGTTT	CAGAAGGGAGAT

Table 2.8 PCR primers used to amplify chromatin immunoprecipitated DNA. Primers were designed against experimentally defined MAREs in CD13 (Mahoney et al., 2007) and Cyclin D2 (Hurt et al., 2004) or putative MAREs identified in the HDAC9 3'UTR. As a negative control primers were also designed against a region of HDAC9 lacking a putative MARE (HDAC9 upstream).

2.11 miRNA target prediction

miRNA target prediction was performed using PITA software (Kertesz et al., 2007) with the help of Dr. S. Henderson (CR-UK Viral Oncology group, UCL). The PITA algorithm was used to calculate both a single miRNA to target interaction score (ddG) and a cumulative score for multiple miRNA to target interactions. All 3' UTR sequences of genes which were expressed in LEC, as determined by previous GEM data (Lagos et al., 2007) were obtained from Biomart (http://www.ensembl.org/Multi/martview). The positions of potential KSHV miRNAs interactions were identified using the PITA algorithm according to the authors recommended formula:

http://genie.weizmann.ac.il/pubs/mir07/mir07_notes.html:

$$ddGsum = -\log(\Sigma(e^{-ddG}))$$

The strength of the interaction (ddGsum) was calculated, only those with an energetically favourable interaction, i.e. a negative ddG value were considered as potential KSHV miRNA targets. In order to minimise the number of false positives, only those potential interactions of 8mer target sites with either one G:U wobble or one mismatch but not both, were considered. The cumulative interaction scores for genes down-regulated in the presence of the KSHV miRNA Cluster were calculated for only those KSHV miRNAs that were found to be significantly expressed in AIDS-KS relative to skin.

2.12 Gene set enrichment analysis (GSEA)

GSEA (Subramanian et al., 2005) was used to assess the enrichment of a gene set within a GEM experiment and was performed by Dr. S. Henderson (CR-UK, Viral Oncology group, UCL) on three GEM data sets generated by myself (LEC-Cluster and LEC-siMAF) or previously by Dr. D. Lagos (KLEC) (CR-UK Viral Oncology group, UCL) (Lagos et al., 2007). Briefly, the GSEA method compares an experimental dataset to a set or sets of genes of interest (Mootha et al., 2003; Subramanian et al., 2005). In this case, the experimental datasets were GEM profiles and the gene set of interest were BEC or LEC specific genes as determined by comparing LEC and BEC expression profiles. Lists of 50-250 genes, increasing in 50 gene increments, were analysed. This method firstly determines whether the order of the set of interest is random within the sorted experimental dataset, that is whether the set of interest is significantly correlated within the experimental dataset assigning a false discovery rate (FDR) q-value based on a permutation test. The resulting Enrichment Score (ES) is a metric of the skew of a gene set within the rank of genes sorted by their GEM expression difference. Secondly, if the gene set is significantly correlated it finds a 'leading edge' or subset of the genes that form a 'core' of the most significantly changed genes. Leading edge genes are the subset that contributes most to the ES.

2.13 Statistical analysis

Standard deviation (SD) was used to calculate the error bars for *in vitro* experiments. SD is the square root of the variance (σ^2), it is a measure of the spread of a particular distribution and indicates how much variability there is about the mean. It is used to measure the variation between sample values:

$$\sigma = \sqrt{\sigma^2} \qquad \sigma 2 = \frac{\sum (x - \mu) 2}{\mathrm{N}}$$

(Where X is a sample value and μ is the mean of the sample values)

To determine whether the difference between two experimental conditions was significant (except in GEM analysis, where the FDR was used) p values were calculated using a two-tailed Student's t test. The difference was considered significant if $p < 0.05$.

Chapter 3. Identification of KSHV miRNA targets

3.1 Introduction and aims

The aim of this chapter was to establish an experimental system in which to identify the cellular targets of the KSHV-encoded miRNAs. Specifically, to discover target genes deregulated in LEC, the closest cell type to the KS spindle cell (Wang et al., 2004). To achieve this aim a combination of experimental and in silico analysis techniques were employed. The viral miRNA expression profile in KS lesions was determined in order to refine analysis to miRNAs relevant to KS biology.

Previously, a subset of cellular KSHV miRNA targets were identified in latently infected B cells and 293 cell lines (Samols et al., 2007; Ziegelbauer et al., 2009; Gottwein et al., 2007; Skalsky et al., 2007). To date there has been no investigation into KSHV miRNA targets in LEC. Since miRNA targets are likely to be highly cell context dependant, identification of mRNAs deregulated in LEC through the action of KSHV-encoded miRNAs may generate more relevant insight into the functional roles of the KSHV miRNAs during primary infection and KS pathogenesis.

miRNAs act to subtly suppress expression of their target mRNAs and, subsequently, modulate the proteome of the cell in which they are expressed (Baek et al., 2008; Selbach et al., 2008). miRNAs exert their effect by inducing small fold-changes in the steady state levels of multiple mRNAs, such changes in mRNA abundance can be quantified by GEM analysis (Lim et al., 2005; Krutzfeldt et al., 2005). To identify changes in mRNA abundance attributed solely to the KSHV miRNAs it was necessary to work with the viral DNA encoding the miRNAs in isolation. Previously in our laboratory, an HIV-based lentiviral vector system was established to study the function of individual KSHV genes in LEC (Vart et al., 2007). Employing this system, the KSHV miRNA Cluster was cloned into the lentiviral vector to permit LEC target identification. This lentiviral system has proven efficacious in expressing exogenous genes in LEC (Naldini et al., 1996; Lagos et al., 2007; Vart et al., 2007), as lentiviruses can infect both dividing and non-dividing cells, an advantage when working with slowly dividing primary cells (Naldini et al., 1996). Transduction of LEC with lentiviral vectors permits delivery of exogenous DNA to primary cells that are sensitive to transfection reagents such as Oligofectamine and FuGENE. In addition, following infection, lentiviral-encoded RNA is reverse transcribed into DNA which inserts into the host genome, allowing stable expression. The resultant expression levels are also more physiologically relevant than those obtained after plasmid transfection.

The KSHV miRNA expression profile has been extensively characterised in latently infected tumour cells (Cai et al., 2005; Samols et al., 2005; Pfeffer et al., 2005); at the onset of this work expression of the KSHV viral miRNAs had not been confirmed in KS lesions. miRNA microarray profiling was performed to confirm and characterise viral miRNA expression in KS lesions, identifying miRNAs which were of relevance to KS pathogenesis. To identify cellular targets not picked up by the array, in silico miRNA target prediction analysis was performed using the publically available prediction algorithm PITA (Probability of Interaction by Target Accessibility) (Kertesz et al., 2007). PITA identifies putative

miRNA targets according to a defined set of criteria that are primarily miRNA-target seed sequence complementation and thermodynamic feasibility of binding. Target prediction analysis was only applied to those miRNAs expressed in KS lesions, restricting analysis those miRNAs relevant to the disease.

3.2 KSHV miRNA expression in Kaposi sarcoma

The KSHV miRNA profile of five AIDS-KS lesions was characterized using Agilent miRNA microarray profiling. The aim was to determine the expression profile of the KSHV miRNAs, therefore three KSHV-negative skin biopsies were used as controls, allowing a baseline to be set for viral miRNA detection in samples lacking the viral genome. KS biopsies are largely comprised of spindle cells, whereas skin biopsies contain additional cell types as well as LEC. For this reason skin is not an optimal comparison for profiling experiments analysing global gene expression; however, in the context of this experiment, the essential criterion was the absence of KSHV infection in control tissue so that viral miRNA expression could be compared, therefore skin was deemed an acceptable control tissue. Normal skin was harvested from three participants with AIDS-KS at sites distal from any obvious KS lesions and qRT-PCR for viral gene expression confirmed KSHV infection of the KS biopsies (Fig. 3.1A). LANA was detected in all KS biopsies, whereas the key lytic reactivator ORF50 was detected at a lower level in four out of five biopsies (Fig. 3.1A). This difference in viral gene expression reflects increased proportion of KS spindle cells that are latently infected with KSHV, with only 5% undergoing lytic replication (Staskus et al., 1997). No viral gene expression was detected in the skin biopsies, confirming their KSHV negative status (Fig. 3.1A). Since the miRNA fraction is often lost or degraded during sample preparation it was important to confirm the quality and quantity of RNA prior to profiling. The miRNA content of RNA extracted from all KS and skin biopsies was assessed using the Agilent small RNA kit (Fig. 3.1B

and C). The Bioanalyzer (Agilent, California) identified samples with sufficient miRNA content and only this RNA was included in further processing for miRNA profiling (Fig. 3.1C).

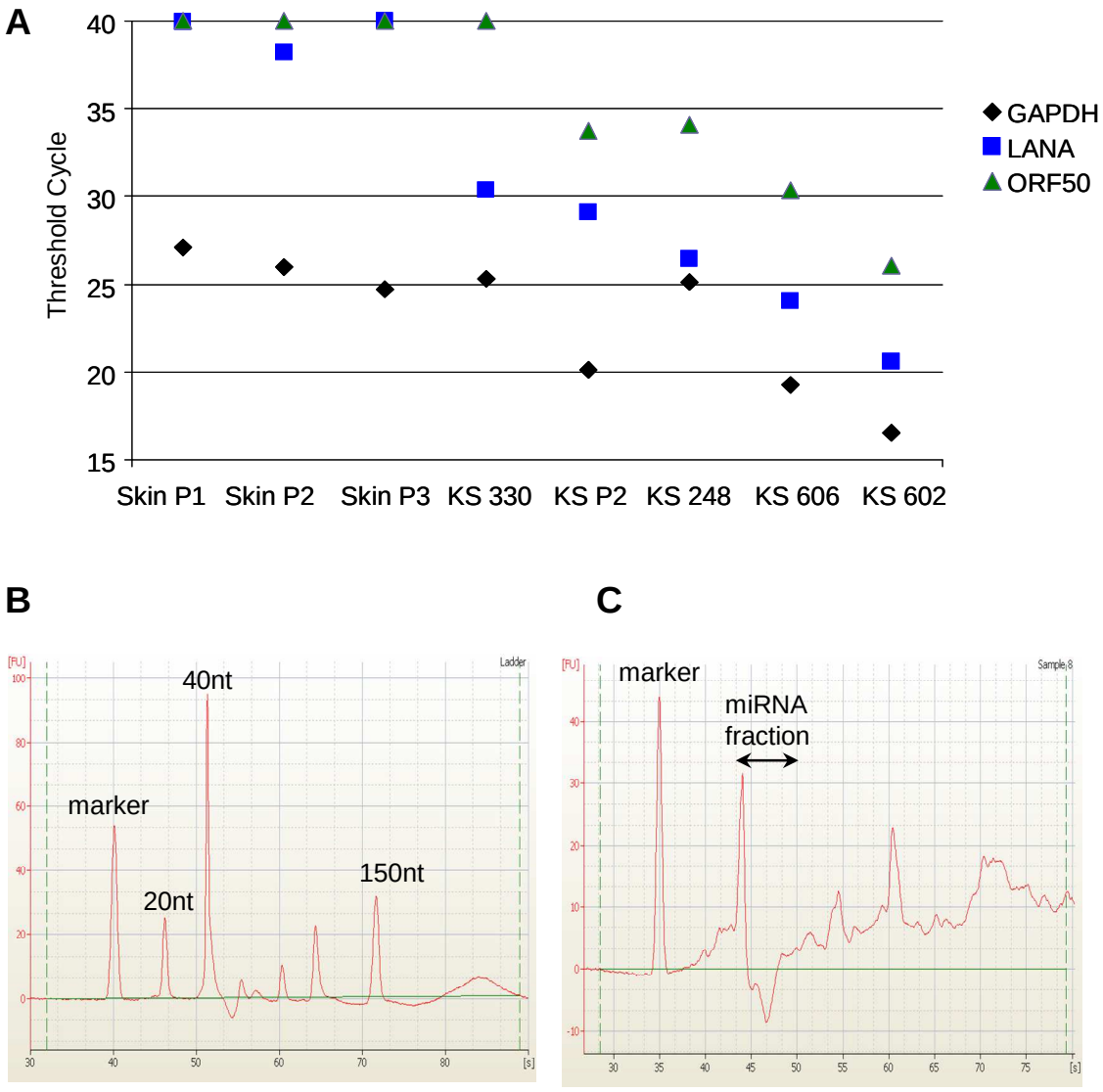

Figure 3.1. Skin and KS biopsies used for miRNA profiling. *A* Viral gene expression was detectable in Kaposi sarcoma, but not in uninfected skin biopsies. qRT-PCR detection of KSHV-encoded genes LANA and ORF 50, and cellular housekeeping gene GAPDH. The threshold cycle of detection is shown. Expressed transcripts have a threshold cycle of less than 35. Values for all skin and KS biopsies profiled are shown. *B* An electropherogram of the small RNA ladder used to quantify the miRNA fraction of total RNA to be profiled. The size of the RNA molecule is proportional to the time taken for fractionation [S]. Peaks corresponding to 20nt, 40nt and 150nt are indicated. *C* Representative electropherogram of total RNA extracted from tissue. Mature miRNAs are ~22nt long, and fractionated between 45-50s. Peak height corresponds to proportion of RNAs within total RNA.

Expression levels of individual KSHV miRNAs from all KS biopsies and normal skin are shown in the boxplots describing the $\log_2$ expression levels (Fig. 3.2A and 3.3A). Each participant had a different viral load and therefore participants express varying levels of KSHV miRNAs. This is reflected in the spread of the data and by the presence of sample outliers. Those miRNAs with significant differential expression between skin and KS are shown in figure 3.2A. Ten out of the 17 mature viral miRNAs had significantly higher expression in KS lesions than in uninfected skin and were therefore classed as expressed (Fig. 3.2A). miR-K12-4, miR-K12-1, miR-K12-11 and miR-K12-6-5p show the most significant differential expression (Fig. 3.2A).

To confirm the viral miRNA microarray data, qRT-PCR quantification of the mature form of KSHV miRNAs was performed (Fig. 3.2B). The difference in threshold detection cycle (delta Ct) between each KSHV miRNA and RNU66 is shown in both KS lesions and skin. RNU66 is a small nucleolar RNA whose expression does not vary between KSHV infected and uninfected tissue. Therefore, in a similar manner to the cellular housekeeping gene GAPDH, RNU66 is used as a loading control for normalisation. Viral miRNAs with a delta Ct of greater than zero are detected at earlier PCR cycles and are therefore more abundant than RNU66. miRNAs expressed in KS lesions were largely undetectable after 40 cycles of amplification in normal skin samples, generating a delta Ct of -8 (Fig. 3.2B). miR-K12-10a was amplified in KSHV negative tissue generating a higher delta Ct than other viral miRNAs (Fig. 3.2B). However, there was a significant difference in the delta Ct of miR-K12-10a between skin and KS. Detection of miR-K12-10a above background levels detected in skin, suggests this miRNA is expressed in KS lesions.

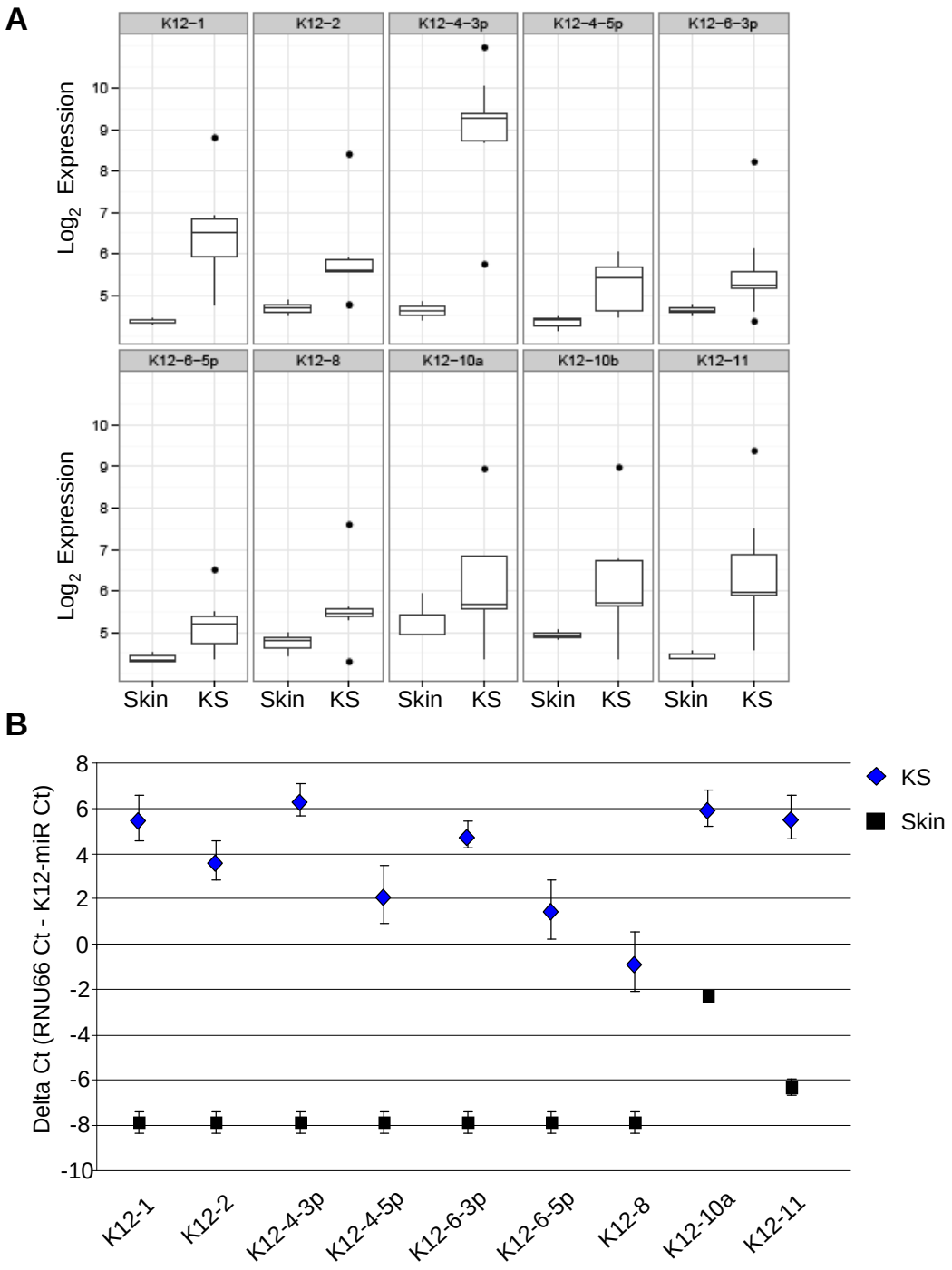

Figure 3.2. Differential expression of KSHV miRNAs in KS lesions *A* miRNA microarray $\log_2$ expression values of significantly expressed miRNAs in KS biopsies (relative to KSHV-negative skin, $p<0.05$). Boxplots show the median, interquartile boxes, 95th percentile range, and outliers as points. Five AIDS-KS biopsies and three KSHV-negative reference skin samples were profiled. *B* qRT-PCR confirmation of the miRNA profiling data. All miRNAs assayed were expressed at higher levels in KS lesions compared to normal skin. Values were normalised to RNU66. The delta Ct represents the difference in threshold detection cycle between RNU66 and viral miRNA. Viral miRNAs were undetectable in skin biopsies. Error bars correspond to standard deviation, n: 5 KS biopsies; 3 normal skin.

Agilent miRNA profiling failed to detect significant differential expression of the remaining seven mature KSHV miRNAs between KS and skin samples (Fig. 3.3A). Five viral miRNAs (miR-K12-3*, miR-K12-5, miR-K12-9, miR-K12-9* and miRK12-12) were undetectable in KS lesions and were therefore classed as unexpressed (Fig. 3.3A). miR-K12-3 and miR-K12-7 cross-reacted in both KSHV positive and negative samples, making it difficult to confirm their expression (Fig. 3.3A). qRT-PCR for miR-K12-3, miR-K12-9 and miR-K12-9* failed to detect these miRNAs in KS tissues, confirming the miRNA microarray data (Fig. 3.3B). However, miR-K12-5 and miRK-12-12 were detected in KS lesions by qRT-PCR (Fig. 3.3B). This discrepancy may be due to a higher detection threshold of the qRT-PCR assay or as a consequence of miRNA microarray probe design. A naturally occurring polymorphism exists in the precursor stem-loop of miR-K12-5 which inhibits Drosha processing and leads to diminished levels of the mature miRNA (Gottwein et al., 2006). It is possible that KS biopsies were infected with a viral strain possessing this polymorphism and that miR-K12-5 is present at low levels. Similar to the miRNA microarray data, miR-K12-7 amplified in both KS and KSHV negative skin samples; therefore it was not possible to confirm expression of this miRNA in KS lesions (Fig. 3.3B). However, significant differential expression of miR-K12-3 was detected in KS above the background levels detected skin, suggesting this miRNA may be expressed (Fig. 3.3B).

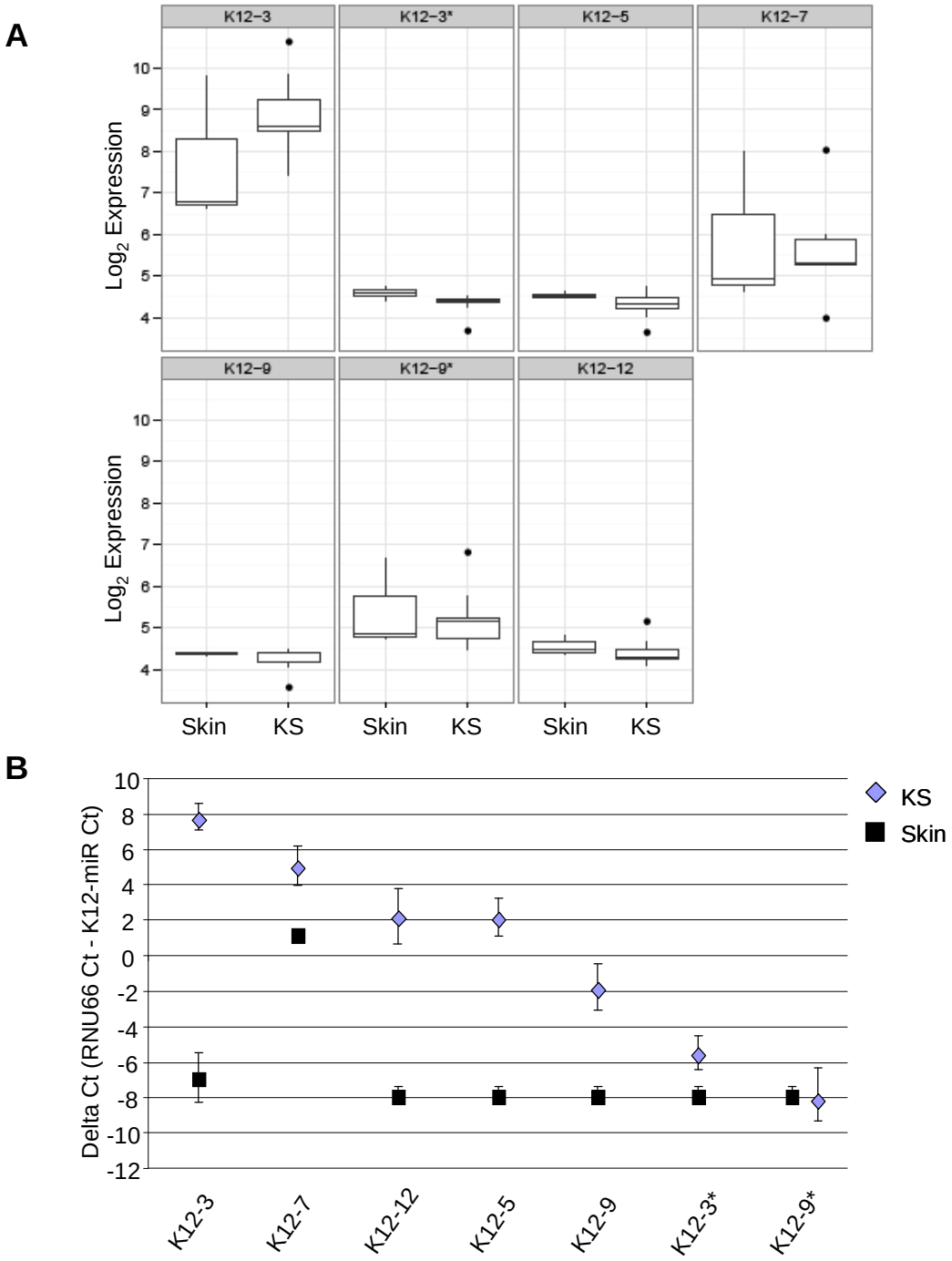

Figure 3.3. KSHV miRNAs not expressed in KS lesions. The microarray log_2 expression value of KSHV miRNAs whose expression is not significantly differ between KS and KSHV negative skin ($p>0.05$). miR-K12-3 and miR-K12-7 both show high background levels in uninfected skin samples. The remaining miRNAs are undetectable in KS lesions. Boxplots show the median, interquartile boxes, 95th percentile range, and outliers as points. Five AIDS-KS biopsies and three KSHV-negative reference skin samples were profiled. *B* qRT-PCR quantification of the KSHV miRNAs whose expression did not significantly differ between KS and skin biopsies. Contrary to the miRNA microarray data miR-K12-3, miR-K12-5 and miR-K12-12 were detectable in KS lesions, but not in KSHV negative skin. Similar to the miRNA profiling data, miR-K12-7 was detected in both KS and skin. The remaining miRNAs were undetected in KS lesions. Values were normalised to RNU66. The delta Ct represents the difference in threshold detection cycle between viral miRNA and RNU66. Error bars correspond to standard deviation, n: 5 KS biopsies; 3 normal skin.

3.3 Sub-cloning the KSHV miRNAs

KSHV encodes 17 mature miRNAs which are generated from 12 pre-miRNAs (Fig. 3.4A). Ten of these pre-miRNAs, generating 14 mature miRNAs, are organised as a Cluster located in the latency-associated region of the genome, in an intergenic region between vFLIP and Kaposin (Fig. 3.4A). The other two pre-miRNAs are located further upstream. miR-K12-10 is unusual due to its location within the Kaposin ORF, processing of miR-K12-10 generates two isoforms referred to as miR-K12-10a and b. miR-K12-12 is located upstream of the Kaposin ORF (Fig. 3.4A).

Previously, nucleotides 119,365 to 122,481 from the KSHV genome had been cloned into the pcDNA3.1/V5/HisA vector (Samols et al., 2007). This construct, along with a subset of individual KSHV pre-miRNAs, also in the context of pcDNA3.1/V5/HisA, were provided by Dr. R. Renne (University of Florida). The individual pre-miRNA vectors consisted of 200 nucleotides surrounding the pre-miRNA (Samols et al., 2007). To allow expression in the lentiviral system, the KSHV miRNA Cluster and individual miRNAs were excised from the pcDNA plasmid by restriction digest with BamHI and NotI; the digested DNA fragments were ligated into the similarly cut pSIN-MCS vector. Subsequent restriction enzyme digestion confirmed the presence of inserts of the correct size in pSIN-K miR vectors (Fig. 3.4B). The sequence of the miRNA insert was confirmed by DNA sequencing, only plasmid DNA with miRNA inserts lacking mutations were used.

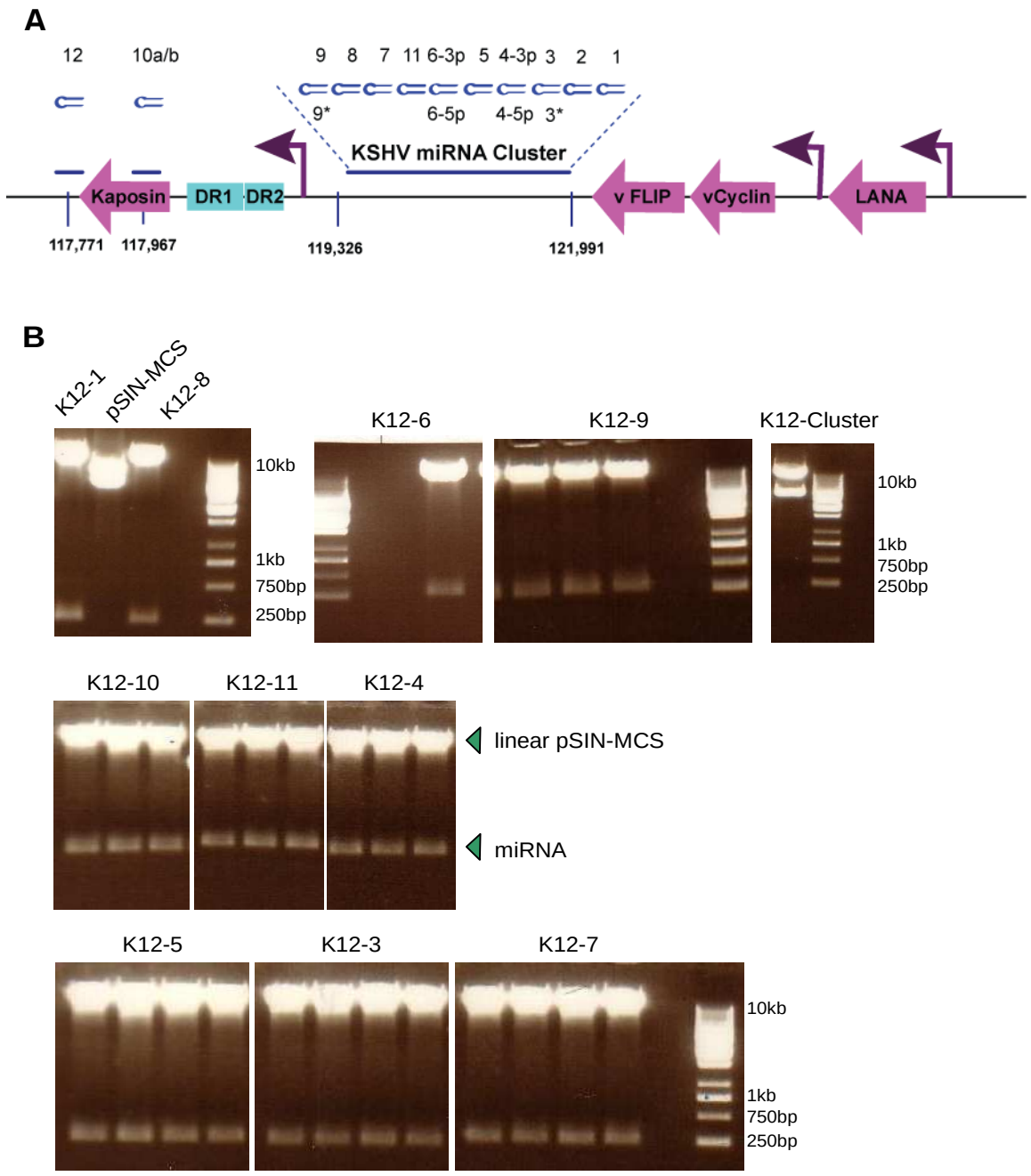

Figure 3.4. Restriction enzyme digestion of pSIN-MCS constructs. *A* Schematic showing the genomic organisation of KSHV miRNAs in the latency-associated region of the viral genome. The KSHV miRNAs are indicated by horizontal blue lines with the genomic locations noted below. Individual KSHV miRNA hairpins are shown above. Promoters are represented by dark purple arrows, protein coding open reading frames are shown in pink. The Kaposin open reading frame is preceded by two sets of direct repeats (Blue rectangles, DR1 and DR2). *B* ~1µg of pSIN-MCS constructs were digested with BamHI and NotI to excise the cloned KSHV miRNA from pSIN-MCS. The top band is empty linearised pSIN-MCS and bands running at ~200bp are the excised pre-miRNAs. Uncut pSIN-MCS was run with K12-1 and K12-8, this plasmid DNA is supercoiled and therefore runs faster than linearised vector.

3.4 KSHV miRNA activity from pSIN-K-Cluster

It was necessary to confirm the cloned miRNAs were expressed from the lentiviral vectors and capable of silencing. miRNA activity was assessed using reporter vectors containing two inverse copies of individual miRNA target sites located downstream of the luciferase firefly coding sequence in the 3'UTR (Luciferase plasmids provided by Dr. R. Renne, [Samols et al., 2007]). miRNA-mediated silencing reduces levels of the firefly luciferase enzyme, the magnitude of silencing is quantified by the reduction in light emitted after addition of luciferase enzyme substrate. The resistance of LEC to transfection necessitated these assays being performed in 293T cells where the reporter constructs could be expressed.

Increasing concentrations of pGL3 control plasmid, that lacks KSHV miRNA target sites, were transfected into 293T cells to determine the range of sensitivity and concentration of sensor vectors to be used when testing KSHV miRNA expression (Fig 3.5). The standard curve of luminescence is linear from 6µg to 78.14ng of pGL3 control plasmid, therefore low concentrations of plasmid can be transfected and accurately quantified (Fig 3.5). 100ng was selected as the optimal concentration of miRNA sensor vector. To determine the concentration of miRNA-expressing lentivirus at which miRNA silencing is detected, increasing concentrations of pSIN-K-miR11 with 100ng of pGL3-T-miR-11 were titrated (Fig. 3.6A). A reduction in luminescence was detected with 50ng of pSIN-K12-11 when compared to control pGL3 plasmid. Increasing concentrations of miRNA-expressing plasmid induced a corresponding decrease in luminescence, confirming cloned miR-K12-11 was expressed and capable of silencing target sites (Fig. 3.6A). 500ng of pSIN-K-miR11 caused a 97% reduction in luciferase activity compared to pGL3 control (Fig. 3.6A); this concentration of miRNA-lentiviral vector was used in all subsequent experiments.

A time-course experiment was performed to determine the time at which maximal miRNA silencing occurred. 500ng of pSIN-K-miR11 and 100ng of sensor vector pGL3-T-miR-11 were co-transfected into 293T cells and luciferase activity measured 24, 48 and 72hrs post-transfection (Fig. 3.6B). Maximal repression was detected 24hrs post-transfection, silencing persisted until 72hrs (Fig. 3.6B). Forty-eight hours post-transfection, pSIN-K-miR11 induced an 87% reduction in luciferase activity compared to empty lentiviral vector (Fig. 3.6B). In some instances the miRNA expression vector had to be transfected and then on the following day the sensor vector was transfected. Therefore, although maximal repression was observed 24hrs post transfection, to ensure consistency, all luciferase assays were harvested 48hrs post-transfection.

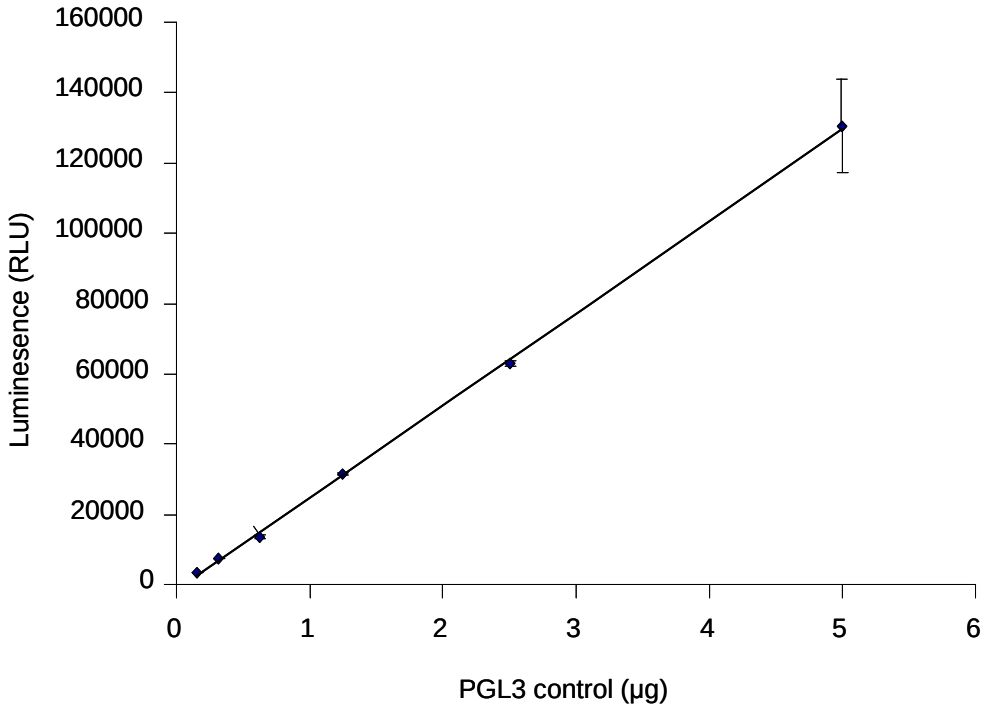

Figure 3.5. Luciferase activity standard curve. Increasing concentrations of pGL3 control plasmid were transfected into 293T cells. The standard curve is linear from 6µg to 78.14ng of transfected plasmid DNA, therefore plasmids can be transfected within these concentrations and accurately quantified. RLU: relative light units. Error bars correspond to standard deviation, n = 3.

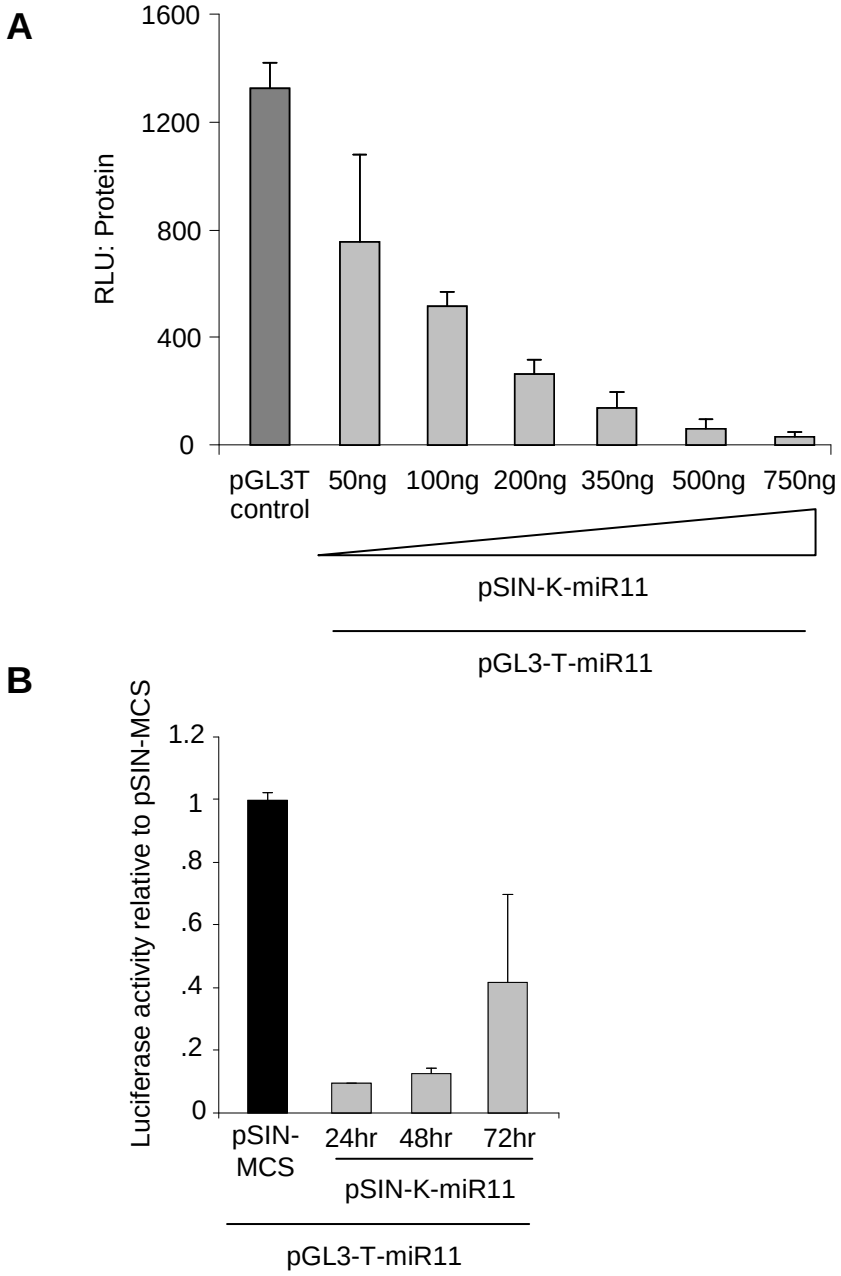

Figure 3.6 KSHV miRNA-mediated reporter silencing. *A* Increasing concentrations of pSIN-K-miR11 silenced synthetic luciferase reporter vector pGL3-T-miR11. 293T cells were co-transfected with 0ng, 250ng or 500ng of pSIN-K-miR11 plasmid and KSHV miRNA sensor vectors. Relative light units (RLU) were normalised to total protein content and the ratio shown. *B* Maximal silencing occurs 24hrs post pSIN-K-miR11 transfection. 293T cells were co-transfected with pSIN-K-miR11 and pGL3-T-miR11 and harvested 24, 48 or 72hrs post transfection. Relative light units (RLU) were normalised to total protein content and the ratio relative to pSIN-MCS is shown. Error bars correspond to standard deviation, n = 3.

Sensor vectors for nine out of 17 mature KSHV miRNAs were provided by Dr. R. Renne (University of Florida). For those mature miRNAs that generated two effector miRNAs, one sensor was constructed. miR-K12-2 was the only miRNA not to have a sensor vector for either branch of the mature miRNA. To test KSHV miRNA activity from pSIN-K-Cluster, increasing plasmid concentrations were transfected in the presence of 100ng of individual miRNA sensor vector (Fig 3.7); this induced a corresponding decrease in luciferase activity for all sensor vectors tested (Fig. 3.7). These data confirm KSHV miRNA expression and activity from the pSIN-K-Cluster lentiviral vector.

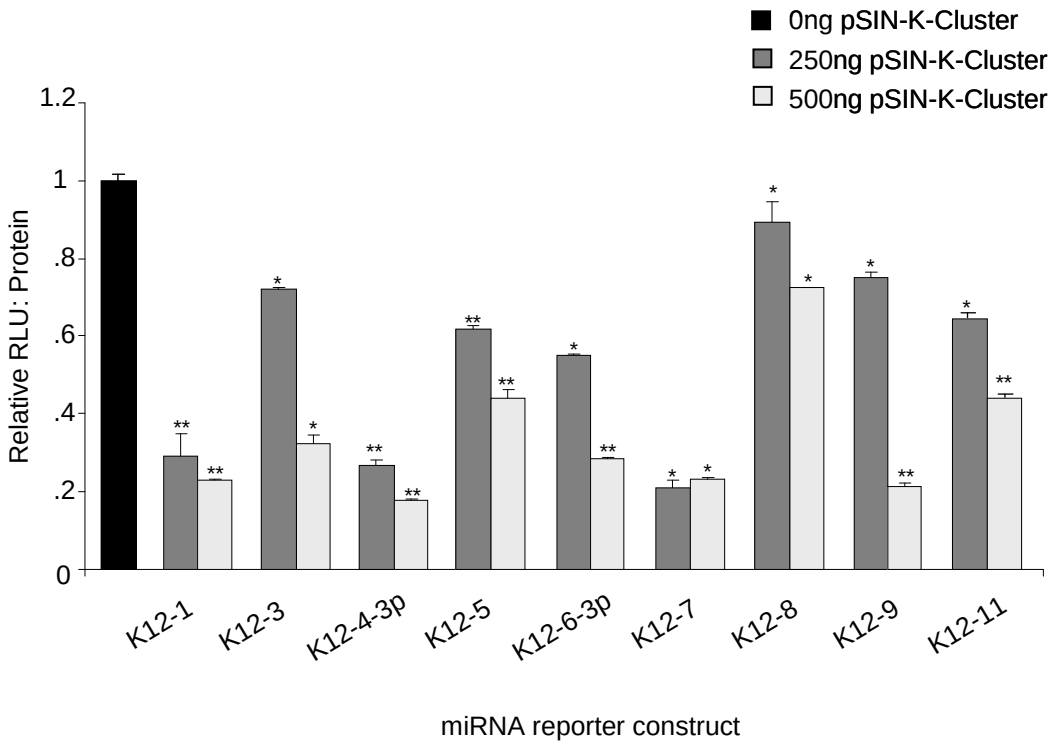

Figure 3.7. KSHV miRNAs expressed from pSIN-K-Cluster silence reporter constructs. 293T cells were co-transfected with 0ng, 250ng or 500ng of pSIN-K-Cluster plasmid and KSHV miRNA sensor vectors. Luminescence (RLU) was normalised to total protein content and the ratio is shown. Increasing concentration of pSIN-K-Cluster corresponds to decreased RLU:Protein ratio. P values (Student's T-test) relative to 0ng pSIN-K-Cluster: *<0.05 **<0.005. Error bars correspond to standard deviation, n = 3.

3.5 KSHV miRNA expression from pSIN-K-miR

miRNA Cluster-encoding lentivirus was produced in 293T cells after transfection of pSIN-K-Cluster vector and the two packaging plasmids, p8.91 and pMD.G. The infectivity of lentiviral preparations was determined by qPCR for the lentiviral packaging signal. LEC were initially infected with 1ml of un-concentrated lentivirus, which yielded 0.81 lentiviral copies per cell (c/c) (Fig. 3.8A). This confirmed the Cluster lentivirus was infective and capable of integrating into the host cell genome. There are approximately ten viral genomes per latently infected KS spindle cell (Asahi-Ozaki et al., 2006), thus a lentiviral titre of approximately ten c/c was used to achieve expression levels comparable to KS spindle cells. Various optimisation steps were performed to increase the lentiviral copy number (Fig. 3.8A). Viral preparations were concentrated 10-fold, leading to increased viral titre; all subsequent experiments were performed with concentrated lentivirus. Lentivirus-containing supernatant was harvested from 293T cells between 48-72hrs post-transfection. To determine whether harvesting at a later time point would yield more concentrated viral preparations, virus was harvested at both 48 and 72hrs post-transfection and c/c compared. Harvesting virus 72hrs post-transfection led to an increase in titre (Fig. 3.8A). However, infecting cells with 0.5ml of virus from both time points did not result in increased infection (Fig. 3.8A). Based on these optimisation steps, harvesting at 72hrs post-transfection and infecting LEC with 1.5ml of Cluster-expressing lentivirus achieved the highest titre (Fig. 3.8A).

To confirm KSHV miRNA expression in LEC transduced with pSIN-K-Cluster, miRNA expression was quantified by qRT-PCR for the mature form of the miRNA. This method is preferable to assaying early precursor miRNA forms as the mature miRNA is directly responsible for silencing, and in general in higher abundance than the precursor. Furthermore, due to differences in processing or stability, levels of pre or pri-miRNA are not always synonymous with levels of mature

miRNA. At the time of this work there existed no commercially available qRT-PCR assays for the KSHV miRNAs. Therefore, the sequence of all KSHV mature miRNAs was taken from miRBase (www.mirbase.org/) and provided to Applied Biosystems™ (California, USA) who designed and synthesized custom TaqMan assays.

Using optimized experimental conditions, KSHV miRNA expression was assessed. The difference in threshold detection cycle (delta Ct) between each KSHV miRNA and RNU66 is shown (Fig. 3.8B). Viral miRNAs with a delta Ct of greater than zero are detected at earlier PCR cycles and are therefore more abundant than RNU66 (Fig. 3.8B). The majority of mature viral miRNAs were expressed from the lentiviral vector. qRT-PCR of two miRNAs, miR-K12-10a and miR-K12-12, not present in the Cluster generated a delta Ct of less than -4.8. Typically one strand of the mature miRNA is preferentially loaded into the RISC complex and consistently used as the guide strand, the other passenger strand is degraded; miRNA cloning strategies may sometimes identify two guide miRNAs from the same mature miRNA (Bartel, 2009). Relative abundance of the cloned miRNAs indicate the predominately expressed miRNA, in this case the less abundant form is denoted with a *. This has been reported for miR-K12-3* and miR-K12-9* (Pfeffer et al., 2005). However, the qRT-PCR data presented here (Fig. 3.2 and 3.3) indicated that these miRNAs had delta Ct values of less than -4.8, which is comparable with miRNAs not present in the Cluster and suggests that these miRNAs were not expressed. When cloning data identify equal abundances for both arms of the mature miRNA, these miRNAs are denoted by “3p” or “5p” to indicate from which arm of the mature miRNA they originated. This was observed for KSHV miR-K12-6 and miR-K12-4 (Pfeffer et al., 2005). Concurring with the nomenclature, both isoforms of miR-K12-6 and miR-K12-4 were detected in Cluster expressing LEC.

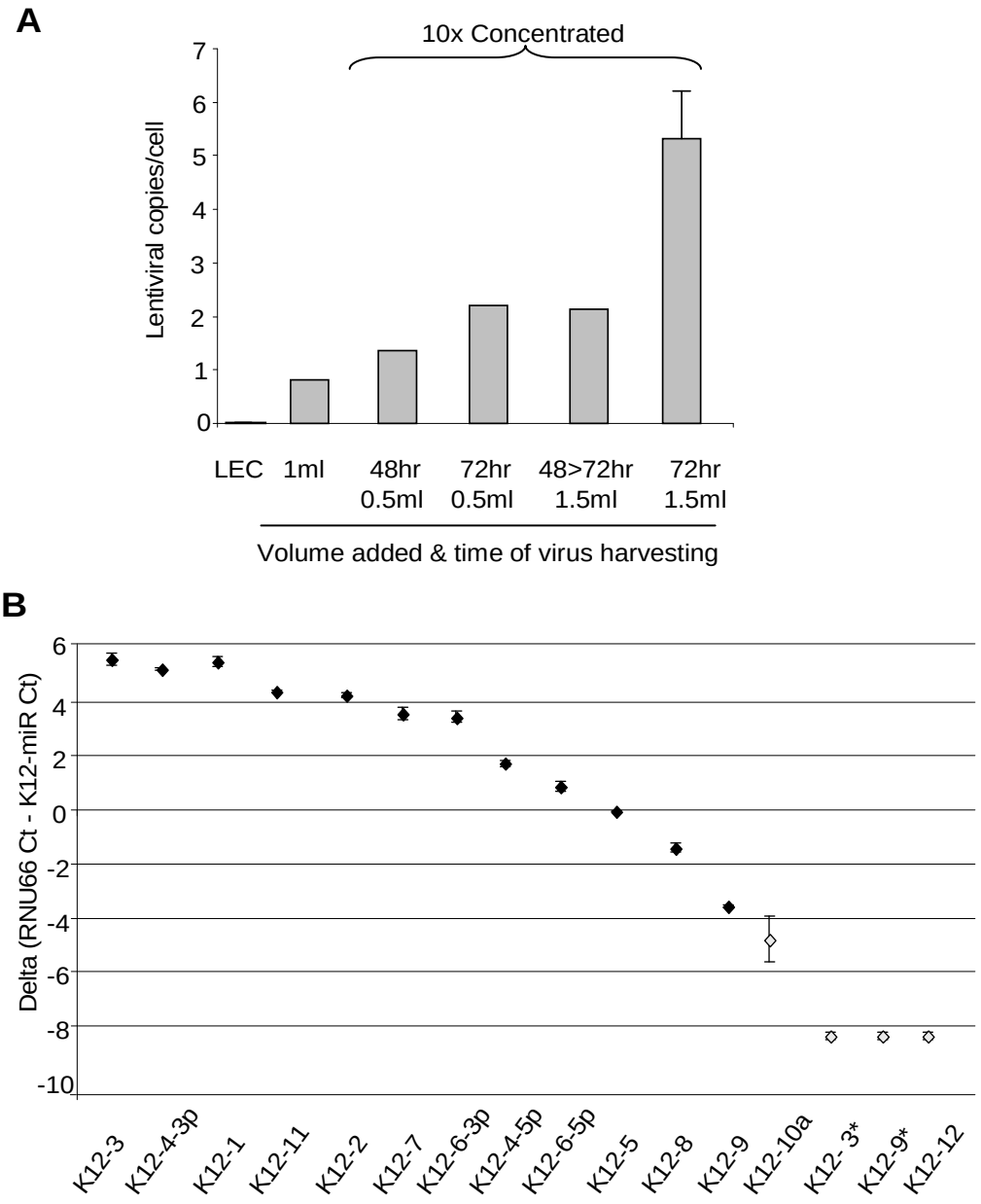

Figure 3.8. LEC transduced with the KSHV miRNA Cluster. *A* Optimisation of Cluster lentivirus infection. Lentiviral copies per cell in LEC transduced with Cluster lentivirus as determined by q-PCR for lentivirus packaging signal and GAPDH. The time of lentivirus harvesting (hr) and the volume of virus (ml) added to 10^5 LEC is shown. Harvesting 72hr post transfection and infecting LEC with 1.5ml of virus yielded the highest lentivirus c/c. 48>72hr 1.5ml: 0.5ml of virus harvested at 48hrs was added, plus 1ml of virus harvested at 72hrs post transfection. *B* qRT-PCR quantification of mature KSHV miRNAs in LEC transduced with KSHV miRNA Cluster. Delta Ct represents the difference in threshold detection cycle between viral miRNA and RNU66. Higher delta Cts correspond to more abundant transcripts. miR-K12-10a and miR-K12-12 are not present in the Cluster, KSHV miRNAs K12-3* and K12-9* which have delta Ct of less than -4 are therefore classed as unexpressed (grey diamonds). Error bars correspond to standard deviation, n = 3.

3.6 KSHV miRNAs induce changes in LEC gene expression

miRNAs regulate their targets by inducing mRNA degradation, such changes in mRNA steady-state levels are quantifiable by GEM profiling (Lim et al., 2005; Ziegelbauer et al., 2009). To detect targets of the KSHV miRNAs whose expression was regulated by mRNA degradation, the GEM profile of LEC transduced with KSHV miRNA Cluster was compared to LEC expressing empty lentiviral vector (Fig. 3.9). An average viral titre of approximately 12 c/c was achieved, as confirmed by qPCR (Fig. 3.9). Although this approach included the majority of KSHV miRNAs, it will not detect those genes deregulated by the three mature miRNAs encoded outside the Cluster.

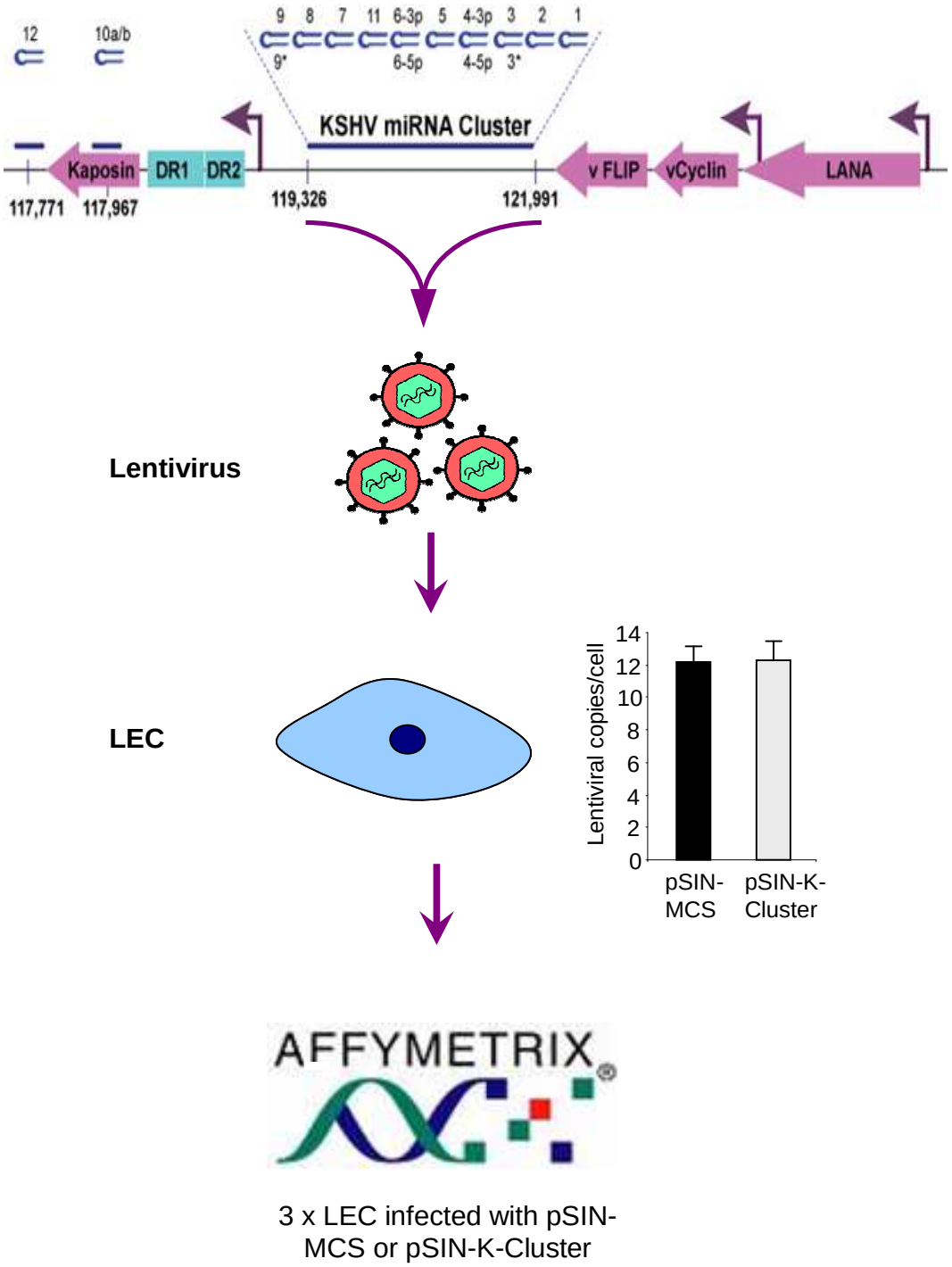

Figure 3.9. Experimental overview of KSHV miRNA Cluster GEM profiling. Schematic representation of KSHV miRNA organization in the latency-associated region of the viral genome. Nucleotides 119,326-121,991 were cloned into pSIN-MCS lentiviral vector. Cluster and empty vector lentivirus were produced and used to infect LEC. Three independent infections per condition at a lentiviral titre of ~12 copies per cell were profiled using Affymetrix Human Genome U133 Plus 2.0 Arrays. Error bars correspond to standard deviation, n = 3.

GEM analysis was performed on RNA from three independent infections per condition using Human Genome U133 Plus 2.0 Affymetrix arrays. Probes significantly deregulated ($q<0.13$) across all samples are shown in Figure 3.10A. Down-regulated probes represent candidate KSHV miRNA target genes. As observed in other studies of this kind, numerous small fold-changes in gene expression were detected, ranging from 25-50% down-regulation, this is in accordance with the fine tuning nature of viral miRNA silencing (Appendix 1) (Ziegelbauer et al., 2009). In addition to decreases in gene expression, a number of probes were up-regulated in the presence of the KSHV miRNA Cluster (Fig. 3.10A). These changes may be a secondary effect induced by miRNA silencing of an upstream repressor. Alternatively, contrary to the dogma of miRNAs as negative regulators of gene expression there have been contentious reports of miRNA-induced up-regulation (Vasudevan et al., 2007; Ghosh et al., 2008; Place et al., 2008). Therefore, it can not be excluded that the up-regulated probes are also direct KSHV miRNA targets. Over-expression of the KSHV miRNAs may saturate the silencing machinery, this would alleviate silencing of endogenous miRNA targets. Therefore, the up-regulated genes may be targets of endogenous miRNAs highly expressed in LEC. Previously this effect was shown to be a consequence of over-expressing miRNAs (Khan et al., 2009). Further work will be needed to determine the mechanism behind these observed increases in mRNA abundance.

The top three down-regulated probes were H19 (imprinted maternally expressed transcript), MAF (v-maf musculoaponeurotic fibrosarcoma oncogene homologue) and HES1 (hairy and enhancer of split) (Fig. 3.10A). Cluster-induced down-regulation of these three genes was confirmed at the mRNA level in three independent infections by qRT-PCR (Fig. 3.10B).

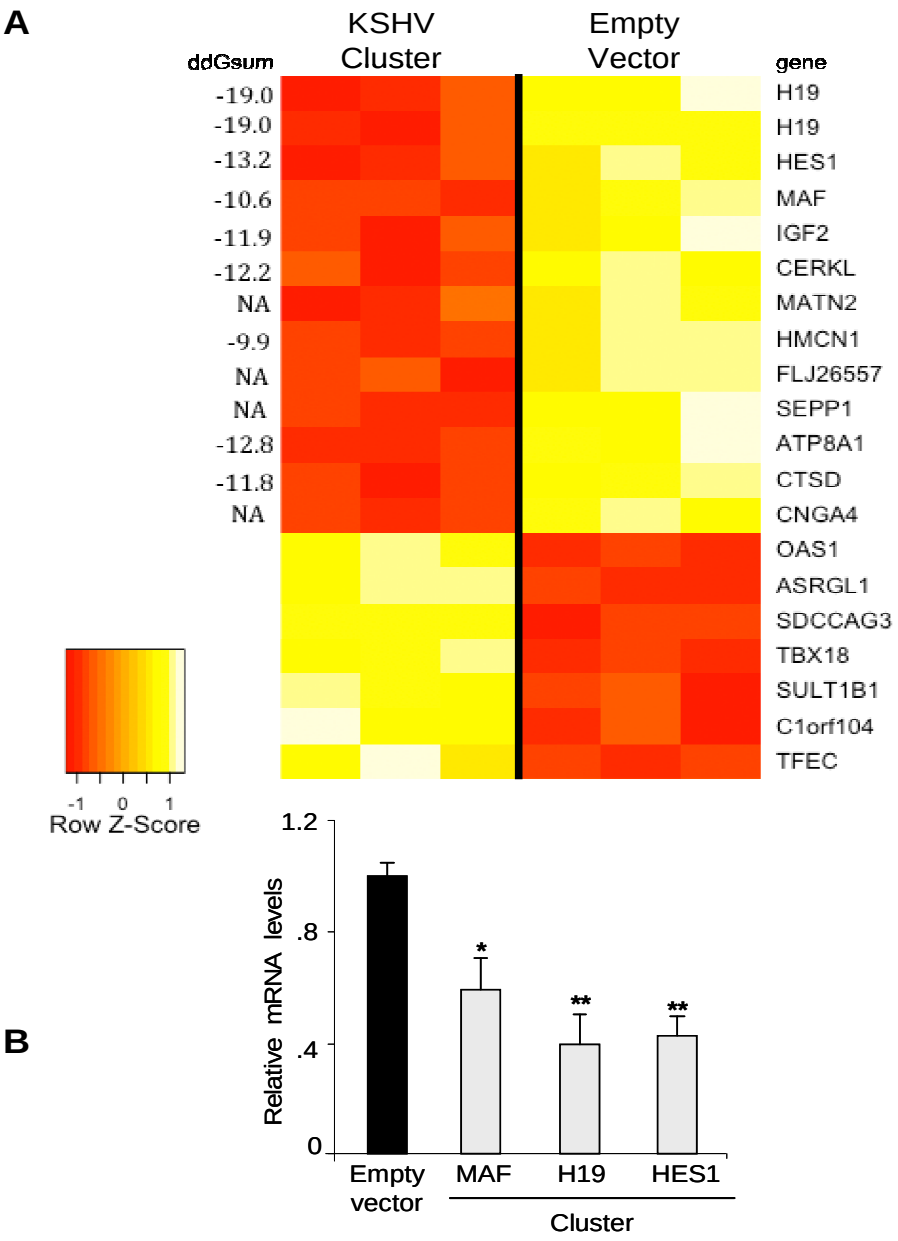

Figure 3.10. KSHV miRNA Cluster induces changes in LEC gene expression. *A* Heatmap of deregulated probes after transduction of LEC with either the KSHV miRNA Cluster or empty vector (pSIN-MCS) 72hrs post infection. This set of most significantly different genes has a false discovery rate (q value) of 0.13. The Z-score scale shows mean scaled and zero centered $\log_2$ GEM expression values for each row. For all down-regulated genes (shown in red), a cumulative interaction score (ddGsum) with the expressed KSHV miRNAs is shown. *B* Down-regulation of the top three cellular genes in LEC transduced with the miRNA Cluster confirmed by qRT-PCR. Expression is relative to empty vector, pSIN-MCS. Values were normalised to GAPDH. p values relative to LEC transduced with pSIN-MCS: *<0.05 **<0.005. Error bars correspond to standard deviation, n = 3.

3.7 KSHV miRNA target prediction

A single miRNA can regulate multiple mRNAs, with over a third of the human genome predicted to be under miRNA regulation (Stark et al., 2005; Farh et al., 2005). In response to this widespread regulation, in silico miRNA target prediction algorithms have been developed to facilitate global target identification (Bartel, 2009). Target prediction algorithms provide a complimentary approach to experimental target identification and are able to identify targets regulated by both mRNA degradation and translation inhibition, whereas GEM analysis only identifies the former. To further investigate KSHV miRNA function, target prediction analysis was performed for all the KSHV miRNAs expressed in KS lesions. The GEM data were used to validate the prediction algorithm, and to test whether such algorithms provided further support for favourable targeting of experimentally identified targets.

3.7.1 Prediction strategy

The main determinant for miRNA-target recognition is the sequence complementation of 6-8 nucleotides comprising the miRNA seed region. However, prediction algorithms working on this principle alone would produce an excessive number of false positive results. Additional parameters based on empirical and theoretical principles are incorporated to improve prediction sensitivity. The target prediction algorithm PITA (Probability of Interaction by Target Accessibility) (Kertesz et al., 2007) was used to identify KSHV miRNA targets.

This programme incorporates the degree of target-seed sequence complementation, as well as the role of target-site accessibility in determining miRNA-target pairing and subsequent silencing. Complex mRNA secondary structure embedding a target site will restrict RISC access to the target and thereby impair silencing, even if the site has high sequence complementation, as secondary structure and any intramolecular base pairing would have to be unwound to permit RISC access (Kertesz et al., 2007). There is an energetic cost to facilitating miRNA accessibility under these circumstances, which may render the miRNA-target interaction unviable.

To ensure the viability of predicted targets, PITA takes these factors into consideration when analysing 3'UTRs for miRNA target sites (Illustrated in Fig. 3.11). The free energy generated upon miRNA-target duplex formation is calculated (Δ_{duplex}), followed by calculation of the energetic cost of unwinding any secondary miRNA structure and unpairing intramolecular bases as well as additional bases flanking the seed (Δ_{open}). RNA secondary structures are modeled using built-in structure prediction algorithms and the final score represents the difference between these two factors and is expressed as ΔΔG (Kertesz et al., 2007). Gibbs free energy (G) refers to the amount of energy capable of doing work in a reaction. Favourable, exergonic reactions generate products with a lower free energy than the reactants; this is expressed as a negative ΔG value. Conversely, unfavourable endergonic reactions require an input of energy generating a positive ΔG value. Such reactions are physically impossible. Therefore, the more negative the ΔΔG score calculated by PITA the higher the likelihood of a miRNA regulating a specific target site (Kertesz et al., 2007).

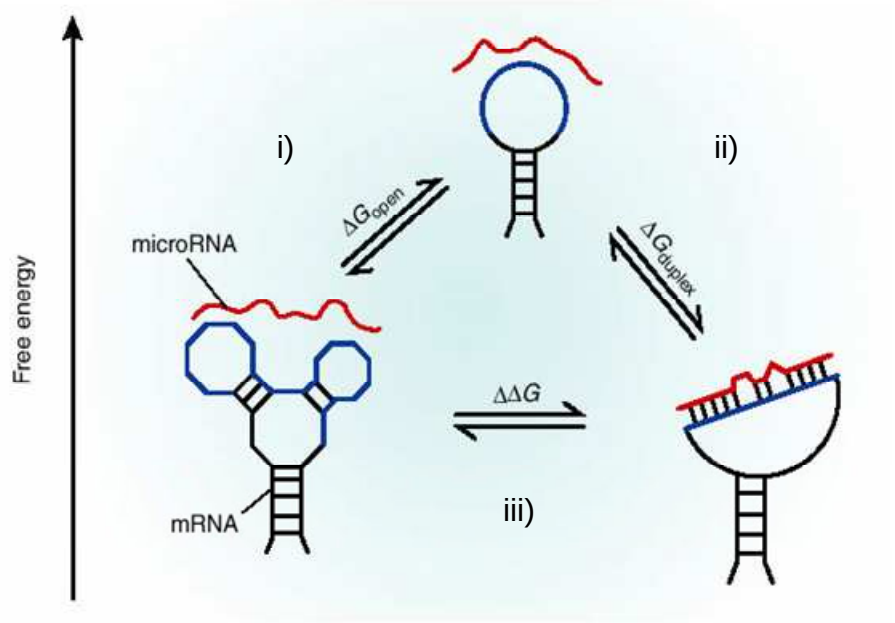

Figure 3.11. Schematic describing PITA scores based on thermodynamic modelling. i) miRNA target sites located within mRNA secondary structures must be unwound before miRNA-target binding can occur. There is an energetic cost to freeing mRNA secondary structure (ΔGopen). ii) Free energy is gained from miRNA-target duplex formation (ΔGDuplex). iii) The resulting ΔΔG score is the combination of energy invested and energy gained. Energetically feasible reactions have negative ΔΔG scores. Schema taken from (Hofacker, 2007).

The accuracy of miRNA target prediction algorithms is greatly improved by considering species conservation, whereby a site is only considered if it is also present in a number of orthologous 3'UTRs (Lewis et al., 2005). Although this approach improves detection it also excludes a large number of species-specific miRNA targets (Bentwich et al., 2005). As KSHV is a human-specific herpesvirus, which has co-evolved with its host, filtering results on the basis of species conservation would provide no additional benefit. This choice is supported by the lack of sequence conservation between the KSHV miRNAs and their counterparts in murine and primate herpesviruses, suggesting that viral miRNAs have evolved to target host-specific mRNAs. Other than thermodynamic modelling, PITA enforces no additional filters.

To create a more sophisticated search, a number of additional filters and parameters were incorporated into PITA (with the help of Dr. S. Henderson, CR-UK, Viral Oncology group, UCL). An overview of target prediction with additional parameters is shown in Figure 3.12. The primary interest was in LEC-specific targets, only the 3'UTRs of genes expressed in LEC where used as input for miRNA target prediction. To improve prediction sensitivity only those target sites with an 8bp seed, which contained either a G:U wobble or a mismatch, but not both, were considered. A number of additional determinants beyond seed pairing have been characterized (Grimson et al., 2007). These findings highlighted the impact of target site context on miRNA regulation, in terms of sequence composition and target site location. Once PITA analysis had generated ΔΔG scores for all predicted targets, the results were filtered according to additional context parameters defined by Grimson et al (Grimson et al., 2007). miRNA sites located within 40bp of one another have been shown to function cooperatively, therefore a boost of -2 was added to closely positioned sites (Fig. 3.12).

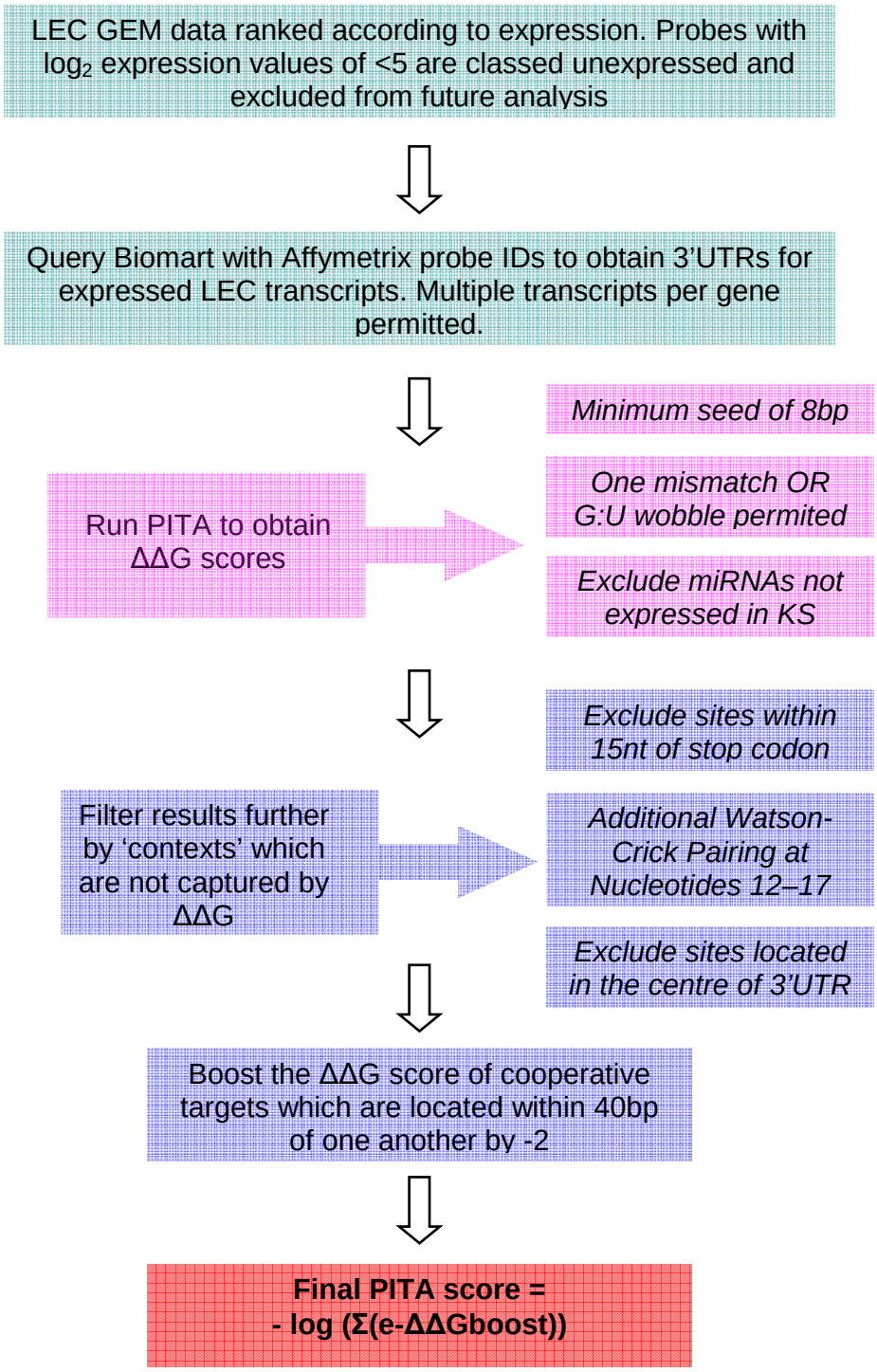

Figure 3.12. Overview of PITA KSHV miRNA target prediction analysis. 3'UTRs from all genes expressed in LEC were used as input for target prediction. Shown in pink are the PITA defined parameters used to generate ΔΔG scores. In purple are additional filters added based on parameters defined in Grimson *et al*. The equation generating the final PITA score is shown.

3.7.2 Prediction results

A ΔΔG threshold of -15 was set and only those miRNAs within the KSHV miRNA Cluster and expressed in KS lesions were considered. These conditions generated 205 predicted targets (Appendix A2). None of the down-regulated genes identified in the GEM target identification were present in this list, neither were any of the up-regulated genes (Table 3.1 and Fig. 3.10A). Likewise, none of the top 20 PITA predicted targets were significantly de-regulated in the GEM experiment, at a significance threshold of $q<0.13$. miRNAs are known to induce small fold changes in steady state mRNA levels when targets are silenced by both mRNA degradation and translation inhibition (Baek et al., 2008; Selbach et al., 2008). Predicted targets may show decreased expression in the presence of the Cluster which fell below the significance threshold of $q<0.13$. Table 3.1 shows the $\log_2$ fold change in expression of the top 20 PITA targets in the Cluster GEM experiment. Although none of these genes had significant q values ($q<0.13$), a quarter were down-regulated by <10% at the mRNA level in the presence of the Cluster (Table 3.1). Abundance of the remaining 15 genes either stayed constant or increased slightly in Cluster expressing LEC (Table 3.1). Therefore, there is minimal overlap between those genes identified in the Cluster-GEM experiment and the PITA prediction analysis.

Gene	microRNA	Seed	Sum for Gene	Average LFC	Ratio Cluster:pSIN
HS3ST3B1	miR-K12-6-3p	08:00:00	-19.15	-0.393	0.761
RAB31	miR-K12-4-3p	08:01:00	-21.86	-0.359	0.780
SENP7	miR-K12-4-3p	08:00:00	-22.62	-0.208	0.866
ERMP1	miR-K12-6-3p	08:00:01	-35.3	-0.188	0.878
IRF2BP2	miR-K12-6-5p	08:00:00	-20.03	-0.145	0.904
FOXP1	miR-K12-1	08:01:00	-40.4	-0.058	0.961
C1orf151	miR-K12-1	08:00:00	-21.2	-0.056	0.962
KPNA6	miR-K12-6-3p	08:00:01	-33.2	-0.039	0.973
KIF1B	miR-K12-6-3p	08:00:01	-33.96	-0.024	0.983
MTMR9	miR-K12-4-3p	08:00:00	-21.4	-0.023	0.984
MTRF1L	miR-K12-1	08:01:00	-21.68	-0.009	0.994
CYP2U1	miR-K12-6-5p	08:01:00	-22.07	-0.008	0.995
SLC25A29	miR-K12-4-3p	08:00:01	-19.19	0.015	1.011
PIN4	miR-K12-6-3p	08:00:00	-36.02	0.023	1.016
C2orf18	miR-K12-11	08:00:00	-20.09	0.049	1.034
DCTN4	miR-K12-1	08:00:01	-35.51	0.068	1.049
RAD21	miR-K12-1	08:00:00	-21.31	0.080	1.057
C2orf60	miR-K12-6-5p	08:00:00	-20.44	0.090	1.064
RABEPK	miR-K12-6-3p	08:01:00	-20.26	0.174	1.128
EXO1	miR-K12-2	08:01:00	-33.95	0.247	1.187

Table 3.1 mRNA abundance of top PITA predicted targets in the presence of the KSHV miRNA cluster. The top PITA predicted KSHV miRNA targets and targeting miRNA are shown, along with the average log fold change (LFC) in expression in presence of the KSHV miRNA Cluster compared with empty vector (pSIN).

Target prediction algorithms are known to generate a high number of false positive results. To test the modified algorithm, PITA prediction analysis was performed for three validated miRNA targets selected from the literature (Table 3.2). PITA was able to predict experimentally identified miRNA target sites in all three instances (Table 3.2, blue text). However, in the 3'UTRs of MAF and PTEN, PITA also predicted energetically feasible sites for other non-related miRNAs, which were included as negative controls. The experimentally validated sites in HOXD10 had a ΔΔG score of -11.22, which is below the threshold of -15 ΔΔG set in KSHV miRNA target prediction. In the case of MAF and PTEN the experimentally validated sites were not the sites with the most favourable ΔΔG score, and were both significantly lower than -15ΔΔG. This analysis reveals the high signal to noise ratio of PITA and highlights the difficulty in identifying bone fide miRNA targets from the noise of false positive results.

Gene	microRNA	Start	End	Seed	PTIA score
HOXD10	hsa-miR-10b	282	274	08:00:01	-11.22
MAF	hsa-miR-10b	706	698	08:01:01	-1.57
MAF	hsa-miR-10b	2439	2431	08:01:01	-4.55
MAF	hsa-miR-10b	3078	3070	08:01:01	-3.49
MAF	hsa-miR-10b	3877	3869	08:01:00	-5.28
MAF	hsa-miR-155	863	855	08:01:01	-1.74
MAF	hsa-miR-155	891	885	06:00:00	-4.41
MAF	hsa-miR-155	1071	1063	08:01:01	1.24
MAF	hsa-miR-155	1076	1068	08:01:01	-2.83
MAF	hsa-miR-155	1756	1748	08:01:01	-5.42
MAF	hsa-miR-155	2484	2476	08:01:00	-12.99
MAF	hsa-miR-155	4368	4360	08:01:01	-7.17
MAF	hsa-miR-155	4371	4363	08:01:01	-7.18
MAF	hsa-miR-214	540	532	08:00:01	-11.68
MAF	hsa-miR-214	903	895	08:01:01	-7.55
MAF	hsa-miR-214	993	985	08:01:00	-6.67
MAF	hsa-miR-214	2219	2211	08:01:01	-4.15
MAF	hsa-miR-214	2608	2600	08:01:01	-2.77
MAF	hsa-miR-214	3967	3959	08:01:01	-8.08
PTEN	hsa-miR-10b	167	159	08:01:00	-4.89
PTEN	hsa-miR-10b	1473	1465	08:01:01	-1.63
PTEN	hsa-miR-10b	3195	3187	08:01:00	-3.67
PTEN	hsa-miR-155	86	78	08:01:01	-4.47
PTEN	hsa-miR-155	263	255	08:01:00	-6.91
PTEN	hsa-miR-155	2243	2235	08:01:01	1.69
PTEN	hsa-miR-155	2385	2377	08:00:01	-2.8
PTEN	hsa-miR-155	2521	2513	08:01:01	-1.9
PTEN	hsa-miR-155	2741	2733	08:01:00	-1.05
PTEN	hsa-miR-214	1021	1013	08:01:00	-8.57

Table 3.2 Testing the ability of PITA to identify experimentally validated miRNA target sites. All three genes are validated miRNA targets, MAF is targeted by miR-155 (Rodriguez et al., 2007), HOXD10 by miR-10a (Ma et al., 2007) and PTEN by miR-214 (Yang et al., 2008). PITA identifies the experimentally confirmed site in each target (blue text), other high scoring false positive sites are also detected for both the targeting and non-targeting miRNAs.

The 3'UTRs of all genes with decreased mRNA abundance in the presence of the Cluster were scanned for potential KSHV miRNA binding sites (Fig 3.10A). For each down-regulated transcript the cumulative PITA score for all expressed viral miRNAs (Fig. 3.2) was calculated (Fig. 3.10). Although these down-regulated genes were not amongst the top PITA predicted targets, nine out of thirteen genes had negative ΔΔG values, which is indicative of miRNA regulation. Given that experimentally validated targets sites also generated relatively low ΔΔG scores (Table 3.2) these genes could be considered as putative KSHV miRNA targets. Employing multiple prediction algorithms and focusing on the overlap between programmes, is one method of increasing confidence in target prediction. However, this approach was not suitable for the KSHV miRNAs as PITA is one of the few prediction programmes which does not require species conservation as a prediction parameter, therefore there was no suitable additional programme with which to compare prediction results.

3.8 Discussion

The data presented here have confirmed expression of the KSHV miRNAs in KS lesions. Since only a limited number of gene products are expressed in latently infected KS spindle cells, it is likely that the viral miRNAs contribute to KSHV-mediated oncogenesis. Expression of ten out of 17 mature miRNAs was confirmed by both miRNA microarray and qRT-PCR; three miRNAs were detected by qRT-PCR only, this may reflect differences in detection thresholds of the two techniques adopted. Another three miRNAs were undetectable by either qRT-PCR or miRNA microarray. Probes for the miRNA, miR-K12-7, cross-reacted in both skin and KS samples and this miRNA cannot be classified as either expressed or unexpressed in KS.

The miRNA profiling data reported here differs from the KSHV miRNA expression data from PEL cell lines, a larger repertoire of KSHV viral miRNAs were detected in PEL compared to KS lesions (Cai et al., 2005; Pfeffer et al., 2005; Samols et al., 2005). PEL cells have approximately 65 KSHV episomes per cell (Lallemand et al., 2000), whereas KS spindle cells typically have approximately 10. This discrepancy in viral titre may explain why less abundant KSHV miRNAs were not detected in KS lesions. Furthermore, the different cellular origin of PEL and KS may favour expression of a distinct repertoire of miRNAs which have evolved to silence cell-type specific genes, thus explaining the differing KSHV miRNA expression profiles.

While this work was being completed a report describing the expression of a subset of KSHV pre-miRNAs in KS lesions was published (O'Hara et al., 2009). The methods employed to identify these miRNAs differ from those presented here. O'Hara et al used primer pairs for nine out of 12 pre-miRNAs and confirmed expression of five of these in AIDS-KS biopsies and provide preliminary evidence of viral miRNAs expression in KS, which is corroborated and expanded upon in

this thesis. The quantification of the mature miRNA by microarray or qRT-PCR used here is more informative than assaying the pre-miRNA alone, as differences in processing or stability of miRNA intermediates mean pre and pri-miRNA levels are not always synonymous with the mature, effector miRNA.

qRT-PCR of mature KSHV miRNAs confirmed a similar expression profile in KS lesions and Cluster-expressing LEC. miR-K12-3*, miR-K12-9 and miR-K12-9* were undetectable in both samples. The other miRNAs showed comparable expression levels in KS and Cluster-expressing LEC. This suggests similar processing and expression from the cloned miRNA Cluster with that present in KSHV infected spindle cells. Therefore the lentiviral system is a good model with which to study KSHV miRNA function and perform miRNA target identification in LEC.

GEM profiling of LEC transduced with the KSHV miRNA Cluster identified a cohort of putative viral miRNA targets. Down-regulation of the top three genes was confirmed by qRT-PCR in independent infections. Two of these genes, MAF and HES1, are transcription factors. Viral-induced silencing of a single transcription factor could potentially modulate the expression of a much larger set of downstream genes from multiple pathways, thereby increasing the functional outcome of miRNA-directed silencing. H19 is a non-coding RNA molecule which is maternally imprinted. This RNA was shown to encode a mature miRNA miR-675, which is expressed during vertebrate embryonic development, although the targets of this miRNA are yet to be characterised (Cai and Cullen, 2007). This may represent a novel function for viral miRNAs, whereby they directly regulate host cellular miRNAs through silencing pre-miRNA transcripts. Importantly, GEM analysis will only identify those targets silenced by mRNA degradation. A proteomics approach such as stable isotope labeling by amino acids in cell culture (SILAC) is required to identify KSHV miRNA targets in LEC silenced by translation inhibition (Vinther et al., 2006).

A number of additional putative KSHV miRNA targets were identified using the target prediction algorithm PITA (Kertesz et al., 2007). PITA was selected on the basis of its dynamic user interface and extensive thermodynamic modelling to predict miRNA targets. The stringency of search parameters was increased in an attempt to improve the typically high signal to noise ratio of prediction programmes. However, experimentally validated miRNA targets can deviate from these rules, some having seed matches of only 6 base pairs and containing mismatches and G:U wobbles (Bartel, 2009). Through computational and experimental analysis Grimson et al identified five additional factors beyond seed complementation which influenced miRNA-mediated repression (Grimson et al., 2007). Two of these site-context features, preferential location of sites in an A/U rich regions and flanking A's surrounding the target site, were already captured by PITA analysis. The other three factors were incorporated into PITA analysis by filtering results or boosting PITA prediction scores.

A comparison of experimental and in silco target identification revealed a quarter of genes were both predicted targets and down-regulated in the GEM target identification experiment. This minimal degree of overlap may be due to the high rate of false positives of PITA obscuring identification of bone fide miRNA targets. Importantly, the mRNA secondary structure prediction algorithm (modified RNA fold algorithm) employed by PITA to model the structure of the 3'UTR does not take into account the affect of RNA binding proteins on mRNA structure. RNA binding proteins are important regulators of miRNA silencing, these proteins have the potential to alter the mRNA secondary structure either facilitating or blocking miRNA silencing (Kedde et al., 2007). Unknown RNA binding proteins may mediate silencing, as these factors are not considered by PITA this may explain the relatively low ΔΔG scores of experimentally validated miRNA targets and suggests the target genes down-regulated by the KSHV miRNA Cluster with poor ΔΔG scores may still be genuine KSHV miRNA targets. Experimental validation of these putative targets and identification of RNA binding proteins regulating KSHV

miRNA-mediated silencing will provide greater insight and facilitate miRNA target identification. Furthermore, specific rules pertaining to viral miRNA targeting may be discovered in the future which influence target prediction.

Chapter 4. MAF is a KSHV miRNA target

4.1 Introduction and aims

Amongst the multiple putative KSHV miRNA targets described in Chapter 3, the transcription factor MAF was one of the most significantly down-regulated genes. The aim of this chapter was to experimentally validate MAF as a KSHV miRNA target.

MAF represented an interesting KSHV miRNA target as transcription factor silencing has potentially wide-reaching secondary effects, dependant on the repertoire of target genes. In this manner, miRNA repression of a single gene following viral infection could present an elegant means of controlling the expression of multiple proteins. Previous gene expression studies have classified LEC and BEC on the basis of their differing transcriptional profiles (Petrova et al., 2002; Hong et al., 2004). In this analysis MAF was classified as a LEC-specific transcript due to its higher level of expression in LEC compared to BEC (Petrova et al., 2002; Hong et al., 2004). Despite this classification, the function of MAF and its target genes in LEC are unknown. LEC are the most similar primary cells to KS tumour cells, and are subject to KSHV-directed transcriptional reprogramming (Wang et al., 2004; Hong et al., 2004). I hypothesised that KSHV miRNA-mediated regulation of a LEC-specific transcription factor could have an important role in viral-mediated oncogenesis.

4.2 MAF is down-regulated by the KSHV miRNA Cluster

qRT-PCR analysis of LEC expressing the KSHV miRNA Cluster confirmed a 25-50% repression of MAF mRNA levels compared to empty lentiviral vector (pSIN-MCS, Fig. 4.1A). This magnitude of repression is comparable to other validated KSHV miRNA targets and is in keeping with the fine-tuning nature of miRNA regulation (Samols et al., 2007; Ziegelbauer et al., 2009). In addition, MAF mRNA was reduced in 293T cells transduced with the Cluster and in a 293 cell line stably expressing the miRNA Cluster (Fig. 4.1A). Increasing copy number of Cluster-lentivirus per cell induced a corresponding decrease in MAF mRNA levels, suggesting MAF silencing is a function of the KSHV miRNAs (Fig. 4.1B). MAF mRNA was down-regulated by 13% 24hrs post infection with lentivirus encoding the miRNA Cluster (Fig. 4.1C). Silencing increased with time, maximal MAF repression occurred at 72hrs post infection when MAF mRNA levels were reduced by -40% compared to empty vector control (Fig. 4.1C). These data confirm MAF down-regulation at the mRNA level in the presence of the KSHV miRNA Cluster and validate the GEM data (Fig. 3.10A). MAF mRNA reduction was also evident at the protein level, whereby MAF protein was reduced by approximately 40% in LEC expressing the Cluster compared to empty lentiviral vector (Fig. 4.1D).

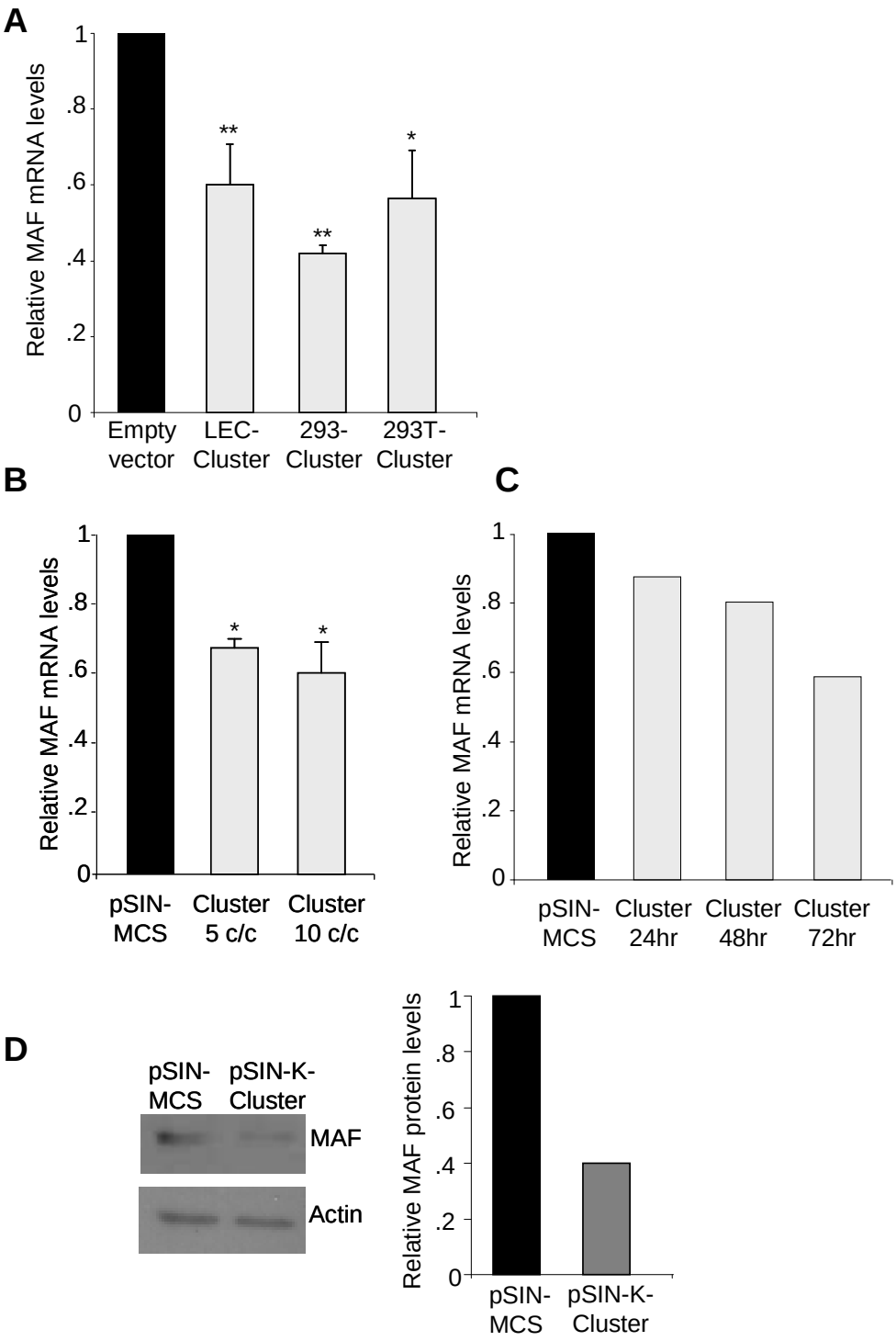

Figure 4.1. KSHV miRNA Cluster induces MAF down-regulation. *A* MAF mRNA down-regulation in LEC and 293T cells transduced with the miRNA Cluster (72hr post infection) and in 293 cell line stably expressing the Cluster. p values relative to empty vector in the respective cell type: *<0.05; **<0.005. *B* MAF mRNA levels in LEC transduced with Cluster lentivirus. Magnitude of silencing increases with viral titre c/c: copies per cell. p values relative to pSIN-MCS at the equivalent viral titre: *<0.05 *C* Cluster-lentivirus time course infection of LEC. MAF mRNA was maximally repressed at 72hrs post infection. *D* Western blot analysis of MAF and loading control actin in LEC transduced with either miRNA Cluster or pSIN-MCS 48hrs post infection. Quantification of relative intensity was performed by Scion Image software. Error bars correspond to standard deviation, n = 3.

4.3 MAF is down-regulated by miR-K12-11 and miR-K12-6

To identify individual KSHV miRNAs capable of silencing MAF a lentiviral screen was performed. Ten KSHV pre-miRNAs were individually expressed in LEC, which were then assayed for MAF repression (Fig. 4.2A). miR-K12-6 and miR-K12-11 induced a small but significant decrease in MAF mRNA compared to empty lentiviral vector in all three screens (Fig. 4.2A). miR-K12-11 is a viral orthologue of cellular miR-155 (Skalsky et al., 2007; Gottwein et al., 2007) and previous work has characterised MAF as a miR-155 target in Th2 cells (Rodriguez et al., 2007). In this study, a number of mouse miR-155 target sites were identified in the Maf 3'UTR and mRNA levels were elevated or suppressed in mice lacking or over-expressing miR-155, respectively (Rodriguez et al., 2007). miR-155 regulation of Maf in murine T helper cells led to decreased expression of the Maf target gene IL4 and a shift in the balance between a Th1 and Th2 immune response in favour of Th2 cells (Rodriguez et al., 2007). In the context of these data from Rodriguez et al, the identification of miR-K-12-11 as a MAF repressor, confirms previous work showing that viral and cellular homologues regulate an over-lapping set of target genes (Skalsky et al., 2007; Gottwein et al., 2007).

miR-K12-10 lentivirus, which encodes for two of the three miRNAs located outside the Cluster failed to reproducibly silence MAF (Fig. 4.2A). This suggests that the Cluster is primarily responsible for MAF silencing and that further experiments performed with this Cluster-expressing lentivirus would capture the majority of MAF silencing and any down-stream effects.

qRT-PCR for miR-K12-6-5p and miR-K12-11 confirmed KSHV miRNA expression in LEC transduced with lentivirus expressing individual pre-miRNAs (Fig. 4.2B). This analysis revealed differences in the relative abundances of Cluster-encoded miRNAs. miR-K12-11 was more abundant than miR-K12-6-5p in LEC transduced with the whole Cluster and at equivalent titres of individual miRNA-expressing lentivirus (Fig. 4.2B). This may be due to differences in miRNA processing since two mature miRNAs are expressed in LEC transduced with miR-K12-6 compared to just one from the miR-K12-11 lentivirus. MAF mRNA levels decreased with increasing titre of both miR-K12-6 and miR-K12-11 lentivirus (Fig. 4.2C). These data identify two miRNAs from the KSHV Cluster capable of silencing MAF at the mRNA level. This concurs with other validated cellular miRNA targets which are regulated by multiple KSHV miRNAs (Samols et al., 2007; Ziegelbauer et al., 2009; Qin et al., 2010).

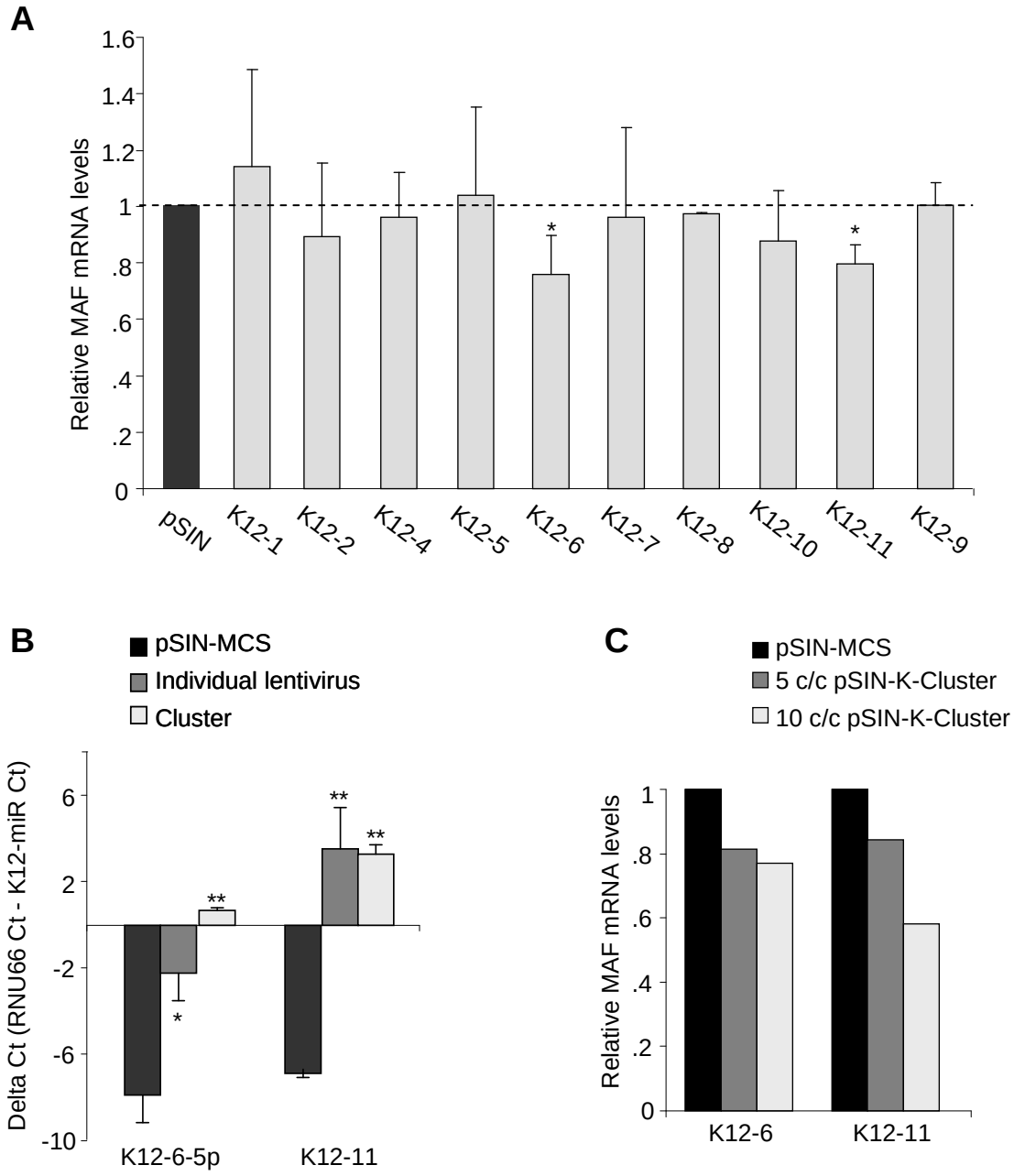

Figure 4.2. miR-K12-6 and miR-K-12-11 induce MAF silencing. *A* Screen for MAF repression in LEC transduced with ten individual KSHV miRNAs. miR-K-12-6 and miR-K12-11 are the only two miRNAs to induce a significant, reproducible reduction in MAF mRNA. Values are relative to GAPDH and normalised to LEC transduced with empty lentiviral vector (pSIN-MCS). p values relative to pSIN-MCS: *<0.05. *B* miR-K12-6-5p and miR-K12-11 are expressed in LEC transduced with lentivirus encoding the entire Cluster and individual miRNAs, expressed miRNAs have a positive delta Ct value. Values are relative to RNU66. p values relative to pSIN-MCS: *<0.05; **<0.005. *C* MAF mRNA levels in LEC transduced with increasing titre of individual miRNA expressing lentivirus. MAF silencing decreased with increasing viral titre, c/c: copies per cell. Error bars correspond to standard deviation, n = 3.

4.4 KSHV miRNAs are predicted to target the MAF 3'UTR

miRNAs predominantly regulate their targets through binding sites located in the 3'UTR (Bartel, 2009). The MAF 3' UTR was scanned for potential KSHV miRNA binding sites using the PITA prediction algorithm (Kertesz et al., 2007). The number of identified sites was refined by considering only those viral miRNAs expressed in KS lesions and including sites with either a perfect match, one GU wobble or mismatch, but not both, in an 8bp seed. This analysis identified 11 putative KSHV miRNA binding sites located throughout the 4.45kb MAF 3'UTR (Fig. 4.3). The alignment of mature KSHV miRNAs with their predicted binding sites is shown (Fig. 4.3B). To avoid missing any potential KSHV miRNA binding sites, all sites with a negative ΔΔG score were considered. miR-K12-6-5p had the strongest predicted site (approximately -10 ΔΔG) (Fig. 4.3A). With four predicted targets, miR-K12-6-3p had the highest number of sites and is the only miRNA with a target site showing perfect sequence complementation across the entire 8bp seed region (Fig. 4.3A and B). The degree of sequence complementation between miRNA seed and 3'UTR has been shown to correlate with increased prediction ability and silencing via mRNA degradation (Bartel, 2009). miR-K12-11 was the only other miRNA to have more than one predicted target site. Despite relatively weak ΔΔG scores, the PITA prediction analysis is supportive of a role for KSHV miRNA regulation of MAF. In particular, miR-K12-6 and miR-K12-11 have multiple PITA-predicted target sites throughout the MAF 3'UTR and were the two miRNAs identified as suppressors of MAF mRNA in the lentiviral screen.

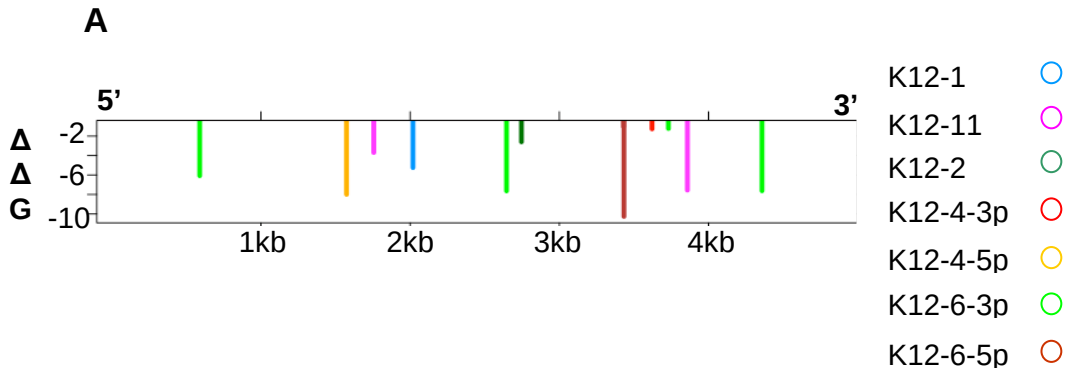

Figure 4.3. Predicted KSHV miRNA bindings sites in the MAF 3'UTR. *A* The positions of energetically favorable predicted seed site interactions of expressed KSHV miRNAs are shown for the MAF 3'UTR. On the Y axis (ΔΔG), the length of each line corresponds to the predicted strength of individual interactions. The more negative the value, the more energetically favorable the interaction. *B* Sequence alignment of the mature KSHV miRNAs and their predicted binding sites in the MAF 3'UTR. Predicted sites for all KSHV miRNAs expressed in KS are shown. Complementary bases are indicated by vertical lines. Seed regions of 8 bases were considered, one mismatch or G:U wobble (indicated by :) but not both was permitted across the seed. Predictions were made using the PITA algorithm (Kertesz et al., 2007). miR-K12-6-3p site at 3723bp highlighted in blue bold is the only predicted site with full sequence complementation across the entire 8bp seed.

B

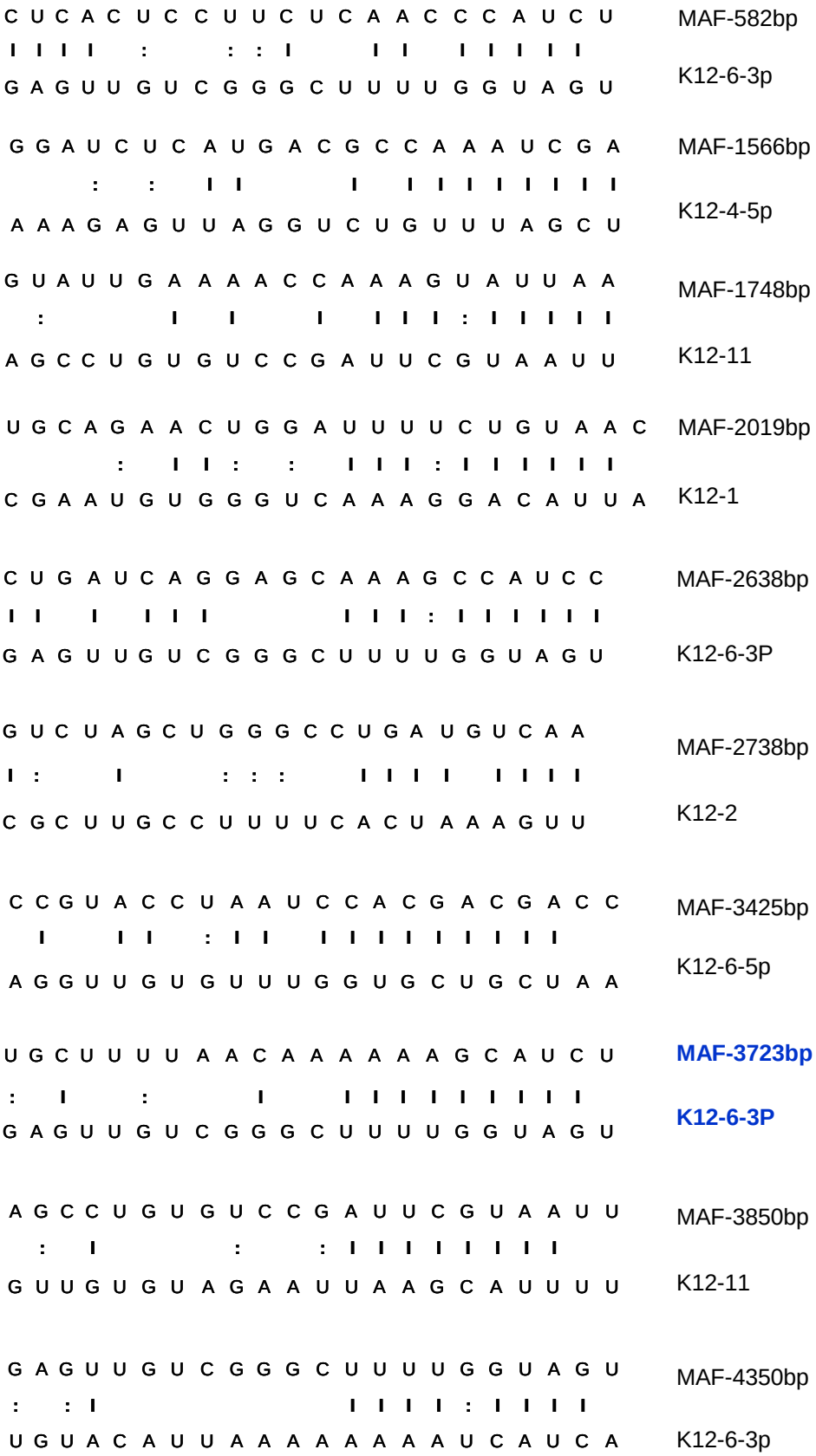
C U C A C U C C U U C U C A A C C C A U C U
MAF-582bp
G A G U U G U C G G G C U U U U G G U A G U
K12-6-3p
G G A U C U C A U G A C G C C A A A U C G A
MAF-1566bp
A A A G A G U U A G G U C U G U U U A G C U
K12-4-5p
G U A U U G A A A A C C A A A G U A U U A A
MAF-1748bp
A G C C U G U G U C C G A U U C G U A A U U
K12-11
U G C A G A A C U G G A U U U U C U G U A A C
MAF-2019bp
C G A A U G U G G G U C A A A G G A C A U U A
K12-1
C U G A U C A G G A G C A A A G C C A U C C
MAF-2638bp
G A G U U G U C G G G C U U U U G G U A G U
K12-6-3P
G U C U A G C U G G G C C U G A U G U C A A
MAF-2738bp
C G C U U G C C U U U U C A C U A A A G U U
K12-2
C C G U A C C U A A U C C A C G A C G A C C
MAF-3425bp
A G G U U G U G U U U G G U G C U G C U A A
K12-6-5p
U G C U U U U A A C A A A A A A G C A U C U
MAF-3723bp
G A G U U G U C G G G C U U U U G G U A G U
K12-6-3P
A G C C U G U G U C C G A U U C G U A A U U
MAF-3850bp
G U U G U G U A G A A U U A A G C A U U U U
K12-11
G A G U U G U C G G G C U U U U G G U A G U
MAF-4350bp
U G U A C A U U A A A A A A A A U C A U C A
K12-6-3p

4.5 MAF silencing via KSHV miRNA binding sites in the 3'UTR

To confirm the KSHV miRNAs were regulating MAF mRNA through interaction with the 3'UTR at the PITA-predicted sites, luciferase-reporter assays were performed (Fig. 4.4). These assays permit quantification of the magnitude of target silencing by miRNAs. The 3'UTR associated with the target mRNA is cloned downstream of the renilla ORF into a dual-luciferase reporter vector (psi-check2) and binding of the miRNA to a target site located in the cloned 3'UTR, reduces expression of the renilla luciferase protein (Fig. 4.4A). The reduction in renilla protein levels corresponds to a reduction in enzymatic activity, which is represented as a reduction in light emitted after the addition of substrate. This vector also encodes the firefly luciferase ORF, which is resistant to miRNA-mediated silencing. Firefly luciferase expression and activity is therefore used to control for transfection efficiency and normalise loading between samples, without requiring co-transfection of an additional plasmid.

The repetitive and G/C-rich nature of the 3'UTR sequence increases its propensity to generate hairpins and complex secondary structure. These structural elements can impede polymerase processing and impair efficient PCR amplification, making cloning problematic. The MAF 3'UTR is 4.3kb long, which in addition to the G/C rich sequence, further impeded PCR cloning. Only accurate amplification of the initial 2.3kb of the MAF 3'UTR closest to the STOP codon was achieved and subject to further study. This region was inserted downstream of the renilla ORF into a dual-luciferase reporter vector (Fig. 4.4A and B). This fragment of the MAF 3'UTR contained four predicted KSHV miRNA target sites, including one site for each of the two candidate MAF repressors miR-K12-6 and miR-K12-11, as well as a site for miR-K12-1 and miR-K12-4-3p (Fig. 4.3A). However, there are limitations to using a fragment of the 3'UTR compared with the full length sequence in assessing miRNA-mediated silencing. The 3'UTR is not linear but instead forms a complex secondary structure. This structure has an important role in miRNA mediated silencing, by regulating access to miRNA target sites and providing structural features which are recognised by RISC-associated and

regulatory RNA binding proteins. Reducing the length of the 3'UTR, as in the case of MAF, creates a different secondary structure which could inhibit or promote miRNA-mediated silencing. Furthermore, the location of miRNA target sites has been shown to play a role in the probability of silencing (Grimson et al., 2007). Halving the 3'UTR moves sites located in the middle of the full length sequence to the end, which is a more favourable location for silencing (Grimson et al., 2007). Therefore, the MAF 3'UTR reporter assay can only inform on whether a KSHV miRNA regulates a specific site within the context of this experiment.

The 293T cells used previously for luciferase assays (Chapter 3) express high levels of MAF mRNA, as evidenced by low a delta Ct value (Fig. 4.4C). miRNA binding sites in the endogenous MAF 3'UTR may sequester viral miRNAs away from the luciferase reporter vector. To limit this effect, 3'UTR experiments were performed in cells expressing low levels of endogenous MAF. Four cell lines were tested for MAF mRNA and HeLa cells were found to express MAF at the lowest levels. These cells were used for 3' UTR KSHV miRNA repression studies (Fig. 4.4C).

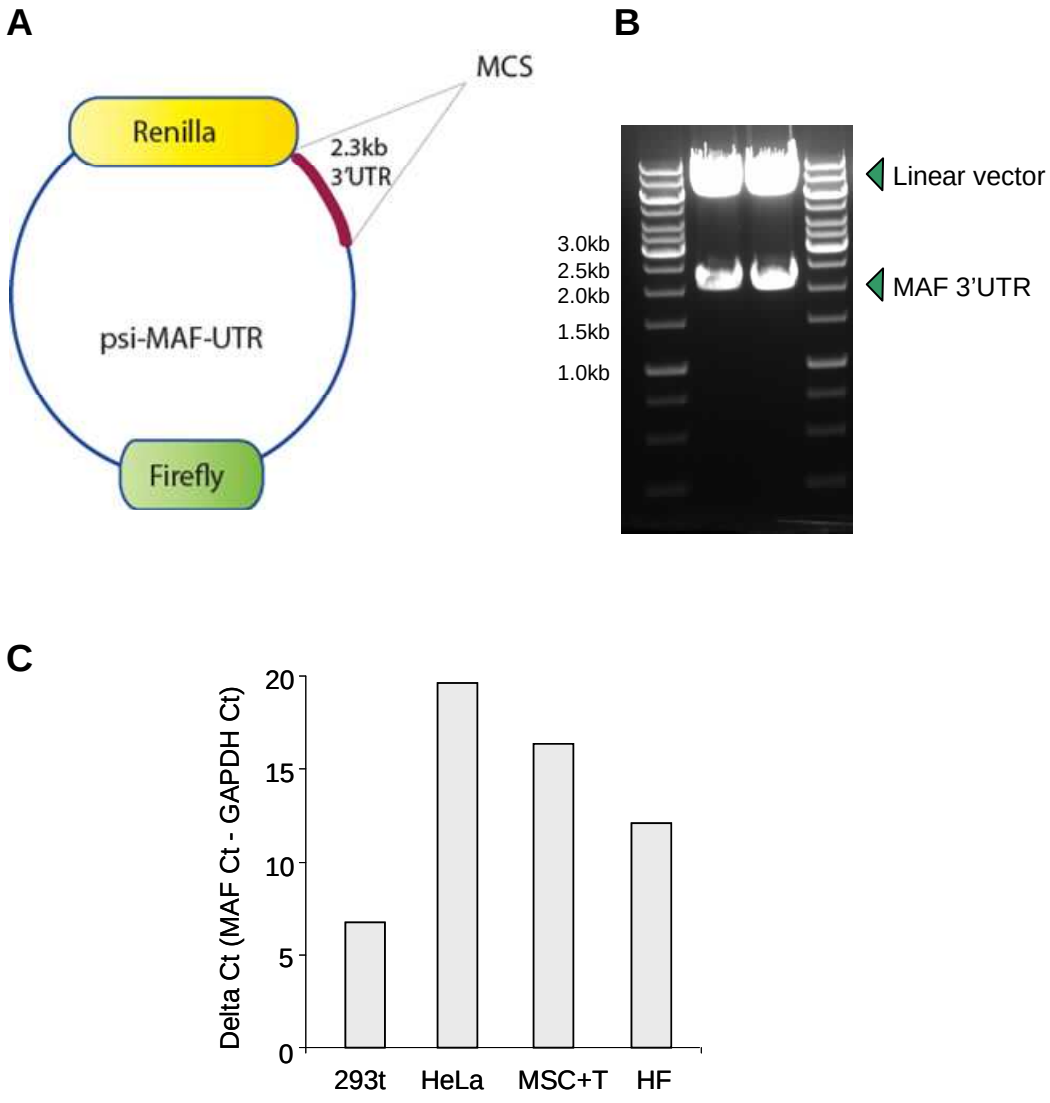

. **Figure 4.4. A Schematic of the psi-MAF-UTR plasmid**. *A* The first 2.3kb of the MAF 3'UTR was inserted into the multiple cloning site (MCS) down-stream of the renilla luciferase ORF (yellow box) into the psi-Check2 vector. This vector also encodes the firefly luciferase enzyme (green box) which is used to normalise for transfection efficiency and sample loading. *B* ~1µg of psi-MAF-UTR was digested with XhoI and NotI to excise the MAF 3'UTR. The top band is empty, linearised psi-Check2 plasmid, bands running at ~2.3kb are the excised MAF 3'UTR. *C* MAF mRNA levels in four cell lines. The difference in threshold detection cycle (Ct) between GAPDH and MAF is shown (delta Ct). HeLa cells gave the highest delta Ct and therefore express the lowest levels of MAF mRNA. MSC+T: mesenchymal stem cells plus tert, HF: human fibroblasts.

MAF 3'UTR luciferase assays were performed using the experimental conditions optimised for the miRNA sensor luciferase assays (Section 3.3). Expression of the KSHV miRNA Cluster induced a significant reduction in renilla activity compared to empty vector control (Fig. 4.5B). Similarly, co-transfection of pSIN-K-miR-6 and pSIN-K-miR-11 also led to a significant reduction in renilla activity (Fig. 4.5B). pSIN-K-miR-6 induced a 50% reduction compared with 23% induced by the pSIN-K-Cluster (Fig. 4.5B). Eleven mature miRNAs are expressed and processed from pSIN-K-Cluster, four of which have predicted binding sites in the fragment of the MAF 3'UTR tested. Conversely, only two mature miRNAs are encoded by pSIN-K-miR-6, with half of the expressed miRNAs having a target site in the MAF 3'UTR. This relative difference in the proportion of expressed MAF-targeting miRNAs may explain why pSIN-K-miR-6 induced greater repression than the entire Cluster (Fig. 4.5B). pSIN-K-miR-6 was a more potent MAF silencer compared to pSIN-K-miR-11, which reduced renilla activity by 21%. This may be due to differences in levels of mature miRNA. Alternatively, in the context of the shortened MAF 3'UTR the target site for miR-K12-6-3p may be more accessible than that for miR-K12-11, explaining the increased silencing by miR-K12-6-3p (Fig. 4.5). miR-K12-1 failed to induce MAF down-regulation when LEC were transduced with a lentivirus encoding for this miRNA (Fig. 4.2A). However, when transfected into HeLa cells miR-K12-1 significantly reduced MAF 3'UTR luciferase reporter activity by approximately 43% (Fig. 4.5B). This discrepancy may be due to higher miRNA expression levels in 293T cells transfected with the miR-K12-1 plasmid, or as a result of increased accessibility in shortened 3'UTR compared to endogenous, full length sequence. Absence of miR-K12-1 induced MAF mRNA down-regulation (Fig. 4.2A) suggests that miR-K12-1 does not significantly contribute to KSHV miRNA MAF regulation. Expression of two viral miRNAs (miR-K12-7 and miR-K12-8) with no predicted binding sites in the MAF 3'UTR failed to induce silencing (Fig. 4.5B). These data strongly suggest MAF regulation is mediated through miRNA interactions with the 3'UTR.

To confirm KSHV miRNA regulation was specifically via the PITA predicted sites, site directed mutagenesis was performed, disrupting the seed region so that the mature miRNA was no longer complimentary to its predicted target (Fig. 4.5C). Three bases in the seed were changed to a non-specific sequence, one mutant UTR was made for each predicted site. Seeds were disrupted for miR-K12-1, K12-6-3p and K12-11 (Fig. 4.5C). Site directed mutagenesis of these predicted targets ablated KSHV miRNA silencing induced by all three miRNAs, restoring renilla levels to that comparable to empty vector (Fig. 4.5B). These data support MAF down-regulation by way of KSHV miRNA binding to target sites located in the 3'UTR and identify potential sites of KSHV miRNA interaction. These data also show miR-K12-1 is capable of targeting the shortened MAF 3'UTR, although it is not clear this miRNA also silences the full length 3'UTR.

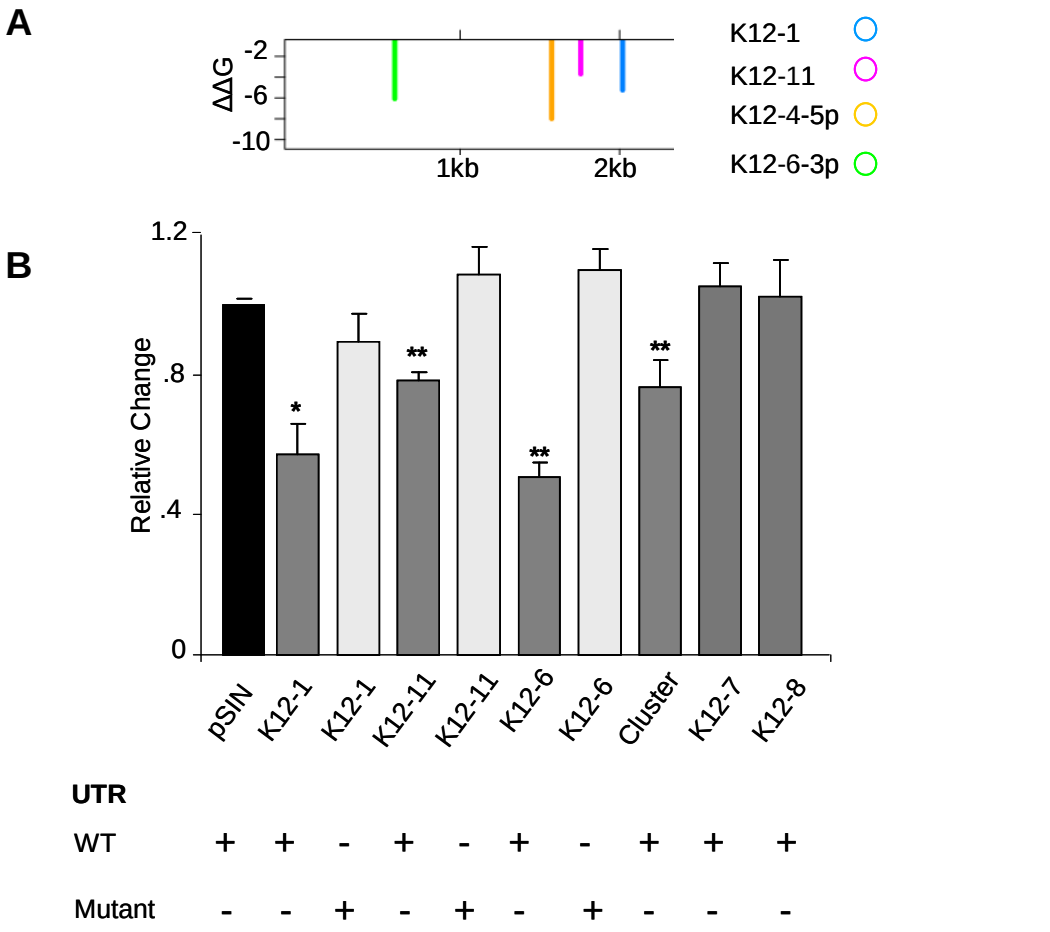

Figure 4.5. miR-K12-6, miR-K12-1 and miR-K-12-11 target the MAF 3'UTR. *A* Rug plot analysis of the section of MAF 3'UTR cloned into psiCheck2. This portion contains four predicted KSHV miRNA binding sites. *B* KSHV miRNA-induced repression of MAF 3'UTR. Individual KSHV miRNAs were co-transfected with the MAF 3'UTR luciferase reporter plasmid. Either wild type or mutated MAF 3'UTR was transfected. Mutated UTRs had the seed region of the corresponding miRNA disrupted by site directed mutagenesis. The ratio of renilla to firefly luciferase relative light units was normalized to empty vector (pSIN-MCS) and the relative change is shown. p values relative to pSIN co-transfected with WT MAF 3'UTR: *<0.05; **<0.005. *C* Sequence alignment of the KSHV miRNAs and their predicted seed regions in the MAF 3'UTR. The black line identifies bases disrupted by site directed mutagenesis, altered bases are shown above in red. Error bars correspond to standard deviation, n = 3.

4.6 MAF is down-regulated during primary KSHV infection

To study the relevance of MAF silencing by KSHV miRNAs, regulation of MAF expression during primary KSHV infection of LEC was investigated. MAF belongs to the AP1 super-family of basic leucine zippers and is the founding member of the Maf family of transcription factors (Nishizawa et al., 1989). To determine whether expression of MAF, or any other family members, was deregulated during primary KSHV infection the gene expression profiles of infected and uninfected LEC were compared. MAF was the only transcription factor from this family that decreased upon primary infection (Fig. 4.6A). The Maf family is classified into two groups: large and small Mafs. In addition to MAF down-regulation, there was a significant up-regulation of two other small Maf transcription factors: MAFF and MAFK at the mRNA level (Fig. 4.6A).

To determine whether MAF down-regulation occurred early during infection, MAF mRNA levels were quantified during a time-course infection of LEC. MAF mRNA was down-regulated early at 6hrs post KSHV infection, this down-regulation was significant and persisted until 72hrs post infection (Fig. 4.6B). MAF down-regulation was also observed at the protein level by approximately 50% 48hrs post KSHV infection of LEC (Fig. 4.6C). Although MAF mRNA was down-regulated at 6hrs post infection, a decrease in protein levels was not observed until 48hrs. This lag in protein down-regulation reflects the time required for a decrease in mRNA levels to yield a corresponding decrease in protein. MAF down-regulation occurs in the context of KSHV miRNA Cluster but is also detected during whole virus infection of LEC. These data highlight MAF as a relevant KSHV miRNA target for further investigation in the context of KSHV infected LEC.

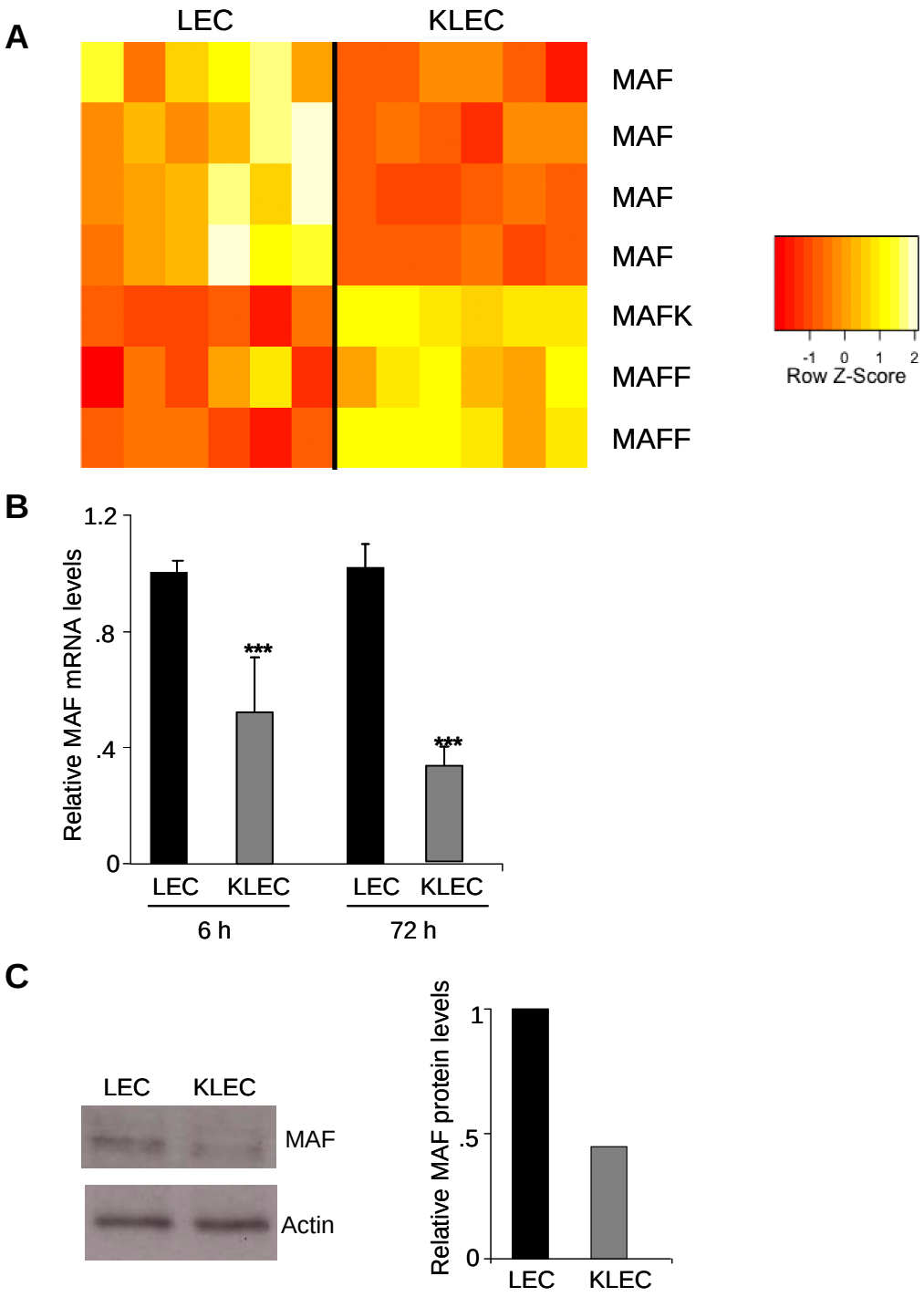

Figure 4.6. MAF is down-regulated during primary KSHV LEC infection. *A* MAF mRNA was down-regulated in LEC 72hrs post KSHV infection (KLEC). The heatmap shows the z-score of the GEM data in which each normalized expression value is divided by the mean and centred around zero (n=6). Down-regulated probes are shown in red, up-regulated probes in yellow. *B* MAF mRNA down-regulation at 6 and 72hrs post KSHV infection of LEC, as quantified by qRT-PCR. p values relative to uninfected LEC at the equivalent time point: *<0.05; **<0.001. *C* Western blot analysis of MAF and loading control actin in uninfected and KSHV infected LEC (KLEC, 48hrs post infection). Quantification of relative intensity was performed by Scion Image software. Error bars correspond to standard deviation, n = 3.

4.7 KSHV miRNA expression during primary LEC infection

Agilent miRNA microarray profiling of KSHV-infected LEC 72hrs post infection was performed by Dr. D. Lagos (Lagos et al., 2010). Analysis of these data confirmed expression of the KSHV miRNAs during primary infection (Fig. 4.7). Figure 4.7 shows the $\log_2$ expression values for those miRNAs significantly differentially expressed between infected and uninfected LEC. Eleven out of 17 mature miRNAs are expressed during primary infection. The viral miRNA profile of KLEC is comparable to that of KS lesions (Fig. 4.7, Fig. 3.2A and 3.3A), with the exception of miR-K12-9*, which was not significantly differentially expressed between KS and normal skin (Fig. 3.3A).

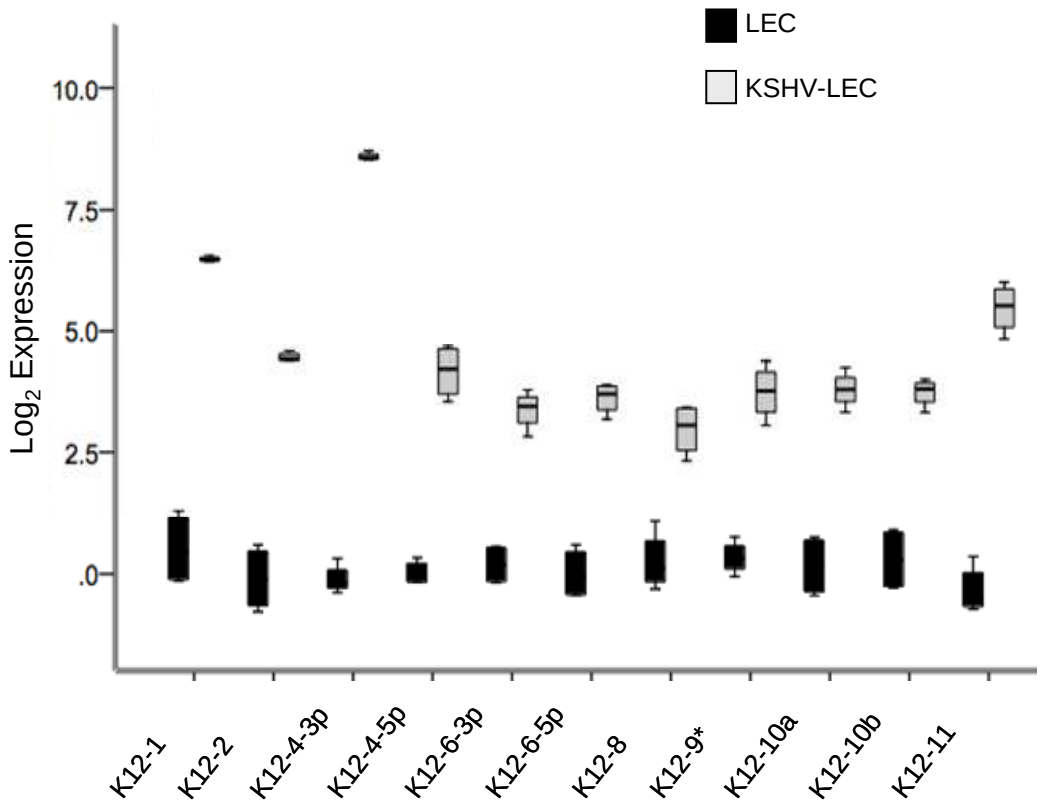

Figure 4.7. KSHV miRNA expression during primary LEC infection. miRNA microarray log2 expression values of significantly expressed miRNAs in KSHV infected LEC 72hrs post infection (relative to uninfected LEC, $p<0.05$). Boxplots show the median, interquartile boxes, 95th percentile range, and outliers as points. Error bars correspond to standard deviation, n = 3.

KSHV miRNA expression in primary infected LEC was confirmed by qRT-PCR for miR-K12-6-5p and miR-K12-11 at 6 and 72hrs post infection (Fig. 4.8). Both miRNAs were detectable at 6hrs, which is the same time point at which MAF mRNA levels begin to decrease (Fig. 4.8). The viral latent protein LANA was also detectable 6hrs post infection (Fig. 4.8). miRNA expression increased between 6 and 72hrs, as evidenced by an increase in the difference between relative miRNA levels between uninfected and infected cells (Fig. 4.8). As LANA and KSHV miRNA expression increased with time, MAF mRNA levels decreased (Figure 4.8).

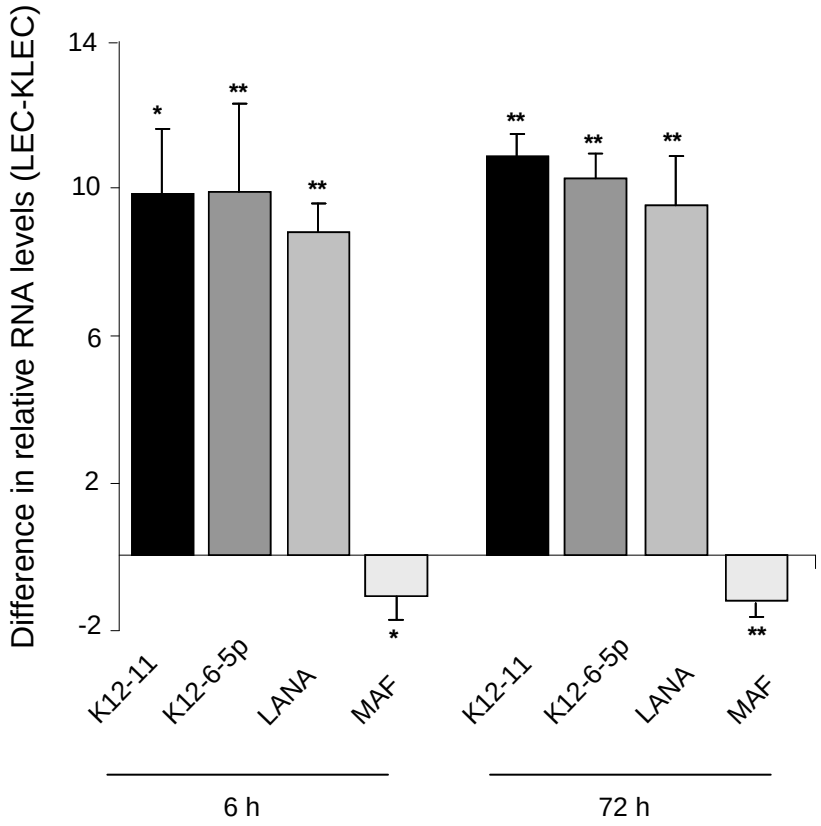

Figure 4.8. KSHV miR-12-6-5p and miR-K12-11 expression during primary infection. The graph shows the relative change in expression of each gene before (LEC) and after KSHV infection of LEC (KLEC) at 6 and 72hrs post infection. KSHV viral gene expression was confirmed by qRT-PCR for LANA, expression is relative to GAPDH. KSHV miRNA expression is relative to RNU66. The bars show the average (n=3) difference in relative expression between LEC and KLEC (DDCt = DCt LEC-DCt KLEC). p values: *<0.001; **<0.005. Error bars correspond to standard deviation, n = 3.

4.8 KSHV miRNA inhibition

4.8.1 miRIDIAN hairpin KSHV miRNA inhibitors

To confirm that MAF down-regulation in KLEC occurred by way of KSHV miRNA-mediated silencing, in particular miR-K12-6 and miR-K12-11, these miRNAs were inhibited during primary KSHV infection. miRNA inhibitors are synthetic oligonucleotides complementary to the mature miRNA of interest. Successful miRNA inhibition impairs silencing, resulting in an increase in mRNA and protein of bone fide targets. The first generation of miRNA inhibitors consisted of 2'-O-methyl modified oligoribonucleotides complementary to the mature miRNA; these inhibitors interacted with the miRNA–RISC nucleoprotein complex successfully blocking target mRNA degradation (Meister et al., 2004; Hutvagner et al., 2004). The 2'O-methyl modification protects oligoribonucleotides from degradation and promotes rapid and stable hybridisation to ssRNA (Meister et al., 2004; Hutvagner et al., 2004). This type of inhibitor was previously used to successfully inhibit KSHV-miRNA RISC-containing complexes in a 293 cell line stably expressing the miRNA Cluster (Samols et al., 2007). The second generation of miRNA inhibitors, referred to as antagomirs, had additional structural and chemical features designed to improve miRNA inhibition. At the time of this work there were no commercially available antagomirs against the KSHV miRNAs. Therefore, custom miRIDIAN miRNA hairpin inhibitors against miR-K12-6-5p and miR-K12-11, the viral miRNAs shown to silence MAF, were purchased from Dharmacon (Thermo-Fisher, Colarado). miRIDIAN miRNA inhibitors contain secondary structural elements flanking the mature miRNA sequence, these hairpins increase inhibitor function and permit multi-miRNA inhibition (Vermeulen et al., 2007). It was proposed that miRIDIAN miRNA inhibitors would allow miRNA inhibition at sub-nanomolar concentrations due to the incorporation of a flanking hairpin; this is necessary when transfecting oligonucleotides into primary LEC which are very sensitive to cytotoxic effects of transfection reagents.

4.8.1.1 KSHV miRNA inhibition of luciferase reporter silencing

miR-K12-11 inhibitor was optimised by confirming the inhibition of silencing of a synthetic luciferase reporter. These initial experiments were performed in 293T cells with miR-K12-11 inhibitor only, as a reporter vector was available for this miRNA. 293T cells were sequentially transfected, first with inhibitors against miR-K12-11, then with luciferase sensor vector (pGL3-T-miR11) and lentiviral plasmid pSIN-K-miR11. Two inhibitor concentrations were tested, and inhibitor miR-K12-6-5p was transfected to control for non-specific effects on silencing (Fig. 4.9A). As expected, miR-K12-11 silenced expression of pGL3-T-miR11, however, the inhibitor specific for miR-K12-11 failed to abolish silencing of the luciferase reporter (Fig. 4.9A). Titrating increasing amounts of this inhibitor slightly augmented silencing, although this was not statistically significant (Fig. 4.9A). Inhibitor miR-K12-6-5p had no significant effects on miR-K-11-mediated silencing. These data suggested the inhibitors may have a non-specific negative effect on luciferase activity. To test this, luciferase activity of pGL3-T-miR11 was measured in the presence of both inhibitors and a non-targeting control (Fig. 4.9B). The inhibitor against miR-K12-11 induced a significant reduction in pGL3-T-miR11 compared to the non-targeting control; the inhibitor against miR-K12-6-5p also induced a reduction in luminescence, although this was not statistically significant (Fig. 4.9B). Therefore, in this experimental system the inhibitor against miR-K12-11 induced significant non-specific affects on reporter luciferase activity.

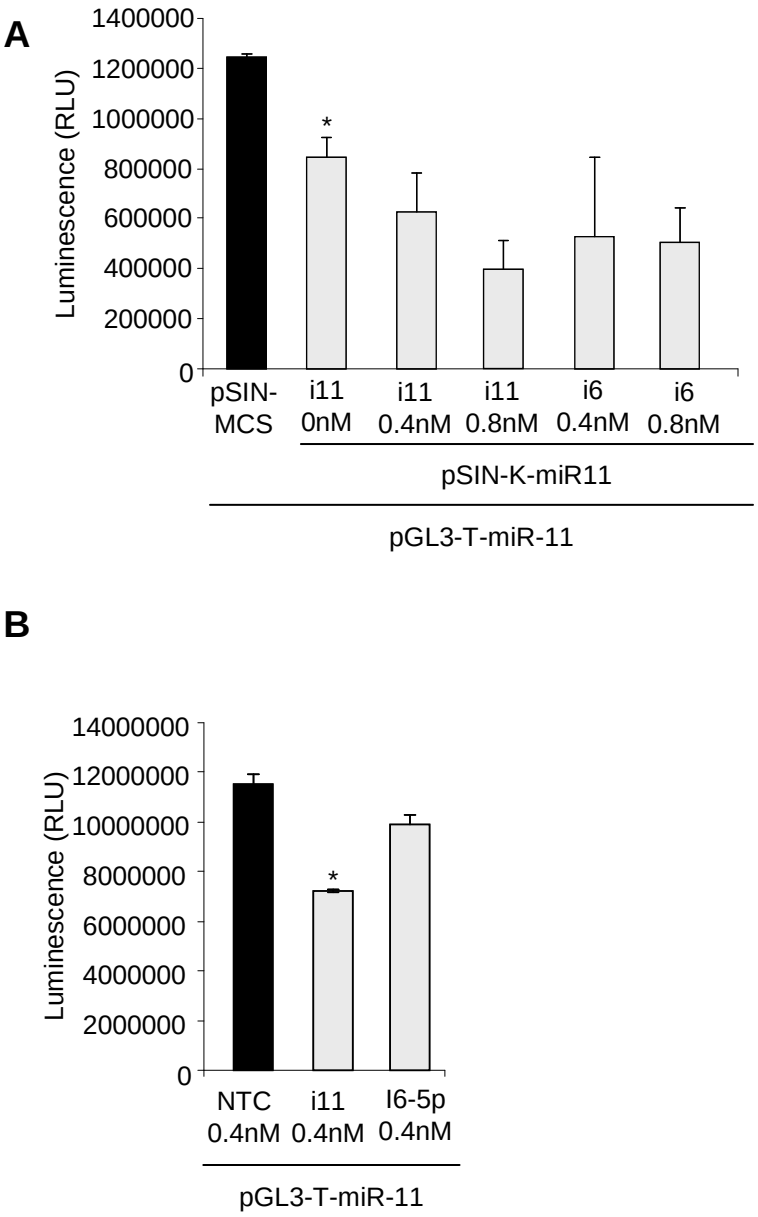

Figure 4.9. KSHV miRNA inhibitor optimisation in 239T cells. *A* pGL3-T-miR11 luciferase activity in 293T cells transfected with inhibitors against miR-K12-11 and as a negative control miR-12-6-5p. In the absence of inhibitors miR-K12-11 induced a significant reduction in luminescence compared to pSIN-MCS. Transfecting increasing concentrations of miR-K12-11 inhibitor failed to ablate silencing, luminescence levels did not vary significantly between 0nM, 0.4nM or 0.8nM i11. Inhibitors against miR-K12-6-5p had no significant effect on pGL3-T-miR11 activity. p values relative to pSIN-MCS: *<0.05. *B* Inhibitor miR-K12-11 has a significant negative effect on pGL3-T-miR11 luciferase activity. Luminescence was significantly reduced in cells transfected with 0.4nM of i11 compared with NTC. Luminescence was also reduced in the presence of i6-5p, although this was not statistically significant. i11: miRNA inhibitor specific for miR-K12-11; i6-5p: miRNA inhibitor specific for miR-k12-6-5p. Error bars correspond to standard deviation, n = 3.

4.8.1.2 KSHV miRNA inhibition in LEC with miRIDIAN inhibitors

To avoid the non-specific effects on luciferase activity observed in the context of these inhibitors, the experimental system was modified and miRNA-mediated MAF silencing was challenged in LEC expressing individual KSHV miRNAs. Previous work in our laboratory using the fluorescent labelled inhibitor analogue siGLO (Dharmacon) confirmed inhibitor delivery to LEC nuclei using the Oligofectamine transfection reagent. A time course monitoring fluorescence post inhibitor-transfection showed maximal fluorescence 24hrs post-transfection, signal remained high until 48hrs, and then significantly decreased by 72hrs post-transfection. Based on these data inhibitors were transfected for 48hrs to allow strong expression and permit time for inhibitor activity. Maximal siGLO fluorescence corresponds to optimal oligonucleotide uptake; however there is no means of directly confirming inhibition of miRNA-mediated silencing. qRT-PCR quantification of the mature miRNA before and after inhibition, would inform on total miRNA levels, but gives no indication of activity. Furthermore, miRNA inhibitors have been shown to comprise the accuracy of miRNA qRT-PCR quantification by directly interfering with the PCR reaction (unpublished observations). Therefore, assessing mRNA levels of a miRNA target is currently the optimal readout of miRNA-inhibitor activity.

Maximal MAF mRNA reduction had previously been observed 72hrs following lentiviral expression of the KSHV miRNAs. To create an optimal environment whereby KSHV miRNAs were expressed during maximal inhibitor uptake, LEC were first infected with the appropriate lentivirus and transfected with inhibitors 24hrs later. miR-K12-11 induced a small but significant reduction in MAF mRNA compared to pSIN-MCS (Fig. 4.10). MAF mRNA levels were similar in cells transfected with miR-K12-11 inhibitors or a non-targeting control, suggesting that the miR-K12-11-specific inhibitor had no effect of MAF silencing (Fig. 4.10). miR-K12-6 caused a significant reduction in MAF mRNA, which was ablated in the presence of miR-K12-6-5p inhibitor (Fig. 4.10). The non-specific effects seen in the luciferase assay were not as significant in this system. In the context of lentivirus expressing empty vector, the inhibitor specific for miR-K12-11 caused a small increase in MAF mRNA compared to NTC, whereas inhibitor against miR-

K12-6-5p induced a decrease in MAF mRNA (Fig. 4.10). However, neither of these effects was statistically significant. These data support MAF silencing by way of miR-K12-6-5p, but are inconclusive for miR-K12-11. Increasing concentration of inhibitors were transfected into LEC in an attempt to titrate miR-K12-6-5p-mediated MAF silencing and to test whether increased inhibitor concentration reversed miR-K12-11 silencing. However, increasing the amount of DNA transfected into LEC requires a reciprocal increase in the volume of transfection reagent Oligofectamine, which LEC are highly sensitive to. Attempts to transfect more than 0.4nM of inhibitors resulted in widespread cell death due to Oligofectamine-induced cytotoxicity, making it impossible to quantify silencing in the presence of higher inhibitor concentration.

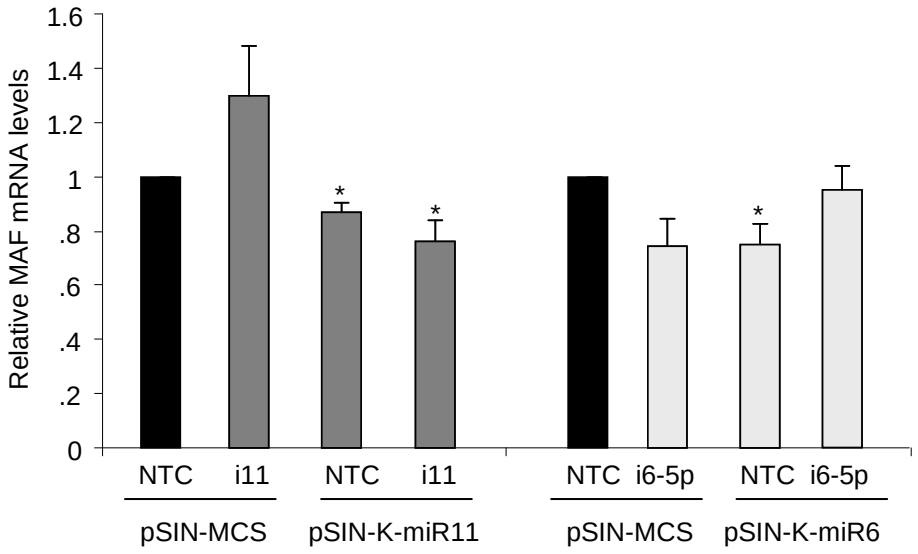

Figure 4.10. KSHV miRNA miRIDIAN inhibitor optimisation in LEC. MAF mRNA levels in LEC transduced with lentivirus expressing individual KSHV miRNAs and transfected with the corresponding miRNA inhibitor or non-targeting control (NTC). pSIN-K-miR11 and pSIN-K-6 induce a small but significant reduction in MAF mRNA compared with pSIN-MCS. The presence of an inhibitor against miR-K12-11 had no effect on MAF silencing, where as miR-k12-6-5p inhibitor led to increased in MAF mRNA. p values relative to pSIN-MCS NTC: *< 0.05. Error bars correspond to standard deviation, n = 3.

Inhibition of viral miRNA function was also performed using the miRIDIAN inhibitors in the context of KSHV infection. In this system, MAF down-regulation occurs 24hrs post infection. To ensure maximal inhibitor uptake, LEC were first transfected with miRNA inhibitors and then infected 24hrs later. Samples were harvested 48hrs post inhibitor transfection, and 24hrs post KSHV infection. MAF mRNA was down-regulated in KSHV-infected cells and in the presence of a non-targeting control (Fig. 4.11A). Inhibitors specific for miR-K12-11 and miR-K12-6-5p had no effect on silencing, MAF mRNA levels were comparable between all KSHV-infected samples regardless of the inhibitor present (Fig. 4.11A).

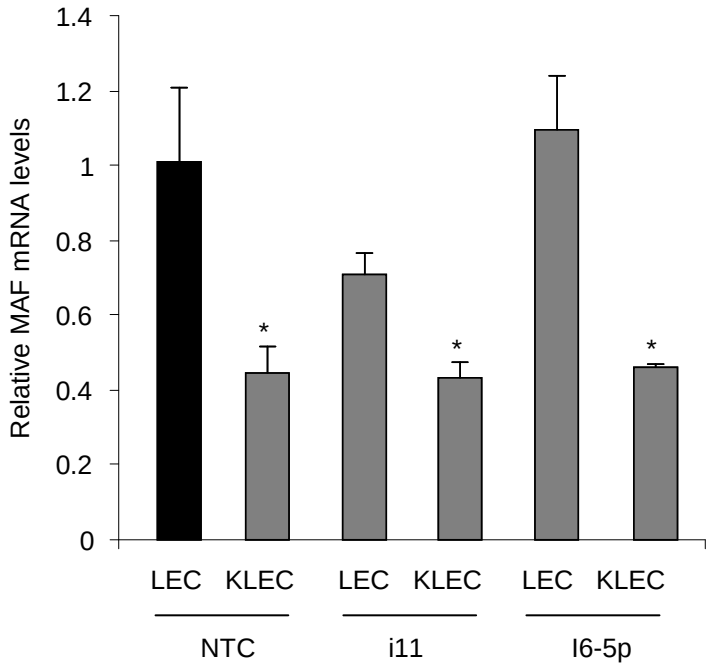

Figure 4.11. KSHV miRNA miRDIAN inhibitor optimisation in KLEC. Viral miRNA inhibitors had no effect on MAF mRNA during KSHV infection. In KSHV infected LEC MAF mRNA is unchanged in the presence of inhibitors specific for miR-K12-11 or miR-k12-6-5p compared with a non-targeting control (NTC). p values relative to LEC NTC: *<0.05. 4.8.2 LNA-modified KSHV miRNA inhibitors. Error bars correspond to standard deviation, n = 3.

4.8.2 LNA-modified KSHV miRNA inhibitors

Due to the inconclusive data obtained with the miRIDIAN hairpin inhibitors, an alternative inhibitor designed was tested to determine whether miRNA inhibition successfully reversed MAF silencing. Locked nucleic acid (LNA) is a three dimensional analogue of RNA. The conformation of the ribose sugar in LNA is 'locked' in the RNA shape by virtue of its rigid bicyclic structure (Petersen et al., 2000). LNA-modified nucleotides undergo conventional Watson-Crick base pairing and, when incorporated into oligonucleotides, the LNA modification conveys dramatically enhanced binding affinity to complementary RNA sequences and greatly increases the stability and specificity of duplexes (Vester and Wengel, 2004). For these reasons LNA-modified oligonucleotides are widely used as miRNA inhibitors. Exiqon (Vedbaek, Denmark) specialise in LNA-modified oligonucleotides and at the time of this work the company was trialling different miRNA inhibitor designs. In collaboration with Exiqon, three independent designs of viral miRNA inhibitors were tested for their ability to reverse MAF silencing. The inhibitors were designed to inhibit exogenous miRNAs and to be active at low concentrations, which would circumvent the need to use toxic concentrations of transfection reagents. Since these reagents were not commercially available, other than the LNA modifications, the specifics of the different versions were not disclosed. LNA inhibitors were provided for MAF-targeting miRNAs, miR-K12-11 and both isoforms of miR-K12-6, as well as a non-targeting KSHV miRNA miR-K12-8. Three versions of each inhibitor were provided.

4.8.2.1 LNA miRNA inhibition of synthetic luciferase targets

As a proof of principle the three LNA miRNA inhibitor designs against miR-K12-11 were tested for the ability to inhibit miRNA-induced silencing of target luciferase constructs in 293T cells. The experiment was complicated by the need to transfect three different reagents into the cell: the miRNA expression vector, the miRNA sensor vector and the miRNA inhibitors. Since optimal oligonucleotide uptake occurs at 48hrs post-transfection, and miR-K12-11 silencing is detected 24hrs post-transfection (Fig. 3.6), 293T cells were first transfected with inhibitors then 24hrs later co-transfected with pSIN-K-miR11 and the corresponding sensor, pGL3-T-miR-11. Cells were harvested 48hrs post inhibitor transfection. These inhibitors were designed to be active a low concentrations, therefore cells were transfected with 10 and 50nM of each of the three inhibitor designs (Fig. 4.12).

miR-K12-11 induced a reduction in sensor luciferase activity, compared to empty vector control. Inhibitor version one caused a slight decrease luminescence at 10nm, but at the higher concentration of 50nM luminescence increased by approximately 20% compared to mock transfected cells (Fig. 4.12A). Inhibitor Version 2 was active at the lower concentration of 10nM, with luminescence increasing slightly with increased inhibitor concentration (Fig. 4.12B). Similar to version one, 50nM of inhibitor version two increased luminescence by approximately 20% compared to mock transfected cells (Fig. 4.12B). At 10nM inhibitor version three increased luminescence by approximately 15%, however this effect did not titrate with increasing inhibitor concentration (Fig. 4.12C). These data suggest the LNA miRNA inhibitors were successfully reversing KSHV miRNA silencing. The luciferase assays revealed a difference in inhibitor efficacy and potency between the three different designs. Based on these preliminary findings with inhibitor 11, all inhibitors were then tested in a more physiologically relevant system.

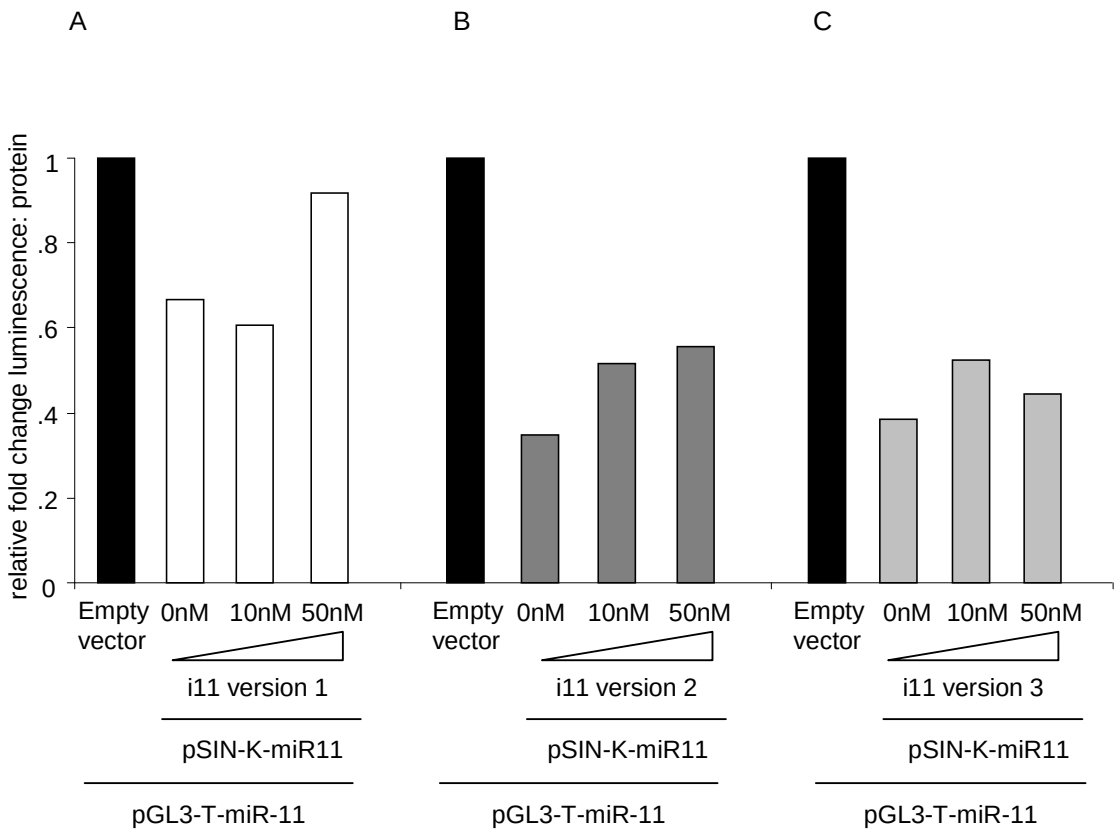

Figure 4.12. KSHV LNA miRNA inhibitor optimisation in 293T cells. The miR-K12-11 expression vector (pSIN-K-miR11) and miRNA sensor (pGL3T-miR-11) were co-transfected into 293T cells which had previously been mock transfected (0nM) or transfected with 10 or 50nM of inhibitor specific for miR-K12-11. Three different inhibitor designs (A-C) were tested for the ability to inhibit miR-K-12-11 induced silencing of the luciferase sensor vector. Luciferase activity is relative to 293T cells transfected with pGL3-T-miR-11 only. pSIN-K-miR11 induces a reduction in luciferase activity; all three inhibitor designs reverse silencing to varying degrees at either 10 or 50nM.

4.8.2.2 LNA miRNA inhibition of KSHV induced MAF silencing

The inhibitors were then tested for the ability to reverse KSHV induced MAF-silencing. This system was selected over LEC expressing lentiviral-encoded KSHV-miRNAs, as the KSHV miRNA expression, and MAF silencing, occurs earliest in KLEC, meaning samples could be harvested at 48hrs post inhibitor transfection, when oligonucleotide uptake is optimal. The inhibitors were tested at the higher concentration of 50nM, which was within the recommended range for the product. LEC were transfected with all three versions of inhibitors specific for the MAF targeting miRNAs: miR-K12-11, miR-K12-6-3p and miR-K12-6-5p, as well as a non-targeting miRNA, miR-K12-8. Twenty four hours post inhibitor transfection, LEC were infected with KSHV and harvested after a further 24hrs.

KSHV infection induced a significant reduction in MAF mRNA, compared to LEC transfected with NTC (Fig. 4.13). KSHV LNA-inhibitors specific for miR-K12-11 and both isoforms of miR-K12-6 successfully reversed MAF silencing, as evidenced by an increase in MAF mRNA levels, relative to KLEC transfected with a non-targeting control (Fig. 4.13). However, similar to the luciferase inhibitor data, there were differences in inhibitor efficacy between the three designs (Fig. 4.13). Design two was the most consistent, reversing silencing mediated by all three MAF-targeting miRNAs (Fig. 4.13). Whereas design one failed to reproducibly reverse silencing induced by any of the three viral miRNAs (Fig. 4.13). Design three was variable, in that it reversed miR-K12-6-3p and miR-K12-6-5p silencing; however the inhibitor specific for miR-K12-11 had no significant effect on MAF mRNA levels, compared with a non-targeting control. In contrast, all three inhibitor designs against miR-K12-8, a miRNA not predicted to target MAF, had no effect on the suppression of MAF mRNA by KSHV (Fig. 4.13). These data confirm that MAF silencing in KSHV infected LEC is mediated specifically by miR-K12-6 and miR-K12-11. Inhibition of both mature isoforms of miR-12-6 led to an increase in MAF mRNA, suggesting both branches of the stem-loop contribute to MAF down-regulation, concurring with the in silico target prediction analysis (Fig. 4.3A).

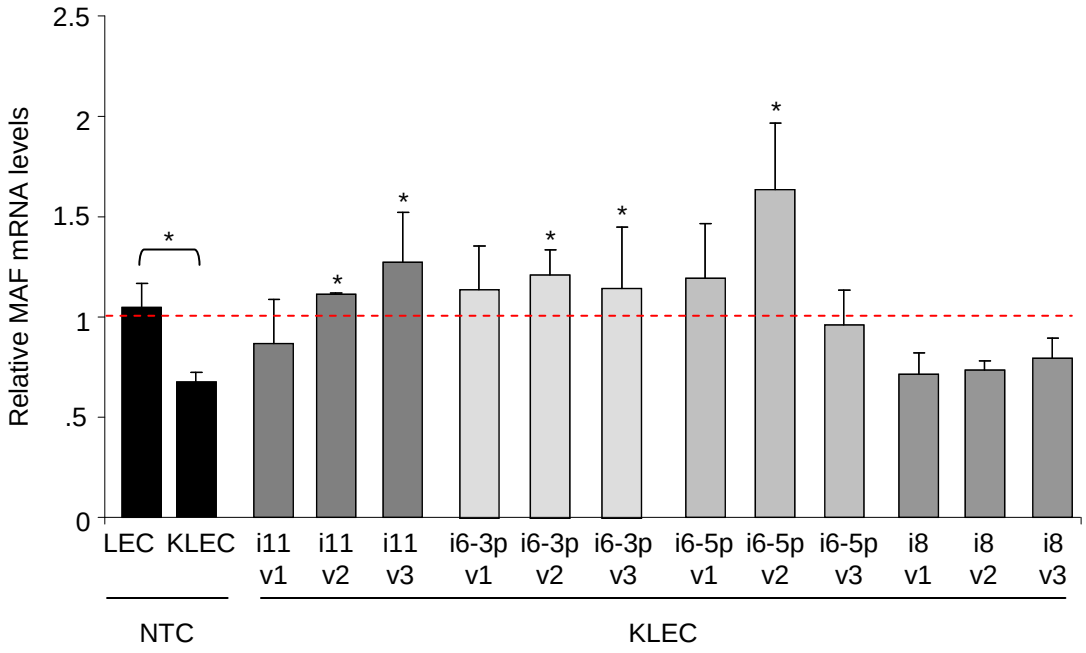

Figure 4.13. Inhibition of miR-K12-6, miR-K12-11 and miR-K12-1 attenuates MAF silencing. LEC were infected with KSHV in the presence of LNA inhibitors against miRK12-11, miR-K12-6-3p, miR-K12-6-5p, miR-K12-8 or a non-targeting control (NTC). Three versions of each inhibitor were tested, denoted by v1-v3. In KSHV infected LEC MAF mRNA was significantly reduced in the presence of a NTC compared to uninfected cells (black bars). Stars indicate samples with significantly different MAF mRNA levels compared to KLEC NTC. Inhibitor version 2 of all targeting miRNAs abolishes silencing. None of the inhibitor designs specific for miR-K12-8, a non-targeting KSHV miRNA had any effect on MAF mRNA levels. Error bars correspond to standard deviation, n = 3.

4.9 Does hsa-miR-155 contribute to MAF silencing?

KSHV miR-K12-11 is a known orthoglogue of cellular miR-155 (Skalsky et al., 2007; Gottwein et al., 2007) (Fig. 4.14A). Since MAF is a validated target of mouse miR-155 in T lymphocytes, it was possible that miR-155 was contributing to MAF silencing observed in KSHV-infected LEC. miRNA profiling data of miR-155 expression in KS and KSHV-infected LEC is shown in Figure 4.14B (LEC and KLEC data provided by D. Lagos (Lagos et al., 2010)). Burkitt's lymphoma (miR-155 positive (Eis et al., 2005)) and PEL cells (miR-155 negative (Gottwein et al., 2007; Skalsky et al., 2007)) were included as controls. miR-155 is expressed in LEC and was found to be induced upon KSHV infection (Fig. 4.14B). However, miR-155 was undetectable in both skin and KS lesions (Fig. 4.14B). The total $\log_2$ expression values for miR-K12-11 and miR-155, 6 and 72 hour post KSHV infection of LEC are shown (Fig. 4.14C). Both miRNAs are expressed at similar total levels in KSHV-infected cells (Fig. 4.14C). Six hours post KSHV infection miR-155 is induced by approximately 2 fold; this induction is maintained 72hrs post infection (Fig. 4.14D). KSHV-encoded miR-K12-11 is detected 6hrs post KSHV infection (Fig. 4.14D) and its expression increases by approximately 30 fold by 72hrs (Fig. 4.14D). Since miR-155 is only marginally induced upon infection, MAF silencing observed in KSHV infected LEC is likely to primarily be as a consequence of the substantial induction of KSHV-encoded miR-K12-11. Furthermore, since miR-155 was undetectable in KS lesions, its role in MAF-regulation during KSHV infection was not investigated any further.

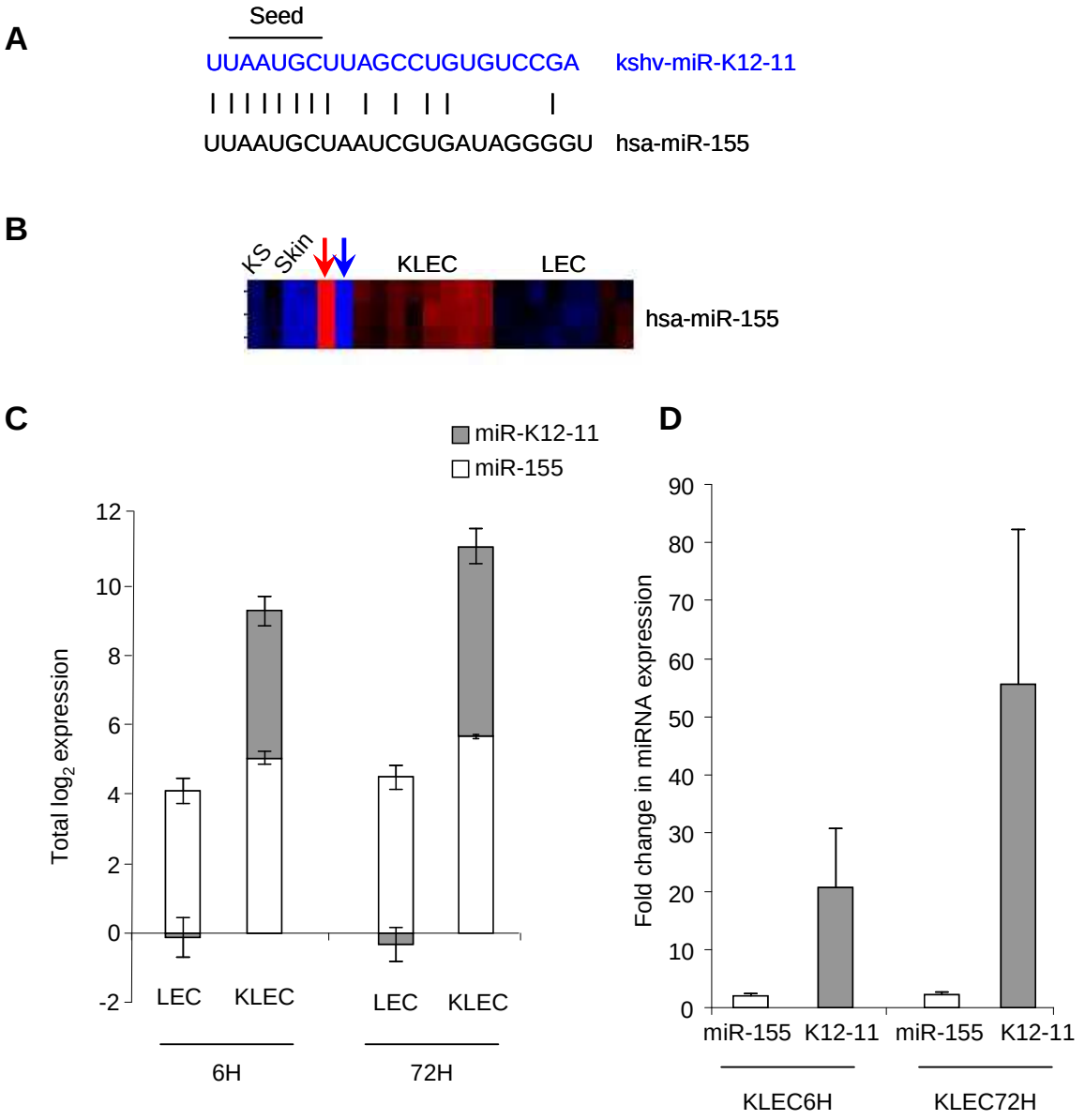

Figure 4.14. KSHV regulation of miR-155. *A* Sequence alignment of mature miR-155 and miR-K12-11. These orthologous miRNAs share the same seed sequence. Lines indicate matching bases. *B* Heatmap showing miRNA profiling data for miR-155. Expressed probes are in red, unexpressed in blue. Red arrow: positive control, Burkitt's lymphoma. Blue arrow: negative control, PEL cell line. miR-155 is not expressed in skin or KS. KSHV infection of LEC induced miR-155 expression. *C* Total microarray $\log_2$ expression levels for miR-155 (white) and miR-K12-11 (gray) in LEC and KLEC at 6 and 72hrs. KSHV-encoded miR-K12-11 is undetectable in uninfected cells, generating negative $\log_2$ expression levels. miR-K12-11 is detected 6hrs post KSHV infection, expression increases with time. miR-155 is expressed in LEC and induced upon KSHV infection. *D* Fold change in miR-155 and miR-K12-11 expression levels upon KSHV infection, at 6 and 72hr time points. miR-155 is induced by 2 fold post infection. There is a ~30 fold induction in miR-K12-11 between 6 and 72hr post KSHV infection. Error bars correspond to standard deviation, n = 3.

4.10 MAF regulation in PEL

miR-155 is essential for normal B cell development (Rodriguez et al., 2007; Thai et al., 2007; Vigorito et al., 2007). miR-155 was one of the first miRNAs to be classified as an oncomir due to it's ability to induce pre-B cell lymphomas in mice (Costinean et al., 2006); miR-155 is up-regulated in a range of B cell lymphomas including diffuse large B cell lymphoma, chronic leukaemia, Burkitt's lymphoma, Hodgkin's Lymphoma and primary mediastinal B cell lymphoma (PMBL) (Eis et al., 2005). Strikingly, miR-155 is not expressed in PEL, instead the viral homologue miR-K12-11 is expressed (Skalsky et al., 2007; Gottwein et al., 2007). Deep sequencing of PEL cells revealed that over 90% of the miRNA content is comprised of viral-encoded miRNAs (Umbach and Cullen, 2010), suggesting an important role for viral miRNAs in the development and maintenance of PEL.

Since both viral and cellular miRNAs are known to target MAF in other cell types (Rodriguez et al., 2007) (and work presented within this thesis), it is plausible that MAF is also under miRNA regulation in KSHV-associated B cell lymphomas. Relative MAF mRNA levels were assessed in a range of transformed B cell lines spanning different stages of B cell development (Fig. 4.15); every cell line tested expressed either miR-155 or miR-K12-11 (Eis et al., 2005; Gottwein et al., 2007; Skalsky et al., 2007). MAF mRNA was undetectable in a range of PEL cell lines, nor was it detectable in B cell lines representing plasma cell leukaemia, diffuse B cell lymphoma or Burkitt's lymphoma, as evidenced by high delta Ct values (Fig. 4.15). The only cell lines expressing MAF were those derived from multiple myeloma; these samples had low delta Ct values of <8 (Fig. 4.15). MAF over-expression in these cells is due to a chromosomal translocation juxtaposing MAF next to the IgG heavy chain promoter (Chesi et al., 1998). Correspondingly, MAF was detected in multiple myeloma cell lines with this mutation but not in a cell line lacking the translocation (see KMS in Fig. 4.15). These data suggest rather than being under miRNA regulation, MAF is not expressed in transformed B cells. The exception to this is a sub-set of multiple myeloma cells lines, where a chromosomal translocation switches on MAF expression.

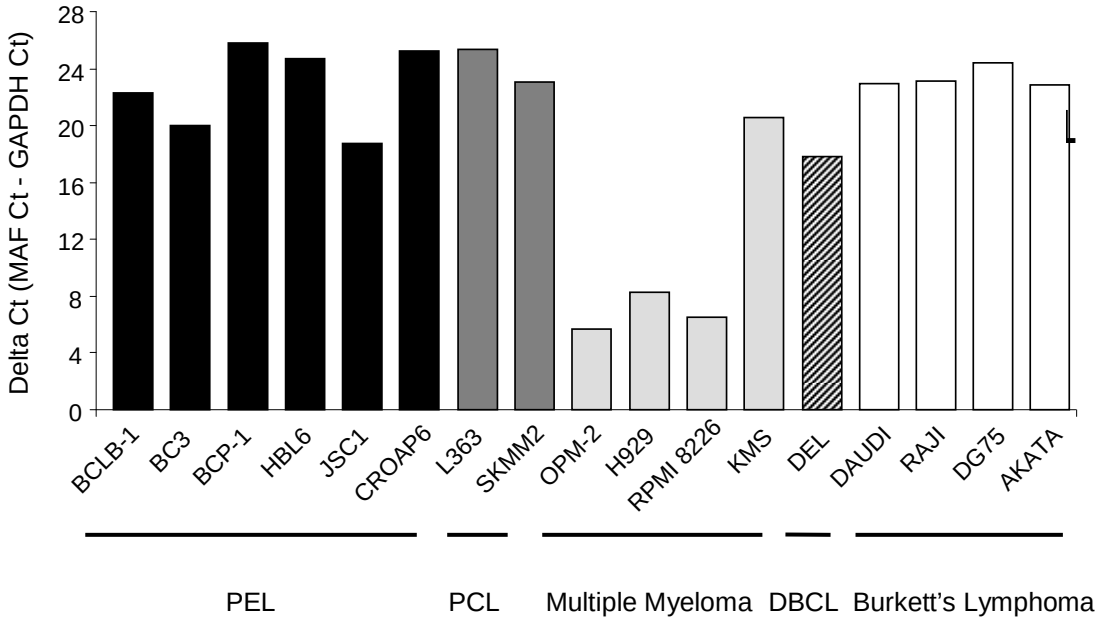

Figure 4.15. MAF expression in B cell lymphoma cell lines. qRT-PCR quantification of MAF mRNA in a range of lymphoma derived B cell lines. The difference in threshold detection cycle (Ct) between MAF and GAPDH is shown. Unexpressed transcripts have a Ct of >35, generating a delta Ct of >17. MAF mRNA was undetectable in the majority of cell lines. MAF mRNA was detected in three multiple myeloma cell lines, OPM-2, H929 and RPMI 8226, as evidenced by low delta Ct values. These three cell lines contain a MAF activating translocation, whereas multiple myeloma cell line KMS does not possess this mutation.

4.11 Discussion

This work shows that multiple KSHV-encoded miRNAs, in particular miR-K12-11 and miR-K12-6, function in concert to target the bZIP transcription factor MAF. Importantly, MAF is the first KSHV miRNA target to be indentified in LEC, the closest primary cells to KS tumour cells (Hong et al., 2004; Wang et al., 2004).

MAF mRNA was down-regulated by approximately 40% in LEC transduced with the viral miRNA Cluster and 60% in KSHV-infected cells; this led to a similar reduction in MAF protein levels. This level of repression is in keeping with other validated miRNA targets. A reduction of this magnitude for a transcription factor could have significant impact, leading to down-stream effects whereby target genes regulated by MAF are no longer activated or repressed. For this reason MAF represented an interesting KSHV miRNA target for further investigation.

Seven out of ten of the expressed KSHV miRNAs have predicted binding sites in the MAF 3'UTR. In particular, expression of miR-K-12-11 and miR-K12-6 induced a significant reduction in MAF mRNA. miR-155 is orthologous to miR-K12-11 and a validated MAF-targeting miRNA (Gottwein et al., 2007; Skalsky et al., 2007; Rodriguez et al., 2007). Since the orthologues share a seed region they are expected to regulate an overlapping set of target genes (Gottwein et al., 2007; Skalsky et al., 2007). In a lentiviral screen testing all the KSHV miRNAs for their ability to silence MAF, the viral homologue of miR-155 was identified as a MAF-repressing miRNA. These data provide evidence of functional homology between viral and cellular miRNAs. miR-155 and MAF are co-expressed in LEC, upon KSHV infection there is a significant induction of viral miRNA expression and only a marginal increase in miR-155. Therefore, it is probable that MAF silencing observed upon KSHV infection is by way of the KSHV miRNAs, including miR-K12-11, and not a consequence of miR-155 expression.

Similar to MAF, the transcriptional repressor BACH1 has also been validated as both a miR-155 and miR-K12-11 target (Qin et al., 2010). Previously, BACH1 was shown to heterodimerise with both MAFK and MAF (Newman and Keating, 2003). However, BACH1 mRNA increases upon KSHV infection of LEC (Lagos et al., 2007). Therefore, either BACH1 is not under KSHV miRNA regulation in LEC or other signalling events are counteracting viral miRNA silencing.

All experimentally validated cellular KSHV miRNA targets, including MAF, are regulated by more than one miRNA (Samols et al., 2007; Ziegelbauer et al., 2009; Qin et al., 2010). Similarly, endogenous cellular miRNA targets are often regulated by multiple members of clustered miRNAs which share the same seed, such as the Let7 family (Lee and Dutta, 2007). Redundancy of targeting by multiple miRNAs may represent a safety mechanism whereby the virus ensures target mRNAs will be down-regulated.

Site directed mutagenesis disrupting PITA predicted KSHV miRNA target sites abolished miRNA silencing of a fragment of the MAF 3'UTR in a luciferase reporter vector. These data confirm KSHV miRNA silencing is via binding sites in the MAF 3'UTR and validate miRNA target prediction analysis. The site directed mutagenesis showed that PITA sites with a seemingly insignificant ΔΔG score (-3 ΔΔG for miR-K12-11), which would fall below stringent threshold cut-offs, can be bone fide miRNA target sites. Interestingly, the magnitude of silencing observed when the Cluster or individual miRNAs were co-transfected with the MAF 3'UTR was consistently less than when they were co-transfected with the synthetic miRNA sensor vectors (Fig. 3.7 and 4.5B). This difference may be due to variations in target site efficiency, or as a consequence of the shortened MAF 3'UTR fragment in the reporter vector. Perfect seed matches were inserted, in tandem, into the sensor vectors; according to miRNA targeting rules regulation of these sites is expected to initiate a high level of silencing. Perfect miRNA target sites are not particularly common in endogenous miRNA targets (Grimson et al., 2007; Bartel, 2009), indeed none of the predicted sites in the cloned region of MAF 3'UTR were fully complementary. Instead all sites contained wobbles or mismatches, which are known to negatively affect silencing. miRNA target sites

located within 40bp of each have been shown to act cooperatively during silencing; whereas sites further apart act independently (Grimson et al., 2007; Baek et al., 2008). Since none of the KSHV miRNA target sites are closely situated, MAF silencing by multiple viral miRNAs is likely to be additive. The magnitude of MAF 3'UTR silencing was greatest in the presence of miR-K12-6 compared to the entire Cluster. This may be due to differences in relative expression levels of MAF-targeting miRNA, and is suggestive of cooperative rather than synergistic regulation by the Cluster. However, maximal MAF mRNA repression was observed both in Cluster expressing and KSHV-infected LEC compared to LEC expressing individual miRNAs. Clearly further experimental work is needed to fully understand the mode of regulation by multiple KSHV miRNAs.

Agilent miRNA profiling of KSHV-infected LEC confirmed viral miRNA expression during primary infection (Lagos et al., 2010). Expression of KSHV miRNAs had previously been confirmed in KSHV-infected human umbilical endothelial cells (O'Hara et al., 2009). However, these are the first data confirming viral miRNA expression in KLEC, the experimental model of primary infection most closely related to KSHV infected spindle cells (Hong et al., 2004; Wang et al., 2004). Importantly, the viral miRNA profile of KS lesions and KSHV-infected LEC were identical, with the exception of miR-K12-9* which was only detected in KLEC. This similarity in miRNA expression profile supports the choice to exclude those miRNAs not expressed in KS lesions in prediction analysis as these miRNAs not only appear to be irrelevant to KS biology, but also during primary infection. It is possible that viral miRNAs not expressed in KS or KLEC target specific transcripts only relevant KSHV infection of B cells.

MAF was down-regulated at both the RNA and protein level in KSHV-infected LEC. MAF repression during whole virus infection, and not only in the presence of the KSHV miRNA Cluster, makes it a physiologically relevant target. GEM analysis of the entire Maf family of transcription factors revealed MAF to be the only member down-regulated upon KSHV infection. There was also significant up-regulation of two small Maf transcription factors, MAFF and MAFK. Small Maf transcription factors lack a transactivation domain, therefore as homodimers these proteins act as repressors (Motohashi et al., 2002; Blank and Andrews, 1997). However, small Mafs can also activate transcription when in complex with other leucine zipper proteins (Motohashi et al., 2002). There is limited functional redundancy between the different family members, especially between the small and large Mafs (Blank and Andrews, 1997; Eychene et al., 2008). MAFF regulates expression of the oxytocin receptor (OTR) during pregnancy (Kimura et al., 1999). All small Mafs heterodimerise with the NF-E2 transcription factor, this transcriptional complex is crucial for the regulation of erythroid gene expression and platelet formation (Toki et al., 1997). Therefore, due to the difference in both dimer partner and target genes it is unlikely that the small Maf upregulation observed upon KSHV infection serves to functionally compensate for MAF silencing.

Failure to detect inhibition of the synthetic luciferase miRNA targets and lack of a positive control meant it was not possible to determine whether the Dharmacon miRIDIAN inhibitors were functional. This made it difficult to draw conclusions on the lack of MAF silencing seen in the presence of the miRIDIAN inhibitors. When inhibiting exogenous miRNAs, both inhibitor and miRNA must be added separately to the cell. The timing and order of events may be important factors in determining whether silencing occurs and whether it can be quantified. In addition, LEC are toxic to high levels of the transfection reagent, oligofectamine making it difficult to determine whether increasing inhibitor concentration would have successfully inhibited MAF silencing.

In contrast, KSHV miRNA-mediated silencing of a luciferase reporter and MAF mRNA, was successfully inhibited by LNA-modified inhibitors. Three different LNA inhibitor designs were tested for their ability to reverse viral miRNA silencing. Since these were pilot experiments for the purpose of product optimisation, the differences in inhibitor design were not disclosed. Preliminary experiments with miR-K12-11 inhibitor, revealed increased luminescence from the reporter vector in the presence of all three inhibitor designs, suggesting the LNA modified oligonucleotides were inhibiting KSHV miRNA activity. Different levels of inhibition were observed between the three designs. The inhibitors were then tested in a more physiologically relevant system for the ability to reverse KSHV-induced MAF down-regulation in LEC. Inhibitor design two successfully inhibited miR-K12-11 silencing of a luciferase reporter vector, and reversed MAF silencing mediated by all three MAF-targeting miRNAs. Importantly, design two specific for miR-K12-8, a non MAF-targeting miRNA, had no affect on MAF mRNA levels in KLEC. Inhibitor design one reversed miR-K12-11 mediated luciferase silencing at 50nM, however at the same concentration this design had no significant affect on MAF mRNA levels for any of the MAF-targeting KSHV miRNAs. Inhibitor design three reversed MAF silencing induced by two out of three targeting miRNAs. These findings supported experimental optimisation performed by Exiqon and the second version of inhibitor design is now commercially available.

Inhibition of all three individual MAF-targeting miRNAs with inhibitor design two restored MAF mRNA levels back to that comparable with LEC. This was surprising since inhibiting a single viral miRNA in KLEC would only affect a fraction of targeting miRNAs. It was therefore expected that MAF would continue to be silenced, albeit to a lesser degree, by the other non-inhibited miRNAs. However, since the window of down-regulation is relatively small (approximately 40%) it may be beyond the sensitivity of the assay to dissect the individual contributions of multiple KSHV miRNAs in this experiment.

Due to MAF miRNA regulation by either miR-155 or miR-K12-11 in T cells and LEC respectively, I hypothesised that MAF may also be under miRNA regulation in transformed B cells. MAF mRNA was undetectable in KSHV positive PEL cell lines and a range of cells spanning different stages of B cell development. It is unlikely that miRNA regulation of a target gene would lead to complete absence of the mRNA as miRNAs do not function as on/off switches. MAF is not expressed in primary B cells isolated from bone marrow (Vigorito et al., 2007) and GEM analysis of miR-155 deficient mouse B cells compared to normal B cells did not reveal up-regulation of Maf, at the RNA level (Vigorito et al., 2007). Therefore, these data suggest that MAF is not under miR-155 or miR-K12-11 regulation in B cells, and MAF is unlikely to be relevant to B cell biology or transformation. With exception of a subset of multiple myeloma cases in which MAF over-expression promotes transformation (Chesi et al., 1998).

Chapter 5. KSHV miRNA regulation of MAF induces endothelial reprogramming

5.1 Introduction and aims

The aim of this chapter was to investigate the functional significance of miRNA-mediated MAF down-regulation during KSHV infection of LEC.

MAF is involved in tissue specification and terminal differentiation of the lens, T-lymphocytes and endochondral bone (Kim et al., 1999b; Ring et al., 2000; Kawauchi et al., 1999; MacLean et al., 2003; Kim et al., 1999a) and regulates a distinct repertoire of target genes specific to each cell type (Eychene et al., 2008). Genome-wide identification of MAF targets has been problematic due to the degeneracy of MAF recognition elements (MARE) (Kataoka, 2007). Consequently, the targets of MAF and its role in LEC are unknown. This section of work focussed on characterising MAF function in LEC, through the identification of LEC-specific MAF target genes; these observations were used to determine the role of viral miRNA-dependent MAF regulation during primary KSHV infection.

5.2 Hypothesis: MAF plays a role in LEC fate determination

LEC are derived from venous endothelial cells and have a plastic, rather than irreversible, differentiation potential (Srinivasan et al., 2007; Johnson et al., 2008). Consequently, continual expression of PROX1 is required during embryogenesis and throughout adulthood to maintain a LEC phenotype and prevent cells from reverting to the default BEC-like state (Wigle et al., 2002; Johnson et al., 2008). Previous work from our laboratory and others has shown that KSHV infection of LEC induces transcriptional reprogramming, altering the differentiation status of the infected cell (Carroll et al., 2004; Hong et al., 2004; Wang et al., 2004). As a result of this transcriptional reprogramming, KSHV infected endothelial cells of either BEC or LEC lineage are more similar to each other in their transcriptional profile than uninfected cells (Wang et al., 2004). KLEC are therefore transcriptionally closer to BEC than uninfected LEC, as evidence by the reduced inter-sample distance of transcriptional profiles (Fig. 5.1, data taken from (Wang et al., 2004)). Despite the up-regulation in corresponding lineage markers, this phenotypic convergence is largely due to decreased expression of unique LEC or BEC markers in the infected cell (Wang et al., 2004). However, the mechanism behind KSHV-induced endothelial reprogramming is unknown. MAF is expressed early during embryogenesis and directs cell lineage specification contributing to tissue development (Yang and Cvekl, 2007; Eychene et al., 2008). MAF is also differentially expressed between LEC and BEC, and has been previously characterised as a LEC-specific transcript (Petrova et al., 2002; Hong et al., 2004). These findings highlight a potential role for MAF in specifying the LEC phenotype. Consequently, miRNA dysregulation of MAF could contribute to the mechanism of endothelial reprogramming following KSHV infection.

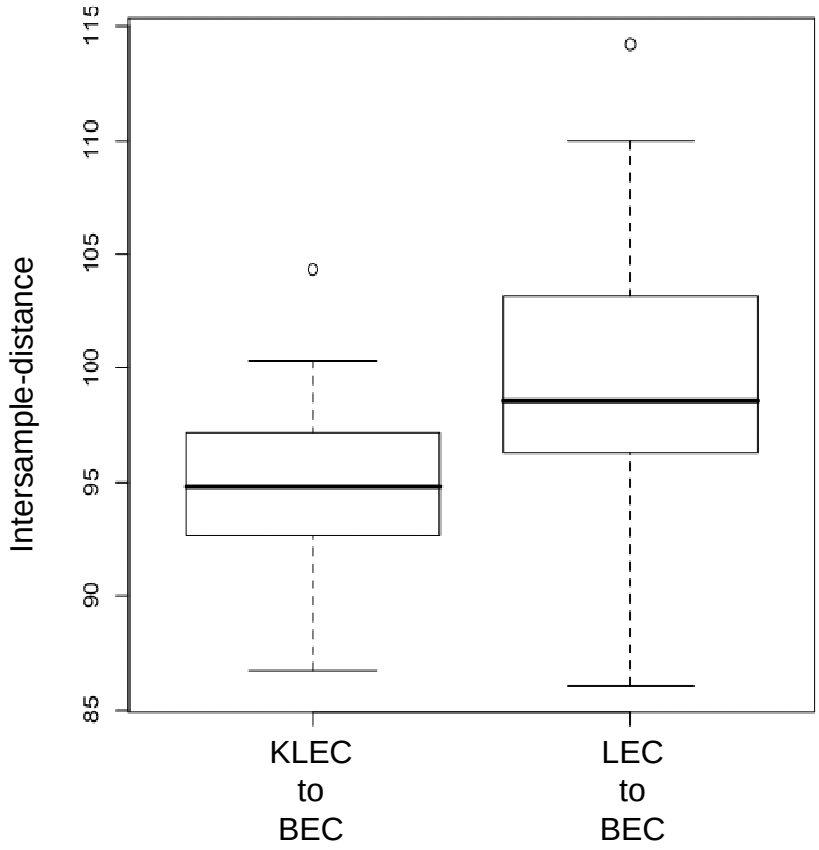

Figure 5.1. KSHV induced transcriptional reprogramming Boxplots of transcriptional profile inter-sample distances between uninfected LEC and BEC and following KSHV infection of LEC (KLEC). The reduced inter-sample distance between KLEC and BEC compared with LEC and BEC, marks convergence in gene expression profile upon KSHV infection of LEC (t-test, p = 0.0002459).

5.3 MAF target identification in LEC

siRNA-mediated knock-down of MAF in LEC was used to identify potential MAF target genes. Cells with reduced MAF levels were subjected to GEM analysis to identify significant changes in mRNA abundance. MAF mRNA undergoes RNA processing to generate two isoforms: a long species which encodes a short single exon encoded protein (MAF-S) or a shorter isoform which is alternatively spliced to give a longer, double exon protein (MAF-L) (Fig. 5.2A) (Chesi et al., 1998). The splicing reaction removes the majority of the 3'UTR, containing miRNA binding sites, from the MAF-L isoform. To ensure neither isoform was preferentially knocked down, a pool of four targeting siRNAs was used, which recognised regions homologous to both MAF isoforms (Fig. 5.2A). To control for non-sequence specific effects, LEC were transfected with a non-targeting pool of siRNA designed against C. elegans-specific sequences. A time-course experiment was performed to determine the time point post-siRNA transfection at which to conduct the GEM. MAF mRNA was quantified 48, 72 and 96hrs post siRNA transfection (Fig. 5.2B). MAF mRNA was maximally repressed by approximately 75% 48hrs post-transfection, relative MAF mRNA levels then began to increase (Fig. 5.2B). The GEM experiment was therefore performed 48hrs post-siRNA transfection.

It was important to quantify the relative expression levels of the two MAF isoforms, to determine how they were regulated during KSHV infection. Previously MAF mRNA quantification was performed using a commercial TaqMan assay in which the primers recognised a sequence common to both MAF mRNA isoforms. To determine the relative mRNA abundances of each isoform primers were designed against sequences unique to MAF-S or MAF-L. qRT-PCR analysis revealed concordant repression of both isoforms when LEC were infected with KSHV, in the presence of the miRNA Cluster or MAF siRNA (Fig. 5.3B). The miRNA Cluster induced silencing of MAF-L which lacks many of the predicated KSHV miRNA binding sites due to splicing of the 3'UTR sequence. This could

perhaps be due to miRNA binding sites retained within the second MAF exon. Both mRNA isoforms increased in the presence of MAF-expressing lentivirus, which encodes the single ORF of MAF-S. It was therefore surprising that MAF-L levels also increased slightly and this could be due to MAF auto-activation of the endogenous promoter. Concurring with previous findings, MAF-S was more abundant than MAF-L as evidence by the lower delta Ct values (Fig. 5.3C) (Chesi et al., 1998). These data suggest MAF-S is the predominant MAF isoform in LEC (Fig. 5.3C).

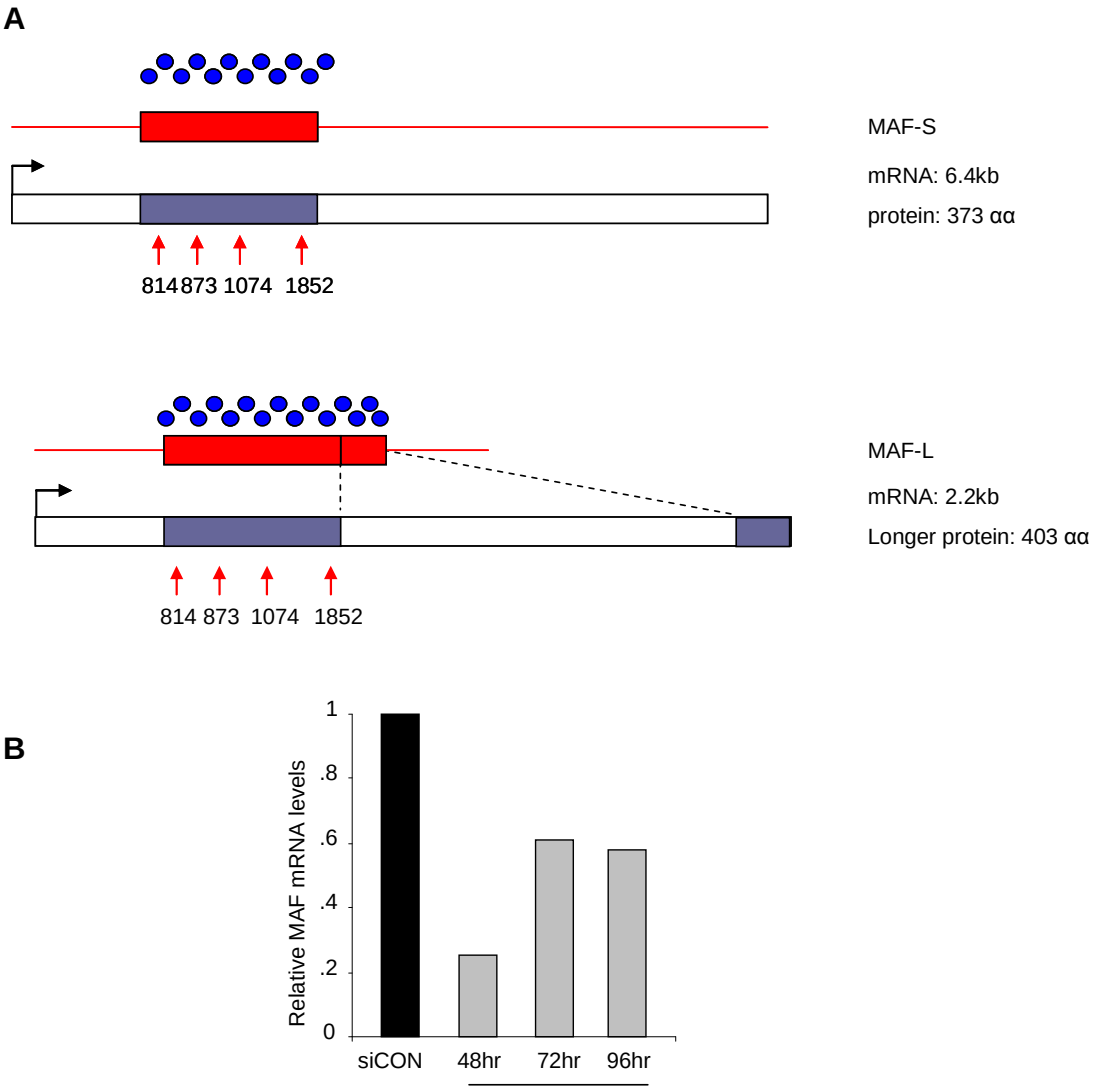

Figure 5.2. siRNA-mediated MAF knock-down *A* Schematic depicting alternatively spliced MAF isoforms. MAF-S is an intron-less 6.4kb mRNA which generates a 373 amino acid protein. MAF-L is alternatively spliced removing a large internal intron and generating a shorter double-exon mRNA of 2.2kb. The additional exon encodes 30 amino acids. DNA is represented by white and blue rectangles, mRNA is shown in red and protein in blue circles. Arrow represents the promoter. Positions of the four targeting siRNAs are indicated, the nucleotide position is shown below the red arrows. All four siRNA molecules recognise sequences common to both MAF isoforms. *B* MAF siRNA time course. MAF mRNA was maximally repressed 48 hours post siRNA transfection compared to control siRNA (siCON). siMAF mRNA was compared to siCON at the equivalent time point, for comparison only one control bar is shown.

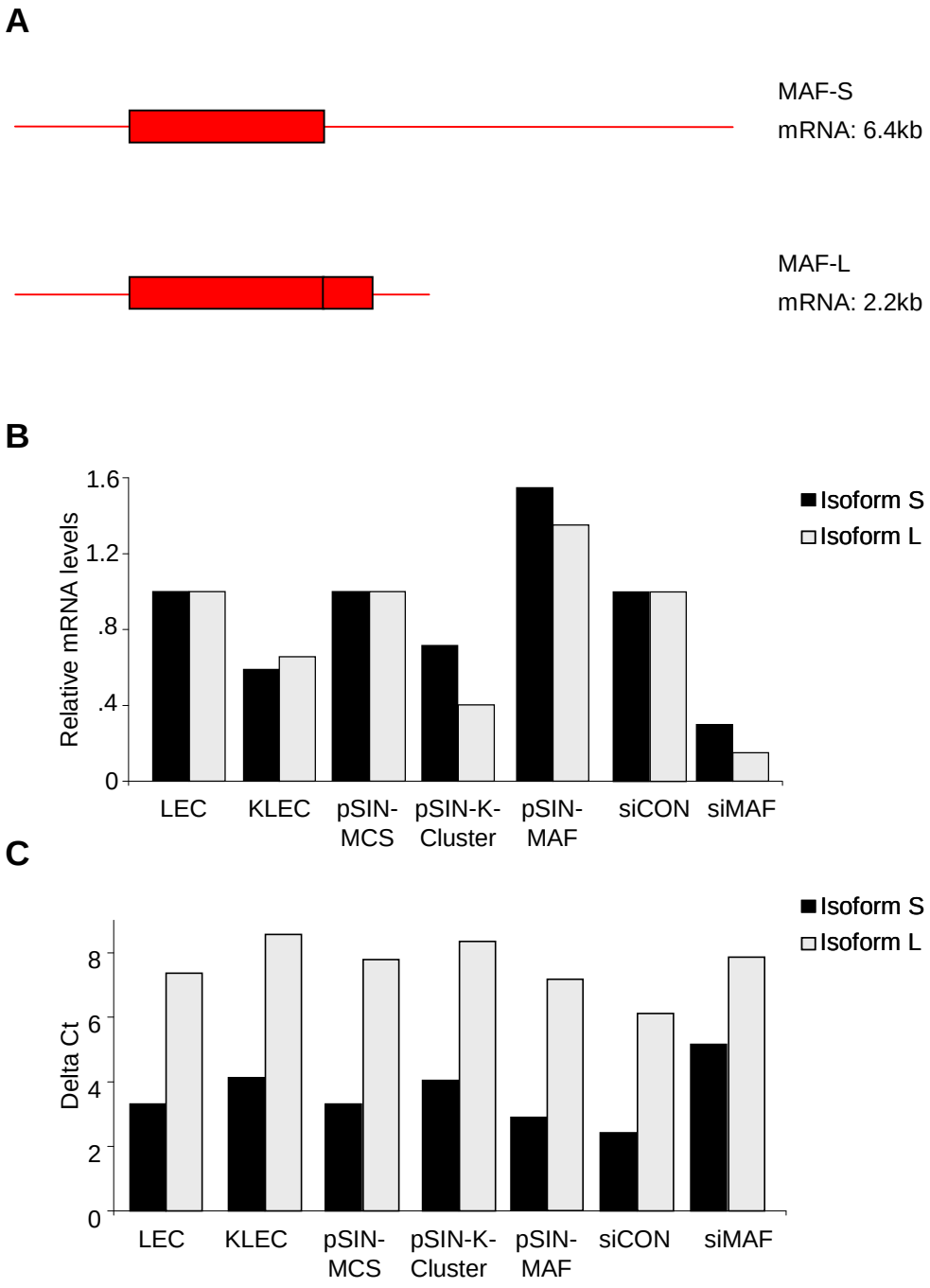

Figure 5.3 MAF mRNA isoforms are concordantly regulated. *A* Schematic depicting alternatively spliced MAF mRNA isoforms. *B* Relative mRNA levels of both MAF isoforms normalised to LEC, pSIN-MCS or siCON. Both isoforms are down-regulated upon KSHV infection, expression of the KSHV miRNA Cluster and after transfection of MAF siRNA. Both isoforms increase slightly when LEC are transduced with pSIN-MAF lentivirus. *C* Difference in threshold detection cycle (Delta Ct) between MAF and GAPDH for both mRNA isoforms. More abundant transcripts have lower delta Ct values, therefore isoform S mRNA is expressed at a higher level than isoform L.

GEM profiling of LEC in the absence of MAF identified a cohort of genes with significantly ($q<0.05$) altered mRNA abundance compared to LEC transfected with the non-targeting control. The heatmap in Figure 5.3A shows the top twenty most significantly up- and down-regulated probes, which represent potential MAF target genes. In the absence of MAF, mRNA of MAF-repressed targets will increase, whereas MAF-activated genes will decrease in abundance (Fig. 5.4A). Importantly, MAF was the most significantly down-regulated probe, indicating that siRNA knock-down was successful. However, qRT-PCR analysis showed only a 50% reduction 48hrs post-transfection (Fig. 5.4B). This reduction in MAF expression was less pronounced than observed during the time-course experiment (Fig. 5.2B), meaning that a larger pool of potential targets may have been identified in the context of more robust knock-down. However, those targets identified here may represent those genes most sensitive to MAF regulation and their expression is affected even in the context of small changes in MAF level, similar to those changes observed due to miRNA-mediated regulation. These data were subsequently analysed in the context of genes significantly altered following KSHV-induced MAF down-regulation to determine whether MAF, and its target genes, were involved in the KSHV-mediated LEC transcriptional reprogramming.

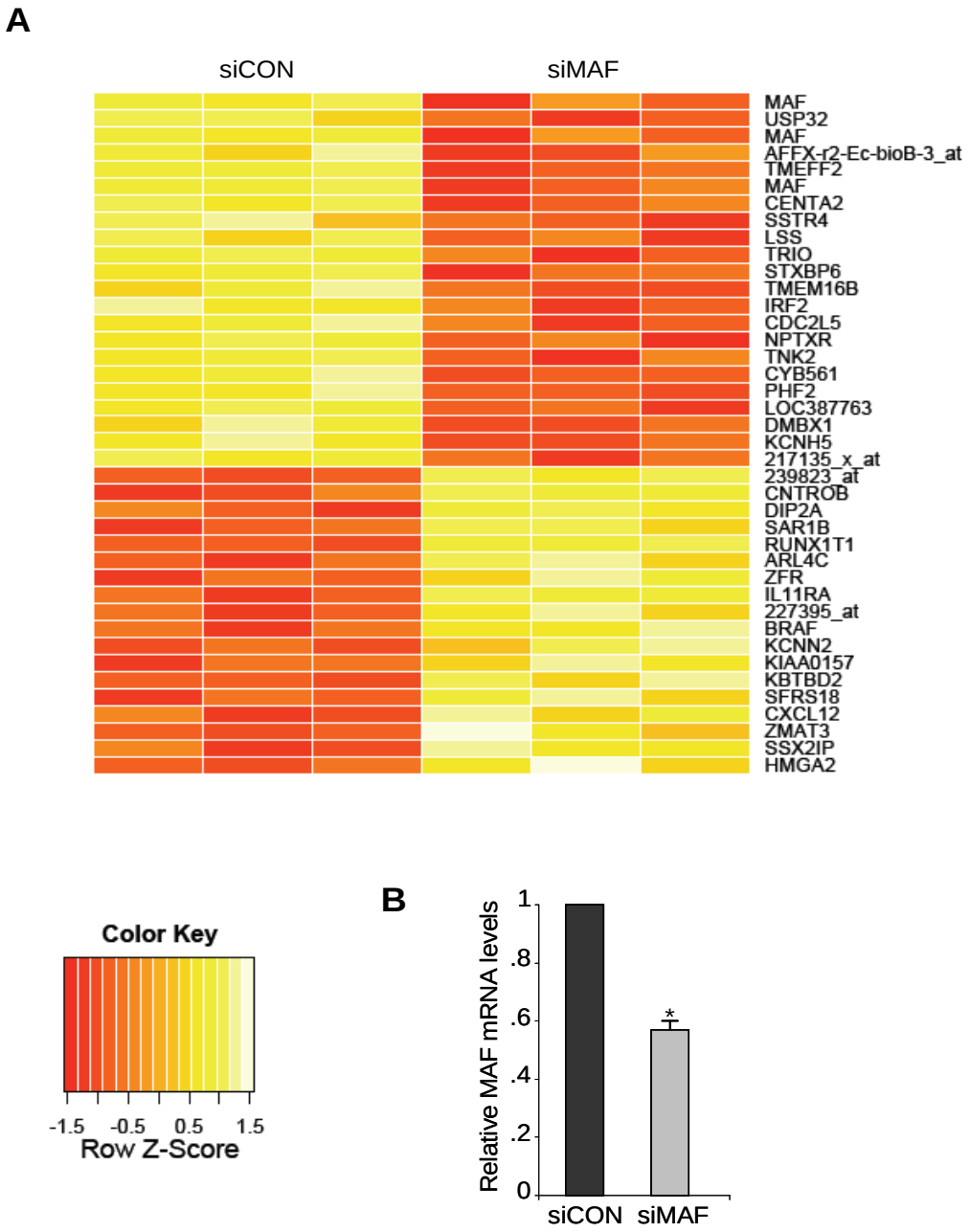

Figure 5.4. MAF knock-down induces changes in gene expression. *A* Heatmap showing probes de-regulated in LEC when MAF is knocked-down by siRNA. The transcriptional profile of LEC transfected with siRNA specific for MAF (siMAF) was compared with cells transfected with a non-targeting control (siCON) 48hrs post-transfection. Down-regulated genes are in red, up-regulated in yellow. This set of most significantly different genes has a false discovery rate (q value) of <0.05. The Z-score scale shows mean scaled and zero centred $\log_2$ GEM expression values for each row. Up-regulated probes are in yellow, down-regulated probes in red. *B* qRT-PCR quantification of MAF mRNA in cells transfected with either MAF or control siRNA. MAF mRNA was reduced by ~55% compared to cells transfected with a non-targeting control. MAF mRNA is normalised to GAPDH and relative to siCON, p: *<0.005. . Error bars correspond to standard deviation, n = 3.

5.4 MAF knock-down induces up-regulation of BEC markers

KSHV-mediated endothelial reprogramming of LEC results in increased expression of BEC marker genes, with a corresponding decrease in LEC-associated transcripts (Fig. 5.1) (Wang et al., 2004). To determine whether MAF knock-down by the KSHV miRNAs played a role in this transcriptional shift, the expression of BEC and LEC-specific genes were examined in the context of MAF repression. LEC and BEC markers were selected as those with the most significant difference in expression between the two cell types (Fig. 5.5, data taken from (Lagos et al., 2007). These genes were selected on the basis of expression rather than function, and therefore include classic cell surface markers and additional BEC- or LEC-specific proteins.

Data from three independent GEM data sets where MAF was down-regulated were analysed: KSHV-infected versus non-infected LEC (Lagos et al., 2007); LEC transduced with the KSHV miRNA Cluster versus empty lentiviral vector; and LEC transfected with siRNA targeting MAF versus non-targeting siRNA control. The primary data set was generated previously (Lagos et al., 2007), the remaining two data sets were generated as described in Sections 3.5 and 5.3.

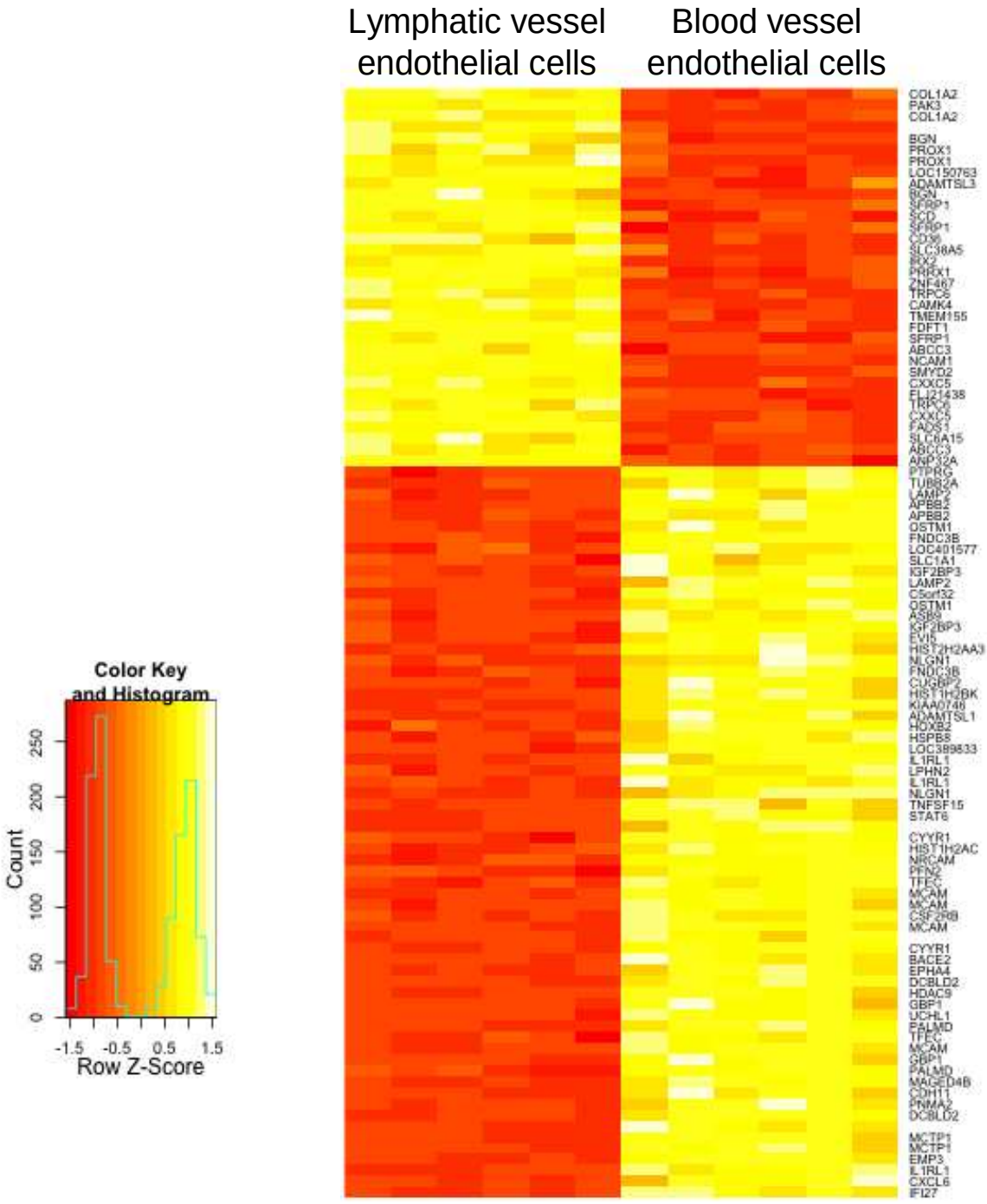

Figure 5.5. LEC and BEC are distinguished on the basis of their transcriptional profiles. Heatmap showing the top 100 differentially expressed probes between LEC and BEC (n=34 LEC, n=66 BEC). The gene set has a false discovery rate (FDR q-value) of 0.05. The Z-score scale shows mean scaled and zero centred $\log_2$ GEM expression values for each row. Up-regulated probes are in yellow, down-regulated probes in red.

Data were analysed using the pathway orientated method Gene Set Enrichment Analysis (GSEA), by the bioinformatician Dr. S. Henderson (CR-UK Viral Oncology group, UCL) (Subramanian et al., 2005). This method considers a set of related genes, in this instance BEC or LEC markers, and determines whether these genes are randomly distributed or localised at the top or bottom of ranked expression data. This method enables the identification of changes in gene expression in a number of related genes in the context of the whole gene-set, which if looked at as changes in individual genes may be missed. Significance is placed on concordant changes within a pathway as opposed to large single differences in gene expression (Subramanian et al., 2005). An enrichment score (ES) was calculated to indicate whether the BEC/LEC markers were significantly distributed in any of the three ranked expression data sets; this corresponded to a weighted Kolmogorov-Smirnov-like statistic (Subramanian et al., 2005). The statistical significance (p value) of the ES score was estimated using a permutation test, in which multiple random lists of the same gene number were tested to see whether they shared the same distribution as the BEC/LEC markers. An ES score was significant if the distribution of more than 95% ($p<0.05$) of control gene sets was considered random. The p value was then adjusted to account for multiple hypotheses testing to give a false discovery rate, or q value. Lists of 50-250 BEC markers, increasing in 50 gene increments were tested across all three GEM data sets. As previously reported, KSHV infection of LEC induced an up-regulation in BEC marker genes (Wang et al., 2004) and this positive enrichment was identified by GSEA (Fig. 5.5, grey plot), illustrating that this is a suitable method of analysis in this context. GSEA also identified a significant enrichment in up-regulated BEC marker genes in LEC expressing the KSHV miRNA Cluster (Fig. 5.5, green plot) and when MAF was knocked-down by siRNA, as evidence by the skewed distribution to the left (Fig. 5.6, red plot).

The vertical dotted lines on the distribution plots represent the leading edge gene subset for each experiment (Fig. 5.5). This represents the core of a gene set which accounts for the enrichment signal (ES score). Leading core edge genes (i.e. those genes most highly up-regulated) were compared within each GSEA analysis to identify concordantly regulated BEC markers potentially under MAF control (Fig. 5.7 and Table 5.1). The proportional Venn diagram shows the number of genes present within each leading core edge data set and how many of these genes were shared between all three sets (Fig. 5.7). Gene names and leading core edge subsets in which they were found are detailed in Table 5.1. Three putative MAF targets were highly up-regulated under all three conditions (KSHV infection, expression of the miRNA Cluster and siRNA knockdown of MAF): TFEC, NRCAM and SLC1A1 (Table 5.1). Two additional genes, HDAC9 and GULP1, were also included as potential MAF targets, since they were two of the most highly up-regulated genes following both KSHV infection and MAF siRNA knockdown and were also up-regulated by the miRNA Cluster, although not present in the leading edge (Table 5.1).

MAF knock-down in LEC, in three different contexts, led to an increase in BEC marker gene expression; therefore this analysis identified a putative role for MAF as a transcriptional repressor of BEC identity in LEC. The concordant change across all three data sets suggests that the viral miRNAs could contribute to KSHV-induced transcriptional reprogramming of LEC through suppression of the transcription factor MAF.

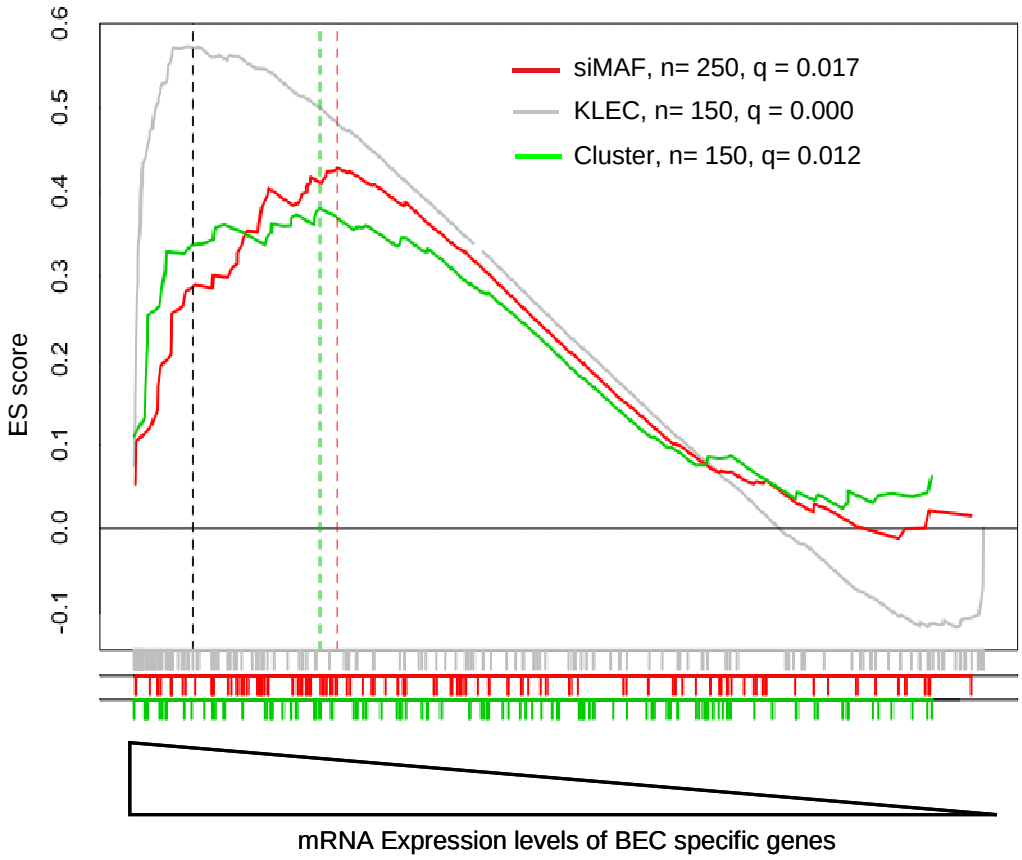

Figure 5.6. BEC markers increase upon MAF knock-down. Gene Set Enrichment Analysis (GSEA) demonstrates a significant enrichment of BEC markers in three different GEM experiments: LEC infected with KSHV (KLEC, grey line), LEC transfected with siRNA against MAF (siMAF, red), and LEC infected with the KSHV miRNA Cluster (green). Several lists of the topmost BEC markers (top 50, 100, 150, 200, 250,) were tested and the most significant list for each experiment is plotted. Note that in the case of KSHV-LEC q=0.000 exceeds the precision of the test. All curves display a similar skewed distribution to the left indicating increased expression. The peak enrichment score (ES) shows the strength of the BEC marker enrichment for each experiment and determines the genes that are within the 'leading edge' of the GSEA analysis, this is indicated by hatched lines. Vertical lines below the plots represent BEC specific probes. The significance calculation shown (q) is a false discovery rate

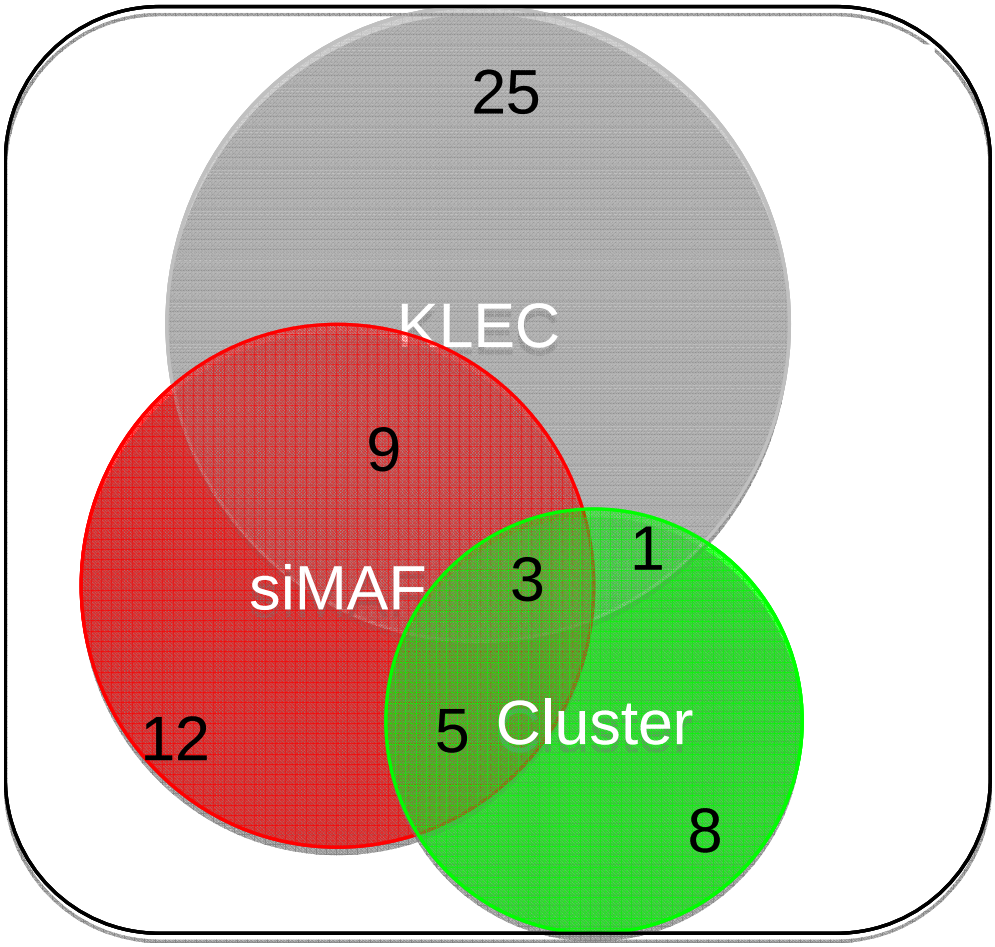

Figure 5.7. BEC markers increased in the context of MAF repression. The intersection of genes within the leading edge between the three GEM experiments is represented as an area proportional Venn diagram. The numbers indicate how many genes are shared between the different leading core edge data sets. The total number of leading core edge genes between all three data sets is 88.

Gene	siMAF	KLEC	Cluster	Total
NRCAM	**1**	**1**	**1**	**3**
TFEC	1	1	1	3
SLC1A1	**1**	**1**	**1**	**3**
CYYR1	1	1	0	2
PALMD	1	0	1	2
HDAC9	**1**	**1**	**0**	**2**
OSTM1	1	1	0	2
IFI27	1	1	0	2
APBB2	1	0	1	2
HSPB8	1	0	1	2
IGF2BP3	1	0	1	2
CSF2RB	1	1	0	2
EVI5	1	1	0	2
PTPRG	1	1	0	2
LOC40157	0	1	1	2
TNIK	1	0	1	2
GULP1	**1**	**1**	**0**	**2**
AKAP12	1	1	0	2

Table 5.1 Leading core edge genes. BEC marker genes concordantly up-regulated in multiple GEM data sets. 1 indicates genes present within the leading core edge, 0 indicates genes which are not present. Only genes present in two or more leading core edge sets are shown. Genes highlighted in bold represent candidate MAF target genes selected for experimental validation.

5.5 MAF knock-down has no effect on LEC marker expression

KSHV infection of LEC leads to decreased expression of LEC-specific genes (Wang et al., 2004) and the GSEA analysis confirmed this negative enrichment as evidenced by a skewed distribution to the right (Fig. 5.78). GSEA identified no significant change in LEC marker expression in the presence of the KSHV miRNA Cluster or when MAF was knocked-down specifically by siRNA (Fig. 5.8B and C). These data suggest neither the KSHV miRNA Cluster nor MAF play a role in regulating LEC marker expression.

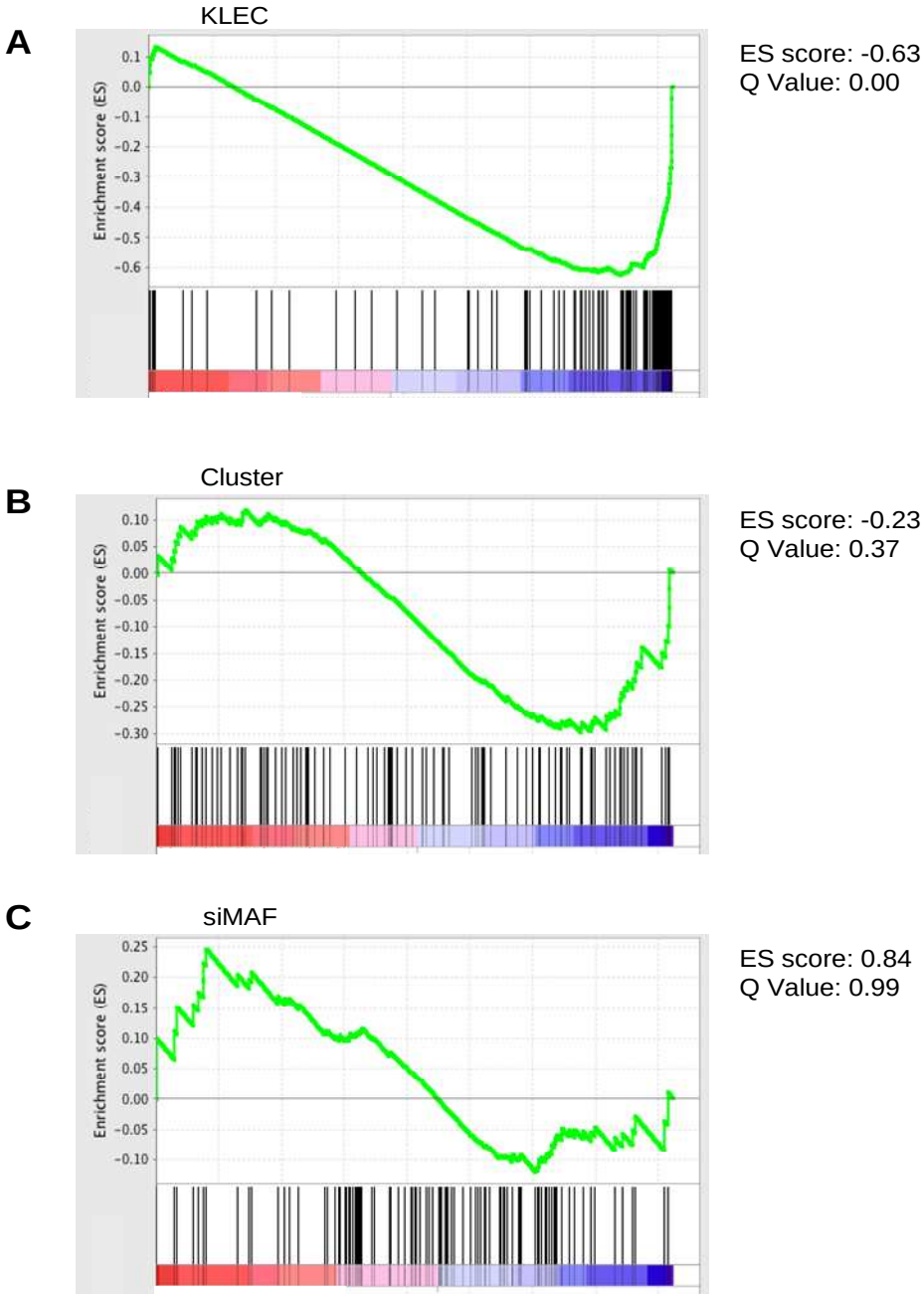

Figure 5.8. siRNA MAF knock-down or KSHV miRNA Cluster has no effect on LEC marker expression *A* GSEA demonstrates a significant enrichment in decreased LEC marker expression upon KSHV infection. Several lists of the topmost LEC markers (top 50, 100, 150, 200, 250,) were tested and the most significant list is plotted (150). Note that q = 0.000 exceeds the precision of the test. Skewed distribution to the right indicates decreased marker expression. Vertical lines below the plots represent LEC specific probes. The colour scale represents expression, from red (increased expression) to blue (decreased expression). The significance calculation shown (q) is a false discovery rate. *B* KSHV miRNA Cluster expression has no significant effect on LEC marker gene expression: q >0.05 C Knock-down MAF by siRNA also has no significant effect on LEC markers: q >0.05.

5.6 MAF is a repressor of BEC identity

5.6.1 MAF knock-down induces increased BEC marker expression

The up-regulation of putative MAF target genes identified by GSEA was confirmed in independent experiments by qRT-PCR analysis (Fig. 5.9). All five putative MAF target genes showed increased expression by this method when MAF was knocked-down by siRNA compared to a non-targeting control (Fig. 5.9A). In the presence of the Cluster, four out of five genes increased compared to empty lentiviral vector (Fig. 5.9B). GULP1 did not increase, however this gene was not present in the leading core edge of the Cluster GSEA profile (Table 5.1). Up-regulation of three out of five genes identified by GSEA was confirmed in KSHV infected LEC (Fig. 5.9C). This represents the most complex experimental system, whereby additional mechanisms may be influencing gene expression. Up-regulation of additional BEC markers was confirmed when MAF was knocked-down (Fig. 5.10). Four standard BEC markers: MAML2, FLT1, CXCR4 and CXCL12, were up-regulated in LEC when MAF was knocked-down by siRNA, compared to a non-targeting control (Fig. 5.10). These data further supported a role for MAF as a transcriptional repressor of BEC identity in LEC.

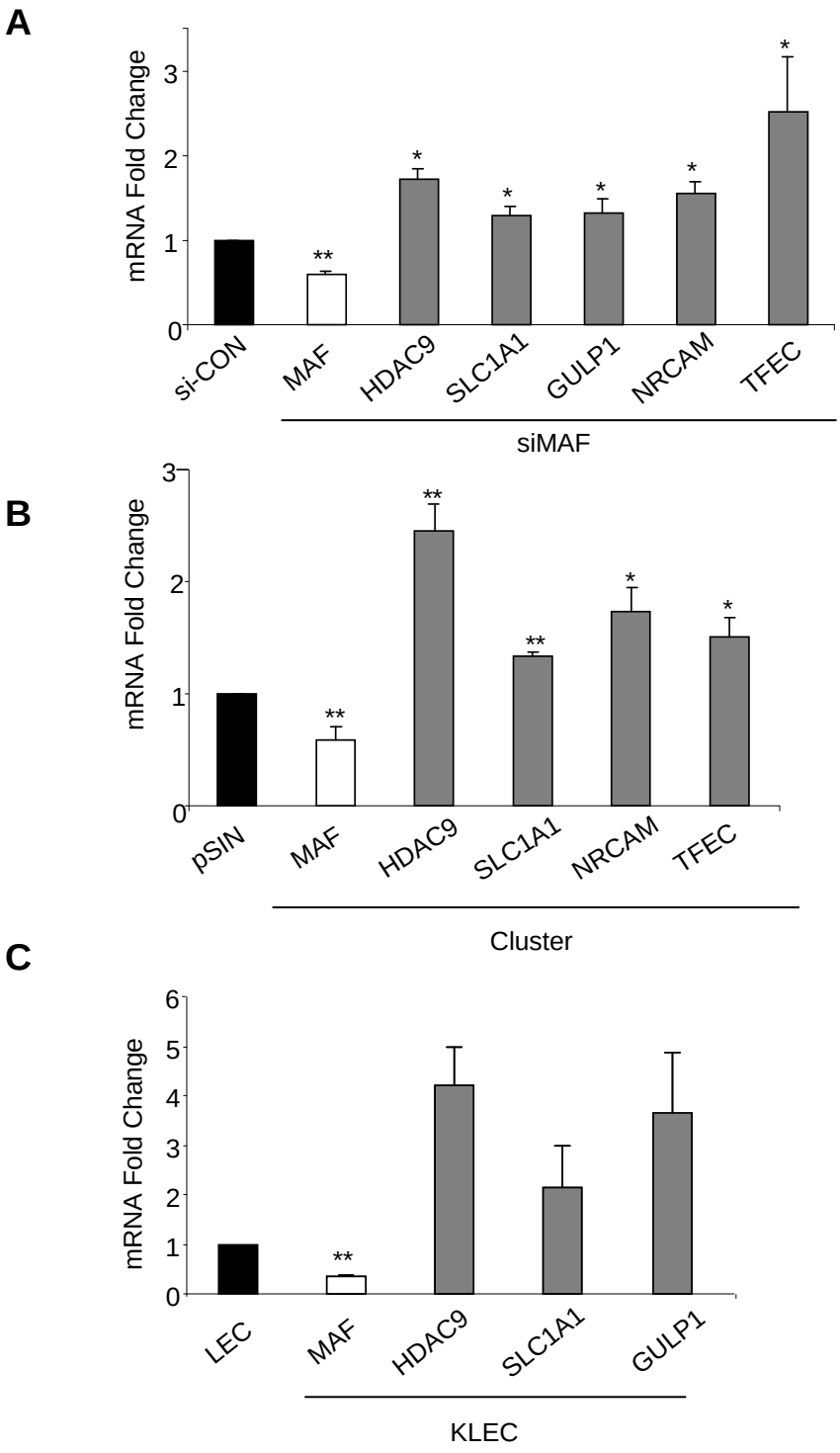

Figure 5.9. GSEA validation. *A-C* qRT-PCR analysis confirmed the up-regulation of candidate MAF target genes identified by GSEA (grey bars). MAF down-regulation by siRNA *(A)*, miRNA Cluster *(B)* and KSHV is shown *(C)* (white bars). All values were normalised to GAPDH. In each condition, expression is relative to the corresponding control siCON, pSIN or LEC (black bar). p values: *<0.05; **<0.005. Error bars correspond to standard deviation, n = 3.

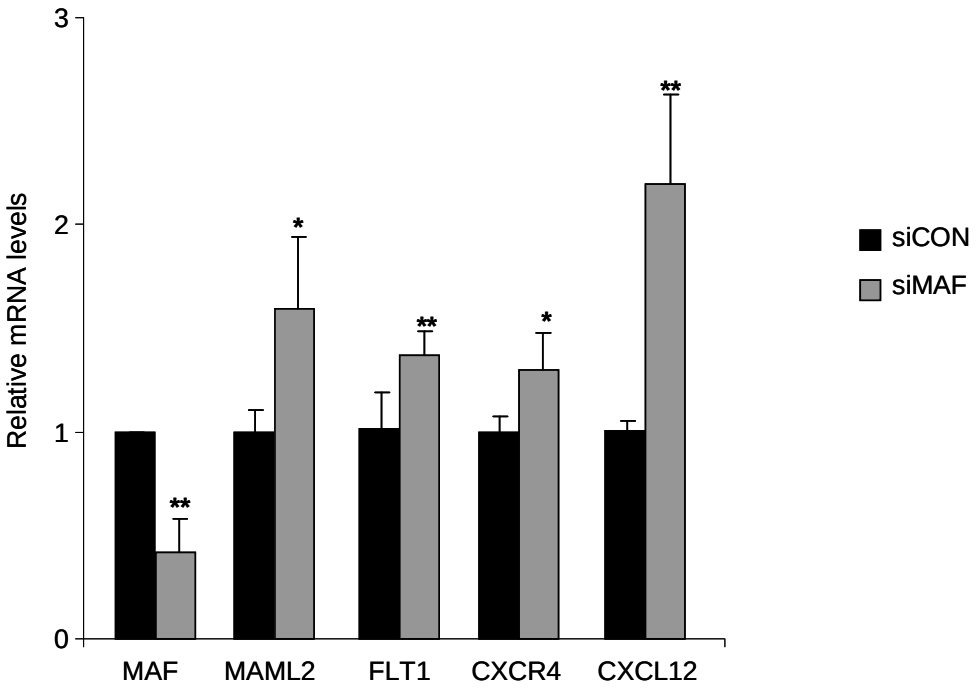

Figure 5.10. MAF knock-down leads to up-regulation of additional BEC markers. qRT-PCR analysis confirmed an up-regulation of additional BEC-specific markers when MAF was knocked-down by siRNA. LEC were transfected with either a non-targeting control (siCON, black bars) or an siRNA pool specific for MAF (siMAF, grey bars). Expression is relative to GAPDH and normalised to LEC transfected with siCON. p values: *<0.05 **<0.005. Error bars correspond to standard deviation, n = 3.

To confirm KSHV miRNA regulation of BEC markers occurs through a mechanism dependent on MAF silencing, this phenotype was rescued using a miRNA-insensitive MAF construct. The MAF ORF (MAF-S, Fig. 5.3A) lacking the 3'UTR was cloned into the lentiviral vector pSIN-MCS (Fig. 5.11); in the absence of the 3'UTR MAF mRNA lacks KSHV miRNA binding sites and is no longer under miRNA-regulation. Expression of exogenous MAF ablated the miRNA Cluster-induced up-regulation of four BEC markers, restoring these mRNA levels to that comparable with cells expressing empty lentiviral vector (Fig. 5.11). These data suggest that the KSHV miRNA Cluster contributes to endothelial reprogramming through silencing of MAF, which normally functions as transcriptional repressor of BEC identity in LEC.

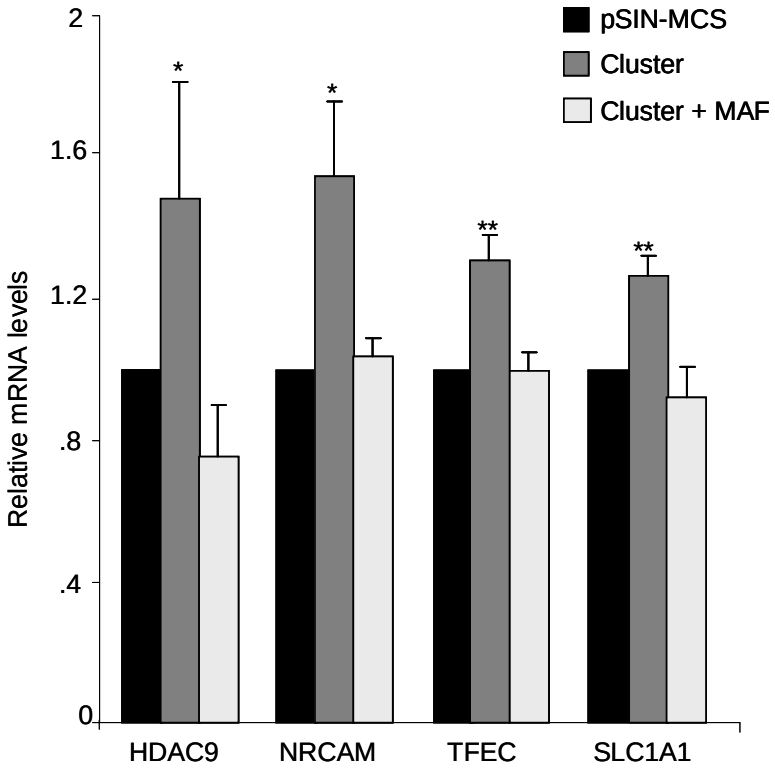

Figure 5.11. miRNA-insensitive MAF ORF rescues Cluster-mediated up-regulation
Exogenous MAF lacking the 3'UTR suppressed miRNA Cluster-induced up-regulation of candidate MAF target genes. MAF target genes were up-regulated in LEC transduced with the KSHV miRNA Cluster as confirmed by qRT-PCR (dark grey bars). Co-infection with Cluster and lentivirus expressing the MAF ORF abolished this upregulation (light grey bars). p values comparing KSHV Cluster to pSIN-MCS: *<0.05 and **<0.005. Differences between LEC transduced with Cluster plus MAF and pSIN-MCS were not significant. Error bars correspond to standard deviation, n = 3.

5.6.2 MAF over-expression reduces BEC marker expression

The data presented here show that knock-down of MAF in LEC induced an up-regulation of BEC-specific genes. To validate MAF as a transcriptional repressor, MAF was over-expressed in BEC, where endogenous levels of MAF are much lower than in LEC (Fig. 5.12B) (Petrova et al., 2002; Hong et al., 2004). LEC and BEC are two closely related endothelial cell lineages and, when isolating either cell type from tissue such as the skin, their close physical proximity may result in a mixed cell population. It was therefore important to confirm the BEC status of cells used in the MAF over-expression experiment. Microvascular endothelial cells isolated from the dermis (PromoCell, Heidelberg, Germany) and the myometrium (provided by Dr. L. Nikitenko, CR-UK Viral Oncology group, UCL) were subjected to qRT-PCR quantification of a range of lineage-specific endothelial cell markers to determine which cell type faithfully represented BEC (Fig. 5.12A). Levels of LEC marker mRNA were similar in both LEC and dermal microvascular endothelial cells (DMVEC) (Fig. 5.12A). Specifically, PROX1 was expressed at a high level in DMVEC, as evidenced by a low delta Ct, indicating these cells were primarily LEC, and not BEC (Fig. 5.12A). Conversely, the lowest levels of PROX1 mRNA were detected in the myometrium microvascular endothelial cells (MMVEC), as evidenced by highest delta Ct value (Fig. 5.12A). Furthermore, MMVEC had the lowest delta Ct values for all BEC markers assayed, indicating increased mRNA abundance (Fig. 5.12A). MMVEC therefore have increased BEC marker expression and express low levels of LEC-associated genes, compared to LEC and DMVEC. qRT-PCR of BEC markers identified in the GSEA analysis confirmed MMVEC faithfully represented BEC (Fig. 5.12B). Interestingly, MAF mRNA levels, similar to PROX1, were negligible in the MMVEC (Fig. 5.12). Both transcription factors were undetectable in MMVEC, at the mRNA level, with threshold detection cycles of over 35, generating high delta Ct values (Fig. 5.12). These data both confirm MAF as a LEC-specific transcription factor and validate

the MMVEC as the appropriate cell type in which to study MAF transcriptional repression. Hereafter, MMVEC are referred to as BEC.

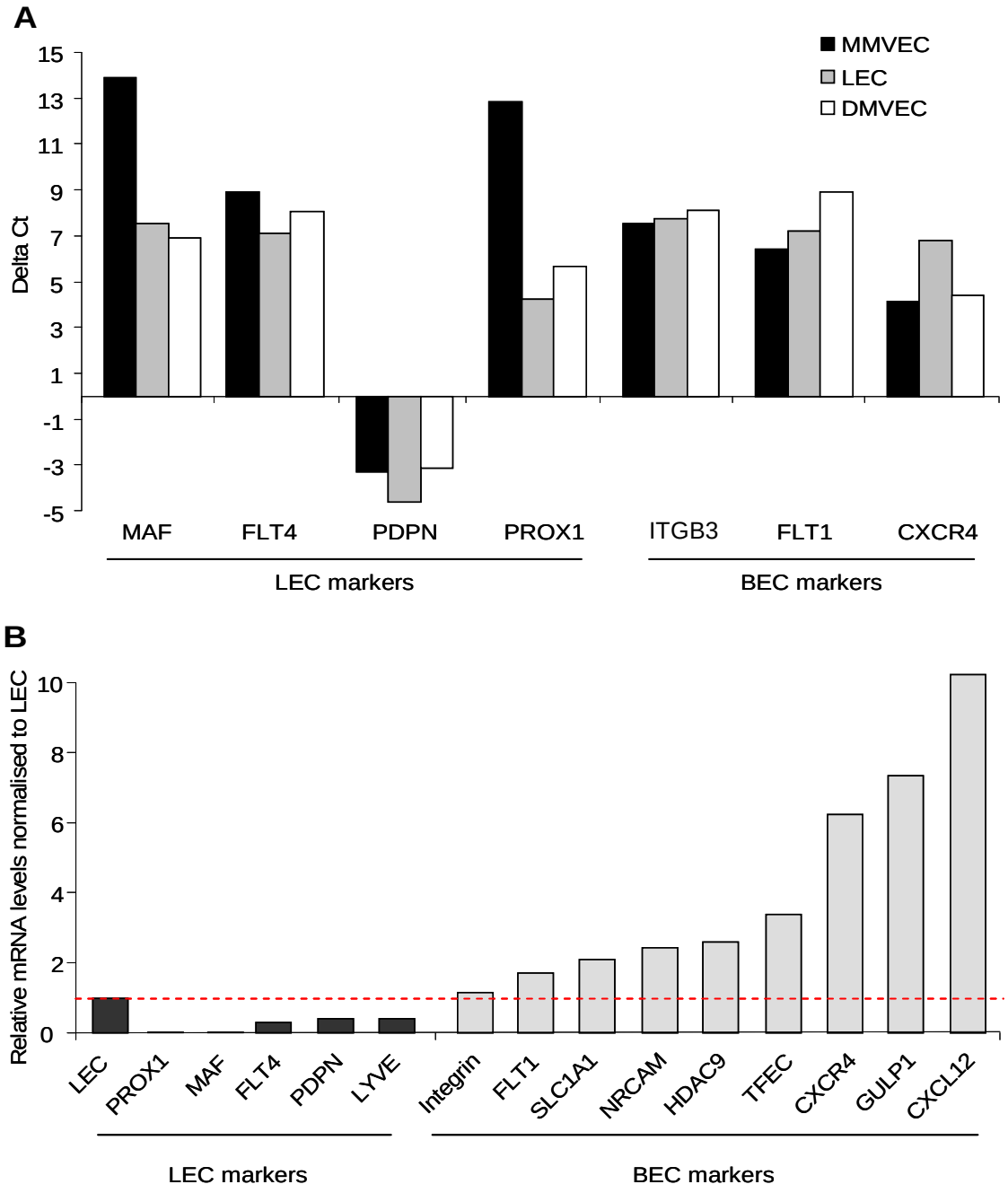

Figure 5.12. qRT-PCR characterisation of BEC. *A* MMVEC express lower levels of LEC, and higher levels of BEC markers compared with DMVEC or LEC. qRT-PCR quantification of a range of BEC and LEC markers in three different cell types. Delta Ct corresponds to the difference in threshold detection cycle (Ct) between the marker and GAPDH. Unexpressed transcripts have a high delta Ct value. MMVEC: myometrium microvascular endothelial cells, DMVEC: dermal microvascular endothelial cells *B* Relative mRNA levels of a range of LEC and BEC markers in MMVEC normalised to LEC. MMVEC express lower levels of MAF and other LEC markers, including the master regulator PROX1. Conversely, higher levels of BEC markers were detected. Hereafter these cells will be referred to as BEC.

BEC were infected with MAF-expressing lentivirus and MAF over-expression confirmed by western blotting (Fig. 5.13A). MAF protein levels increased by approximately 40 fold in BEC transduced with MAF lentivirus compared to empty lentiviral vector (Fig. 5.13A). MAF over-expression in BEC suppressed MAF target genes compared to BEC expressing empty lentiviral vector (Fig. 5.13B). MAF over-expression reduced HDAC9, CXCR4 and CXCL12 mRNA levels by more than 50% (Fig. 5.13B). The remaining BEC marker genes were reduced by 20-35% at the mRNA level in the presence of exogenous MAF (Fig. 5.13B). These data confirm MAF as a transcriptional repressor of BEC markers.

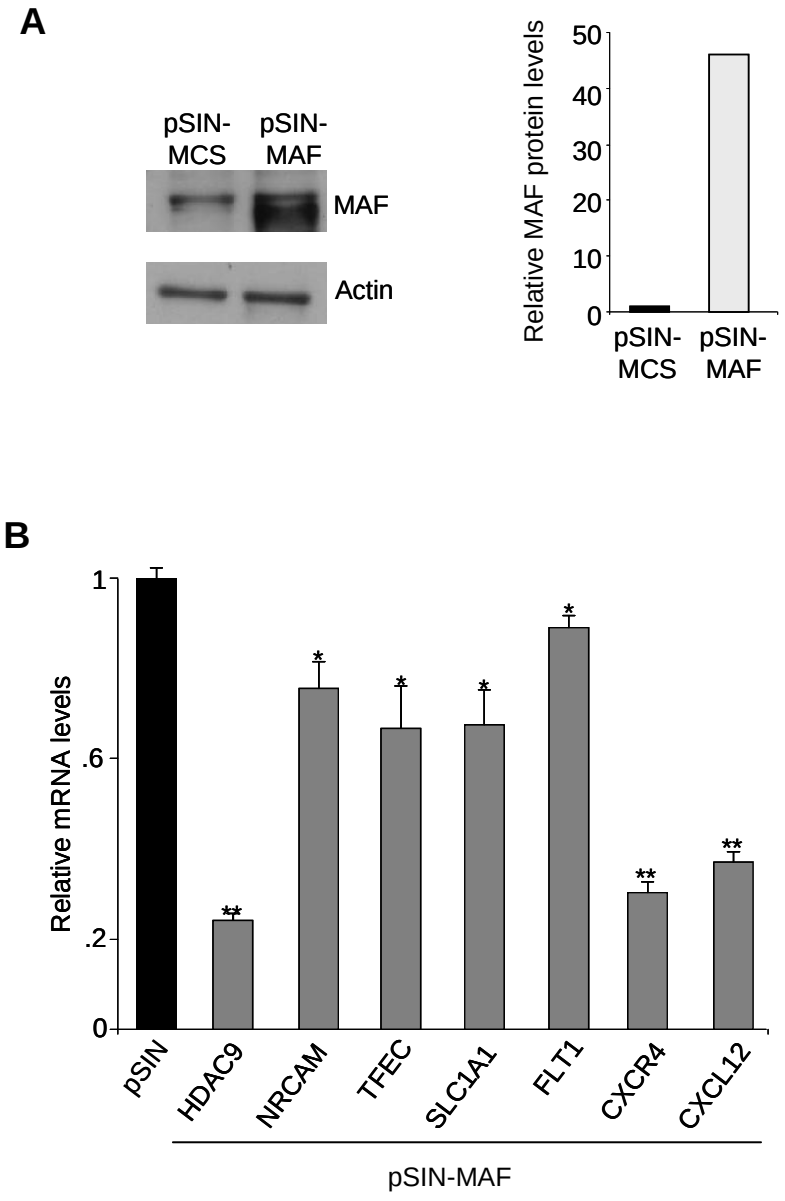

Figure 5.13. Exogenous MAF represses BEC marker expression. *A* Western blot analysis of MAF and loading control actin protein in LEC transduced with either empty lentiviral vector (pSIN-MCS) or MAF expressing lentivirus (pSIN-MAF). Quantification of relative intensity was performed by Scion Image software. *B* In BEC exogenous MAF represses MAF target genes. qRT-PCR analysis of BEC marker genes in BEC transduced with pSIN-MCS or MAF lentivirus (pSIN-MAF). Values normalised to GAPDH and relative to empty vector, pSIN. p values: *<0.05; **<0.005. Error bars correspond to standard deviation, n = 3.

5.7 MAF target validation by ChIP

To continue validating MAF target genes, chromatin immunoprecipitation (ChIP) was used to assess the occupation of target gene promoters by MAF. Successful target gene PCR amplification from precipitated MAF-bound DNA would confirm MAF-regulation of GSEA-identified targets.

5.7.1 MAF immunoprecipitation

Before proceeding to ChIP, the MAF antibody was assessed by immunuprecipitation for the ability to recognise and precipitate native MAF protein. As MAF is a nuclear protein, immunoprecipitation experiments were performed on fractionated cell lysates, enriched for nuclear proteins. Western blotting for p53 and GAPDH were used to confirmed lysates had been fractionated and enriched for either nuclear or cytoplasmic proteins, respectively and depleted of proteins from the reciprocal fraction (Fig. 5.14A).

MAF ChIP was previously performed using a rabbit polyclonal antibody (M153) to confirm MAF regulation of individual target genes in a range of different cell types (Suzuki et al., 2005; Mahoney et al., 2007; Leavenworth et al., 2009). In Figures 4.1, 4.6 and 5.12, MAF protein was quantified by western blotting using an alternative rabbit polyclonal antibody (IMG-6076A), as this antibody gave the lowest background and highest sensitivity compared to M153. However, since the M153 antibody had been shown to recognise MAF in its native form, and the IMG-6076A had never been used for ChIP, the M153 antibody was selected for immunoprecipitation studies. Equal concentrations of M153 and species matched IgG antibodies were used to control for specific enrichment of MAF protein. To accurately quantify the relative IgG levels in the control and test antibody, increasing volumes of a 1/400 antibody dilution were resolved by SDS-PAGE, both antibodies were detected using a goat-anti-rabbit secondary antibody. The

IgG heavy chain runs at approximately 50kDa and densitometry analysis was performed to quantify this signal for each antibody (Fig. 5.14B). After subtracting background signal, the density of M153 band was compared to IgG and corrected for dilution factor. M153 antibody was 7.37 times more concentrated than the control rabbit IgG. Therefore, for use in the immunoprecipitation, M153 was corrected by a factor of 7.4 ensuring an accurate comparison between the test MAF antibody and control IgG.

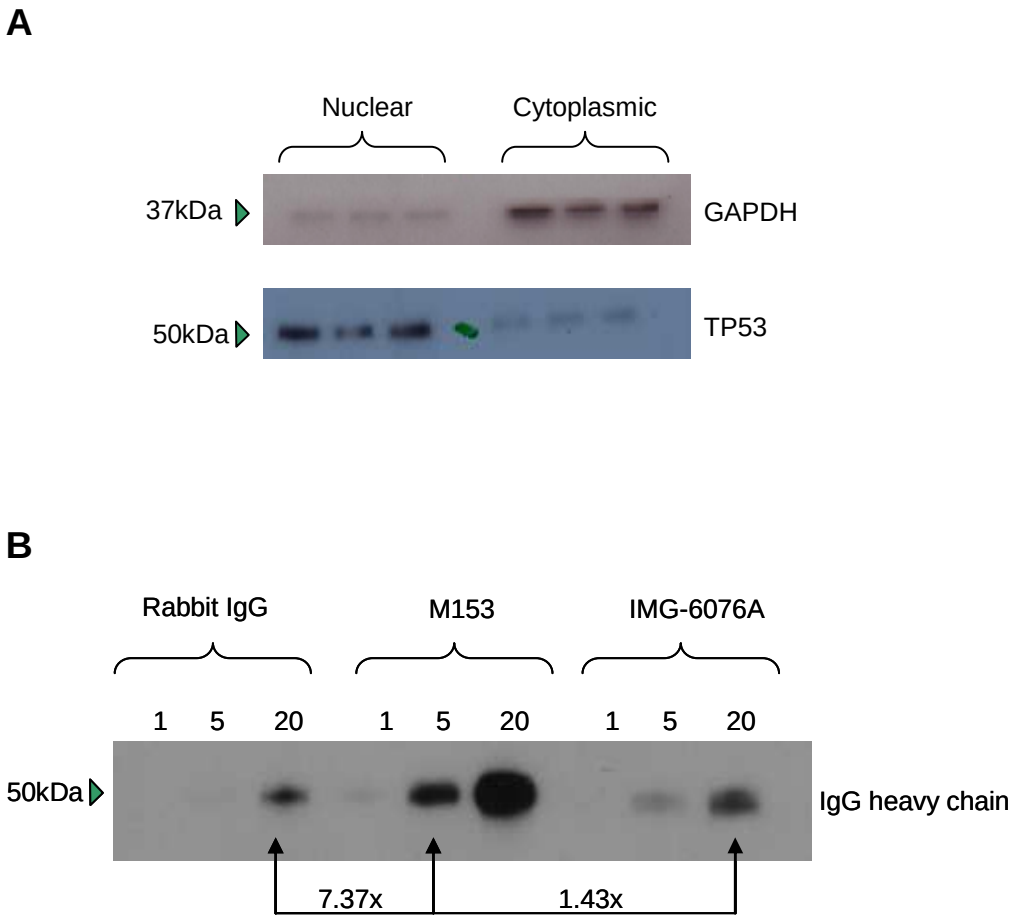

Figure 5.14. Antibody optimisation *A* Nuclear and cytoplasmic fractions were isolated from 293T cells. Western blotting for cytoplasmic protein GAPDH showed a significant enrichment in the cytoplasmic fraction (top blot). Conversely, TP53 protein was enriched in the nuclear fraction only (bottom blot). *B* Western blot quantifying increasing volume of 1/400 dilution of the indicated antibodies. The band running at 50kDa corresponds to the IgG heavy chain. Numbers above the blot indicate µl of 1/400 dilution which were resolved. The density of 5µl M153 heavy chain band was compared to the 20µl rabbit IgG band. The relative intensities shown below the blot were corrected for background and dilution factor.

The large amount of protein required for the ChIP assay necessitated the use of the 293T cell line rather than primary LEC for these experiments. The ChIP assay was optimised using 293T nuclear extracts to reflect this. To enrich for MAF, nuclear extracts were produced from 293T cells transduced with the MAF lentivirus. Nuclear extracts from pSIN-MCS were also tested to determine whether endogenous MAF could be immunoprecipitated. Precipitated protein was resolved by SDS-PAGE along with the following control samples: total nuclear extract (input); pre-cleared sample (input incubated with protein A/G beads only); depleted IgG and depleted MAF (protein not precipitated by antibody-bound beads). Previously, the M153 antibody was shown to recognise MAF, as well as the large Maf proteins MAFA and MAFB (Kataoka et al., 2004). Therefore, to ensure the immunoprecipitation specifically enriched for MAF, and not other large Mafs, precipitated protein was detected using the N15 antibody, which recognises the unique MAF N-terminus and does not recognise either MAFA or MAFB (Kataoka et al., 2004).

A band corresponding to MAF at approximately 40kDa was detected in nuclear input from 293T cells transduced with pSIN-MCS and MAF (Fig. 5.15A and B). This band was also present in pre-cleared and IgG depleted samples, indicating MAF does not bind non-specially to the protein A/G beads or rabbit IgGs (Fig. 5.15A and B). A differential band running just above 37kDa was enriched in M153 precipitated samples compared with the rabbit IgG and indicated MAF immunoprecipitation (Fig. 5.15A and B). This differential band was present in MAF over-expressing (Fig. 5.15A) and empty vector control cells (Fig. 5.15B); therefore the MAF antibody was capable of precipitating exogenous and endogenous protein. MAF levels were comparable in the depleted IgG and M153 samples (Fig. 5.15A and B), possibly as a result of high MAF expression whereby MAF was successfully pulled down without detectable protein depletion in the M153 precipitated samples (Fig. 5.15A). To determine whether the correction factor of 7.4 led to equal concentrations of control IgG and M153 antibodies, blots were

stripped and re-probed with secondary goat-anti-rabbit antibody (Fig. 5.15B). Although more comparable with the dilution factor correction, IgG heavy chain levels were still higher in the M153 samples (Fig. 5.15B). However, this difference is unlikely to account for the strong MAF enrichment observed in the M153 precipitated samples (Fig. 5.15A and B).

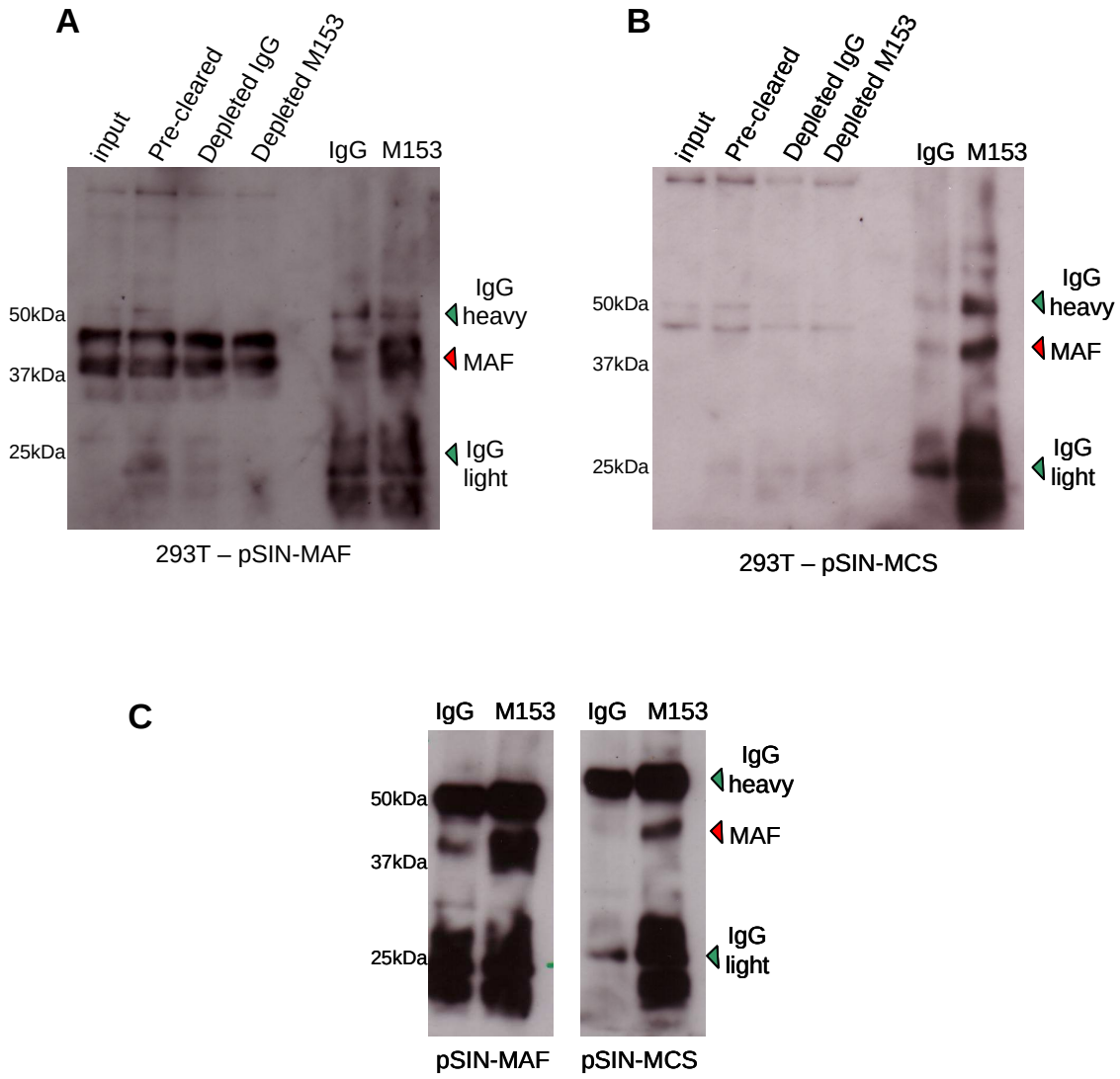

Figure 5.15. MAF immunoprecipitation *A* 293T Nuclear extracts from cells transduced with pSIN-MAF lentivirus were immunoprecipitated with MAF M153 antibody, or as a control rabbit IgG antibody. MAF protein levels in antibody precipitated samples and aliquots from sequential experimental stages were quantified by western blotting with the MAF N15 antibody. In both MAF expressing cells (left blot) and in cells expressing control empty vector the band running just above 37kDa corresponding to MAF protein and is enriched in the M153 precipitated samples compared with the rabbit IgG (right blot). Increased MAF protein is detected in MAF over-expressing cells. Bands corresponding to antibody light and heavy chains at 25 and 50kDa, respectively, are indicated. *B* As in *A*, except with 293T nuclear extracts from cells transduced with pSIN-MCS lentivirus *C* Blots were stripped of N15 and re-probed with a goat-anti-rabbit secondary antibody to quantify levels of rabbit IgG and M153. IgG heavy chain at 50kDa is more abundant in the M153 lane compared to the IgG, although this difference has been corrected somewhat by running 7.4 times less M153 than IgG. M153: MAF antibody.

5.7.2 MAF ChIP-PCR

Immunoprecipitation confirmed antibody recognition and precipitation of endogenous MAF protein. The M153 antibody was therefore considered suitable for use in ChIP-PCR. To design PCR primers for MAF target genes, the MAF DNA binding sequence is required. Since the MAF targets identified in the GSEA were all novel, the MAF recognition elements (MARE) in these target genes were unknown. HDAC9 was selected as a candidate MAF target for ChIP-PCR validation. HDAC9 and MAF are both expressed in 293T cells, therefore although HDAC9 was identified as a MAF target in LEC, it may also be under MAF regulation in 293T cells. To identify putative MAF binding sites 1kb up and downstream of the HDAC9 transcription start site was scanned for putative MAREs using TRANSFAC. This sequence spans the transcription start site of all HDAC9 mRNA isoforms, and contains several areas of high sequence conservation (Fig. 5.16A), which is suggestive of highly conserved regulator elements. Promoter analysis identified four potential MAF binding sites, one proximal and three distal to the transcription start site (Fig. 5.16B). PCR primers were designed against these four putative MAREs, and as a negative control a region of upstream DNA which contained no predicted MAF binding sites. Since there are no validated MAF target genes in 293T cells for use as a positive control, PCR primers were designed against experimentally defined MAREs in CD13 (Mahoney et al., 2007) and Cyclin D2 (Hurt et al., 2004). Primers against the putative HDAC9 MAREs generated a single amplicon of approximately 100bp from genomic DNA, as did primers for the experimentally validated MAREs (Fig. 5.16.C). These primers were therefore considered suitable for ChIP-PCR analysis.

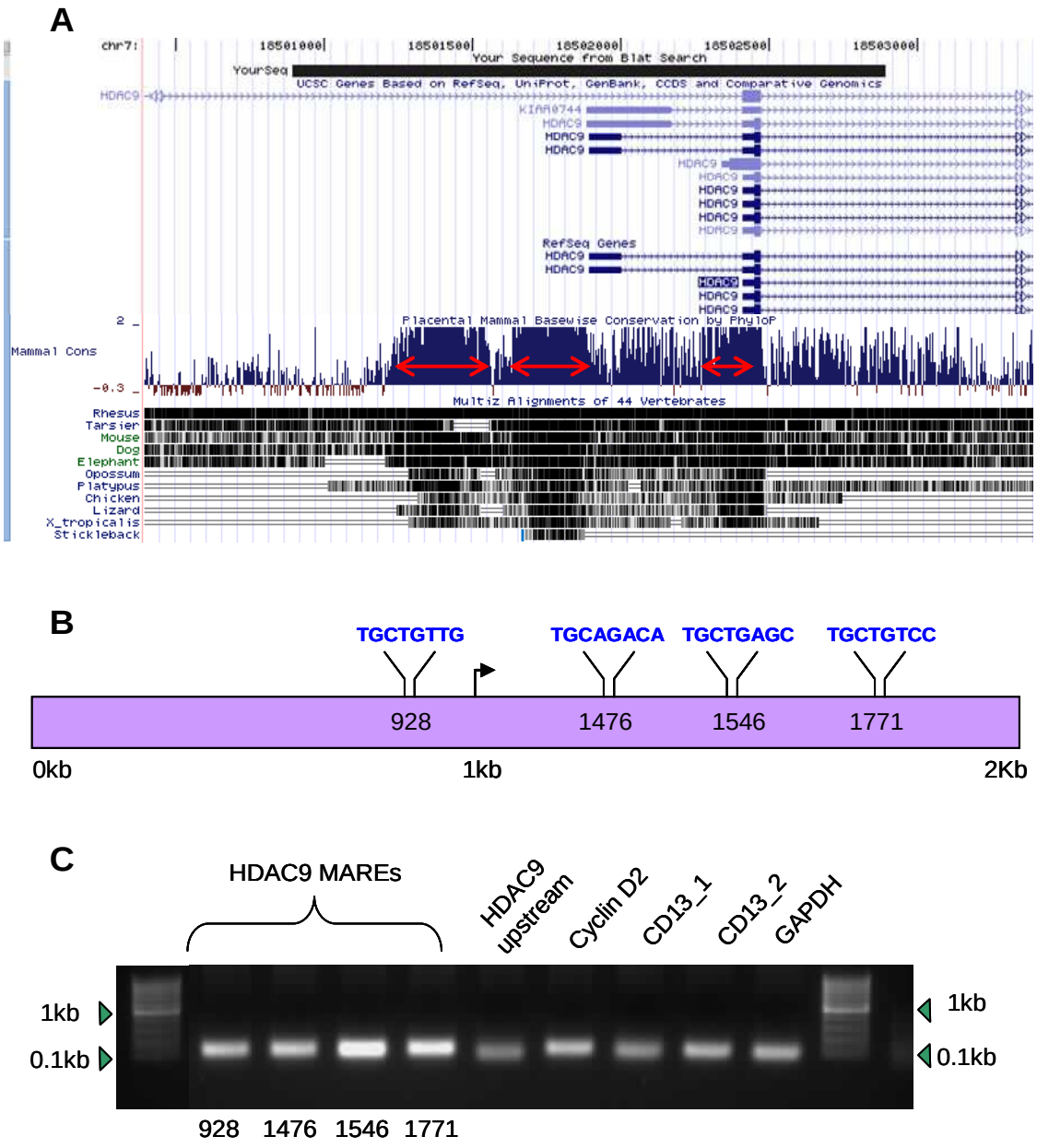

Figure 5.16 HDAC9 promoter *A* One kilobase upstream and downstream of HDAC9 transcription start site was selected for MARE analysis (black bar). USCS genome browser showing sequence overlap with the five HDAC9 mRNA isoforms and regions of sequence conservation with placental mammals and vertebrates. Blocks of sequence conservation, indicated by the red arrows, are encompassed in the 2kb HDAC9 sequence, these may represent potential regulatory sequences. *B* Location and sequence of four putative MARE's identified in the 2kb HDAC9 sequence. The transcription start site is indicated by a black arrow. *C* PCR from genomic DNA testing primers designed against the putative HDAC9 MAREs, experimentally validated MAREs (Cyclin D2 and CD13) and an upstream HDAC9 region devoid of MAF binding sites (HDAC9 upstream). PCR with all primer pairs generated a single band of ~100bp. Validated GAPDH PCR primers were included as a positive control

In addition to the M153 and control IgG antibodies, a positive control ChIP for RNA pol II with subsequent PCR analysis of its actin target was performed on 293T nuclear extracts. This served as a positive control for the assay protocol. An aliquot of sonicated whole cell genomic DNA was used for qPCR input to create a standard curve informing on the threshold detection cycle (Ct) of the gene of interest at a specific DNA concentration. The concentration of immunoprecipitated target DNA was extrapolated using the target Ct and standard curve. Fold-enrichment was calculated by comparing the amount of target DNA precipitated by M153 to that precipitated by control IgG antibody. The RNA Pol II positive control ChIP successfully precipitated actin, with a 20-fold DNA enrichment compared with rabbit IgG control (Fig. 5.17 and Table 5.2). There was no significant enrichment of an upstream region, lacking RNA Pol II binding sites, confirming the specificity of the actin promoter enrichment (Fig. 5.17 and Table 5.2). There was also a significant DNA enrichment of the Cyclin D2 MARE for RNA Pol II, giving 90ng DNA per well and a 400-fold DNA enrichment compared to control IgG ChIP (Fig. 5.17 and Table 5.2). This strong enrichment in Cyclin D2 likely reflects the high growth rate of the transformed 293T cells. However, there was no significant enrichment in precipitated DNA for the two MAF positive controls CD13 and Cyclin D2. This is reflected by less than 1ng of MARE-encoding DNA detected by qPCR (Fig. 5.17 and Table 5.2). Similarly, there was no significant enrichment in any of the HDAC9 putative MAREs in the M153 ChIP, in fact the strongest enrichment was observed for the HDAC9 upstream DNA region, lacking a putative MARE (Fig. 5.17 and Table 5.2). Therefore, although the ChIP experiment was successful for RNA POL II, it was not possible to determine whether the M153 ChIP succeeded in precipitating MAF-bound chromatin.

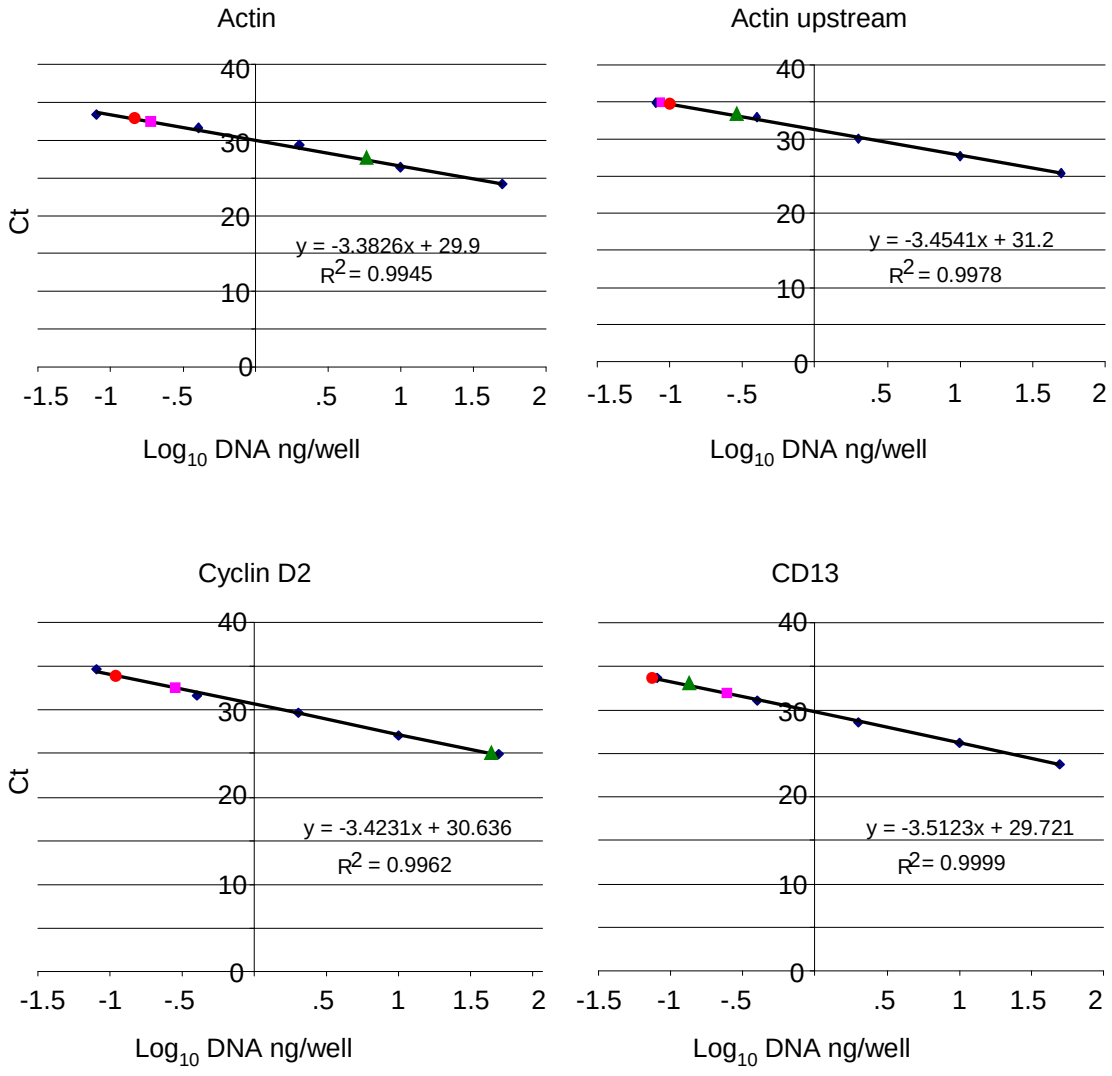

Figure 5.17 MAF Chromatin immunoprecipitation The threshold detection cycle (Ct) of 5 fold serial dilutions of whole cell sonnicated DNA were amplified with the indicated primers and the values plotted as a standard curve (blue diamonds). Target DNA amplification after MAF (pink square), RNA pol II (green triangle) and rabbit IgG (red circle) antibody precipitation was determined using the threshold detection cycle and equation of the standard curve. The equation of each line is shown along with the correlation coefficient, R^2.

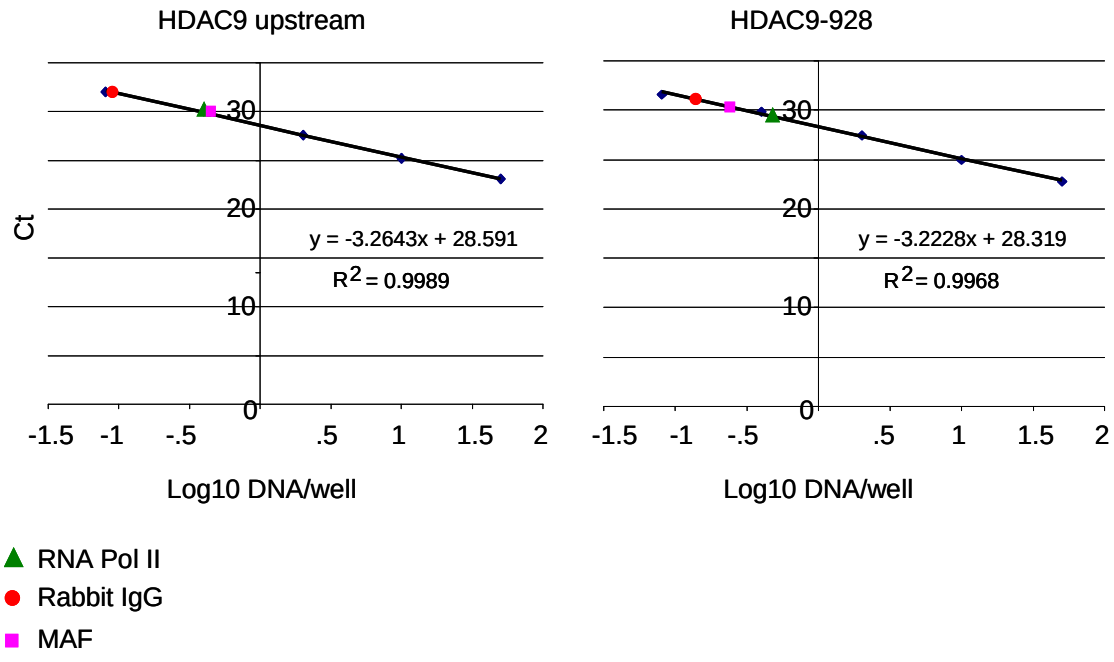

Figure 5.18 MAF Chromatin immunoprecipitation, continued

Target	Fold Enrichment	ng DNA/ well
Actin	20.38	5.90
Actin U.S.	0.58	0.29
Cyclin D2	401	89.61
Cyclin D2	2.65	0.65
CD13	1.80	0.27
HDAC9 U.S.	4.84	0.89
HDAC9 928	1.73	0.48
HDAC9 1476	1.14	0.28
HDAC9 1546	1.35	0.30

Table 5.2 ChIP Target enrichment. Targets in blue correspond to RNA POL II ChIP, whereas targets in black represent MAF ChIP. Fold enrichment is amount of DNA precipitated by either RNA POL II or MAF antibodies relative to ng DNA/well precipitated by rabbit IgG antibody. Total ng DNA per well is also shown.

5.8 MAF auto-regulation

Previously Sakai et al reported auto-activation of the rat Maf promoter in which two Maf binding sites were identified, one resembled a MARE with a cAMP responsive element at its core (C-MARE) and the other contained a core MARE element (Sakai et al., 2001). MafB and Jun also activate their own promoters; suggesting auto-regulation may be a common feature of Maf and bZIP transcription factors (Angel et al., 1988; Huang et al., 2000). To determine whether MAF expression in LEC is subject to auto-regulation, MAF mRNA levels were assessed in three different endothelial cell types transduced with MAF lentivirus (Fig. 5.18A). MAF mRNA levels were elevated in LEC infected with 0.06ml and 0.3ml of MAF lentivirus compared to empty lentiviral vector (Fig. 5.18A); but were reduced by approximately 30% in cells infected with 1.5ml of MAF-lentivirus, compared to empty vector control (Fig. 5.18A). In BEC and human umbilical vein endothelial cells (HUVEC), MAF mRNA levels failed to increase when cells were transduced with exogenous MAF, instead mRNA expression decreased with increasing concentration of lentivirus (Fig. 5.18A). A time-course infection of BEC transduced with MAF lentivirus, showed a modest increase in MAF mRNA 8hrs post transduction, after which MAF mRNA began to decrease until levels were approximately half that of cells transduced with empty vector control (Fig. 5.13B). Despite the reduction in MAF mRNA (Fig. 5.18), MAF protein was up-regulated by approximately 40 fold as determined by western blotting of lysates from BEC transduced with MAF lentivirus (Fig. 5.13A). Similarly, immunofluorescence quantification of LEC transduced with MAF confirmed a strong increase in MAF protein compared to cells infected with pSIN-MCS (Fig. 5.19). These findings suggest a negative feedback loop, which reduces MAF mRNA levels once MAF protein accumulates to a threshold level. This repression of MAF transcription by exogenous MAF may be context-specific as, conversely, auto-activation of rat Maf has been described using luciferase assay data (Sakai et al., 2001),

MAF localised predominantly to the nucleus of over-expressing cells (Fig. 5.19). Nuclear localisation suggests exogenous MAF protein is functional and not aberrantly distributed or degraded. In LEC transduced with pSIN-MCS, MAF localised to both the nucleus and cytoplasm (Fig. 5.19). Cytoplasmic staining could represent newly synthesised MAF protein located in the endoplasmic reticulum, or degraded protein located in the ubiquitin-proteosome. This suggests endogenous MAF is being actively synthesised and degraded in LEC and may be under dynamic regulation.

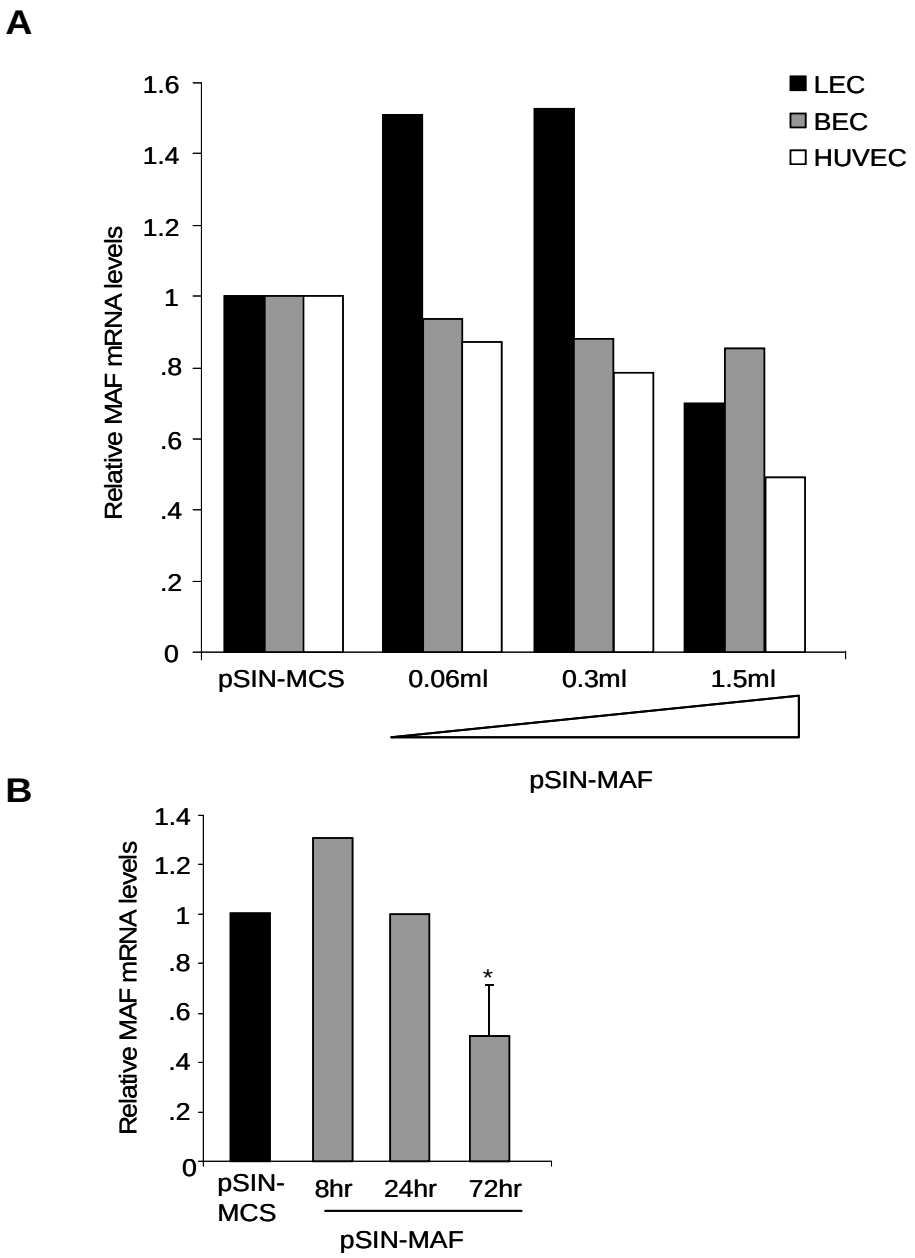

Figure 5.18. MAF auto regulation *A* MAF mRNA in endothelial cells transduced with MAF-expressing lentivirus. At low concentrations of MAF lentivirus, mRNA levels increase in LEC, relative mRNA levels then decrease to below that of empty vector when cells are infected with 1.5ml. In BEC and HUVEC (human umbilical vein endothelial cells) MAF mRNA decreases with increasing concentration of MAF-expressing lentivirus. MAF mRNA levels are relative to cells infected with equal volume of pSIN-MCS for brevity one representative bar is shown. *B* Time-course infection assaying MAF mRNA in BEC transduced with 1ml of MAF-lentivirus. MAF mRNA increases slightly 8hrs post infection, mRNA levels then decrease with time. MAF mRNA levels are normalised to GAPDH and relative to cells infected for the same time period with pSIN-MCS. p *: <0.05.

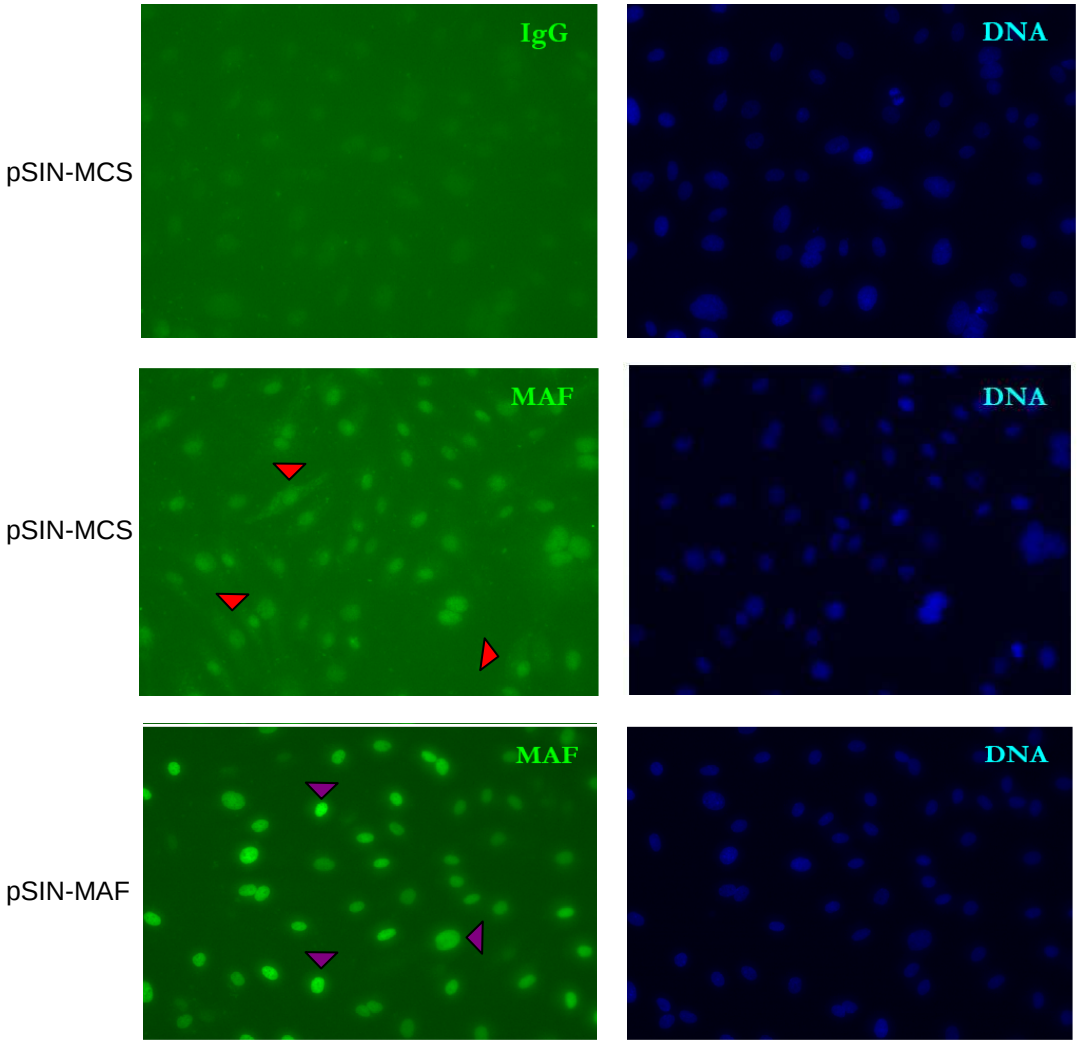

Figure 5.19. MAF protein in LEC. MAF protein levels in LEC transduced with pSIN-MCS or pSIN-MAF as quantified by immunofluorescence. Primary antibody (MAF or IgG) is indicated in the top left corner. Cells on the left were stained with FITC-labelled goat-anti-rabbit secondary antibody. Right hand panels show DAPI stained cells, nuclear DNA is stained blue. FITC staining was more intense in LEC transduced with MAF compared with pSIN-MCS, indicating increased MAF protein. MAF protein was detected in both the nucleus and cytoplasm of pSIN-MCS cells (middle panel, red arrowheads). Whereas MAF staining was predominantly nuclear in over-expressing cells (bottom panel, purple arrowheads). Low signal in cells incubated with IgG primary reveal low background signal, and confirm specificity of MAF staining.

5.9 MAF and PROX1 regulate an overlapping set of target genes

PROX1 is the master regulator of the LEC differentiated phenotype; knock-out mice are embryonic lethal and lack a lymphatic vasculature (Wigle and Oliver, 1999; Wigle et al., 2002). Whereas MAF knock-out mice die shortly after birth, with the most striking embryonic phenotype a failure of lens fibre elongation and microphthalmia (Kim et al., 1999b; Kawauchi et al., 1999; Ring et al., 2000). Similar to LEC, high levels of both MAF and PROX1 are expressed in the lens, and PROX1 was previously shown to enhance MAF activation of β-crystallin transcription in this context (Chen et al., 2002; Cui et al., 2004). However, the mechanism behind MAF and PROX1 cooperation is unclear and direct interaction has not been demonstrated. Petrova et al observed a set of 63 genes that were repressed in BEC following PROX1 over-expression (Petrova et al., 2002). To determine whether MAF and PROX1 could act together to repress transcription, GSEA was performed to analyse this set of 63 genes, in the context of MAF repression following siRNA knockdown in LEC. This analysis identified a significant enrichment in this gene set following siRNA knockdown of MAF in LEC (Fig. 5.20); genes repressed by PROX1 in BEC, increased when MAF was knocked-down in LEC. In agreement with the data presented here suggesting a role for MAF as a repressor of BEC identity, PROX1 also suppressed expression of BEC markers in LEC (Fig. 5.20) (Johnson et al., 2008). These data suggest PROX1 and MAF may act in concert to repress the default BEC state, through regulating an overlapping set of target genes, thereby promoting a LEC phenotype.

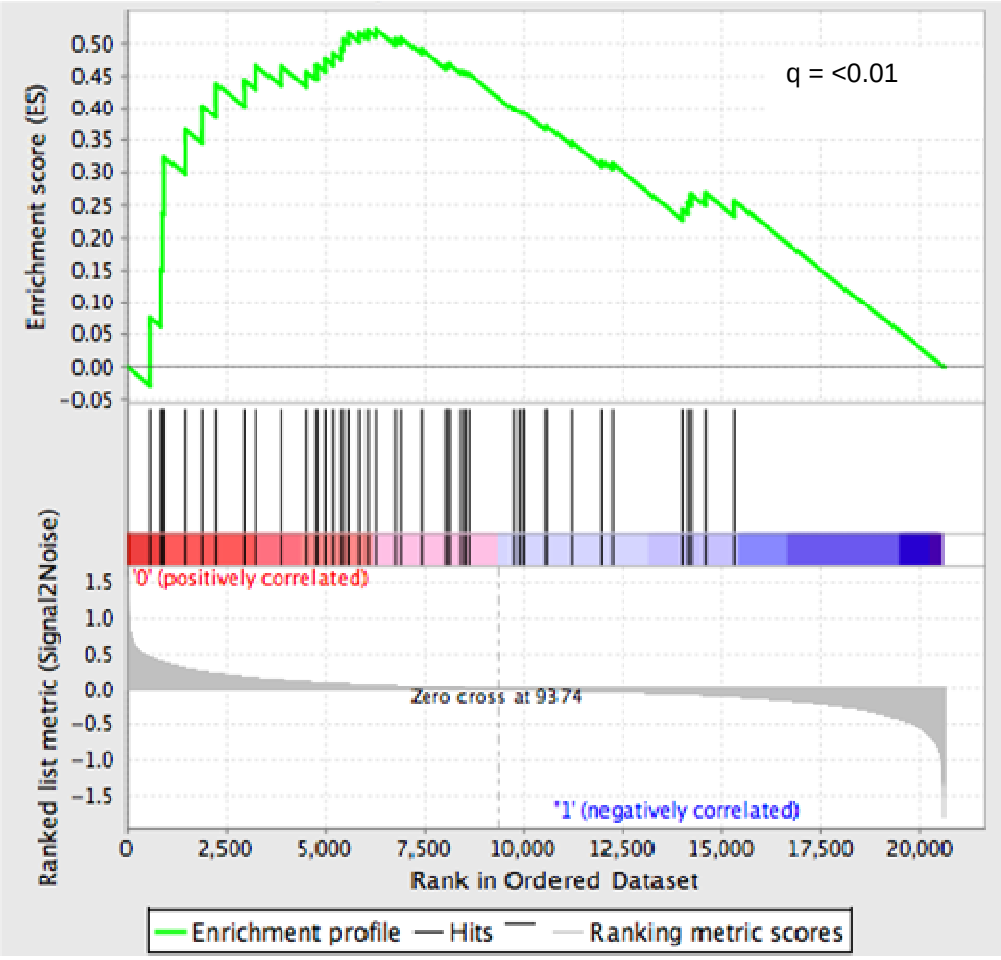

Figure 5.20 Reciprocal regulation of BEC markers by PROX1 and MAF. Gene Set Enrichment Analysis (GSEA) shows a significant enrichment in a set of 63 genes which were repressed by PROX1 in BEC (Petrova et al., 2002). In LEC, upon siRNA knock-down of MAF, there is a significant increase in mRNA abundance of this gene set. The significance calculation shown (q) is a false discovery rate.

5.10 Discussion

Although originally classified as a transforming oncogene (Nishizawa et al., 1989; Kawai et al., 1992), MAF has subsequently been shown to mediate terminal differentiation in a range of cell types (Eychene et al., 2008). Therefore, it was hypothesised that MAF may be involved in endothelial differentiation and that de-regulation of this transcription factor could play a role in KSHV-mediated endothelial reprogramming. In concordance with its role in tissue differentiation, MAF regulates the expression of distinct target genes according to cell type (Hegde et al., 1999; Kim et al., 1999a; Kim et al., 1999b; Ring et al., 2000; Aziz et al., 2009). In combination with cell-type specific targets, the degenerate MAF DNA recognition element has hindered genome-wide identification of MAF target genes (Kataoka, 2007). To gain insight into the genes in LEC which are under MAF regulation, GEM analysis was performed using LEC in which MAF had been silenced. A cohort of genes was de-regulated in the context of MAF repression and these genes were classed as potential MAF targets. Within a set of eighteen experimentally validated MAF targets (Table 1.2 and (Eychene et al., 2008)), only Cyclin D2 was de-regulated when MAF was silenced in LEC. These data support the context-specific regulation of distinct sets of genes by MAF according to cell type.

GSEA of siMAF, LEC transduced with the miRNA Cluster and KLEC GEM data sets were performed to determine whether MAF de-regulation was responsible for the transcriptional convergence of KLEC towards a more BEC-like phenotype. Strikingly, a concordant up-regulation in the expression of BEC markers was observed in LEC when MAF was silenced; this pattern in gene expression was similar to that observed upon KSHV infection of LEC (Wang et al., 2004; Hong et al., 2004). Similarly, when the KSHV miRNA Cluster was expressed in LEC, there was a significant up-regulation in genes associated BEC differentiation status. This analysis suggested the KSHV miRNAs are involved in the transcriptional

reprogramming of infected LEC through a mechanism involving MAF silencing. Furthermore, the data presented here suggest that MAF functions as a transcriptional repressor in LEC. siRNA silencing of MAF led to an increase in additional BEC–specific marker genes, supporting a role for MAF as a repressor of BEC identity.

MAF contains a transactivation domain and the majority of studies into its function show MAF to be a transcriptional activator (Yang and Cvekl, 2007). However, the data presented here is consistent with other reports showing that MAF can also function as a repressor (Dhakshinamoorthy and Jaiswal, 2002; Aziz et al., 2009). The activity of bZIP transcription factors is dependant on both dimerization partners and cooperating proteins present within the larger transcription regulation complex. An analysis of bZIP dimerization activity identified MAF as preferentially forming heterodimers (Vinson et al., 2002) and multiple proteins are capable of dimerizing with MAF *in vitro* (Newman and Keating, 2003). Therefore, it is possible that in LEC, MAF associates with a dimerization partner that confers a repressive function to regulate BEC-associated genes, compared to other cell types which express higher levels of activating dimerization partners.

A MAF rescue experiment was performed to confirm the up-regulation of BEC markers induced by the KSHV miRNA Cluster was by way of MAF targeting. The MAF ORF, minus the 3'UTR, was expressed in the context of Cluster-expressing LEC. This form of MAF is insensitive to miRNA regulation as it no longer contains the miRNA binding sites present in endogenous MAF 3'UTR. Co-expression of the MAF ORF ablated the up-regulation of candidate MAF-target genes induced by the Cluster. Lentivirus expressing the MAF-S single ORF rescued the miRNA induced phenotype, this suggests that there are no miRNA binding sites located in the MAF ORF and that MAF-S is predominantly regulated through the 3'UTR. This implies that miRNA Cluster-induced silencing of MAF-L (Fig. 5.3) may be a result of binding sites in the additional exon. However, the majority of miRNA binding

sites are functionally restrained to the 3'UTR, due to ribosomal displacement of miRNA containing RISC from target sites situated in ORFs (Gu et al., 2009). Further work is needed to clarify the mechanism of Cluster-induced MAF-L down-regulation and whether this of relevance to KSHV infection.

LEC and BEC were classified by the differential expression of lymphatic and blood vessel-specific makers. qRT-PCR analysis presented here showed that, in addition to expressing low levels of LEC cell surface markers, negligible PROX1 and MAF mRNA levels were detected in BEC. This confirmed previous reports classifying MAF as a LEC specific protein (Petrova et al., 2002; Hong et al., 2004). Transducing BEC with MAF lentivirus led to an increase in MAF protein and a corresponding decrease in mRNA abundance of BEC-specific genes, suggesting the role of MAF in LEC is as a transcriptional repressor. Previously, MAF was included in a list of LEC specific genes increased upon KSHV infection of BEC (Hong et al., 2004). It could be envisaged that this reciprocal increase in MAF, compared to the decrease in KLEC, is responsible for the repression of BEC identity, contributing to the move towards a LEC-phenotype in KBEC. Since the KSHV miRNAs are also likely to be expressed in KBEC, another mechanism could exist which over-rides viral miRNA-mediated MAF silencing in KBEC.

Together these results provide insight into the function of the KSHV miRNAs, identify a novel role for viral miRNAs in regulating the cellular differentiation state, and identify MAF as a transcription factor involved in the plasticity of LEC (Fig. 5.21). Sustained PROX1 expression is necessary in the adult mouse to maintain the LEC phenotype, otherwise cells revert to the default blood vessel endothelial state (Johnson et al., 2008). In suppressing BEC markers, MAF also contributes to LEC identity. KSHV miRNA silencing of MAF and the subsequent increase in BEC marker expression, explain in part the mechanism behind the reprogramming of infected LEC (Fig. 5.21). However, the move towards a BEC-like phenotype was most pronounced in KSHV-infected LEC, suggesting that

there may be factors other than MAF de-regulation contributing to the transcriptional reprogramming. Although overall the poorly differentiated KS tumour cells are most similar to LEC (Wang et al., 2004), these findings provide an explanation for the BEC-like features of KS spindle cells.

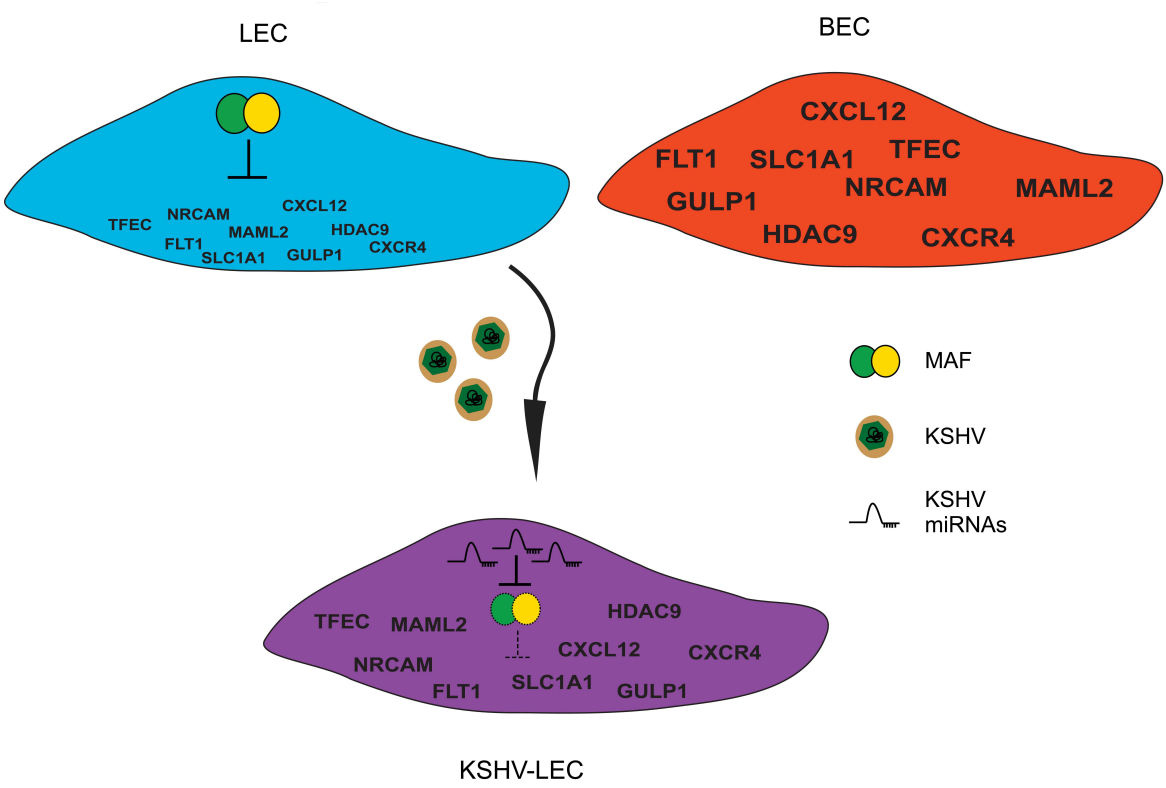

Figure 5.21 KSHV miRNAs contribute to LEC reprogramming. MAF represses the transcription of BEC marker genes in LEC (blue cell). BEC markers, but not MAF, are expressed in BEC (orange cell). Upon KSHV infection and expression of the viral miRNAs, MAF is silenced (purple cell), leading to increased expression of BEC marker genes. The resulting KSHV infected LEC is more similar to BEC than an uninfected cell. BEC marker gene names are shown in black.

In addition to an increase in BEC-specific genes, KSHV infection represses genes associated with LEC differentiation status (Wang et al., 2004; Hong et al., 2004). Expression of the KSHV miRNA Cluster or MAF silencing had no effect on LEC marker expression. These data show that the viral miRNA contribution to endothelial reprogramming is by way of BEC marker regulation only. Instead, the reduction in LEC markers is likely by way of PROX1 down-regulation upon KSHV infection, although other mechanisms may also contribute (Wang et al., 2004). PROX1 was significantly up-regulated in KSHV infected BEC, resulting in an increase in LEC specific genes in KBEC (Carroll et al., 2004; Hong et al., 2004). These data support the idea that PROX1 has an important role in mediating the effects of KSHV on endothelial reprogramming (Carroll et al., 2004; Hong et al., 2004).

MAF regulates transcription by synergising with an additional transcription factor, for example PAX6 in the lens (Kawauchi et al., 1999) and SOX9 in the bone (MacLean et al., 2003). Previously, PROX1 and MAF were shown to cooperate in the activation of β-crystallin transcription (Chen et al., 2002; Cui et al., 2004). Therefore, it was hypothesised that MAF and PROX1 may be acting in concert to specify LEC fate. PROX1 expression in BEC repressed a set of BEC-related genes (Petrova et al., 2002) and this same set of genes was enriched following MAF knockdown in LEC. These data support the hypothesis that these transcription factors form a repressor complex, suppressing BEC markers and helping to maintain the LEC phenotype.

PROX1 is expressed at mouse E9.5 in a subset of venous endothelial cells (Wigle and Oliver, 1999). MAF mRNA is first detected at E9 in the mouse lens placode (Kawauchi et al., 1999). However, the timing of MAF expression in the developing lymphatic system has not yet been determined. The hierarchy of transcriptional regulation by MAF and PROX1 is unknown. However, since MAF knock-out mice have no reported lymphatic defect and PROX1 knock-out mice fail to develop a

lymphatic system, is seems plausible that MAF is under PROX1 regulation, rather than the opposite. As a LEC-specific transcript, MAF was up-regulated upon KSHV infection of BEC, as was PROX1 (Hong et al., 2004). However, when PROX1 was silenced in KBEC, there was a corresponding reduction in MAF mRNA. These data support the hypothesis that MAF is under PROX1 regulation. Further work will clarify the relationship between PROX1 and MAF and delineate the members of the transcriptional repressor complex acting to specific LEC fate.

ChIP-PCR was performed in an attempt to directly confirm *in situ* MAF promoter occupation of the BEC genes identified through GSEA. Immunoprecipitation of MAF protein in its native form, confirmed the MAF antibody was suitable for use in ChIP studies. HDAC9 was selected as a candidate target gene with which to test the ChIP-PCR. PCR primers were designed around putative MAF binding sites identified in the region surrounding the HDAC9 transcription start site. Although the ChIP-PCR was successful for the positive RNA POl II control, there was no significant enrichment in any of the putative HDAC9 predicted MAREs. Similarly, there was there no enrichment in two experimentally defined MAREs in the MAF target genes CD13 or Cyclin D2, included as positive controls. The cell-type specific nature of MAF-regulation could explain the failure of the MAF ChIP to precipitate the positive controls as these genes may not be under MAF regulation in 293T cells. This could hold true for HDAC9 which was identified as a MAF target in LEC. Alternatively, HDAC9 may be under MAF regulation but the correct MARE was not identified. HDAC9 was selected as a candidate target since it was expressed at a high level in 293T cells, however PCR primers could also be designed against other putative MAREs identified in additional MAF targets genes, such as NRCAM or SLC1A1, to confirm the negative ChIP results obtained for HDAC9.

Experimentally validated MAREs often deviate from the canonical sequence, and MAF has been shown to regulate genes through a range of different DNA motifs

(Kerppola and Curran, 1994; Yoshida et al., 2005; Kataoka, 2007). Furthermore, MAF heterodimers will recognise distinct shorter sequences from the palindromic MARE bound by MAF homodimers, making it difficult to identify putative MAREs through in silico promoter analysis.

Failure to precipitate MAF binding sequences could also be a consequence of the antibody used. M153 not only recognises MAF, but also MAFB and MAFA (Kataoka et al., 2004). MAFB is expressed at high levels in the kidney and has a major role in renal function (Moriguchi et al., 2006). Therefore, it is possible that in the kidney-derived 293T cell line the M153 antibody preferentially precipitated MAFB protein over MAF. qPCR for a MAFB target in the M153 precipitated DNA would address this issue, however as yet no targets have been characterised. Using lysates from MAF over-expressing 293T cells would potentially favour MAF precipitation; however exogenous protein does not always regulate targets in the same manner as endogenous, potentially skewing the results. As a positive control to confirm the experimental conditions employed were suitable for M153, ChIP could be performed using this antibody on a validated target in the appropriate cell type, such as IL4 which was precipitated with M153 in T lymphocyte cell lines (Tykocinski et al., 2005).

These findings highlight the difficulty of performing ChIP-PCR without a validated positive control and a strong consensus DNA binding sequence around which to design PCR primers. Therefore, ChIP-Seq or ChIP-chip, two methods which do not require prior knowledge of DNA binding regions will be more successful at confirming and identifying new MAF target genes. Approximately 100 million cells are required per ChIP, making this a challenging experiment to perform with primary human LEC. Therefore, 293T cells were selected for ChIP optimisation because they are easier to grow and obtain in large numbers. However, for a tissue specific transcription factor with a distinct target repertoire in each cell type, global target identification studies must be performed in the cell type of interest.

Chapter 6. Discussion and future work

6.1 Summary

An investigation into KSHV miRNA function in lymphatic endothelial cells identified a role for viral miRNAs in reprogramming KSHV infected cells through silencing the cellular transcription factor MAF. The main findings of my work are:

Identification of KSHV miRNA targets in LEC (Chapter Three)

- Characterisation of the viral miRNA profile of Kaposi sarcoma lesions.
- Development of an experimental system in which to investigate KSHV miRNA function in endothelial cells.
- Identification of putative KSHV miRNA cellular targets in LEC:
    - Experimental identification through GEM analysis of LEC expressing the viral miRNA cluster.
    - In silico target prediction analysis.

MAF is a KSHV miRNA target (Chapter Four)

- MAF is an experimentally validated target of the KSHV miRNA Cluster.
- Individual KSHV miRNAs, miR-K12-6 and miR-K12-11, regulate MAF through specific binding sites located in the 3'UTR.
- MAF is down-regulated by way of the KSHV miRNAs in KSHV infected primary LEC.

KSHV miRNA regulation of MAF induces endothelial reprogramming (Chapter Five)

- MAF is a transcriptional repressor of BEC markers, contributing to the maintenance of LEC identity.

- The viral miRNA Cluster contributes to KSHV-induced endothelial reprogramming through silencing MAF, leading to an up-regulation of BEC-associated genes in LEC.

6.2 Conclusions

Despite encoding many conserved ORFs and large numbers of clustered miRNAs in similar genomic locations, gammaherpesvirus miRNAs share little sequence conservation. This observation suggests that viral miRNAs have evolved to target host and tissue-specific genes to facilitate infection of distinct cell lineages. Cellular target identification in a range of KSHV infected cell types identified distinct target repertoires according to cellular origin and the method adopted (Samols et al., 2007; Ziegelbauer et al., 2009). However, at the onset of this work, there had been no investigations into KSHV miRNAs targets in LEC. Since LEC are the closest uninfected cell type to the KS spindle cell (Wang et al., 2004), it was of primary importance to determine the cellular targets of the viral miRNAs during KSHV infection of LEC. Furthermore, due to the reduced mode of latent gene expression, the viral miRNAs are some of the few gene products expressed in KSHV infected spindle cells. Therefore they are likely to play an important role in KSHV-mediated oncogenesis.

6.2.1 Novel role for viral miRNAs

Only a small number of viral miRNA targets have been identified, making it difficult to gain a full understanding of viral miRNA function. To date, validated viral miRNA targets tend to fall into three categories: immune modulators, apoptosis inhibitors and regulators of viral reactivation (Umbach and Cullen, 2009; Cullen, 2010). Since their identification in 2005 (Cai et al., 2005; Pfeffer et al., 2005; Samols et al., 2005), there have been six experimentally validated KSHV miRNA targets, five of which are cellular (Table 1.4). Silencing of three of these targets (IkBα, RBL and KSHV-encoded lytic reactivator RTA) inhibits viral replication thereby promoting persistent latent infection (Bellare and Ganem, 2009; Lei et al., 2010; Lu et al., 2010). Although not the primary regulators of the lytic switch, the KSHV miRNAs likely function as a back-up mechanism, controlling fluctuations in cellular and viral genes which may trigger lytic reactivation. Viral miRNA regulation of the other three cellular genes (BCLAF1, BACH1, THSD1), inhibits apoptosis (Ziegelbauer et al., 2009), increases permissiveness to KSHV infection and protects cells against oxidative stress (Qin et al., 2010), as well as contributing to a pro-angiogenic environment (Samols et al., 2007). These studies confirmed that KSHV miRNA-target regulation promotes a favourable environment in which to establish persistent infection. Currently there is little evidence for a role in pathogenesis for viral miRNAs. Indeed, the main reported phenotype of KSHV genomes lacking the viral miRNA Cluster was enhanced lytic replication (Lei et al., 2010; Lu et al., 2010).

miRNAs were first identified through their control of C. elegans larval development, and subsequently have been shown to mediate differentiation and development in a range of tissues from drosophila to mammals (Chen et al., 2004; Thum et al., 2007; Davidson-Moncada et al., 2010). The work presented in this thesis provides the first example of viral miRNAs modulating the differentiation status of an infected cell (Hansen et al., 2010). Although this is the first example of viral miRNAs modulating differentiation, certain oncogenic viruses have long been known to regulate the cellular differentiation status to promote infection. EBV hijacks the normal development of B cells to establish life long infection in the B cell compartment (Kuppers, 2003). EBV infection of naïve B cells induces proliferation and germinal center reaction; these EBV positive germinal centers then differentiate into memory B cells which are the long term reservoir of EBV (Babcock et al., 1998). Similarly, it has been proposed that KSHV may directly interfere with the B cell development pathway, through vIL6 promoting naïve infected B cells to differentiate directly into plasmablasts (Jenner et al., 2003; Barozzi et al., 2007). This could explain the plasmablastic features of KSHV-related PEL and multicentric Castleman's disease (MCD) (Dupin et al., 1995). Furthermore, HPV makes use of epithelial differentiation during the productive lifecycle phase (Fehrmann and Laimins, 2003). Following cell division, HPV infected daughter cells leave the basal layer and migrate towards the suprabasal region where they begin to differentiate, uninfected cells exit the cell cycle here whereas infected cells continue to enter S-phase (Doorbar et al., 1997). The data presented within this thesis showing KSHV miRNA regulation of MAF altering the differentiation status of infected LEC, highlights the importance of differentiation status during viral infection.

6.2.2 Mechanism underlying KSHV-induced reprogramming

In 2004 three groups independently reported KSHV-induced endothelial cell reprogramming (Carroll et al., 2004; Hong et al., 2004; Wang et al., 2004). All groups described induction of a lymphatic signature upon KSHV infection of BEC; Wang *et al* also showed the reverse phenotype in KSHV infected LEC (Carroll et al., 2004; Hong et al., 2004; Wang et al., 2004). These studies clearly highlight the capacity of KSHV to reprogram the endothelial transcriptome; however the mechanism underlying these changes was poorly defined. Silencing PROX1 in KSHV-infected BEC, decreased expression of multiple lymphatic genes (Hong et al., 2004), suggesting that in KBEC, lymphatic-specific genes may be switched on as a consequence of PROX1 induction. Notably, ectopic expression of PROX1 in BEC failed to recapitulate the full phenotype of KBEC, suggesting there are other KSHV-induced mechanisms contributing to this reprogramming (Hong et al., 2002; Petrova et al., 2002; Carroll et al., 2004). Wang et al reported a significant reduction in PROX1 mRNA in KLEC, which could be responsible, in part, for inducing a BEC signature in LEC (Wang et al., 2004). However, the mechanism responsible for PROX1 induction in KBEC and repression in KLEC has yet to be determined.

Expression of the KSHV miRNA Cluster was sufficient to induce BEC-specific genes in LEC. This induction was shown to be by way of MAF silencing. Therefore, the work presented in this thesis identifies a novel mechanism contributing to the KSHV-induced reprogramming of LEC (Hansen et al., 2010) and expands on previous studies documenting this reprogramming (Wang et al., 2004). The induction of a BEC-like signature in LEC was most prominent after infection with the whole virus, suggesting that multiple factors work in concert to reprogram LEC. Down-regulation of the lymphatic specific transcription factors PROX1 and MAF could be two of the main mechanisms driving the transition towards a BEC phenotype. The KSHV-encoded miRNAs are responsible for MAF down-regulation, however no significant change in PROX1 mRNA was observed

in LEC expressing the miRNA Cluster. A number of cellular miRNAs are also induced upon KSHV infection (Lagos et al., 2010); therefore it is possible that cellular miRNAs may also contribute to KSHV-induced reprogramming, potentially through silencing PROX1. Further work is needed to elucidate the additional mechanisms contributing to the reprogramming, such as the factors responsible for suppression of LEC markers in KLEC.

The *in vitro* experimental system employed within this thesis models primary KSHV infection of LEC; under these conditions MAF silencing induces a BEC-like signature. Differentiated LEC are slow dividing primary cells, therefore *in vivo* the global effect of KSHV-induced reprogramming could be to drive LEC towards a less differentiated phenotype, promoting cell division and hence viral propagation. Although KLEC in culture display no growth advantage compared with LEC, infected cells may need the stimulus of the tumour inflammatory microenvironment to initiate proliferation. Alternatively, the observed reprogramming could reflect KSHV infection of circulating endothelial progenitor cells *in vivo*. Here KSHV infection may drive the progenitors towards poorly differentiated spindle precursor cells, expressing both LEC and BEC markers. However, the down-regulation of key LEC transcription factors, which are only switched on after LEC specification, suggests that KSHV has evolved mechanisms to alter the status of fully differentiated cells, rather than progenitors. Clearly, there are many questions still to be answered regarding the *in vivo* cellular reservoirs of KSHV and the functional significance of the reprogramming. For example, it is not known whether the poorly differentiated status of spindle cells and endothelial progenitors is more conducive to latency. The inability to maintain long-term culture of KSHV infected LEC and the lack a suitable mouse model has hindered investigations into the role of reprogrammed cells during primary infection and throughout disease progression.

6.2.3 MAF: a novel LEC-specifying protein

The LEC phenotype is initiated upon expression of PROX1 in a subset of venous endothelial cells in the anterior cardinal vein during embryogenesis (Wigle and Oliver, 1999). PROX1 triggers a cascade of gene expression driving cells towards a lymphatic fate (Wigle et al., 2002). Despite the established role of PROX1 as the lymphatic master regulator, there still remains much to be discovered regarding lymphangiogenesis. The initiating lymphatic signal is still unknown, as are many PROX1-responsive genes responsible for the lymphatic phenotype (Oliver and Alitalo, 2005). Identification of MAF as a KSHV miRNA target prompted investigations into its function in LEC. This work identified a novel role for MAF in suppressing BEC-specific genes, helping to maintain the LEC phenotype. A report describing the plasticity of LEC (Johnson et al., 2008), showed PROX1 expression was required both for the initiation and maintenance of the lymphatic phenotype. Loss of PROX1 in adult murine lymphatic vessels induced a morphological shift towards blood vessels (Johnson et al., 2008). Similarly, MAF expression is required in differentiated LEC to suppress the BEC phenotype; consequently loss of MAF through KSHV infection induces a shift towards a BEC phenotype. These data support the reported plasticity of LEC and highlight the sensitivity of these cells to the dosage of lineage-specifying transcription factors. The findings of this thesis add the lymphatic vasculature to the list of tissues in which MAF plays a lineage specifying role (Yang and Cvekl, 2007).

6.3 Future Work

6.3.1 KSHV miRNA target identification

The GEM experiment in Chapter Three identified a cohort of genes de-regulated at the mRNA level in the presence of the KSHV miRNA Cluster; subsequently a single miRNA target was experimentally validated. Further experiments will be performed to gain insight into additional KSHV miRNA targets and the significance of target regulation during primary infection and in KS. This approach identified only the viral miRNA targets that were affected at the mRNA level. As an alternative to GEM analysis, stable isotope labeling by amino acids in cell culture (SILAC) has been employed to investigate the effects of miRNAs on the proteome (Vinther et al., 2006). This approach has the benefit of monitoring changes in abundance of protein, and therefore can identify viral miRNA targets silenced solely by translation inhibition which may have been missed in the GEM experiment. In addition, SILAC data can be used to substantiate some of the small fold changes in mRNA abundance identified in the GEM experiment, as many genes silenced via translation inhibition were also shown to be marginally down-regulated at the RNA level (Baek et al., 2008; Selbach et al., 2008). SILAC could be performed on LEC expressing the Cluster and KSHV infected LEC. The overlap of genes would inform on viral miRNA targets compared to genes regulated by cellular miRNAs induced upon infection. Performing SILAC on samples throughout a time course of KSHV infection could provide insight into how viral and cellular miRNA activity changes during infection.

Another method of identifying functional miRNA interaction sites is by immunoprecipitation of Argonaute bound to target RNAs which are subsequently identified by high-throughput sequencing (Chi et al., 2009). This technique known as HITS-CLIP (high-throughput sequencing of RNA isolated by crosslinking immunoprecipitation) could be employed on KLEC and Cluster expressing LEC to generate a genome-wide interaction map, informing on which miRNAs are actively associated with Argonaute during infection. This method could also be employed on KS biopsies, which will inform on how miRNA targets change from primary infection towards late stage disease.

Two groups have independently created a KSHV bacmid (Bacterial artificial chromosome, BAC36) lacking the viral miRNA Cluster (Lei et al., 2010; Lu et al., 2010). Infection of cells with this mutated BAC increased viral lytic gene expression and lytic replication, confirming a role for the KSHV miRNAs in stabilising latency (Lei et al., 2010; Lu et al., 2010). Infection of LEC with KSHV lacking the miRNA Cluster would compliment target identification by GEM and SILAC, as well as facilitating investigations into viral miRNA function. For example, KLEC infected with wild-type virus or virus lacking the miRNA Cluster could be assayed for differences in lymphangiogenic assays, such as tube formation in three dimensional culture (Bruyere and Noel, 2010). This system could also be employed to confirm the role of KSHV miRNAs in endothelial reprogramming by comparing markers of endothelial differentiation in LEC infected with wild type KSHV and those infected with the miRNA deletion mutant. In addition to target identification, functional assays will be employed in the future to identify pathways and processes manipulated by the KSHV miRNAs.

6.3.2 MAF and PROX1

A set of PROX1 responsive genes in BEC (Petrova et al., 2002), were also de-regulated upon MAF siRNA-mediated silencing in LEC. In the lens, MAF and PROX1 have been shown to cooperate in the activation of β-crystallin transcription (Chen et al., 2002; Cui et al., 2004). Given the tendency for MAF to synergise with additional transcription factors (Kataoka, 2007), it is plausible that MAF and PROX1 form a transcriptional repressor complex acting to maintain the LEC phenotype. Future work will characterise the relationship between these two transcription factors in LEC and determine whether PROX1 augments MAF repression of BEC genes. In addition, COUPTFII will be also investigated, as this transcription factor augments PROX1 activation of certain LEC genes, helping to establish LEC fate (Lee et al., 2009; Yamazaki et al., 2009). Therefore, it is possible that all three LEC-specifying transcription factors are working in concert. Co-immunoprecipitation for all three proteins will determine whether they interact within a transcription complex. Alternatively, MAF immunoprecipitation in LEC, followed by mass spectrometry analysis would fully characterise all proteins cooperating in the repressor complex. Furthermore, this analysis could potentially identify the MAF bZIP dimerization partners. Since MAF is primarily a transcriptional activator, identification of its dimer partner in LEC where it acts as a repressor, would shed light on which proteins are responsible for conferring repressor activity.

Future work will also delineate whether there is reciprocal regulation between PROX1 and MAF. The phenotype of PROX1 and MAF homozygous mice partially overlapped (Ring et al., 2000). However, in Maf homozygous null mice there was no change in Prox1 mRNA in the mutant lens, suggesting that at least in this tissue, Prox1 expression is not under Maf control (Ring et al., 2000). Conversely, MAF up-regulation in KSHV infected BEC could be reduced through silencing PROX1 (Hong et al., 2004), implying that PROX1 may control MAF expression. The effect of both proteins on levels of the corresponding

transcription factor should be assessed to confirm whether MAF is a genuine PROX1 target. Luciferase promoter studies and competitive DNA binding assays such as electric mobility shift assay (EMSA) could be employed to identify the site of PROX1 binding in the MAF promoter.

6.3.3 The role of *MAF role during lymphangiogenesis*

The work in this thesis identified MAF as a LEC-specifying transcription factor. Experiments were performed solely on differentiated LEC, whereas there has been no investigation into MAF function in the development of the lymphatic system. Previously, three groups independently created Maf homozygous null mice, the most striking embryonic phenotype was microphthalmia and defective lens formation (Kim et al., 1999; Kawauchi et al., 1999; Ring et al., 2000). Homozygous null mice were born at the expected Mendelian frequency, but died shortly after birth of undetermined causes (Kim et al., 1999; Kawauchi et al., 1999; Ring et al., 2000). Heterozygous mice were born at the expected frequency, survived past weaning and displayed no eye defects (Kim et al., 1999; Kawauchi et al., 1999; Ring et al., 2000). None of the studies reported any gross defects in the lymphatic system (Kim et al., 1999; Kawauchi et al., 1999; Ring et al., 2000). This may be due to functional redundancy between LEC-specifying transcription factors, including COUPTFII and PROX1. Alternatively, MAF may play a role after development of the lymphatic system, helping to maintain the adult LEC phenotype.

Future work will employ the use of Maf knock out mice and pups to determine whether Maf plays an important role in lymphangiogenesis. First the expression profile of Maf will be characterised throughout the stages of lymphatic development to determine when in the LEC-specifying transcription cascade Maf is expressed. The timing and location of MAF expression during lymphangiogenesis will be compared with that of PROX1 and COUPTFII. The lymphatic system of MAF homozygous null mice will be closely inspected at the

four main steps of development: LEC competence, LEC bias, LEC specification and lymphatic vessel differentiation and maturation (Oliver, 2004).

References

Abtahian,F., Guerriero,A., Sebzda,E., Lu,M.M., Zhou,R., Mocsai,A., Myers,E.E., Huang,B., Jackson,D.G., Ferrari,V.A., Tybulewicz,V., Lowell,C.A., Lepore,J.J., Koretzky,G.A., and Kahn,M.L. (2003). Regulation of blood and lymphatic vascular separation by signaling proteins SLP-76 and Syk. Science 299, 247-251.

Adams,R.H. and Alitalo,K. (2007). Molecular regulation of angiogenesis and lymphangiogenesis. Nat. Rev. Mol. Cell Biol. 8, 464-478.

Akula,S.M., Pramod,N.P., Wang,F.Z., and Chandran,B. (2001a). Human herpesvirus 8 envelope-associated glycoprotein B interacts with heparan sulfate-like moieties. Virology 284, 235-249.

Akula,S.M., Pramod,N.P., Wang,F.Z., and Chandran,B. (2002). Integrin alpha3beta1 (CD 49c/29) is a cellular receptor for Kaposi's sarcoma-associated herpesvirus (KSHV/HHV-8) entry into the target cells. Cell 108, 407-419.

Akula,S.M., Wang,F.Z., Vieira,J., and Chandran,B. (2001b). Human herpesvirus 8 interaction with target cells involves heparan sulfate. Virology 282, 245-255.

Alitalo,K. and Carmeliet,P. (2002). Molecular mechanisms of lymphangiogenesis in health and disease. Cancer Cell 1, 219-227.

Al-Rawi,M.A., Watkins,G., Mansel,R.E., and Jiang,W.G. (2005). The effects of interleukin-7 on the lymphangiogenic properties of human endothelial cells. Int. J. Oncol. 27, 721-730.

Ambros,V. (2004). The functions of animal microRNAs. Nature 431, 350-355.

Ambros,V., Bartel,B., Bartel,D.P., Burge,C.B., Carrington,J.C., Chen,X., Dreyfuss,G., Eddy,S.R., Griffiths-Jones,S., Marshall,M., Matzke,M., Ruvkun,G., and Tuschl,T. (2003). A uniform system for microRNA annotation. RNA. 9, 277-279.

Angel,P., Hattori,K., Smeal,T., and Karin,M. (1988). The jun proto-oncogene is positively autoregulated by its product, Jun/AP-1. Cell 55, 875-885.

Antman,K. and Chang,Y. (2000). Kaposi's sarcoma. N. Engl. J. Med. 342, 1027-1038.

Aoki,Y., Jaffe,E.S., Chang,Y., Jones,K., Teruya-Feldstein,J., Moore,P.S., and Tosato,G. (1999). Angiogenesis and hematopoiesis induced by Kaposi's sarcoma-associated herpesvirus-encoded interleukin-6. Blood 93, 4034-4043.

Aravin,A.A., Hannon,G.J., and Brennecke,J. (2007). The Piwi-piRNA pathway provides an adaptive defense in the transposon arms race. Science 318, 761-764.

Arvanitakis,L., Geras-Raaka,E., Varma,A., Gershengorn,M.C., and Cesarman,E. (1997). Human herpesvirus KSHV encodes a constitutively active G-protein-coupled receptor linked to cell proliferation. Nature 385, 347-350.

Arvanitakis,L., Yaseen,N., and Sharma,S. (1995). Latent membrane protein-1 induces cyclin D2 expression, pRb hyperphosphorylation, and loss of TGF-beta 1-mediated growth inhibition in EBV-positive B cells. J. Immunol. 155, 1047-1056.

Asahi-Ozaki,Y., Sato,Y., Kanno,T., Sata,T., and Katano,H. (2006). Quantitative analysis of Kaposi sarcoma-associated herpesvirus (KSHV) in KSHV-associated diseases. J. Infect. Dis. 193, 773-782.

Asellius,G. (1627). Asellii Cremonensis Antomici Ticiensis Qua Sententiae Anatomicae multae, nel perperam receptae illustrantur, De Lacteibus sive lacteis venis Quarto Vasorum Mesaroicum genere novo invente Gasp. Milan: Mediolani.

Aziz,A., Soucie,E., Sarrazin,S., and Sieweke,M.H. (2009). MafB/c-Maf deficiency enables self-renewal of differentiated functional macrophages. Science 326, 867-871.

Babcock,G.J., Decker,L.L., Volk,M., and Thorley-Lawson,D.A. (1998). EBV persistence in memory B cells in vivo. Immunity. 9, 395-404.

Backhed,F., Crawford,P.A., O'Donnell,D., and Gordon,J.I. (2007). Postnatal lymphatic partitioning from the blood vasculature in the small intestine requires fasting-induced adipose factor. Proc. Natl. Acad. Sci. U. S. A 104, 606-611.

Baek,D., Villen,J., Shin,C., Camargo,F.D., Gygi,S.P., and Bartel,D.P. (2008). The impact of microRNAs on protein output. Nature.

Bagneris,C., Ageichik,A.V., Cronin,N., Wallace,B., Collins,M., Boshoff,C., Waksman,G., and Barrett,T. (2008). Crystal structure of a vFlip-IKKgamma complex: insights into viral activation of the IKK signalosome. Mol. Cell 30, 620-631.

Bais,C., Santomasso,B., Coso,O., Arvanitakis,L., Raaka,E.G., Gutkind,J.S., Asch,A.S., Cesarman,E., Gershengorn,M.C., and Mesri,E.A. (1998). G-protein-coupled receptor of Kaposi's sarcoma-associated herpesvirus is a viral oncogene and angiogenesis activator. Nature 391, 86-89.

Baldwin,M.E., Halford,M.M., Roufail,S., Williams,R.A., Hibbs,M.L., Grail,D., Kubo,H., Stacker,S.A., and Achen,M.G. (2005). Vascular endothelial growth factor D is dispensable for development of the lymphatic system. Mol. Cell Biol. 25, 2441-2449.

Ballestas,M.E. and Kaye,K.M. (2001). Kaposi's sarcoma-associated herpesvirus latency-associated nuclear antigen 1 mediates episome persistence through cis-acting terminal repeat (TR) sequence and specifically binds TR DNA. J. Virol. 75, 3250-3258.

Ballestas,M.E., Chatis,P.A., and Kaye,K.M. (1999). Efficient persistence of extrachromosomal KSHV DNA mediated by latency-associated nuclear antigen. Science 284, 641-644.
Baluk,P. and McDonald,D.M. (2008). Markers for microscopic imaging of lymphangiogenesis and angiogenesis. Ann. N. Y. Acad. Sci. 1131, 1-12.

Baluk,P., Fuxe,J., Hashizume,H., Romano,T., Lashnits,E., Butz,S., Vestweber,D., Corada,M., Molendini,C., Dejana,E., and McDonald,D.M. (2007). Functionally specialized junctions between endothelial cells of lymphatic vessels. J. Exp. Med. 204, 2349-2362.

Banerji,S., Ni,J., Wang,S.X., Clasper,S., Su,J., Tammi,R., Jones,M., and Jackson,D.G. (1999). LYVE-1, a new homologue of the CD44 glycoprotein, is a lymph-specific receptor for hyaluronan. J. Cell Biol. 144, 789-801.

Barbera,A.J., Chodaparambil,J.V., Kelley-Clarke,B., Joukov,V., Walter,J.C., Luger,K., and Kaye,K.M. (2006). The nucleosomal surface as a docking station for Kaposi's sarcoma herpesvirus LANA. Science 311, 856-861.

Barozzi,P., Potenza,L., Riva,G., Vallerini,D., Quadrelli,C., Bosco,R., Forghieri,F., Torelli,G., and Luppi,M. (2007). B cells and herpesviruses: a model of lymphoproliferation. Autoimmun. Rev. 7, 132-136.

Bartel,B. and Bartel,D.P. (2003). MicroRNAs: at the root of plant development? Plant Physiol 132, 709-717.

Bartel,D.P. (2004). MicroRNAs: genomics, biogenesis, mechanism, and function. Cell 116, 281-297.

Bartel,D.P. (2009). MicroRNAs: target recognition and regulatory functions. Cell 136, 215-233.
Barth,S., Pfuhl,T., Mamiani,A., Ehses,C., Roemer,K., Kremmer,E., Jaker,C., Hock,J., Meister,G., and Grasser,F.A. (2008). Epstein-Barr virus-encoded microRNA miR-BART2 down-regulates the viral DNA polymerase BALF5. Nucleic Acids Res. 36, 666-675.

Bechtel,J.T., Liang,Y., Hvidding,J., and Ganem,D. (2003). Host range of Kaposi's sarcoma-associated herpesvirus in cultured cells. J. Virol. 77, 6474-6481.

Beckstead,J.H., Wood,G.S., and Fletcher,V. (1985). Evidence for the origin of Kaposi's sarcoma from lymphatic endothelium. Am. J. Pathol. 119, 294-300.

Behm-Ansmant,I., Rehwinkel,J., Doerks,T., Stark,A., Bork,P., and Izaurralde,E. (2006). mRNA degradation by miRNAs and GW182 requires both CCR4:NOT deadenylase and DCP1:DCP2 decapping complexes. Genes Dev. 20, 1885-1898.

Bellare,P. and Ganem,D. (2009). Regulation of KSHV lytic switch protein expression by a virus-encoded microRNA: an evolutionary adaptation that fine-tunes lytic reactivation. Cell Host. Microbe 6, 570-575.

Benkhelifa,S., Provot,S., Lecoq,O., Pouponnot,C., Calothy,G., and Felder-Schmittbuhl,M.P. (1998). mafA, a novel member of the maf proto-oncogene family, displays developmental regulation and mitogenic capacity in avian neuroretina cells. Oncogene 17, 247-254.

Bentwich,I., Avniel,A., Karov,Y., Aharonov,R., Gilad,S., Barad,O., Barzilai,A., Einat,P., Einav,U., Meiri,E., Sharon,E., Spector,Y., and Bentwich,Z. (2005). Identification of hundreds of conserved and nonconserved human microRNAs. Nat. Genet. 37, 766-770.

Beral,V., Peterman,T.A., Berkelman,R.L., and Jaffe,H.W. (1990). Kaposi's sarcoma among persons with AIDS: a sexually transmitted infection? Lancet 335, 123-128.

Bernstein,E., Caudy,A.A., Hammond,S.M., and Hannon,G.J. (2001). Role for a bidentate ribonuclease in the initiation step of RNA interference. Nature 409, 363-366.

Blank,V. and Andrews,N.C. (1997). The Maf transcription factors: regulators of differentiation. Trends Biochem. Sci. 22, 437-441.

Bloomston,M., Frankel,W.L., Petrocca,F., Volinia,S., Alder,H., Hagan,J.P., Liu,C.G., Bhatt,D., Taccioli,C., and Croce,C.M. (2007). MicroRNA expression patterns to differentiate pancreatic adenocarcinoma from normal pancreas and chronic pancreatitis. JAMA 297, 1901-1908.

Boneschi,V., Brambilla,L., Berti,E., Ferrucci,S., Corbellino,M., Parravicini,C., and Fossati,S. (2001). Human herpesvirus 8 DNA in the skin and blood of patients with Mediterranean Kaposi's sarcoma: clinical correlations. Dermatology *203*, 19-23

Boshoff,C. and Weiss,R. (2002). AIDS-related malignancies. Nat. Rev. Cancer 2, 373-382.
Boshoff,C. and Weiss,R.A. (1998). Kaposi's sarcoma-associated herpesvirus. Adv. Cancer Res. 75, 57-86.

Boshoff,C. and Weiss,R.A. (1998). Kaposi's sarcoma-associated herpesvirus. Adv. Cancer Res. *75*, 57-86.

Boshoff,C., Endo,Y., Collins,P.D., Takeuchi,Y., Reeves,J.D., Schweickart,V.L., Siani,M.A., Sasaki,T., Williams,T.J., Gray,P.W., Moore,P.S., Chang,Y., and Weiss,R.A. (1997). Angiogenic and HIV-inhibitory functions of KSHV-encoded chemokines. Science 278, 290-294.

Boshoff,C., Gao,S.J., Healy,L.E., Matthews,S., Thomas,A.J., Coignet,L., Warnke,R.A., Strauchen,J.A., Matutes,E., Kamel,O.W., Moore,P.S., Weiss,R.A., and Chang,Y. (1998). Establishing a KSHV+ cell line (BCP-1) from peripheral blood and characterizing its growth in Nod/SCID mice. Blood 91, 1671-1679.

Boshoff,C., Schulz,T.F., Kennedy,M.M., Graham,A.K., Fisher,C., Thomas,A., McGee,J.O., Weiss,R.A., and O'Leary,J.J. (1995). Kaposi's sarcoma-associated herpesvirus infects endothelial and spindle cells. Nat. Med. 1, 1274-1278.

Bourboulia,D., Aldam,D., Lagos,D., Allen,E., Williams,I., Cornforth,D., Copas,A., and Boshoff,C. (2004). Short- and long-term effects of highly active antiretroviral therapy on Kaposi sarcoma-associated herpesvirus immune responses and viraemia. AIDS 18, 485-493.

Boyer,L.A., Lee,T.I., Cole,M.F., Johnstone,S.E., Levine,S.S., Zucker,J.P., Guenther,M.G., Kumar,R.M., Murray,H.L., Jenner,R.G., Gifford,D.K., Melton,D.A., Jaenisch,R., and Young,R.A. (2005). Core transcriptional regulatory circuitry in human embryonic stem cells. Cell 122, 947-956.

Breiteneder-Geleff,S., Soleiman,A., Kowalski,H., Horvat,R., Amann,G., Kriehuber,E., Diem,K., Weninger,W., Tschachler,E., Alitalo,K., and Kerjaschki,D. (1999). Angiosarcomas express mixed endothelial phenotypes of blood and lymphatic capillaries: podoplanin as a specific marker for lymphatic endothelium. Am. J. Pathol. 154, 385-394.

Brennecke,J., Stark,A., Russell,R.B., and Cohen,S.M. (2005). Principles of microRNA-target recognition. PLoS. Biol. 3, e85.

Brousset,P., Cesarman,E., Meggetto,F., Lamant,L., and Delsol,G. (2001). Colocalization of the viral interleukin-6 with latent nuclear antigen-1 of human herpesvirus-8 in endothelial spindle cells of Kaposi's sarcoma and lymphoid cells of multicentric Castleman's disease. Hum. Pathol. *32*, 95-100

Bruyere,F. and Noel,A. (2010). Lymphangiogenesis: in vitro and in vivo models. FASEB J. 24, 8-21.

Burger,R., Neipel,F., Fleckenstein,B., Savino,R., Ciliberto,G., Kalden,J.R., and Gramatzki,M. (1998). Human herpesvirus type 8 interleukin-6 homologue is functionally active on human myeloma cells. Blood 91, 1858-1863.

Burysek,L., Yeow,W.S., and Pitha,P.M. (1999). Unique properties of a second human herpesvirus 8-encoded interferon regulatory factor (vIRF-2). J. Hum. Virol. 2, 19-32.

Byzova,T.V., Goldman,C.K., Jankau,J., Chen,J., Cabrera,G., Achen,M.G., Stacker,S.A., Carnevale,K.A., Siemionow,M., Deitcher,S.R., and DiCorleto,P.E. (2002). Adenovirus encoding vascular endothelial growth factor-D induces tissue-specific vascular patterns in vivo. Blood 99, 4434-4442.

Cai,X. and Cullen,B.R. (2006). Transcriptional origin of Kaposi's sarcoma-associated herpesvirus microRNAs. J. Virol. 80, 2234-2242.

Cai,X. and Cullen,B.R. (2007). The imprinted H19 noncoding RNA is a primary microRNA precursor. RNA. 13, 313-316.

Cai,X., Lu,S., Zhang,Z., Gonzalez,C.M., Damania,B., and Cullen,B.R. (2005). Kaposi's sarcoma-associated herpesvirus expresses an array of viral microRNAs in latently infected cells. Proc. Natl. Acad. Sci. U. S. A 102, 5570-5575.

Calin,G.A., Dumitru,C.D., Shimizu,M., Bichi,R., Zupo,S., Noch,E., Aldler,H., Rattan,S., Keating,M., Rai,K., Rassenti,L., Kipps,T., Negrini,M., Bullrich,F., and Croce,C.M. (2002). Frequent deletions and down-regulation of micro- RNA genes miR15 and miR16 at 13q14 in chronic lymphocytic leukemia. Proc. Natl. Acad. Sci. U. S. A 99, 15524-15529.

Calin,G.A., Sevignani,C., Dumitru,C.D., Hyslop,T., Noch,E., Yendamuri,S., Shimizu,M., Rattan,S., Bullrich,F., Negrini,M., and Croce,C.M. (2004). Human microRNA genes are frequently located at fragile sites and genomic regions involved in cancers. Proc. Natl. Acad. Sci. U. S. A 101, 2999-3004.

Campbell,T.B., Borok,M., Gwanzura,L., MaWhinney,S., White,I.E., Ndemera,B., Gudza,I., Fitzpatrick,L., and Schooley,R.T. (2000). Relationship of human herpesvirus 8 peripheral blood virus load and Kaposi's sarcoma clinical stage. AIDS *14*, 2109-2116.

Cannon,M., Philpott,N.J., and Cesarman,E. (2003). The Kaposi's sarcoma-associated herpesvirus G protein-coupled receptor has broad signaling effects in primary effusion lymphoma cells. J. Virol. 77, 57-67.

Cannon,M.J., Dollard,S.C., Black,J.B., Edlin,B.R., Hannah,C., Hogan,S.E., Patel,M.M., Jaffe,H.W., Offermann,M.K., Spira,T.J., Pellett,P.E., and Gunthel,C.J. (2003). Risk factors for Kaposi's sarcoma in men seropositive for both human herpesvirus 8 and human immunodeficiency virus. AIDS 17, 215-222.

Carmell,M.A., Xuan,Z., Zhang,M.Q., and Hannon,G.J. (2002). The Argonaute family: tentacles that reach into RNAi, developmental control, stem cell maintenance, and tumorigenesis. Genes Dev. 16, 2733-2742.

Carroll,P.A., Brazeau,E., and Lagunoff,M. (2004). Kaposi's sarcoma-associated herpesvirus infection of blood endothelial cells induces lymphatic differentiation. Virology 328, 7-18.

Cesarman,E., Chang,Y., Moore,P.S., Said,J.W., and Knowles,D.M. (1995a). Kaposi's sarcoma-associated herpesvirus-like DNA sequences in AIDS-related body-cavity-based lymphomas. N. Engl. J. Med. *332*, 1186-1191.

Cesarman,E., Moore,P.S., Rao,P.H., Inghirami,G., Knowles,D.M., and Chang,Y. (1995b). In vitro establishment and characterization of two acquired immunodeficiency syndrome-related lymphoma cell lines (BC-1 and BC-2) containing Kaposi's sarcoma-associated herpesvirus-like (KSHV) DNA sequences. Blood 86, 2708-2714.

Cesarman,E., Nador,R.G., Bai,F., Bohenzky,R.A., Russo,J.J., Moore,P.S., Chang,Y., and Knowles,D.M. (1996). Kaposi's sarcoma-associated herpesvirus contains G protein-coupled receptor and cyclin D homologs which are expressed in Kaposi's sarcoma and malignant lymphoma. J. Virol. 70, 8218-8223.

Chang,T.C., Wentzel,E.A., Kent,O.A., Ramachandran,K., Mullendore,M., Lee,K.H., Feldmann,G., Yamakuchi,M., Ferlito,M., Lowenstein,C.J., Arking,D.E., Beer,M.A., Maitra,A., and Mendell,J.T. (2007). Transactivation of miR-34a by p53 broadly influences gene expression and promotes apoptosis. Mol. Cell 26, 745-752.

Chang,Y., Cesarman,E., Pessin,M.S., Lee,F., Culpepper,J., Knowles,D.M., and Moore,P.S. (1994). Identification of herpesvirus-like DNA sequences in AIDS-associated Kaposi's sarcoma. Science 266, 1865-1869.

Chang,Y., Moore,P.S., Talbot,S.J., Boshoff,C.H., Zarkowska,T., Godden,K., Paterson,H., Weiss,R.A., and Mittnacht,S. (1996). Cyclin encoded by KS herpesvirus. Nature 382, 410.

Chauhan,B.K., Yang,Y., Cveklova,K., and Cvekl,A. (2004). Functional interactions between alternatively spliced forms of Pax6 in crystallin gene regulation and in haploinsufficiency. Nucleic Acids Res. 32, 1696-1709.

Chen,C.Z., Li,L., Lodish,H.F., and Bartel,D.P. (2004). MicroRNAs modulate hematopoietic lineage differentiation. Science 303, 83-86.

Chen,J., Ueda,K., Sakakibara,S., Okuno,T., Parravicini,C., Corbellino,M., and Yamanishi,K. (2001). Activation of latent Kaposi's sarcoma-associated herpesvirus by demethylation of the promoter of the lytic transactivator. Proc. Natl. Acad. Sci. U. S. A 98, 4119-4124.

Chen,Q., Dowhan,D.H., Liang,D., Moore,D.D., and Overbeek,P.A. (2002). CREB-binding protein/p300 co-activation of crystallin gene expression. J. Biol. Chem. 277, 24081-24089.

Chendrimada,T.P., Finn,K.J., Ji,X., Baillat,D., Gregory,R.I., Liebhaber,S.A., Pasquinelli,A.E., and Shiekhattar,R. (2007). MicroRNA silencing through RISC recruitment of eIF6. Nature 447, 823-828.

Chesi,M., Bergsagel,P.L., Shonukan,O.O., Martelli,M.L., Brents,L.A., Chen,T., Schrock,E., Ried,T., and Kuehl,W.M. (1998). Frequent dysregulation of the c-maf proto-oncogene at 16q23 by translocation to an Ig locus in multiple myeloma. Blood 91, 4457-4463.

Chi,S.W., Zang,J.B., Mele,A., and Darnell,R.B. (2009). Argonaute HITS-CLIP decodes microRNA-mRNA interaction maps. Nature 460, 479-486.
Choudhuri,S. (2009). Lesser known relatives of miRNA. Biochem. Biophys. Res. Commun. 388, 177-180.

Chow,M. and Rubin,H. (1999a). Clonal dynamics of progressive neoplastic transformation. Proc. Natl. Acad. Sci. U. S. A 96, 6976-6981.

Chow,M. and Rubin,H. (1999b). The cellular ecology of progressive neoplastic transformation: a clonal analysis. Proc. Natl. Acad. Sci. U. S. A 96, 2093-2098.

Choy,E.Y., Siu,K.L., Kok,K.H., Lung,R.W., Tsang,C.M., To,K.F., Kwong,D.L., Tsao,S.W., and Jin,D.Y. (2008). An Epstein-Barr virus-encoded microRNA targets PUMA to promote host cell survival. J. Exp. Med. 205, 2551-2560.

Cimmino,A., Calin,G.A., Fabbri,M., Iorio,M.V., Ferracin,M., Shimizu,M., Wojcik,S.E., Aqeilan,R.I., Zupo,S., Dono,M., Rassenti,L., Alder,H., Volinia,S., Liu,C.G., Kipps,T.J., Negrini,M., and Croce,C.M. (2005). miR-15 and miR-16 induce apoptosis by targeting BCL2. Proc. Natl. Acad. Sci. U. S. A 102, 13944-13949.

Cobaleda,C. and Busslinger,M. (2008). Developmental plasticity of lymphocytes. Curr. Opin. Immunol. 20, 139-148.

Cobaleda,C., Jochum,W., and Busslinger,M. (2007). Conversion of mature B cells into T cells by dedifferentiation to uncommitted progenitors. Nature 449, 473-477.

Coolen,M., Sii-Felice,K., Bronchain,O., Mazabraud,A., Bourrat,F., Retaux,S., Felder-Schmittbuhl,M.P., Mazan,S., and Plouhinec,J.L. (2005). Phylogenomic analysis and expression patterns of large Maf genes in Xenopus tropicalis provide new insights into the functional evolution of the gene family in osteichthyans. Dev. Genes Evol. 215, 327-339.

Costinean,S., Zanesi,N., Pekarsky,Y., Tili,E., Volinia,S., Heerema,N., and Croce,C.M. (2006). Pre-B cell proliferation and lymphoblastic leukemia/high-grade lymphoma in E(mu)-miR155 transgenic mice. Proc. Natl. Acad. Sci. U. S. A 103, 7024-7029.

Cotter,M.A. and Robertson,E.S. (1999). The latency-associated nuclear antigen tethers the Kaposi's sarcoma-associated herpesvirus genome to host chromosomes in body cavity-based lymphoma cells. Virology 264, 254-264.

Croce,C.M. (2009). Causes and consequences of microRNA dysregulation in cancer. Nat. Rev. Genet. 10, 704-714.

Cueni,L.N. and Detmar,M. (2006). New insights into the molecular control of the lymphatic vascular system and its role in disease. J. Invest Dermatol. 126, 2167-2177.

Cueni,L.N. and Detmar,M. (2008). The lymphatic system in health and disease. Lymphat. Res. Biol. 6, 109-122.

Cui,W., Tomarev,S.I., Piatigorsky,J., Chepelinsky,A.B., and Duncan,M.K. (2004). Mafs, Prox1, and Pax6 can regulate chicken betaB1-crystallin gene expression. J. Biol. Chem. 279, 11088-11095.

Cullen,B.R. (2009). Viral and cellular messenger RNA targets of viral microRNAs. Nature 457, 421-425.

Cullen,B.R. (2010). Five questions about viruses and microRNAs. PLoS. Pathog. 6, e1000787.
Dagenais,S.L., Hartsough,R.L., Erickson,R.P., Witte,M.H., Butler,M.G., and Glover,T.W. (2004). Foxc2 is expressed in developing lymphatic vessels and other tissues associated with lymphedema-distichiasis syndrome. Gene Expr. Patterns. 4, 611-619.

Davidovici,B., Karakis,I., Bourboulia,D., Ariad,S., Zong,J., Benharroch,D., Dupin,N., Weiss,R., Hayward,G., Sarov,B., and Boshoff,C. (2001). Seroepidemiology and molecular epidemiology of Kaposi's sarcoma-associated herpesvirus among Jewish population groups in Israel. J. Natl. Cancer Inst. 93, 194-202.

Davidson-Moncada,J., Papavasiliou,F.N., and Tam,W. (2010). MicroRNAs of the immune system: roles in inflammation and cancer. Ann. N. Y. Acad. Sci. 1183, 183-194.

Davis,E., Caiment,F., Tordoir,X., Cavaille,J., Ferguson-Smith,A., Cockett,N., Georges,M., and Charlier,C. (2005). RNAi-mediated allelic trans-interaction at the imprinted Rtl1/Peg11 locus. Curr. Biol. 15, 743-749.

Davison,A.J. (2002). Evolution of the herpesviruses. Vet. Microbiol. 86, 69-88.

Davison,A.J. (2007). Overview of classification. In Human Herpesviruses. Biology, Therapy, and Immunorophylaxis, Cambridge University Press), pp. 3-9.

Dejana,E. (2004). Endothelial cell-cell junctions: happy together. Nat. Rev. Mol. Cell Biol. 5, 261-270.

Dhakshinamoorthy,S. and Jaiswal,A.K. (2002). c-Maf negatively regulates ARE-mediated detoxifying enzyme genes expression and anti-oxidant induction. Oncogene 21, 5301-5312.

Di,B.D. and Cesarman,E. (2004). Uncovering the complexities of Kaposi's sarcoma through genome-wide expression analysis. Genome Biol. 5, 247.

Direkze,S. and Laman,H. (2004). Regulation of growth signalling and cell cycle by Kaposi's sarcoma-associated herpesvirus genes. Int. J. Exp. Pathol. 85, 305-319.

Dittmer,D., Lagunoff,M., Renne,R., Staskus,K., Haase,A., and Ganem,D. (1998). A cluster of latently expressed genes in Kaposi's sarcoma-associated herpesvirus. J. Virol. 72, 8309-8315.

Dittmer,D.P. (2003). Transcription profile of Kaposi's sarcoma-associated herpesvirus in primary Kaposi's sarcoma lesions as determined by real-time PCR arrays. Cancer Res. 63, 2010-2015.

Djerbi,M., Screpanti,V., Catrina,A.I., Bogen,B., Biberfeld,P., and Grandien,A. (1999). The inhibitor of death receptor signaling, FLICE-inhibitory protein defines a new class of tumor progression factors. J. Exp. Med. 190, 1025-1032.

Dlakic,M., Grinberg,A.V., Leonard,D.A., and Kerppola,T.K. (2001). DNA sequence-dependent folding determines the divergence in binding specificities between Maf and other bZIP proteins. EMBO J. 20, 828-840.

Doench,J.G. and Sharp,P.A. (2004). Specificity of microRNA target selection in translational repression. Genes Dev. 18, 504-511.

Doench,J.G., Petersen,C.P., and Sharp,P.A. (2003). siRNAs can function as miRNAs. Genes Dev. 17, 438-442.

Doorbar,J., Foo,C., Coleman,N., Medcalf,L., Hartley,O., Prospero,T., Napthine,S., Sterling,J., Winter,G., and Griffin,H. (1997). Characterization of events during the late stages of HPV16 infection in vivo using high-affinity synthetic Fabs to E4. Virology 238, 40-52.

Dorfman,R.F. (1988). Kaposi's sarcoma: evidence supporting its origin from the lymphatic system. Lymphology 21, 45-52.

Dourmishev,L.A., Dourmishev,A.L., Palmeri,D., Schwartz,R.A., and Lukac,D.M. (2003). Molecular genetics of Kaposi's sarcoma-associated herpesvirus (human herpesvirus-8) epidemiology and pathogenesis. Microbiol. Mol. Biol. Rev. *67*, 175-212, table.

Du,M.Q., Liu,H., Diss,T.C., Ye,H., Hamoudi,R.A., Dupin,N., Meignin,V., Oksenhendler,E., Boshoff,C., and Isaacson,P.G. (2001). Kaposi sarcoma-associated herpesvirus infects monotypic (IgM lambda) but polyclonal naive B cells in Castleman disease and associated lymphoproliferative disorders. Blood 97, 2130-2136.

Du,T. and Zamore,P.D. (2005). microPrimer: the biogenesis and function of microRNA. Development 132, 4645-4652.

Dumont,D.J., Jussila,L., Taipale,J., Lymboussaki,A., Mustonen,T., Pajusola,K., Breitman,M., and Alitalo,K. (1998). Cardiovascular failure in mouse embryos deficient in VEGF receptor-3. Science 282, 946-949.

Dupin,N., Diss,T.L., Kellam,P., Tulliez,M., Du,M.Q., Sicard,D., Weiss,R.A., Isaacson,P.G., and Boshoff,C. (2000). HHV-8 is associated with a plasmablastic variant of Castleman disease that is linked to HHV-8-positive plasmablastic lymphoma. Blood 95, 1406-1412.

Dupin,N., Fisher,C., Kellam,P., Ariad,S., Tulliez,M., Franck,N., van,M.E., Salmon,D., Gorin,I., Escande,J.P., Weiss,R.A., Alitalo,K., and Boshoff,C. (1999). Distribution of human herpesvirus-8 latently infected cells in Kaposi's sarcoma, multicentric Castleman's disease, and primary effusion lymphoma. Proc. Natl. Acad. Sci. U. S. A 96, 4546-4551.

Dupin,N., Grandadam,M., Calvez,V., Gorin,I., Aubin,J.T., Havard,S., Lamy,F., Leibowitch,M., Huraux,J.M., Escande,J.P., and . (1995). Herpesvirus-like DNA sequences in patients with Mediterranean Kaposi's sarcoma. Lancet 345, 761-762.

Duprez,R., Lacoste,V., Briere,J., Couppie,P., Frances,C., Sainte-Marie,D., Kassa-Kelembho,E., Lando,M.J., Essame Oyono,J.L., Nkegoum,B., Hbid,O., Mahe,A., Lebbe,C., Tortevoye,P., Huerre,M., and Gessain,A. (2007). Evidence for a multiclonal origin of multicentric advanced lesions of Kaposi sarcoma. J. Natl. Cancer Inst. 99, 1086-1094.

Duus,K.M., Lentchitsky,V., Wagenaar,T., Grose,C., and Webster-Cyriaque,J. (2004). Wild-type Kaposi's sarcoma-associated herpesvirus isolated from the oropharynx of immune-competent individuals has tropism for cultured oral epithelial cells. J. Virol. 78, 4074-4084.

Eferl,R. and Wagner,E.F. (2003). AP-1: a double-edged sword in tumorigenesis. Nat. Rev. Cancer 3, 859-868.

Eis,P.S., Tam,W., Sun,L., Chadburn,A., Li,Z., Gomez,M.F., Lund,E., and Dahlberg,J.E. (2005). Accumulation of miR-155 and BIC RNA in human B cell lymphomas. Proc. Natl. Acad. Sci. U. S. A 102, 3627-3632.

Elbashir,S.M., Lendeckel,W., and Tuschl,T. (2001). RNA interference is mediated by 21- and 22-nucleotide RNAs. Genes Dev. 15, 188-200.

Ellis,M., Chew,Y.P., Fallis,L., Freddersdorf,S., Boshoff,C., Weiss,R.A., Lu,X., and Mittnacht,S. (1999). Degradation of p27(Kip) cdk inhibitor triggered by Kaposi's sarcoma virus cyclin-cdk6 complex. EMBO J. 18, 644-653.

Elmen,J., Lindow,M., Schutz,S., Lawrence,M., Petri,A., Obad,S., Lindholm,M., Hedtjarn,M., Hansen,H.F., Berger,U., Gullans,S., Kearney,P., Sarnow,P., Straarup,E.M., and Kauppinen,S. (2008). LNA-mediated microRNA silencing in non-human primates. Nature 452, 896-899.

Ensoli,B. and Sturzl,M. (1998). Kaposi's sarcoma: a result of the interplay among inflammatory cytokines, angiogenic factors and viral agents. Cytokine Growth Factor Rev. 9, 63-83.

Ensoli,B., Nakamura,S., Salahuddin,S.Z., Biberfeld,P., Larsson,L., Beaver,B., Wong-Staal,F., and Gallo,R.C. (1989). AIDS-Kaposi's sarcoma-derived cells express cytokines with autocrine and paracrine growth effects. Science 243, 223-226.

Ensoli,B., Sgadari,C., Barillari,G., Sirianni,M.C., Sturzl,M., and Monini,P. (2001). Biology of Kaposi's sarcoma. Eur. J. Cancer 37, 1251-1269.

Eulalio,A., Huntzinger,E., and Izaurralde,E. (2008). Getting to the root of miRNA-mediated gene silencing. Cell 132, 9-14.

Eychene,A., Rocques,N., and Pouponnot,C. (2008). A new MAFia in cancer. Nat. Rev. Cancer 8, 683-693.

Fabbri,M., Garzon,R., Cimmino,A., Liu,Z., Zanesi,N., Callegari,E., Liu,S., Alder,H., Costinean,S., Fernandez-Cymering,C., Volinia,S., Guler,G., Morrison,C.D., Chan,K.K., Marcucci,G., Calin,G.A., Huebner,K., and Croce,C.M. (2007). MicroRNA-29 family reverts aberrant methylation in lung cancer by targeting DNA methyltransferases 3A and 3B. Proc. Natl. Acad. Sci. U. S. A 104, 15805-15810.

Farh,K.K., Grimson,A., Jan,C., Lewis,B.P., Johnston,W.K., Lim,L.P., Burge,C.B., and Bartel,D.P. (2005). The widespread impact of mammalian MicroRNAs on mRNA repression and evolution. Science 310, 1817-1821.

Fehrmann,F. and Laimins,L.A. (2003). Human papillomaviruses: targeting differentiating epithelial cells for malignant transformation. Oncogene 22, 5201-5207.

Felli,N., Fontana,L., Pelosi,E., Botta,R., Bonci,D., Facchiano,F., Liuzzi,F., Lulli,V., Morsilli,O., Santoro,S., Valtieri,M., Calin,G.A., Liu,C.G., Sorrentino,A., Croce,C.M., and Peschle,C. (2005). MicroRNAs 221 and 222 inhibit normal erythropoiesis and erythroleukemic cell growth via kit receptor down-modulation. Proc. Natl. Acad. Sci. U. S. A 102, 18081-18086.

Field,N., Low,W., Daniels,M., Howell,S., Daviet,L., Boshoff,C., and Collins,M. (2003). KSHV vFLIP binds to IKK-gamma to activate IKK. J. Cell Sci. 116, 3721-3728.

Filipowicz,W., Bhattacharyya,S.N., and Sonenberg,N. (2008). Mechanisms of post-transcriptional regulation by microRNAs: are the answers in sight? Nat. Rev. Genet. 9, 102-114.

Fire,A., Xu,S., Montgomery,M.K., Kostas,S.A., Driver,S.E., and Mello,C.C. (1998). Potent and specific genetic interference by double-stranded RNA in Caenorhabditis elegans. Nature 391, 806-811.

Franceschi,S. and Geddes,M. (1995). Epidemiology of classic Kaposi's sarcoma, with special reference to mediterranean population. Tumori 81, 308-314.

Friborg,J., Jr., Kong,W., Hottiger,M.O., and Nabel,G.J. (1999). p53 inhibition by the LANA protein of KSHV protects against cell death. Nature 402, 889-894.

Friedman,J.S., Khanna,H., Swain,P.K., Denicola,R., Cheng,H., Mitton,K.P., Weber,C.H., Hicks,D., and Swaroop,A. (2004). The minimal transactivation domain of the basic motif-leucine zipper transcription factor NRL interacts with TATA-binding protein. J. Biol. Chem. 279, 47233-47241.

Fujimuro,M., Wu,F.Y., ApRhys,C., Kajumbula,H., Young,D.B., Hayward,G.S., and Hayward,S.D. (2003). A novel viral mechanism for dysregulation of beta-catenin in Kaposi's sarcoma-associated herpesvirus latency. Nat. Med. 9, 300-306.

Fujiwara,K.T., Kataoka,K., and Nishizawa,M. (1993). Two new members of the maf oncogene family, mafK and mafF, encode nuclear b-Zip proteins lacking putative trans-activator domain. Oncogene 8, 2371-2380.

Gale,N.W., Prevo,R., Espinosa,J., Ferguson,D.J., Dominguez,M.G., Yancopoulos,G.D., Thurston,G., and Jackson,D.G. (2007). Normal lymphatic development and function in mice deficient for the lymphatic hyaluronan receptor LYVE-1. Mol. Cell Biol. 27, 595-604.

Gale,N.W., Thurston,G., Hackett,S.F., Renard,R., Wang,Q., McClain,J., Martin,C., Witte,C., Witte,M.H., Jackson,D., Suri,C., Campochiaro,P.A., Wiegand,S.J., and Yancopoulos,G.D. (2002). Angiopoietin-2 is required for postnatal angiogenesis and lymphatic patterning, and only the latter role is rescued by Angiopoietin-1. Dev. Cell 3, 411-423.

Ganem,D. (1998). Human herpesvirus 8 and its role in the genesis of Kaposi's sarcoma. Curr. Clin. Top. Infect. Dis. 18, 237-251.

Garzon,R., Calin,G.A., and Croce,C.M. (2009). MicroRNAs in Cancer. Annu. Rev. Med. 60, 167-179.

Garzon,R., Garofalo,M., Martelli,M.P., Briesewitz,R., Wang,L., Fernandez-Cymering,C., Volinia,S., Liu,C.G., Schnittger,S., Haferlach,T., Liso,A., Diverio,D., Mancini,M., Meloni,G., Foa,R., Martelli,M.F., Mecucci,C., Croce,C.M., and Falini,B. (2008). Distinctive microRNA signature of acute myeloid leukemia bearing cytoplasmic mutated nucleophosmin. Proc. Natl. Acad. Sci. U. S. A 105, 3945-3950.

Gates,A.E. and Kaplan,L.D. (2002). AIDS malignancies in the era of highly active antiretroviral therapy. Oncology (Williston. Park) 16, 657-665.

Gautier,L., Cope,L., Bolstad,B.M., and Irizarry,R.A. (2004). affy--analysis of Affymetrix GeneChip data at the probe level. Bioinformatics. 20, 307-315.

Gerli,R., Solito,R., Weber,E., and Agliano,M. (2000). Specific adhesion molecules bind anchoring filaments and endothelial cells in human skin initial lymphatics. Lymphology 33, 148-157.
Gessain,A. and Duprez,R. (2005). Spindle cells and their role in Kaposi's sarcoma. Int. J. Biochem. Cell Biol. 37, 2457-2465.

Gessain,A. and Duprez,R. (2005). Spindle cells and their role in Kaposi's sarcoma. Int. J. Biochem. Cell Biol. *37*, 2457-2465.

Gill,P.S., Tsai,Y.C., Rao,A.P., Spruck,C.H., III, Zheng,T., Harrington,W.A., Jr., Cheung,T., Nathwani,B., and Jones,P.A. (1998). Evidence for multiclonality in multicentric Kaposi's sarcoma. Proc. Natl. Acad. Sci. U. S. A 95, 8257-8261.

Giraldez,A.J., Mishima,Y., Rihel,J., Grocock,R.J., van,D.S., Inoue,K., Enright,A.J., and Schier,A.F. (2006). Zebrafish MiR-430 promotes deadenylation and clearance of maternal mRNAs. Science 312, 75-79.

Godden-Kent,D., Talbot,S.J., Boshoff,C., Chang,Y., Moore,P., Weiss,R.A., and Mittnacht,S. (1997). The cyclin encoded by Kaposi's sarcoma-associated herpesvirus stimulates cdk6 to phosphorylate the retinoblastoma protein and histone H1. J. Virol. 71, 4193-4198.

Godfrey,A., Anderson,J., Papanastasiou,A., Takeuchi,Y., and Boshoff,C. (2005). Inhibiting primary effusion lymphoma by lentiviral vectors encoding short hairpin RNA. Blood 105, 2510-2518.

Gottwein,E., Cai,X., and Cullen,B.R. (2006). A novel assay for viral microRNA function identifies a single nucleotide polymorphism that affects Drosha processing. J. Virol. 80, 5321-5326.

Gottwein,E., Mukherjee,N., Sachse,C., Frenzel,C., Majoros,W.H., Chi,J.T., Braich,R., Manoharan,M., Soutschek,J., Ohler,U., and Cullen,B.R. (2007). A viral microRNA functions as an orthologue of cellular miR-155. Nature 450, 1096-1099.

Gradoville,L., Gerlach,J., Grogan,E., Shedd,D., Nikiforow,S., Metroka,C., and Miller,G. (2000). Kaposi's sarcoma-associated herpesvirus open reading frame 50/Rta protein activates the entire viral lytic cycle in the HH-B2 primary effusion lymphoma cell line. J. Virol. 74, 6207-6212.

Grey,F., Meyers,H., White,E.A., Spector,D.H., and Nelson,J. (2007). A human cytomegalovirus-encoded microRNA regulates expression of multiple viral genes involved in replication. PLoS. Pathog. 3, e163.

Griffiths-Jones,S. (2004). The microRNA Registry. Nucleic Acids Res. 32, D109-D111.

Griffiths-Jones,S., Grocock,R.J., van,D.S., Bateman,A., and Enright,A.J. (2006). miRBase: microRNA sequences, targets and gene nomenclature. Nucleic Acids Res. 34, D140-D144.

Griffiths-Jones,S., Saini,H.K., van,D.S., and Enright,A.J. (2008). miRBase: tools for microRNA genomics. Nucleic Acids Res. 36, D154-D158.

Grimson,A., Farh,K.K., Johnston,W.K., Garrett-Engele,P., Lim,L.P., and Bartel,D.P. (2007). MicroRNA targeting specificity in mammals: determinants beyond seed pairing. Mol. Cell 27, 91-105.

Groger,M., Loewe,R., Holnthoner,W., Embacher,R., Pillinger,M., Herron,G.S., Wolff,K., and Petzelbauer,P. (2004). IL-3 induces expression of lymphatic markers Prox-1 and podoplanin in human endothelial cells. J. Immunol. 173, 7161-7169.

Grossmann,C. and Ganem,D. (2008). Effects of NFkappaB activation on KSHV latency and lytic reactivation are complex and context-dependent. Virology 375, 94-102.

Grossmann,C., Podgrabinska,S., Skobe,M., and Ganem,D. (2006). Activation of NF-kappaB by the latent vFLIP gene of Kaposi's sarcoma-associated herpesvirus is required for the spindle shape of virus-infected endothelial cells and contributes to their proinflammatory phenotype. J. Virol. 80, 7179-7185.

Grundhoff,A., Sullivan,C.S., and Ganem,D. (2006). A combined computational and microarray-based approach identifies novel microRNAs encoded by human gamma-herpesviruses. RNA. 12, 733-750.

Gu,S., Jin,L., Zhang,F., Sarnow,P., and Kay,M.A. (2009). Biological basis for restriction of microRNA targets to the 3' untranslated region in mammalian mRNAs. Nat. Struct. Mol. Biol. 16, 144-150.

Guasparri,I., Keller,S.A., and Cesarman,E. (2004). KSHV vFLIP is essential for the survival of infected lymphoma cells. J. Exp. Med. 199, 993-1003.

Guo,H.G., Sadowska,M., Reid,W., Tschachler,E., Hayward,G., and Reitz,M. (2003). Kaposi's sarcoma-like tumors in a human herpesvirus 8 ORF74 transgenic mouse. J. Virol. 77, 2631-2639.

Gwack,Y., Byun,H., Hwang,S., Lim,C., and Choe,J. (2001). CREB-binding protein and histone deacetylase regulate the transcriptional activity of Kaposi's sarcoma-associated herpesvirus open reading frame 50. J. Virol. 75, 1909-1917.

Hale,T.K., Myers,C., Maitra,R., Kolzau,T., Nishizawa,M., and Braithwaite,A.W. (2000). Maf transcriptionally activates the mouse p53 promoter and causes a p53-dependent cell death. J. Biol. Chem. 275, 17991-17999.

Hammond,S.M., Bernstein,E., Beach,D., and Hannon,G.J. (2000). An RNA-directed nuclease mediates post-transcriptional gene silencing in Drosophila cells. Nature 404, 293-296.

Hansen,A., Henderson,S., Lagos,D., Nikitenko,L., Coulter,E., Roberts,S., Gratrix,F., Plaisance,K., Renne,R., Bower,M., Kellam,P., and Boshoff,C. (2010). KSHV-encoded miRNAs target MAF to induce endothelial cell reprogramming. Genes Dev. 24, 195-205.

Harvey,N.L., Srinivasan,R.S., Dillard,M.E., Johnson,N.C., Witte,M.H., Boyd,K., Sleeman,M.W., and Oliver,G. (2005). Lymphatic vascular defects promoted by Prox1 haploinsufficiency cause adult-onset obesity. Nat. Genet. 37, 1072-1081.

Harwood,A.R., Osoba,D., Hofstader,S.L., Goldstein,M.B., Cardella,C.J., Holecek,M.J., Kunynetz,R., and Giammarco,R.A. (1979). Kaposi's sarcoma in recipients of renal transplants. Am. J. Med. 67, 759-765.

Hegde,S.P., Zhao,J., Ashmun,R.A., and Shapiro,L.H. (1999). c-Maf induces monocytic differentiation and apoptosis in bipotent myeloid progenitors. Blood 94, 1578-1589.

Ho,I.C., Hodge,M.R., Rooney,J.W., and Glimcher,L.H. (1996). The proto-oncogene c-maf is responsible for tissue-specific expression of interleukin-4. Cell 85, 973-983.

Ho,I.C., Lo,D., and Glimcher,L.H. (1998). c-maf promotes T helper cell type 2 (Th2) and attenuates Th1 differentiation by both interleukin 4-dependent and -independent mechanisms. J. Exp. Med. 188, 1859-1866.

Hofacker,I.L. (2007). How microRNAs choose their targets. Nat. Genet. 39, 1191-1192.

Hong,Y.K., Foreman,K., Shin,J.W., Hirakawa,S., Curry,C.L., Sage,D.R., Libermann,T., Dezube,B.J., Fingeroth,J.D., and Detmar,M. (2004). Lymphatic reprogramming of blood vascular endothelium by Kaposi sarcoma-associated herpesvirus. Nat. Genet. 36, 683-685.

Hong,Y.K., Harvey,N., Noh,Y.H., Schacht,V., Hirakawa,S., Detmar,M., and Oliver,G. (2002). Prox1 is a master control gene in the program specifying lymphatic endothelial cell fate. Dev. Dyn. 225, 351-357.

Huang,K., Serria,M.S., Nakabayashi,H., Nishi,S., and Sakai,M. (2000). Molecular cloning and functional characterization of the mouse mafB gene. Gene 242, 419-426.

Huang,W., Lu,N., Eberspaecher,H., and De,C.B. (2002). A new long form of c-Maf cooperates with Sox9 to activate the type II collagen gene. J. Biol. Chem. 277, 50668-50675.

Humphreys,D.T., Westman,B.J., Martin,D.I., and Preiss,T. (2005). MicroRNAs control translation initiation by inhibiting eukaryotic initiation factor 4E/cap and poly(A) tail function. Proc. Natl. Acad. Sci. U. S. A 102, 16961-16966.

Hurt,E.M., Wiestner,A., Rosenwald,A., Shaffer,A.L., Campo,E., Grogan,T., Bergsagel,P.L., Kuehl,W.M., and Staudt,L.M. (2004). Overexpression of c-maf is a frequent oncogenic event in multiple myeloma that promotes proliferation and pathological interactions with bone marrow stroma. Cancer Cell 5, 191-199.

Hutvagner,G., Simard,M.J., Mello,C.C., and Zamore,P.D. (2004). Sequence-specific inhibition of small RNA function. PLoS. Biol. 2, E98.

Iorio,M.V., Ferracin,M., Liu,C.G., Veronese,A., Spizzo,R., Sabbioni,S., Magri,E., Pedriali,M., Fabbri,M., Campiglio,M., Menard,S., Palazzo,J.P., Rosenberg,A., Musiani,P., Volinia,S., Nenci,I.,

Calin,G.A., Querzoli,P., Negrini,M., and Croce,C.M. (2005). MicroRNA gene expression deregulation in human breast cancer. Cancer Res. 65, 7065-7070.

Jackson,D.G. (2004). Biology of the lymphatic marker LYVE-1 and applications in research into lymphatic trafficking and lymphangiogenesis. APMIS 112, 526-538.

Jamieson,R.V., Munier,F., Balmer,A., Farrar,N., Perveen,R., and Black,G.C. (2003). Pulverulent cataract with variably associated microcornea and iris coloboma in a MAF mutation family. Br. J. Ophthalmol. 87, 411-412.

Jeltsch,M., Kaipainen,A., Joukov,V., Meng,X., Lakso,M., Rauvala,H., Swartz,M., Fukumura,D., Jain,R.K., and Alitalo,K. (1997). Hyperplasia of lymphatic vessels in VEGF-C transgenic mice. Science 276, 1423-1425.

Jenner,R.G. and Boshoff,C. (2002). The molecular pathology of Kaposi's sarcoma-associated herpesvirus. Biochim. Biophys. Acta 1602, 1-22.

Jenner,R.G., Maillard,K., Cattini,N., Weiss,R.A., Boshoff,C., Wooster,R., and Kellam,P. (2003). Kaposi's sarcoma-associated herpesvirus-infected primary effusion lymphoma has a plasma cell gene expression profile. Proc. Natl. Acad. Sci. U. S. A 100, 10399-10404.

Johnson,L.A. and Jackson,D.G. (2008). Cell traffic and the lymphatic endothelium. Ann. N. Y. Acad. Sci. 1131, 119-133.

Johnson,N.C., Dillard,M.E., Baluk,P., McDonald,D.M., Harvey,N.L., Frase,S.L., and Oliver,G. (2008). Lymphatic endothelial cell identity is reversible and its maintenance requires Prox1 activity. Genes Dev. 22, 3282-3291.

Johnson,S.M., Grosshans,H., Shingara,J., Byrom,M., Jarvis,R., Cheng,A., Labourier,E., Reinert,K.L., Brown,D., and Slack,F.J. (2005). RAS is regulated by the let-7 microRNA family. Cell 120, 635-647.

Joukov,V., Pajusola,K., Kaipainen,A., Chilov,D., Lahtinen,I., Kukk,E., Saksela,O., Kalkkinen,N., and Alitalo,K. (1996). A novel vascular endothelial growth factor, VEGF-C, is a ligand for the Flt4 (VEGFR-3) and KDR (VEGFR-2) receptor tyrosine kinases. EMBO J. 15, 1751.

Judde,J.G., Lacoste,V., Briere,J., Kassa-Kelembho,E., Clyti,E., Couppie,P., Buchrieser,C., Tulliez,M., Morvan,J., and Gessain,A. (2000). Monoclonality or oligoclonality of human herpesvirus 8 terminal repeat sequences in Kaposi's sarcoma and other diseases. J. Natl. Cancer Inst. 92, 729-736.

Jussila,L., Valtola,R., Partanen,T.A., Salven,P., Heikkila,P., Matikainen,M.T., Renkonen,R., Kaipainen,A., Detmar,M., Tschachler,E., Alitalo,R., and Alitalo,K. (1998). Lymphatic endothelium and Kaposi's sarcoma spindle cells detected by antibodies against the vascular endothelial growth factor receptor-3. Cancer Res. 58, 1599-1604.

Kaipainen,A., Korhonen,J., Mustonen,T., van,H., V, Fang,G.H., Dumont,D., Breitman,M., and Alitalo,K. (1995). Expression of the fms-like tyrosine kinase 4 gene becomes restricted to lymphatic endothelium during development. Proc. Natl. Acad. Sci. U. S. A 92, 3566-3570.

Kaleeba,J.A. and Berger,E.A. (2006a). Broad target cell selectivity of Kaposi's sarcoma-associated herpesvirus glycoprotein-mediated cell fusion and virion entry. Virology 354, 7-14.
Kaleeba,J.A. and Berger,E.A. (2006b). Kaposi's sarcoma-associated herpesvirus fusion-entry receptor: cystine transporter xCT. Science 311, 1921-1924.

Kaleeba,J.A. and Berger,E.A. (2006b). Kaposi's sarcoma-associated herpesvirus fusion-entry receptor: cystine transporter xCT. Science *311*, 1921-1924.

Kaposi,M. (1872). Idiopathisches multiples Pigmentsarkomen der. Haut. Archiv Dermatol Syph 4, 265-273.

Karkkainen,M.J., Haiko,P., Sainio,K., Partanen,J., Taipale,J., Petrova,T.V., Jeltsch,M., Jackson,D.G., Talikka,M., Rauvala,H., Betsholtz,C., and Alitalo,K. (2004). Vascular endothelial growth factor C is required for sprouting of the first lymphatic vessels from embryonic veins. Nat. Immunol. 5, 74-80.

Karolchik,D., Kuhn,R.M., Baertsch,R., Barber,G.P., Clawson,H., Diekhans,M., Giardine,B., Harte,R.A., Hinrichs,A.S., Hsu,F., Kober,K.M., Miller,W., Pedersen,J.S., Pohl,A., Raney,B.J., Rhead,B., Rosenbloom,K.R., Smith,K.E., Stanke,M., Thakkapallayil,A., Trumbower,H., Wang,T., Zweig,A.S., Haussler,D., and Kent,W.J. (2008). The UCSC Genome Browser Database: 2008 update. Nucleic Acids Res. 36, D773-D779.

Karpanen,T. and Makinen,T. (2006). Regulation of lymphangiogenesis--from cell fate determination to vessel remodeling. Exp. Cell Res. 312, 575-583.

Kataoka,K. (2007). Multiple mechanisms and functions of maf transcription factors in the regulation of tissue-specific genes. J. Biochem. 141, 775-781.

Kataoka,K., Fujiwara,K.T., Noda,M., and Nishizawa,M. (1994a). MafB, a new Maf family transcription activator that can associate with Maf and Fos but not with Jun. Mol. Cell Biol. 14, 7581-7591.

Kataoka,K., Igarashi,K., Itoh,K., Fujiwara,K.T., Noda,M., Yamamoto,M., and Nishizawa,M. (1995). Small Maf proteins heterodimerize with Fos and may act as competitive repressors of the NF-E2 transcription factor. Mol. Cell Biol. 15, 2180-2190.

Kataoka,K., Noda,M., and Nishizawa,M. (1994b). Maf nuclear oncoprotein recognizes sequences related to an AP-1 site and forms heterodimers with both Fos and Jun. Mol. Cell Biol. 14, 700-712.

Kataoka,K., Shioda,S., Ando,K., Sakagami,K., Handa,H., and Yasuda,K. (2004). Differentially expressed Maf family transcription factors, c-Maf and MafA, activate glucagon and insulin gene expression in pancreatic islet alpha- and beta-cells. J. Mol. Endocrinol. 32, 9-20.

Kawai,S., Goto,N., Kataoka,K., Saegusa,T., Shinno-Kohno,H., and Nishizawa,M. (1992). Isolation of the avian transforming retrovirus, AS42, carrying the v-maf oncogene and initial characterization of its gene product. Virology 188, 778-784.

Kawauchi,S., Takahashi,S., Nakajima,O., Ogino,H., Morita,M., Nishizawa,M., Yasuda,K., and Yamamoto,M. (1999). Regulation of lens fiber cell differentiation by transcription factor c-Maf. J. Biol. Chem. 274, 19254-19260.

Kedde,M., Strasser,M.J., Boldajipour,B., Oude Vrielink,J.A., Slanchev,K., le,S.C., Nagel,R., Voorhoeve,P.M., van,D.J., Orom,U.A., Lund,A.H., Perrakis,A., Raz,E., and Agami,R. (2007). RNA-binding protein Dnd1 inhibits microRNA access to target mRNA. Cell 131, 1273-1286.

Keller,S.A., Schattner,E.J., and Cesarman,E. (2000). Inhibition of NF-kappaB induces apoptosis of KSHV-infected primary effusion lymphoma cells. Blood 96, 2537-2542.

Kerppola,T.K. and Curran,T. (1994). A conserved region adjacent to the basic domain is required for recognition of an extended DNA binding site by Maf/Nrl family proteins. Oncogene 9, 3149-3158.

Kertesz,M., Iovino,N., Unnerstall,U., Gaul,U., and Segal,E. (2007). The role of site accessibility in microRNA target recognition. Nat. Genet. 39, 1278-1284.

Khan,A.A., Betel,D., Miller,M.L., Sander,C., Leslie,C.S., and Marks,D.S. (2009). Transfection of small RNAs globally perturbs gene regulation by endogenous microRNAs. Nat. Biotechnol. 27, 549-555.

Kim,J.I., Li,T., Ho,I.C., Grusby,M.J., and Glimcher,L.H. (1999). Requirement for the c-Maf transcription factor in crystallin gene regulation and lens development. Proc. Natl. Acad. Sci. U. S. A 96, 3781-3785.

Kim,J.I., Ho,I.C., Grusby,M.J., and Glimcher,L.H. (1999b). The transcription factor c-Maf controls the production of interleukin-4 but not other Th2 cytokines. Immunity. 10, 745-751.

Kimura,T., Ivell,R., Rust,W., Mizumoto,Y., Ogita,K., Kusui,C., Matsumura,Y., Azuma,C., and Murata,Y. (1999). Molecular cloning of a human MafF homologue, which specifically binds to the oxytocin receptor gene in term myometrium. Biochem. Biophys. Res. Commun. 264, 86-92.

Kiriakidou,M., Tan,G.S., Lamprinaki,S., De Planell-Saguer,M., Nelson,P.T., and Mourelatos,Z. (2007). An mRNA m7G cap binding-like motif within human Ago2 represses translation. Cell 129, 1141-1151.

Kluiver,J., Poppema,S., de,J.D., Blokzijl,T., Harms,G., Jacobs,S., Kroesen,B.J., and van den Berg,A. (2005). BIC and miR-155 are highly expressed in Hodgkin, primary mediastinal and diffuse large B cell lymphomas. J. Pathol. 207, 243-249.

Knudson,C.B. and Knudson,W. (1993). Hyaluronan-binding proteins in development, tissue homeostasis, and disease. FASEB J. 7, 1233-1241.

Krek,A., Grun,D., Poy,M.N., Wolf,R., Rosenberg,L., Epstein,E.J., MacMenamin,P., da,P., I, Gunsalus,K.C., Stoffel,M., and Rajewsky,N. (2005). Combinatorial microRNA target predictions. Nat. Genet. 37, 495-500.

Krutzfeldt,J., Rajewsky,N., Braich,R., Rajeev,K.G., Tuschl,T., Manoharan,M., and Stoffel,M. (2005). Silencing of microRNAs in vivo with 'antagomirs'. Nature 438, 685-689.

Kukk,E., Lymboussaki,A., Taira,S., Kaipainen,A., Jeltsch,M., Joukov,V., and Alitalo,K. (1996). VEGF-C receptor binding and pattern of expression with VEGFR-3 suggests a role in lymphatic vascular development. Development 122, 3829-3837.

Kuppers,R. (2003). B cells under influence: transformation of B cells by Epstein-Barr virus. Nat. Rev. Immunol. 3, 801-812.

Kurschner,C. and Morgan,J.I. (1995). The maf proto-oncogene stimulates transcription from multiple sites in a promoter that directs Purkinje neuron-specific gene expression. Mol. Cell Biol. 15, 246-254.

Kusunoki,H., Motohashi,H., Katsuoka,F., Morohashi,A., Yamamoto,M., and Tanaka,T. (2002). Solution structure of the DNA-binding domain of MafG. Nat. Struct. Biol. 9, 252-256.

Lacoste,V., Mauclere,P., Dubreuil,G., Lewis,J., Georges-Courbot,M.C., and Gessain,A. (2000). KSHV-like herpesviruses in chimps and gorillas. Nature 407, 151-152.

Lagos,D., Pollara,G., Henderson,S., Gratrix,F., Fabani,M., Milne,R., Gotch,F., and Boshoff,C. (2010). miR-132 regulates antiviral innate immunity through suppression of the p300 transcriptional co-activator. Nat. Cell. Biol.

Lagos,D., Trotter,M.W., Vart,R.J., Wang,H.W., Matthews,N.C., Hansen,A., Flore,O., Gotch,F., and Boshoff,C. (2007). Kaposi sarcoma herpesvirus-encoded vFLIP and vIRF1 regulate antigen presentation in lymphatic endothelial cells. Blood 109, 1550-1558.

Lagos-Quintana,M., Rauhut,R., Lendeckel,W., and Tuschl,T. (2001). Identification of novel genes coding for small expressed RNAs. Science 294, 853-858.

Lallemand,F., Desire,N., Rozenbaum,W., Nicolas,J.C., and Marechal,V. (2000). Quantitative analysis of human herpesvirus 8 viral load using a real-time PCR assay. J. Clin. Microbiol. 38, 1404-1408.

Lan,K., Kuppers,D.A., and Robertson,E.S. (2005). Kaposi's sarcoma-associated herpesvirus reactivation is regulated by interaction of latency-associated nuclear antigen with recombination signal sequence-binding protein Jkappa, the major downstream effector of the Notch signaling pathway. J. Virol. 79, 3468-3478.

Lan,K., Kuppers,D.A., Verma,S.C., and Robertson,E.S. (2004). Kaposi's sarcoma-associated herpesvirus-encoded latency-associated nuclear antigen inhibits lytic replication by targeting Rta: a potential mechanism for virus-mediated control of latency. J. Virol. 78, 6585-6594.

Lau,N.C., Lim,L.P., Weinstein,E.G., and Bartel,D.P. (2001). An abundant class of tiny RNAs with probable regulatory roles in Caenorhabditis elegans. Science 294, 858-862.

Lau,N.C., Seto,A.G., Kim,J., Kuramochi-Miyagawa,S., Nakano,T., Bartel,D.P., and Kingston,R.E. (2006). Characterization of the piRNA complex from rat testes. Science 313, 363-367.

Leak,L.V. (1976). The structure of lymphatic capillaries in lymph formation. Fed. Proc. 35, 1863-1871.

Leavenworth,J.W., Ma,X., Mo,Y.Y., and Pauza,M.E. (2009). SUMO conjugation contributes to immune deviation in nonobese diabetic mice by suppressing c-Maf transactivation of IL-4. J. Immunol. 183, 1110-1119.

Lecoin,L., Sii-Felice,K., Pouponnot,C., Eychene,A., and Felder-Schmittbuhl,M.P. (2004). Comparison of maf gene expression patterns during chick embryo development. Gene Expr. Patterns. 4, 35-46.

Lee,R.C. and Ambros,V. (2001). An extensive class of small RNAs in Caenorhabditis elegans. Science 294, 862-864.

Lee,R.C., Feinbaum,R.L., and Ambros,V. (1993). The C. elegans heterochronic gene lin-4 encodes small RNAs with antisense complementarity to lin-14. Cell 75, 843-854.

Lee,S., Kang,J., Yoo,J., Ganesan,S.K., Cook,S.C., Aguilar,B., Ramu,S., Lee,J., and Hong,Y.K. (2009). Prox1 physically and functionally interacts with COUP-TFII to specify lymphatic endothelial cell fate. Blood 113, 1856-1859.

Lee,Y., Ahn,C., Han,J., Choi,H., Kim,J., Yim,J., Lee,J., Provost,P., Radmark,O., Kim,S., and Kim,V.N. (2003). The nuclear RNase III Drosha initiates microRNA processing. Nature 425, 415-419.

Lee,Y., Kim,M., Han,J., Yeom,K.H., Lee,S., Baek,S.H., and Kim,V.N. (2004). MicroRNA genes are transcribed by RNA polymerase II. EMBO J. 23, 4051-4060.

Lee,Y.S. and Dutta,A. (2007). The tumor suppressor microRNA let-7 represses the HMGA2 oncogene. Genes Dev. 21, 1025-1030.

Lei,X., Bai,Z., Ye,F., Xie,J., Kim,C.G., Huang,Y., and Gao,S.J. (2010). Regulation of NF-kappaB inhibitor IkappaBalpha and viral replication by a KSHV microRNA. Nat. Cell Biol. 12, 193-199.

Lewis,B.P., Burge,C.B., and Bartel,D.P. (2005). Conserved seed pairing, often flanked by adenosines, indicates that thousands of human genes are microRNA targets. Cell 120, 15-20.

Li,H., Komatsu,T., Dezube,B.J., and Kaye,K.M. (2002). The Kaposi's sarcoma-associated herpesvirus K12 transcript from a primary effusion lymphoma contains complex repeat elements, is spliced, and initiates from a novel promoter. J. Virol. 76, 11880-11888.

Li,M., Damania,B., Alvarez,X., Ogryzko,V., Ozato,K., and Jung,J.U. (2000). Inhibition of p300 histone acetyltransferase by viral interferon regulatory factor. Mol. Cell Biol. 20, 8254-8263.

Li,M., Lee,H., Guo,J., Neipel,F., Fleckenstein,B., Ozato,K., and Jung,J.U. (1998). Kaposi's sarcoma-associated herpesvirus viral interferon regulatory factor. J. Virol. 72, 5433-5440.

Li,M., Lee,H., Yoon,D.W., Albrecht,J.C., Fleckenstein,B., Neipel,F., and Jung,J.U. (1997). Kaposi's sarcoma-associated herpesvirus encodes a functional cyclin. J. Virol. 71, 1984-1991.

Liang,Y. and Ganem,D. (2003). Lytic but not latent infection by Kaposi's sarcoma-associated herpesvirus requires host CSL protein, the mediator of Notch signaling. Proc. Natl. Acad. Sci. U. S. A 100, 8490-8495.

Liang,Y., Chang,J., Lynch,S.J., Lukac,D.M., and Ganem,D. (2002). The lytic switch protein of KSHV activates gene expression via functional interaction with RBP-Jkappa (CSL), the target of the Notch signaling pathway. Genes Dev. 16, 1977-1989.

Lim,L.P., Lau,N.C., Garrett-Engele,P., Grimson,A., Schelter,J.M., Castle,J., Bartel,D.P., Linsley,P.S., and Johnson,J.M. (2005). Microarray analysis shows that some microRNAs downregulate large numbers of target mRNAs. Nature 433, 769-773.

Lin,C.W., Tu,P.F., Hsiao,N.W., Chang,C.Y., Wan,L., Lin,Y.T., and Chang,H.W. (2007). Identification of a novel septin 4 protein binding to human herpesvirus 8 kaposin A protein using a phage display cDNA library. J. Virol. Methods 143, 65-72.

Lin,R., Genin,P., Mamane,Y., Sgarbanti,M., Battistini,A., Harrington,W.J., Jr., Barber,G.N., and Hiscott,J. (2001). HHV-8 encoded vIRF-1 represses the interferon antiviral response by blocking IRF-3 recruitment of the CBP/p300 coactivators. Oncogene 20, 800-811.

Linsley,P.S., Schelter,J., Burchard,J., Kibukawa,M., Martin,M.M., Bartz,S.R., Johnson,J.M., Cummins,J.M., Raymond,C.K., Dai,H., Chau,N., Cleary,M., Jackson,A.L., Carleton,M., and Lim,L. (2007). Transcripts targeted by the microRNA-16 family cooperatively regulate cell cycle progression. Mol. Cell Biol. 27, 2240-2252.

Liu,L., Eby,M.T., Rathore,N., Sinha,S.K., Kumar,A., and Chaudhary,P.M. (2002). The human herpes virus 8-encoded viral FLICE inhibitory protein physically associates with and persistently activates the Ikappa B kinase complex. J. Biol. Chem. 277, 13745-13751.

Lo,A.K., To,K.F., Lo,K.W., Lung,R.W., Hui,J.W., Liao,G., and Hayward,S.D. (2007). Modulation of LMP1 protein expression by EBV-encoded microRNAs. Proc. Natl. Acad. Sci. U. S. A 104, 16164-16169.

Longnecker,R. and Neipel,F. (2007). Introduction to the Human gamma-herpesviruses. In Human Herpesviruses. Biology, Therapy, and Immunoprophylaxis, Cambridge University Press), pp. 341-359.

Lu,F., Stedman,W., Yousef,M., Renne,R., and Lieberman,P.M. (2010). Epigenetic regulation of Kaposi's sarcoma-associated herpesvirus latency by virus-encoded microRNAs that target Rta and the cellular Rbl2-DNMT pathway. J. Virol. 84, 2697-2706.

Lu,L.F., Thai,T.H., Calado,D.P., Chaudhry,A., Kubo,M., Tanaka,K., Loeb,G.B., Lee,H., Yoshimura,A., Rajewsky,K., and Rudensky,A.Y. (2009). Foxp3-dependent microRNA155 confers competitive fitness to regulatory T cells by targeting SOCS1 protein. Immunity. *30*, 80-91.

Lu,J., Getz,G., Miska,E.A., varez-Saavedra,E., Lamb,J., Peck,D., Sweet-Cordero,A., Ebert,B.L., Mak,R.H., Ferrando,A.A., Downing,J.R., Jacks,T., Horvitz,H.R., and Golub,T.R. (2005). MicroRNA expression profiles classify human cancers. Nature 435, 834-838.

Lukac,D.M., Renne,R., Kirshner,J.R., and Ganem,D. (1998). Reactivation of Kaposi's sarcoma-associated herpesvirus infection from latency by expression of the ORF 50 transactivator, a homolog of the EBV R protein. Virology *252*, 304-312.

Lukac,D.M., Kirshner,J.R., and Ganem,D. (1999). Transcriptional activation by the product of open reading frame 50 of Kaposi's sarcoma-associated herpesvirus is required for lytic viral reactivation in B cells. J. Virol. 73, 9348-9361.

Lund,E., Guttinger,S., Calado,A., Dahlberg,J.E., and Kutay,U. (2004). Nuclear export of microRNA precursors. Science 303, 95-98.

Lymboussaki,A., Olofsson,B., Eriksson,U., and Alitalo,K. (1999). Vascular endothelial growth factor (VEGF) and VEGF-C show overlapping binding sites in embryonic endothelia and distinct sites in differentiated adult endothelia. Circ. Res. 85, 992-999.

Lyon,M.F., Jamieson,R.V., Perveen,R., Glenister,P.H., Griffiths,R., Boyd,Y., Glimcher,L.H., Favor,J., Munier,F.L., and Black,G.C. (2003). A dominant mutation within the DNA-binding domain of the bZIP transcription factor Maf causes murine cataract and results in selective alteration in DNA binding. Hum. Mol. Genet. 12, 585-594.

Ma,L., Teruya-Feldstein,J., and Weinberg,R.A. (2007). Tumour invasion and metastasis initiated by microRNA-10b in breast cancer. Nature 449, 682-688.

Maby-El,H.H. and Petrova,T.V. (2008). Developmental and pathological lymphangiogenesis: from models to human disease. Histochem. Cell Biol. 130, 1063-1078.

MacLean,H.E., Kim,J.I., Glimcher,M.J., Wang,J., Kronenberg,H.M., and Glimcher,L.H. (2003). Absence of transcription factor c-maf causes abnormal terminal differentiation of hypertrophic chondrocytes during endochondral bone development. Dev. Biol. 262, 51-63.

Mahoney,K.M., Petrovic,N., Schacke,W., and Shapiro,L.H. (2007). CD13/APN transcription is regulated by the proto-oncogene c-Maf via an atypical response element. Gene 403, 178-187.

Maisonpierre,P.C., Suri,C., Jones,P.F., Bartunkova,S., Wiegand,S.J., Radziejewski,C., Compton,D., McClain,J., Aldrich,T.H., Papadopoulos,N., Daly,T.J., Davis,S., Sato,T.N., and Yancopoulos,G.D. (1997). Angiopoietin-2, a natural antagonist for Tie2 that disrupts in vivo angiogenesis. Science 277, 55-60.

Maki,Y., Bos,T.J., Davis,C., Starbuck,M., and Vogt,P.K. (1987). Avian sarcoma virus 17 carries the jun oncogene. Proc. Natl. Acad. Sci. U. S. A 84, 2848-2852.

Makinen,T., Adams,R.H., Bailey,J., Lu,Q., Ziemiecki,A., Alitalo,K., Klein,R., and Wilkinson,G.A. (2005). PDZ interaction site in ephrinB2 is required for the remodeling of lymphatic vasculature. Genes Dev. 19, 397-410.

Mann,D.J., Child,E.S., Swanton,C., Laman,H., and Jones,N. (1999). Modulation of p27(Kip1) levels by the cyclin encoded by Kaposi's sarcoma-associated herpesvirus. EMBO J. 18, 654-663.

Marchio,S., Primo,L., Pagano,M., Palestro,G., Albini,A., Veikkola,T., Cascone,I., Alitalo,K., and Bussolino,F. (1999). Vascular endothelial growth factor-C stimulates the migration and proliferation of Kaposi's sarcoma cells. J. Biol. Chem. 274, 27617-27622.

Maroney,P.A., Yu,Y., Fisher,J., and Nilsen,T.W. (2006). Evidence that microRNAs are associated with translating messenger RNAs in human cells. Nat. Struct. Mol. Biol. 13, 1102-1107.

Marshall,V., Parks,T., Bagni,R., Wang,C.D., Samols,M.A., Hu,J., Wyvil,K.M., Aleman,K., Little,R.F., Yarchoan,R., Renne,R., and Whitby,D. (2007). Conservation of virally encoded microRNAs in Kaposi sarcoma--associated herpesvirus in primary effusion lymphoma cell lines and in patients with Kaposi sarcoma or multicentric Castleman disease. J. Infect. Dis. 195, 645-659.

Martin,J. (2007). The epidemiology of KSHV and its association with malignant disease. In Human Herpesviruses. Biology, therapy and immunoprophylaxis, Cambridge University Press), pp. 960-985.

Martin,J.N., Ganem,D.E., Osmond,D.H., Page-Shafer,K.A., Macrae,D., and Kedes,D.H. (1998). Sexual transmission and the natural history of human herpesvirus 8 infection. N. Engl. J. Med. 338, 948-954.

Martinez,J., Patkaniowska,A., Urlaub,H., Luhrmann,R., and Tuschl,T. (2002). Single-stranded antisense siRNAs guide target RNA cleavage in RNAi. Cell 110, 563-574.

Matsumura,S., Fujita,Y., Gomez,E., Tanese,N., and Wilson,A.C. (2005). Activation of the Kaposi's sarcoma-associated herpesvirus major latency locus by the lytic switch protein RTA (ORF50). J. Virol. *79*, 8493-8505.

McCormick,C. and Ganem,D. (2005). The kaposin B protein of KSHV activates the p38/MK2 pathway and stabilizes cytokine mRNAs. Science 307, 739-741.

McGeoch,D.J., Dolan,A., and Ralph,A.C. (2000). Toward a comprehensive phylogeny for mammalian and avian herpesviruses. J. Virol. 74, 10401-10406.

Meister,G., Landthaler,M., Dorsett,Y., and Tuschl,T. (2004). Sequence-specific inhibition of microRNA- and siRNA-induced RNA silencing. RNA. 10, 544-550.

Mendell,J.T. (2008). miRiad roles for the miR-17-92 cluster in development and disease. Cell 133, 217-222.

Mercader,M., Taddeo,B., Panella,J.R., Chandran,B., Nickoloff,B.J., and Foreman,K.E. (2000). Induction of HHV-8 lytic cycle replication by inflammatory cytokines produced by HIV-1-infected T cells. Am. J. Pathol. 156, 1961-1971.

Metzler,M., Wilda,M., Busch,K., Viehmann,S., and Borkhardt,A. (2004). High expression of precursor microRNA-155/BIC RNA in children with Burkitt lymphoma. Genes Chromosomes. Cancer 39, 167-169.

Miles,S.A., Rezai,A.R., Salazar-Gonzalez,J.F., Vander,M.M., Stevens,R.H., Logan,D.M., Mitsuyasu,R.T., Taga,T., Hirano,T., Kishimoto,T., and . (1990). AIDS Kaposi sarcoma-derived cells produce and respond to interleukin 6. Proc. Natl. Acad. Sci. U. S. A 87, 4068-4072.

Mishima,K., Watabe,T., Saito,A., Yoshimatsu,Y., Imaizumi,N., Masui,S., Hirashima,M., Morisada,T., Oike,Y., Araie,M., Niwa,H., Kubo,H., Suda,T., and Miyazono,K. (2007). Prox1 induces lymphatic endothelial differentiation via integrin alpha9 and other signaling cascades. Mol. Biol. Cell 18, 1421-1429.

Moazed,D. (2009). Small RNAs in transcriptional gene silencing and genome defence. Nature 457, 413-420.

Molden,J., Chang,Y., You,Y., Moore,P.S., and Goldsmith,M.A. (1997). A Kaposi's sarcoma-associated herpesvirus-encoded cytokine homolog (vIL-6) activates signaling through the shared gp130 receptor subunit. J. Biol. Chem. 272, 19625-19631.

Montaner,S., Sodhi,A., Pece,S., Mesri,E.A., and Gutkind,J.S. (2001). The Kaposi's sarcoma-associated herpesvirus G protein-coupled receptor promotes endothelial cell survival through the activation of Akt/protein kinase B. Cancer Res. 61, 2641-2648.

Moore,P.S. and Chang,Y. (1998). Antiviral activity of tumor-suppressor pathways: clues from molecular piracy by KSHV. Trends Genet. 14, 144-150.

Moore,P.S. and Chang,Y. (2003). Kaposi's sarcoma-associated herpesvirus immunoevasion and tumorigenesis: two sides of the same coin? Annu. Rev. Microbiol. 57, 609-639.

Moore,P.S., Boshoff,C., Weiss,R.A., and Chang,Y. (1996). Molecular mimicry of human cytokine and cytokine response pathway genes by KSHV. Science 274, 1739-1744.

Mootha,V.K., Lindgren,C.M., Eriksson,K.F., Subramanian,A., Sihag,S., Lehar,J., Puigserver,P., Carlsson,E., Ridderstrale,M., Laurila,E., Houstis,N., Daly,M.J., Patterson,N., Mesirov,J.P., Golub,T.R., Tamayo,P., Spiegelman,B., Lander,E.S., Hirschhorn,J.N., Altshuler,D., and Groop,L.C. (2003). PGC-1alpha-responsive genes involved in oxidative phosphorylation are coordinately downregulated in human diabetes. Nat. Genet. 34, 267-273.

Mori,Y., Nishimoto,N., Ohno,M., Inagi,R., Dhepakson,P., Amou,K., Yoshizaki,K., and Yamanishi,K. (2000). Human herpesvirus 8-encoded interleukin-6 homologue (viral IL-6) induces endogenous human IL-6 secretion. J. Med. Virol. 61, 332-335.

Moriguchi,T., Hamada,M., Morito,N., Terunuma,T., Hasegawa,K., Zhang,C., Yokomizo,T., Esaki,R., Kuroda,E., Yoh,K., Kudo,T., Nagata,M., Greaves,D.R., Engel,J.D., Yamamoto,M., and Takahashi,S. (2006). MafB is essential for renal development and F4/80 expression in macrophages. Mol. Cell Biol. 26, 5715-5727.

Morito,N., Yoh,K., Fujioka,Y., Nakano,T., Shimohata,H., Hashimoto,Y., Yamada,A., Maeda,A., Matsuno,F., Hata,H., Suzuki,A., Imagawa,S., Mitsuya,H., Esumi,H., Koyama,A., Yamamoto,M., Mori,N., and Takahashi,S. (2006). Overexpression of c-Maf contributes to T-cell lymphoma in both mice and human. Cancer Res. 66, 812-819.

Moses,A.V., Fish,K.N., Ruhl,R., Smith,P.P., Strussenberg,J.G., Zhu,L., Chandran,B., and Nelson,J.A. (1999). Long-term infection and transformation of dermal microvascular endothelial cells by human herpesvirus 8. J. Virol. 73, 6892-6902.

Motohashi,H., O'Connor,T., Katsuoka,F., Engel,J.D., and Yamamoto,M. (2002). Integration and diversity of the regulatory network composed of Maf and CNC families of transcription factors. Gene 294, 1-12.

Murakami,Y.I., Yatabe,Y., Sakaguchi,T., Sasaki,E., Yamashita,Y., Morito,N., Yoh,K., Fujioka,Y., Matsuno,F., Hata,H., Mitsuya,H., Imagawa,S., Suzuki,A., Esumi,H., Sakai,M., Takahashi,S., and Mori,N. (2007). c-Maf expression in angioimmunoblastic T-cell lymphoma. Am. J. Surg. Pathol. 31, 1695-1702.

Muralidhar,S., Pumfery,A.M., Hassani,M., Sadaie,M.R., Kishishita,M., Brady,J.N., Doniger,J., Medveczky,P., and Rosenthal,L.J. (1998). Identification of kaposin (open reading frame K12) as a human herpesvirus 8 (Kaposi's sarcoma-associated herpesvirus) transforming gene. J. Virol. 72, 4980-4988.

Murphy,E., Vanicek,J., Robins,H., Shenk,T., and Levine,A.J. (2008). Suppression of immediate-early viral gene expression by herpesvirus-coded microRNAs: implications for latency. Proc. Natl. Acad. Sci. U. S. A 105, 5453-5458.

Naldini,L., Blomer,U., Gallay,P., Ory,D., Mulligan,R., Gage,F.H., Verma,I.M., and Trono,D. (1996). In vivo gene delivery and stable transduction of nondividing cells by a lentiviral vector. Science 272, 263-267.

Naranatt,P.P., Akula,S.M., and Chandran,B. (2002). Characterization of gamma2-human herpesvirus-8 glycoproteins gH and gL. Arch. Virol. 147, 1349-1370.

Naranatt,P.P., Krishnan,H.H., Smith,M.S., and Chandran,B. (2005). Kaposi's sarcoma-associated herpesvirus modulates microtubule dynamics via RhoA-GTP-diaphanous 2 signaling and utilizes the dynein motors to deliver its DNA to the nucleus. J. Virol. 79, 1191-1206.

Narizhneva,N.V., Razorenova,O.V., Podrez,E.A., Chen,J., Chandrasekharan,U.M., DiCorleto,P.E., Plow,E.F., Topol,E.J., and Byzova,T.V. (2005). Thrombospondin-1 up-regulates expression of cell adhesion molecules and promotes monocyte binding to endothelium. FASEB J. 19, 1158-1160.

Neipel,F., Albrecht,J.C., and Fleckenstein,B. (1997a). Cell-homologous genes in the Kaposi's sarcoma-associated rhadinovirus human herpesvirus 8: determinants of its pathogenicity? J. Virol. 71, 4187-4192.

Neipel,F., Albrecht,J.C., Ensser,A., Huang,Y.Q., Li,J.J., Friedman-Kien,A.E., and Fleckenstein,B. (1997b). Human herpesvirus 8 encodes a homolog of interleukin-6. J. Virol. 71, 839-842.

Newman,J.R. and Keating,A.E. (2003). Comprehensive identification of human bZIP interactions with coiled-coil arrays. Science 300, 2097-2101.

Nicholas,J. (2005). Human gammaherpesvirus cytokines and chemokine receptors. J. Interferon Cytokine Res. 25, 373-383.

Nicholas,J., Ruvolo,V.R., Burns,W.H., Sandford,G., Wan,X., Ciufo,D., Hendrickson,S.B., Guo,H.G., Hayward,G.S., and Reitz,M.S. (1997). Kaposi's sarcoma-associated human herpesvirus-8 encodes homologues of macrophage inflammatory protein-1 and interleukin-6. Nat. Med. 3, 287-292.

Niedt,G.W. and Prioleau,P.G. (1988). Kaposi's sarcoma occurring in a dermatome previously involved by herpes zoster. J. Am. Acad. Dermatol. 18, 448-451.

Nikitenko,L.L., Cross,T., Campo,L., Turley,H., Leek,R., Manek,S., Bicknell,R., and Rees,M.C. (2006). Expression of terminally glycosylated calcitonin receptor-like receptor in uterine leiomyoma: endothelial phenotype and association with microvascular density. Clin. Cancer Res. 12, 5648-5658.

Nilsen,T.W. (2007). Mechanisms of microRNA-mediated gene regulation in animal cells. Trends Genet. 23, 243-249.

Nishizawa,M., Kataoka,K., Goto,N., Fujiwara,K.T., and Kawai,S. (1989). v-maf, a viral oncogene that encodes a "leucine zipper" motif. Proc. Natl. Acad. Sci. U. S. A 86, 7711-7715.

Nottrott,S., Simard,M.J., and Richter,J.D. (2006). Human let-7a miRNA blocks protein production on actively translating polyribosomes. Nat. Struct. Mol. Biol. 13, 1108-1114.

Ny,A., Koch,M., Schneider,M., Neven,E., Tong,R.T., Maity,S., Fischer,C., Plaisance,S., Lambrechts,D., Heligon,C., Terclavers,S., Ciesiolka,M., Kalin,R., Man,W.Y., Senn,I., Wyns,S., Lupu,F., Brandli,A., Vleminckx,K., Collen,D., Dewerchin,M., Conway,E.M., Moons,L., Jain,R.K., and Carmeliet,P. (2005). A genetic Xenopus laevis tadpole model to study lymphangiogenesis. Nat. Med. 11, 998-1004.

Odaka,C., Morisada,T., Oike,Y., and Suda,T. (2006). Distribution of lymphatic vessels in mouse thymus: immunofluorescence analysis. Cell Tissue Res. 325, 13-22.

O'Donnell,K.A., Wentzel,E.A., Zeller,K.I., Dang,C.V., and Mendell,J.T. (2005). c-Myc-regulated microRNAs modulate E2F1 expression. Nature 435, 839-843.

OETTLE,A.G. (1962). Geographical and racial differences in the frequency of Kaposi's sarcoma as evidence of environmental or genetic causes. Acta Unio. Int. Contra. Cancrum. 18, 330-363.

Ogino,H. and Yasuda,K. (1998). Induction of lens differentiation by activation of a bZIP transcription factor, L-Maf. Science 280, 115-118.

Oh,S.J., Jeltsch,M.M., Birkenhager,R., McCarthy,J.E., Weich,H.A., Christ,B., Alitalo,K., and Wilting,J. (1997). VEGF and VEGF-C: specific induction of angiogenesis and lymphangiogenesis in the differentiated avian chorioallantoic membrane. Dev. Biol. 188, 96-109.

O'Hara,A.J., Chugh,P., Wang,L., Netto,E.M., Luz,E., Harrington,W.J., Dezube,B.J., Damania,B., and Dittmer,D.P. (2009). Pre-micro RNA signatures delineate stages of endothelial cell transformation in kaposi sarcoma. PLoS. Pathog. 5, e1000389.

Oliver,G. (2004). Lymphatic vasculature development. Nat. Rev. Immunol. 4, 35-45.

Oliver,G. and Alitalo,K. (2005). The lymphatic vasculature: recent progress and paradigms. Annu. Rev. Cell Dev. Biol. 21, 457-483.

Oliver,G. and Detmar,M. (2002). The rediscovery of the lymphatic system: old and new insights into the development and biological function of the lymphatic vasculature. Genes Dev. 16, 773-783.

Oliver,G. and Harvey,N. (2002). A stepwise model of the development of lymphatic vasculature. Ann. N. Y. Acad. Sci. 979, 159-165.

Olweny,C.L. (1984). Etiology of endemic Kaposi's sarcoma. IARC Sci. Publ. 543-548.

Park,J., Lee,M.S., Yoo,S.M., Jeong,K.W., Lee,D., Choe,J., and Seo,T. (2007). Identification of the DNA sequence interacting with Kaposi's sarcoma-associated herpesvirus viral interferon regulatory factor 1. J. Virol. 81, 12680-12684.

Parravicini,C., Chandran,B., Corbellino,M., Berti,E., Paulli,M., Moore,P.S., and Chang,Y. (2000). Differential viral protein expression in Kaposi's sarcoma-associated herpesvirus-infected diseases: Kaposi's sarcoma, primary effusion lymphoma, and multicentric Castleman's disease. Am. J. Pathol. *156*, 743-749.

Pasquinelli,A.E., Reinhart,B.J., Slack,F., Martindale,M.Q., Kuroda,M.I., Maller,B., Hayward,D.C., Ball,E.E., Degnan,B., Muller,P., Spring,J., Srinivasan,A., Fishman,M., Finnerty,J., Corbo,J., Levine,M., Leahy,P., Davidson,E., and Ruvkun,G. (2000). Conservation of the sequence and temporal expression of let-7 heterochronic regulatory RNA. Nature 408, 86-89.

Paun,A. and Pitha,P.M. (2007). The IRF family, revisited. Biochimie 89, 744-753.

Pearce,M., Matsumura,S., and Wilson,A.C. (2005). Transcripts encoding K12, v-FLIP, v-cyclin, and the microRNA cluster of Kaposi's sarcoma-associated herpesvirus originate from a common promoter. J. Virol. 79, 14457-14464.

Penn,I. (1997). Kaposi's sarcoma in transplant recipients. Transplantation 64, 669-673.
Petersen,C.P., Bordeleau,M.E., Pelletier,J., and Sharp,P.A. (2006). Short RNAs repress translation after initiation in mammalian cells. Mol. Cell 21, 533-542.

Petersen,M., Nielsen,C.B., Nielsen,K.E., Jensen,G.A., Bondensgaard,K., Singh,S.K., Rajwanshi,V.K., Koshkin,A.A., Dahl,B.M., Wengel,J., and Jacobsen,J.P. (2000). The conformations of locked nucleic acids (LNA). J. Mol. Recognit. 13, 44-53.

Petre,C.E., Sin,S.H., and Dittmer,D.P. (2007). Functional p53 signaling in Kaposi's sarcoma-associated herpesvirus lymphomas: implications for therapy. J. Virol. 81, 1912-1922.

Petrova,T.V., Karpanen,T., Norrmen,C., Mellor,R., Tamakoshi,T., Finegold,D., Ferrell,R., Kerjaschki,D., Mortimer,P., Yla-Herttuala,S., Miura,N., and Alitalo,K. (2004). Defective valves and abnormal mural cell recruitment underlie lymphatic vascular failure in lymphedema distichiasis. Nat. Med. 10, 974-981.

Petrova,T.V., Makinen,T., Makela,T.P., Saarela,J., Virtanen,I., Ferrell,R.E., Finegold,D.N., Kerjaschki,D., Yla-Herttuala,S., and Alitalo,K. (2002). Lymphatic endothelial reprogramming of vascular endothelial cells by the Prox-1 homeobox transcription factor. EMBO J. 21, 4593-4599.

Pfeffer,S., Sewer,A., Lagos-Quintana,M., Sheridan,R., Sander,C., Grasser,F.A., van Dyk,L.F., Ho,C.K., Shuman,S., Chien,M., Russo,J.J., Ju,J., Randall,G., Lindenbach,B.D., Rice,C.M., Simon,V., Ho,D.D., Zavolan,M., and Tuschl,T. (2005). Identification of microRNAs of the herpesvirus family. Nat. Methods 2, 269-276.

Pfeffer,S., Zavolan,M., Grasser,F.A., Chien,M., Russo,J.J., Ju,J., John,B., Enright,A.J., Marks,D., Sander,C., and Tuschl,T. (2004). Identification of virus-encoded microRNAs. Science 304, 734-736.

Pillai,R.S., Bhattacharyya,S.N., Artus,C.G., Zoller,T., Cougot,N., Basyuk,E., Bertrand,E., and Filipowicz,W. (2005). Inhibition of translational initiation by Let-7 MicroRNA in human cells. Science 309, 1573-1576.

Platt,G., Carbone,A., and Mittnacht,S. (2002). p16INK4a loss and sensitivity in KSHV associated primary effusion lymphoma. Oncogene *21*, 1823-1831.

Portsmouth,S., Stebbing,J., Gill,J., Mandalia,S., Bower,M., Nelson,M., Bower,M., and Gazzard,B. (2003). A comparison of regimens based on non-nucleoside reverse transcriptase inhibitors or protease inhibitors in preventing Kaposi's sarcoma. AIDS 17, F17-F22.

Pouponnot,C., Sii-Felice,K., Hmitou,I., Rocques,N., Lecoin,L., Druillennec,S., Felder-Schmittbuhl,M.P., and Eychene,A. (2006). Cell context reveals a dual role for Maf in oncogenesis. Oncogene 25, 1299-1310.

Pozharskaya,V.P., Weakland,L.L., Zimring,J.C., Krug,L.T., Unger,E.R., Neisch,A., Joshi,H., Inoue,N., and Offermann,M.K. (2004). Short duration of elevated vIRF-1 expression during lytic replication of human herpesvirus 8 limits its ability to block antiviral responses induced by alpha interferon in BCBL-1 cells. J. Virol. 78, 6621-6635.

Prevo,R., Banerji,S., Ferguson,D.J., Clasper,S., and Jackson,D.G. (2001). Mouse LYVE-1 is an endocytic receptor for hyaluronan in lymphatic endothelium. J. Biol. Chem. 276, 19420-19430.

Punj,V., Matta,H., Schamus,S., Yang,T., Chang,Y., and Chaudhary,P.M. (2009). Induction of CCL20 production by Kaposi sarcoma-associated herpesvirus: role of viral FLICE inhibitory protein K13-induced NF-kappaB activation. Blood 113, 5660-5668.

Qin,Z., Freitas,E., Sullivan,R., Mohan,S., Bacelieri,R., Branch,D., Romano,M., Kearney,P., Oates,J., Plaisance,K., Renne,R., Kaleeba,J., and Parsons,C. (2010). Upregulation of xCT by KSHV-Encoded microRNAs Facilitates KSHV Dissemination and Persistence in an Environment of Oxidative Stress. PLoS. Pathog. 6, e1000742.

Rabkin,C.S., Goedert,J.J., Biggar,R.J., Yellin,F., and Blattner,W.A. (1990). Kaposi's sarcoma in three HIV-1-infected cohorts. J. Acquir. Immune. Defic. Syndr. 3 Suppl 1, S38-S43.

Rabkin,C.S., Janz,S., Lash,A., Coleman,A.E., Musaba,E., Liotta,L., Biggar,R.J., and Zhuang,Z. (1997). Monoclonal origin of multicentric Kaposi's sarcoma lesions. N. Engl. J. Med. 336, 988-993.

Radkov,S.A., Kellam,P., and Boshoff,C. (2000). The latent nuclear antigen of Kaposi sarcoma-associated herpesvirus targets the retinoblastoma-E2F pathway and with the oncogene Hras transforms primary rat cells. Nat. Med. 6, 1121-1127.

Rajaram,N. and Kerppola,T.K. (2004). Synergistic transcription activation by Maf and Sox and their subnuclear localization are disrupted by a mutation in Maf that causes cataract. Mol. Cell Biol. 24, 5694-5709.

Raver-Shapira,N., Marciano,E., Meiri,E., Spector,Y., Rosenfeld,N., Moskovits,N., Bentwich,Z., and Oren,M. (2007). Transcriptional activation of miR-34a contributes to p53-mediated apoptosis. Mol. Cell 26, 731-743.

Regezi,J.A., MacPhail,L.A., Daniels,T.E., DeSouza,Y.G., Greenspan,J.S., and Greenspan,D. (1993). Human immunodeficiency virus-associated oral Kaposi's sarcoma. A heterogeneous cell population dominated by spindle-shaped endothelial cells. Am. J. Pathol. 143, 240-249.

Reinhart,B.J., Slack,F.J., Basson,M., Pasquinelli,A.E., Bettinger,J.C., Rougvie,A.E., Horvitz,H.R., and Ruvkun,G. (2000). The 21-nucleotide let-7 RNA regulates developmental timing in Caenorhabditis elegans. Nature 403, 901-906.

Renne,R., Blackbourn,D., Whitby,D., Levy,J., and Ganem,D. (1998). Limited transmission of Kaposi's sarcoma-associated herpesvirus in cultured cells. J. Virol. 72, 5182-5188.

Renne,R., Lagunoff,M., Zhong,W., and Ganem,D. (1996a). The size and conformation of Kaposi's sarcoma-associated herpesvirus (human herpesvirus 8) DNA in infected cells and virions. J. Virol. 70, 8151-8154.

Renne,R., Zhong,W., Herndier,B., McGrath,M., Abbey,N., Kedes,D., and Ganem,D. (1996b). Lytic growth of Kaposi's sarcoma-associated herpesvirus (human herpesvirus 8) in culture. Nat. Med. 2, 342-346.

Reza,H.M. and Yasuda,K. (2004). Roles of Maf family proteins in lens development. Dev. Dyn. 229, 440-448.

Ring,B.Z., Cordes,S.P., Overbeek,P.A., and Barsh,G.S. (2000). Regulation of mouse lens fiber cell development and differentiation by the Maf gene. Development 127, 307-317.

Rissanen,T.T., Markkanen,J.E., Gruchala,M., Heikura,T., Puranen,A., Kettunen,M.I., Kholova,I., Kauppinen,R.A., Achen,M.G., Stacker,S.A., Alitalo,K., and Yla-Herttuala,S. (2003). VEGF-D is the strongest angiogenic and lymphangiogenic effector among VEGFs delivered into skeletal muscle via adenoviruses. Circ. Res. 92, 1098-1106.

Rivas,C., Thlick,A.E., Parravicini,C., Moore,P.S., and Chang,Y. (2001). Kaposi's sarcoma-associated herpesvirus LANA2 is a B-cell-specific latent viral protein that inhibits p53. J. Virol. 75, 429-438.

Roca,C. and Adams,R.H. (2007). Regulation of vascular morphogenesis by Notch signaling. Genes Dev. 21, 2511-2524.

Rocques,N., Abou,Z.N., Sii-Felice,K., Lecoin,L., Felder-Schmittbuhl,M.P., Eychene,A., and Pouponnot,C. (2007). GSK-3-mediated phosphorylation enhances Maf-transforming activity. Mol. Cell 28, 584-597.

Rodriguez,A., Vigorito,E., Clare,S., Warren,M.V., Couttet,P., Soond,D.R., van,D.S., Grocock,R.J., Das,P.P., Miska,E.A., Vetrie,D., Okkenhaug,K., Enright,A.J., Dougan,G., Turner,M., and Bradley,A. (2007). Requirement of bic/microRNA-155 for normal immune function. Science 316, 608-611.

ROUS,P. (1910). A TRANSMISSIBLE AVIAN NEOPLASM. (SARCOMA OF THE COMMON FOWL.). JEM 12, 696.

Russo,J.J., Bohenzky,R.A., Chien,M.C., Chen,J., Yan,M., Maddalena,D., Parry,J.P., Peruzzi,D., Edelman,I.S., Chang,Y., and Moore,P.S. (1996). Nucleotide sequence of the Kaposi sarcoma-associated herpesvirus (HHV8). Proc. Natl. Acad. Sci. U. S. A 93, 14862-14867.

Saaristo,A., Veikkola,T., Enholm,B., Hytonen,M., Arola,J., Pajusola,K., Turunen,P., Jeltsch,M., Karkkainen,M.J., Kerjaschki,D., Bueler,H., Yla-Herttuala,S., and Alitalo,K. (2002). Adenoviral VEGF-C overexpression induces blood vessel enlargement, tortuosity, and leakiness but no sprouting angiogenesis in the skin or mucous membranes. FASEB J. 16, 1041-1049.

Sabin,F.R. (1902). On the origin of the lymphatic system from the veins and the development of the lymph hearts and thoracic duct in the pig. Am. J. Anat. 1.

Sadagopan,S., Sharma-Walia,N., Veettil,M.V., Bottero,V., Levine,R., Vart,R.J., and Chandran,B. (2009). Kaposi's sarcoma-associated herpesvirus upregulates angiogenin during infection of human dermal microvascular endothelial cells, which induces 45S rRNA synthesis, antiapoptosis, cell proliferation, migration, and angiogenesis. J. Virol. 83, 3342-3364.

Sadler,R., Wu,L., Forghani,B., Renne,R., Zhong,W., Herndier,B., and Ganem,D. (1999). A complex translational program generates multiple novel proteins from the latently expressed kaposin (K12) locus of Kaposi's sarcoma-associated herpesvirus. J. Virol. 73, 5722-5730.

Saharinen,P. and Petrova,T.V. (2004). Molecular regulation of lymphangiogenesis. Ann. N. Y. Acad. Sci. 1014, 76-87.

Sakai,M., Imaki,J., Yoshida,K., Ogata,A., Matsushima-Hibaya,Y., Kuboki,Y., Nishizawa,M., and Nishi,S. (1997). Rat maf related genes: specific expression in chondrocytes, lens and spinal cord. Oncogene 14, 745-750.

Sakai,M., Serria,M.S., Ikeda,H., Yoshida,K., Imaki,J., and Nishi,S. (2001). Regulation of c-maf gene expression by Pax6 in cultured cells. Nucleic Acids Res. 29, 1228-1237.

Sakakibara,S., Pise-Masison,C.A., Brady,J.N., and Tosato,G. (2009). Gene regulation and functional alterations induced by Kaposi's sarcoma-associated herpesvirus-encoded ORFK13/vFLIP in endothelial cells. J. Virol. 83, 2140-2153.

Samols,M.A., Hu,J., Skalsky,R.L., and Renne,R. (2005). Cloning and identification of a microRNA cluster within the latency-associated region of Kaposi's sarcoma-associated herpesvirus. J. Virol. 79, 9301-9305.

Samols,M.A., Skalsky,R.L., Maldonado,A.M., Riva,A., Lopez,M.C., Baker,H.V., and Renne,R. (2007). Identification of cellular genes targeted by KSHV-encoded microRNAs. PLoS. Pathog. 3, e65.

Sampson,V.B., Rong,N.H., Han,J., Yang,Q., Aris,V., Soteropoulos,P., Petrelli,N.J., Dunn,S.P., and Krueger,L.J. (2007). MicroRNA let-7a down-regulates MYC and reverts MYC-induced growth in Burkitt lymphoma cells. Cancer Res. 67, 9762-9770.

Sandler,H. and Stoecklin,G. (2008). Control of mRNA decay by phosphorylation of tristetraprolin. Biochem. Soc. Trans. 36, 491-496.

Sarid,R., Wiezorek,J.S., Moore,P.S., and Chang,Y. (1999). Characterization and cell cycle regulation of the major Kaposi's sarcoma-associated herpesvirus (human herpesvirus 8) latent genes and their promoter. J. Virol. 73, 1438-1446.

Schafer,A., Cai,X., Bilello,J.P., Desrosiers,R.C., and Cullen,B.R. (2007). Cloning and analysis of microRNAs encoded by the primate gamma-herpesvirus rhesus monkey rhadinovirus. Virology 364, 21-27.

Schetter,A.J., Leung,S.Y., Sohn,J.J., Zanetti,K.A., Bowman,E.D., Yanaihara,N., Yuen,S.T., Chan,T.L., Kwong,D.L., Au,G.K., Liu,C.G., Calin,G.A., Croce,C.M., and Harris,C.C. (2008). MicroRNA expression profiles associated with prognosis and therapeutic outcome in colon adenocarcinoma. JAMA 299, 425-436.

Schwarz,D.S., Hutvagner,G., Du,T., Xu,Z., Aronin,N., and Zamore,P.D. (2003). Asymmetry in the assembly of the RNAi enzyme complex. Cell 115, 199-208.

Searles,R.P., Bergquam,E.P., Axthelm,M.K., and Wong,S.W. (1999). Sequence and genomic analysis of a Rhesus macaque rhadinovirus with similarity to Kaposi's sarcoma-associated herpesvirus/human herpesvirus 8. J. Virol. 73, 3040-3053.

Selbach,M., Schwanhausser,B., Thierfelder,N., Fang,Z., Khanin,R., and Rajewsky,N. (2008). Widespread changes in protein synthesis induced by microRNAs. Nature 455, 58-63.

Seo,S., Fujita,H., Nakano,A., Kang,M., Duarte,A., and Kume,T. (2006). The forkhead transcription factors, Foxc1 and Foxc2, are required for arterial specification and lymphatic sprouting during vascular development. Dev. Biol. 294, 458-470.

Seo,T., Lee,D., Lee,B., Chung,J.H., and Choe,J. (2000). Viral interferon regulatory factor 1 of Kaposi's sarcoma-associated herpesvirus (human herpesvirus 8) binds to, and inhibits transactivation of, CREB-binding protein. Biochem. Biophys. Res. Commun. 270, 23-27.

Shaulian,E. and Karin,M. (2002). AP-1 as a regulator of cell life and death. Nat. Cell Biol. 4, E131-E136.

Shepard,L.W., Yang,M., Xie,P., Browning,D.D., Voyno-Yasenetskaya,T., Kozasa,T., and Ye,R.D. (2001). Constitutive activation of NF-kappa B and secretion of interleukin-8 induced by the G protein-coupled receptor of Kaposi's sarcoma-associated herpesvirus involve G alpha(13) and RhoA. J. Biol. Chem. 276, 45979-45987.

Skalsky,R.L., Samols,M.A., Plaisance,K.B., Boss,I.W., Riva,A., Lopez,M.C., Baker,H.V., and Renne,R. (2007). Kaposi's Sarcoma-associated Herpesvirus Encodes an Ortholog of miR-155. J. Virol.

Skobe,M., Brown,L.F., Tognazzi,K., Ganju,R.K., Dezube,B.J., Alitalo,K., and Detmar,M. (1999). Vascular endothelial growth factor-C (VEGF-C) and its receptors KDR and flt-4 are expressed in AIDS-associated Kaposi's sarcoma. J. Invest Dermatol. 113, 1047-1053.

Skobe,M., Hawighorst,T., Jackson,D.G., Prevo,R., Janes,L., Velasco,P., Riccardi,L., Alitalo,K., Claffey,K., and Detmar,M. (2001). Induction of tumor lymphangiogenesis by VEGF-C promotes breast cancer metastasis. Nat. Med. 7, 192-198.

Slack,F.J., Basson,M., Liu,Z., Ambros,V., Horvitz,H.R., and Ruvkun,G. (2000). The lin-41 RBCC gene acts in the C. elegans heterochronic pathway between the let-7 regulatory RNA and the LIN-29 transcription factor. Mol. Cell 5, 659-669.

Smit,M.J., Verzijl,D., Casarosa,P., Navis,M., Timmerman,H., and Leurs,R. (2002). Kaposi's sarcoma-associated herpesvirus-encoded G protein-coupled receptor ORF74 constitutively activates p44/p42 MAPK and Akt via G(i) and phospholipase C-dependent signaling pathways. J. Virol. 76, 1744-1752.

Smyth,G.K. (2004). Linear models and empirical bayes methods for assessing differential expression in microarray experiments. Stat. Appl. Genet. Mol. Biol. 3, Article3.

Song,M.J., Deng,H., and Sun,R. (2003). Comparative study of regulation of RTA-responsive genes in Kaposi's sarcoma-associated herpesvirus/human herpesvirus 8. J. Virol. 77, 9451-9462.

Soulier,J., Grollet,L., Oksenhendler,E., Cacoub,P., Cazals-Hatem,D., Babinet,P., d'Agay,M.F., Clauvel,J.P., Raphael,M., Degos,L., and . (1995). Kaposi's sarcoma-associated herpesvirus-like DNA sequences in multicentric Castleman's disease. Blood 86, 1276-1280.

Sozzani,S., Luini,W., Bianchi,G., Allavena,P., Wells,T.N., Napolitano,M., Bernardini,G., Vecchi,A., D'Ambrosio,D., Mazzeo,D., Sinigaglia,F., Santoni,A., Maggi,E., Romagnani,S., and Mantovani,A. (1998). The viral chemokine macrophage inflammatory protein-II is a selective Th2 chemoattractant. Blood 92, 4036-4039.

Spear,P.G. and Longnecker,R. (2003). Herpesvirus entry: an update. J. Virol. 77, 10179-10185.

Srinivasan,R.S., Dillard,M.E., Lagutin,O.V., Lin,F.J., Tsai,S., Tsai,M.J., Samokhvalov,I.M., and Oliver,G. (2007). Lineage tracing demonstrates the venous origin of the mammalian lymphatic vasculature. Genes Dev. 21, 2422-2432.

Stark,A., Brennecke,J., Bushati,N., Russell,R.B., and Cohen,S.M. (2005). Animal MicroRNAs confer robustness to gene expression and have a significant impact on 3'UTR evolution. Cell 123, 1133-1146.

Staskus,K.A., Zhong,W., Gebhard,K., Herndier,B., Wang,H., Renne,R., Beneke,J., Pudney,J., Anderson,D.J., Ganem,D., and Haase,A.T. (1997). Kaposi's sarcoma-associated herpesvirus gene expression in endothelial (spindle) tumor cells. J. Virol. 71, 715-719.

Stern-Ginossar,N., Elefant,N., Zimmermann,A., Wolf,D.G., Saleh,N., Biton,M., Horwitz,E., Prokocimer,Z., Prichard,M., Hahn,G., Goldman-Wohl,D., Greenfield,C., Yagel,S., Hengel,H., Altuvia,Y., Margalit,H., and Mandelboim,O. (2007). Host immune system gene targeting by a viral miRNA. Science 317, 376-381.

Stine,J.T., Wood,C., Hill,M., Epp,A., Raport,C.J., Schweickart,V.L., Endo,Y., Sasaki,T., Simmons,G., Boshoff,C., Clapham,P., Chang,Y., Moore,P., Gray,P.W., and Chantry,D. (2000). KSHV-encoded CC chemokine vMIP-III is a CCR4 agonist, stimulates angiogenesis, and selectively chemoattracts TH2 cells. Blood 95, 1151-1157.

Storey,J.D. and Tibshirani,R. (2003). Statistical significance for genomewide studies. Proc. Natl. Acad. Sci. U. S. A 100, 9440-9445.

Sturzl,M., Blasig,C., Schreier,A., Neipel,F., Hohenadl,C., Cornali,E., Ascherl,G., Esser,S., Brockmeyer,N.H., Ekman,M., Kaaya,E.E., Tschachler,E., and Biberfeld,P. (1997). Expression of HHV-8 latency-associated T0.7 RNA in spindle cells and endothelial cells of AIDS-associated, classical and African Kaposi's sarcoma. Int. J. Cancer 72, 68-71.

Subramanian,A., Tamayo,P., Mootha,V.K., Mukherjee,S., Ebert,B.L., Gillette,M.A., Paulovich,A., Pomeroy,S.L., Golub,T.R., Lander,E.S., and Mesirov,J.P. (2005). Gene set enrichment analysis: a knowledge-based approach for interpreting genome-wide expression profiles. Proc. Natl. Acad. Sci. U. S. A 102, 15545-15550.

Sullivan,C.S., Grundhoff,A.T., Tevethia,S., Pipas,J.M., and Ganem,D. (2005). SV40-encoded microRNAs regulate viral gene expression and reduce susceptibility to cytotoxic T cells. Nature 435, 682-686.

Sunil-Chandra,N.P., Arno,J., Fazakerley,J., and Nash,A.A. (1994). Lymphoproliferative disease in mice infected with murine gammaherpesvirus 68. Am. J. Pathol. 145, 818-826.

Suzuki,A., Iida,S., Kato-Uranishi,M., Tajima,E., Zhan,F., Hanamura,I., Huang,Y., Ogura,T., Takahashi,S., Ueda,R., Barlogie,B., Shaughnessy,J., Jr., and Esumi,H. (2005). ARK5 is transcriptionally regulated by the Large-MAF family and mediates IGF-1-induced cell invasion in multiple myeloma: ARK5 as a new molecular determinant of malignant multiple myeloma. Oncogene 24, 6936-6944.

Takahashi,K. and Yamanaka,S. (2006). Induction of pluripotent stem cells from mouse embryonic and adult fibroblast cultures by defined factors. Cell 126, 663-676.

Tammela,T. and Alitalo,K. (2010). Lymphangiogenesis: Molecular mechanisms and future promise. Cell 140, 460-476.

Tammela,T., Petrova,T.V., and Alitalo,K. (2005). Molecular lymphangiogenesis: new players. Trends Cell Biol. 15, 434-441.

Tang,S., Bertke,A.S., Patel,A., Wang,K., Cohen,J.I., and Krause,P.R. (2008). An acutely and latently expressed herpes simplex virus 2 viral microRNA inhibits expression of ICP34.5, a viral neurovirulence factor. Proc. Natl. Acad. Sci. U. S. A 105, 10931-10936.

Tang,S., Patel,A., and Krause,P.R. (2009). Novel less-abundant viral microRNAs encoded by herpes simplex virus 2 latency-associated transcript and their roles in regulating ICP34.5 and ICP0 mRNAs. J. Virol. 83, 1433-1442.

Thai,T.H., Calado,D.P., Casola,S., Ansel,K.M., Xiao,C., Xue,Y., Murphy,A., Frendewey,D., Valenzuela,D., Kutok,J.L., Schmidt-Supprian,M., Rajewsky,N., Yancopoulos,G., Rao,A., and Rajewsky,K. (2007). Regulation of the germinal center response by microRNA-155. Science 316, 604-608.

Thome,M., Schneider,P., Hofmann,K., Fickenscher,H., Meinl,E., Neipel,F., Mattmann,C., Burns,K., Bodmer,J.L., Schroter,M., Scaffidi,C., Krammer,P.H., Peter,M.E., and Tschopp,J. (1997). Viral FLICE-inhibitory proteins (FLIPs) prevent apoptosis induced by death receptors. Nature 386, 517-521.

Thomson,T. and Lin,H. (2009). The biogenesis and function of PIWI proteins and piRNAs: progress and prospect. Annu. Rev. Cell Dev. Biol. 25, 355-376.

Thum,T., Galuppo,P., Wolf,C., Fiedler,J., Kneitz,S., van Laake,L.W., Doevendans,P.A., Mummery,C.L., Borlak,J., Haverich,A., Gross,C., Engelhardt,S., Ertl,G., and Bauersachs,J. (2007). MicroRNAs in the human heart: a clue to fetal gene reprogramming in heart failure. Circulation 116, 258-267.

Toki,T., Itoh,J., Kitazawa,J., Arai,K., Hatakeyama,K., Akasaka,J., Igarashi,K., Nomura,N., Yokoyama,M., Yamamoto,M., and Ito,E. (1997). Human small Maf proteins form heterodimers with CNC family transcription factors and recognize the NF-E2 motif. Oncogene 14, 1901-1910.

Turner,M. and Vigorito,E. (2008). Regulation of B- and T-cell differentiation by a single microRNA. Biochem. Soc. Trans. 36, 531-533.

Tykocinski,L.O., Hajkova,P., Chang,H.D., Stamm,T., Sozeri,O., Lohning,M., Hu-Li,J., Niesner,U., Kreher,S., Friedrich,B., Pannetier,C., Grutz,G., Walter,J., Paul,W.E., and Radbruch,A. (2005). A critical control element for interleukin-4 memory expression in T helper lymphocytes. J. Biol. Chem. 280, 28177-28185.

Umbach,J.L. and Cullen,B.R. (2009). The role of RNAi and microRNAs in animal virus replication and antiviral immunity. Genes Dev. 23, 1151-1164.

Umbach,J.L. and Cullen,B.R. (2010). In-depth analysis of Kaposi's sarcoma-associated herpesvirus microRNA expression provides insights into the mammalian microRNA-processing machinery. J. Virol. 84, 695-703.

Umbach,J.L., Kramer,M.F., Jurak,I., Karnowski,H.W., Coen,D.M., and Cullen,B.R. (2008). MicroRNAs expressed by herpes simplex virus 1 during latent infection regulate viral mRNAs. Nature 454, 780-783.

Valanciute,A., le,G.S., Solhonne,B., Pawlak,A., Grimbert,P., Lyonnet,L., Hue,S., Lang,P., Remy,P., Salomon,R., Bensman,A., Guellaen,G., and Sahali,D. (2004). NF-kappa B p65 antagonizes IL-4 induction by c-maf in minimal change nephrotic syndrome. J. Immunol. 172, 688-698.

van der Putte,S.C. (1975). The early development of the lymphatic system in mouse embryos. Acta Morphol. Neerl. Scand. 13, 245-286.

Vart,R.J., Nikitenko,L.L., Lagos,D., Trotter,M.W., Cannon,M., Bourboulia,D., Gratrix,F., Takeuchi,Y., and Boshoff,C. (2007). Kaposi's sarcoma-associated herpesvirus-encoded interleukin-6 and G-protein-coupled receptor regulate angiopoietin-2 expression in lymphatic endothelial cells. Cancer Res. 67, 4042-4051.

Veikkola,T. and Alitalo,K. (2002). Dual role of Ang2 in postnatal angiogenesis and lymphangiogenesis. Dev. Cell 3, 302-304.

Ventura,A., Young,A.G., Winslow,M.M., Lintault,L., Meissner,A., Erkeland,S.J., Newman,J., Bronson,R.T., Crowley,D., Stone,J.R., Jaenisch,R., Sharp,P.A., and Jacks,T. (2008). Targeted deletion reveals essential and overlapping functions of the miR-17 through 92 family of miRNA clusters. Cell 132, 875-886.

Vermeulen,A., Robertson,B., Dalby,A.B., Marshall,W.S., Karpilow,J., Leake,D., Khvorova,A., and Baskerville,S. (2007). Double-stranded regions are essential design components of potent inhibitors of RISC function. RNA. 13, 723-730.

Verschuren,E.W., Klefstrom,J., Evan,G.I., and Jones,N. (2002). The oncogenic potential of Kaposi's sarcoma-associated herpesvirus cyclin is exposed by p53 loss in vitro and in vivo. Cancer Cell 2, 229-241.

Vester,B. and Wengel,J. (2004). LNA (locked nucleic acid): high-affinity targeting of complementary RNA and DNA. Biochemistry 43, 13233-13241.

Vieira,J., O'Hearn,P., Kimball,L., Chandran,B., and Corey,L. (2001). Activation of Kaposi's sarcoma-associated herpesvirus (human herpesvirus 8) lytic replication by human cytomegalovirus. J. Virol. 75, 1378-1386.

Vigorito,E., Perks,K.L., Abreu-Goodger,C., Bunting,S., Xiang,Z., Kohlhaas,S., Das,P.P., Miska,E.A., Rodriguez,A., Bradley,A., Smith,K.G., Rada,C., Enright,A.J., Toellner,K.M., Maclennan,I.C., and Turner,M. (2007). microRNA-155 regulates the generation of immunoglobulin class-switched plasma cells. Immunity. 27, 847-859.

Vinson,C., Acharya,A., and Taparowsky,E.J. (2006). Deciphering B-ZIP transcription factor interactions in vitro and in vivo. Biochim. Biophys. Acta 1759, 4-12.

Vinson,C., Myakishev,M., Acharya,A., Mir,A.A., Moll,J.R., and Bonovich,M. (2002). Classification of human B-ZIP proteins based on dimerization properties. Mol. Cell Biol. 22, 6321-6335.

Vinther,J., Hedegaard,M.M., Gardner,P.P., Andersen,J.S., and Arctander,P. (2006). Identification of miRNA targets with stable isotope labeling by amino acids in cell culture. Nucleic Acids Res. 34, e107.

Voorhoeve,P.M., le,S.C., Schrier,M., Gillis,A.J., Stoop,H., Nagel,R., Liu,Y.P., van,D.J., Drost,J., Griekspoor,A., Zlotorynski,E., Yabuta,N., De,V.G., Nojima,H., Looijenga,L.H., and Agami,R. (2006). A genetic screen implicates miRNA-372 and miRNA-373 as oncogenes in testicular germ cell tumors. Cell 124, 1169-1181.

Wang,H.W., Trotter,M.W., Lagos,D., Bourboulia,D., Henderson,S., Makinen,T., Elliman,S., Flanagan,A.M., Alitalo,K., and Boshoff,C. (2004). Kaposi sarcoma herpesvirus-induced cellular reprogramming contributes to the lymphatic endothelial gene expression in Kaposi sarcoma. Nat. Genet. 36, 687-693.

Watanabe,T., Sugaya,M., Atkins,A.M., Aquilino,E.A., Yang,A., Borris,D.L., Brady,J., and Blauvelt,A. (2003). Kaposi's sarcoma-associated herpesvirus latency-associated nuclear antigen prolongs the life span of primary human umbilical vein endothelial cells. J. Virol. 77, 6188-6196.

Weissman,I.L. (2000). Stem cells: units of development, units of regeneration, and units in evolution. Cell 100, 157-168.

Whitby,D., Luppi,M., Sabin,C., Barozzi,P., Di Biase,A.R., Balli,F., Cucci,F., Weiss,R.A., Boshoff,C., and Torelli,G. (2000). Detection of antibodies to human herpesvirus 8 in Italian children: evidence for horizontal transmission. Br. J. Cancer 82, 702-704.

Wightman,B., Ha,I., and Ruvkun,G. (1993). Posttranscriptional regulation of the heterochronic gene lin-14 by lin-4 mediates temporal pattern formation in C. elegans. Cell 75, 855-862.

Wigle,J.T. and Oliver,G. (1999). Prox1 function is required for the development of the murine lymphatic system. Cell *98*, 769-778.

Wigle,J.T., Harvey,N., Detmar,M., Lagutina,I., Grosveld,G., Gunn,M.D., Jackson,D.G., and Oliver,G. (2002). An essential role for Prox1 in the induction of the lymphatic endothelial cell phenotype. EMBO J. 21, 1505-1513.

Wilson,S.J., Tsao,E.H., Webb,B.L., Ye,H., ton-Griffin,L., Tsantoulas,C., Gale,C.V., Du,M.Q., Whitehouse,A., and Kellam,P. (2007). X box binding protein XBP-1s transactivates the Kaposi's sarcoma-associated herpesvirus (KSHV) ORF50 promoter, linking plasma cell differentiation to KSHV reactivation from latency. J. Virol. 81, 13578-13586.

Wilting,J., Aref,Y., Huang,R., Tomarev,S.I., Schweigerer,L., Christ,B., Valasek,P., and Papoutsi,M. (2006). Dual origin of avian lymphatics. Dev. Biol. 292, 165-173.

Wilting,J., Papoutsi,M., Christ,B., Nicolaides,K.H., von Kaisenberg,C.S., Borges,J., Stark,G.B., Alitalo,K., Tomarev,S.I., Niemeyer,C., and Rossler,J. (2002). The transcription factor Prox1 is a marker for lymphatic endothelial cells in normal and diseased human tissues. FASEB J. 16, 1271-1273.

Winter,J., Jung,S., Keller,S., Gregory,R.I., and Diederichs,S. (2009). Many roads to maturity: microRNA biogenesis pathways and their regulation. Nat. Cell Biol. 11, 228-234.

Witte,M.H., Bernas,M.J., Martin,C.P., and Witte,C.L. (2001). Lymphangiogenesis and lymphangiodysplasia: from molecular to clinical lymphology. Microsc. Res. Tech. 55, 122-145.

Wu,L. and Belasco,J.G. (2008). Chapter 18. Examining the influence of microRNAs on translation efficiency and on mRNA deadenylation and decay. Methods Enzymol. 449, 373-393.

Wu,L., Fan,J., and Belasco,J.G. (2006). MicroRNAs direct rapid deadenylation of mRNA. Proc. Natl. Acad. Sci. U. S. A 103, 4034-4039.

Xia,T., O'Hara,A., Araujo,I., Barreto,J., Carvalho,E., Sapucaia,J.B., Ramos,J.C., Luz,E., Pedroso,C., Manrique,M., Toomey,N.L., Brites,C., Dittmer,D.P., and Harrington,W.J., Jr. (2008). EBV microRNAs in primary lymphomas and targeting of CXCL-11 by ebv-mir-BHRF1-3. Cancer Res. 68, 1436-1442.

Xiao,C., Calado,D.P., Galler,G., Thai,T.H., Patterson,H.C., Wang,J., Rajewsky,N., Bender,T.P., and Rajewsky,K. (2007). MiR-150 controls B cell differentiation by targeting the transcription factor c-Myb. Cell 131, 146-159.

Xiao,C., Srinivasan,L., Calado,D.P., Patterson,H.C., Zhang,B., Wang,J., Henderson,J.M., Kutok,J.L., and Rajewsky,K. (2008). Lymphoproliferative disease and autoimmunity in mice with increased miR-17-92 expression in lymphocytes. Nat. Immunol. 9, 405-414.

Xu,N., Segerman,B., Zhou,X., and Akusjarvi,G. (2007). Adenovirus virus-associated RNAII-derived small RNAs are efficiently incorporated into the rna-induced silencing complex and associate with polyribosomes. J. Virol. 81, 10540-10549.

Xu,Y. and Ganem,D. (2007). Induction of chemokine production by latent Kaposi's sarcoma-associated herpesvirus infection of endothelial cells. J. Gen. Virol. 88, 46-50.
Yamazaki,T., Yoshimatsu,Y., Morishita,Y., Miyazono,K., and Watabe,T. (2009). COUP-TFII regulates the functions of Prox1 in lymphatic endothelial cells through direct interaction. Genes Cells 14, 425-434.

Yanaihara,N., Caplen,N., Bowman,E., Seike,M., Kumamoto,K., Yi,M., Stephens,R.M., Okamoto,A., Yokota,J., Tanaka,T., Calin,G.A., Liu,C.G., Croce,C.M., and Harris,C.C. (2006). Unique microRNA molecular profiles in lung cancer diagnosis and prognosis. Cancer Cell 9, 189-198.

Yang,H., Kong,W., He,L., Zhao,J.J., O'Donnell,J.D., Wang,J., Wenham,R.M., Coppola,D., Kruk,P.A., Nicosia,S.V., and Cheng,J.Q. (2008). MicroRNA expression profiling in human ovarian cancer: miR-214 induces cell survival and cisplatin resistance by targeting PTEN. Cancer Res. 68, 425-433.

Yang,Y. and Cvekl,A. (2007). Large Maf Transcription Factors: Cousins of AP-1 Proteins and Important Regulators of Cellular Differentiation. Einstein. J. Biol. Med. 23, 2-11.

Yang,Y., Chauhan,B.K., Cveklova,K., and Cvekl,A. (2004). Transcriptional regulation of mouse alphaB- and gammaF-crystallin genes in lens: opposite promoter-specific interactions between Pax6 and large Maf transcription factors. J. Mol. Biol. 344, 351-368.

Yao,A. and Rubin,H. (1993). Automatic enumeration and characterization of heterogeneous clonal progression in cell transformation. Proc. Natl. Acad. Sci. U. S. A 90, 10524-10528.
Yekta,S., Shih,I.H., and Bartel,D.P. (2004). MicroRNA-directed cleavage of HOXB8 mRNA. Science 304, 594-596.

Yi,R., Qin,Y., Macara,I.G., and Cullen,B.R. (2003). Exportin-5 mediates the nuclear export of pre-microRNAs and short hairpin RNAs. Genes Dev. 17, 3011-3016.

Yoeffry,J.M. and Courtice,F.C. (1970). Lymphatics, lymph and the lymphomyeloid complex. Academic Press (London, New York).

Yoshida,T., Ohkumo,T., Ishibashi,S., and Yasuda,K. (2005). The 5'-AT-rich half-site of Maf recognition element: a functional target for bZIP transcription factor Maf. Nucleic Acids Res. 33, 3465-3478.

You,L.R., Lin,F.J., Lee,C.T., DeMayo,F.J., Tsai,M.J., and Tsai,S.Y. (2005). Suppression of Notch signalling by the COUP-TFII transcription factor regulates vein identity. Nature 435, 98-104.

Yuan,L., Moyon,D., Pardanaud,L., Breant,C., Karkkainen,M.J., Alitalo,K., and Eichmann,A. (2002). Abnormal lymphatic vessel development in neuropilin 2 mutant mice. Development 129, 4797-4806.

Zhan,F., Huang,Y., Colla,S., Stewart,J.P., Hanamura,I., Gupta,S., Epstein,J., Yaccoby,S., Sawyer,J., Burington,B., Anaissie,E., Hollmig,K., Pineda-Roman,M., Tricot,G., van,R.F., Walker,R., Zangari,M., Crowley,J., Barlogie,B., and Shaughnessy,J.D., Jr. (2006). The molecular classification of multiple myeloma. Blood 108, 2020-2028.

Zhong,W., Wang,H., Herndier,B., and Ganem,D. (1996). Restricted expression of Kaposi sarcoma-associated herpesvirus (human herpesvirus 8) genes in Kaposi sarcoma. Proc. Natl. Acad. Sci. U. S. A 93, 6641-6646.

Ziegelbauer,J.M., Sullivan,C.S., and Ganem,D. (2009). Tandem array-based expression screens identify host mRNA targets of virus-encoded microRNAs. Nat. Genet. 41, 130-134.

Zimring,J.C., Goodbourn,S., and Offermann,M.K. (1998). Human herpesvirus 8 encodes an interferon regulatory factor (IRF) homolog that represses IRF-1-mediated transcription. J. Virol. 72, 701-707.

Affymetrix probe ID	Gene	LFC	Cluster:Empty vector	Average Expresssion	p Value	q Value
224997_x_at	H19	-1.12	0.46	6.2	0.00001	0.09
219764_at	FZD10	-1.09	0.47	6.25	0.00007	0.13
224646_x_at	H19	-0.99	0.50	9.17	0.00000	0.07
203394_s_at	HES1	-0.94	0.52	9.67	0.00002	0.11
1566324_a_at	MAF	-0.88	0.54	6.5	0.00000	0.07
202409_at	IGF2	-0.86	0.55	9.92	0.00003	0.11
213416_at	CERKL	-0.85	0.55	4.58	0.00002	0.11
228793_at	JMJD1C	-0.85	0.55	8.32	0.00007	0.13
202350_s_at	MATN2	-0.84	0.56	8.28	0.00002	0.11
235944_at	HMCN1	-0.82	0.57	5.14	0.00000	0.07
203395_s_at	HES1	-0.81	0.57	8.43	0.00008	0.13
219452_at	DPEP2	-0.71	0.61	7.14	0.00008	0.13
203868_s_at	VCAM1	-0.68	0.62	5.08	0.00012	0.14
231181_at	<NA>	-0.66	0.63	8.94	0.00008	0.13
229004_at	<NA>	-0.61	0.66	6.77	0.00003	0.11
230673_at	PKHD1L1	-0.61	0.66	8.85	0.00006	0.13
205756_s_at	F8	-0.61	0.66	8.35	0.00008	0.13
201427_s_at	SEPP1	-0.60	0.66	11.71	0.00002	0.11
205392_s_at	CCL14	-0.60	0.66	10.05	0.00009	0.13
213106_at	ATP8A1	-0.58	0.67	8.75	0.00002	0.11
209348_s_at	MAF	-0.57	0.67	11.53	0.00007	0.13
204301_at	KBTBD11	-0.56	0.68	9.22	0.00012	0.14
200766_at	CTSD	-0.52	0.70	9.77	0.00003	0.11
1562273_at	CNGA4	-0.51	0.70	3.75	0.00003	0.11
226822_at	STOX2	-0.50	0.71	7.25	0.00014	0.14
229638_at	IRX3	-0.47	0.72	7.27	0.00006	0.13
238764_at	CSAD	-0.47	0.72	4.99	0.00009	0.13
210980_s_at	ASAH1	-0.45	0.73	10.52	0.00005	0.13
234638_at	LARGE	-0.45	0.73	3.91	0.00009	0.13
214660_at	ITGA1	-0.44	0.74	6.94	0.00007	0.13
229327_s_at	MAF	-0.44	0.74	8.89	0.00014	0.14
219262_at	SUV39H2	0.40	1.32	4.11	0.00013	0.14
212806_at	<NA>	0.42	1.34	7.45	0.00013	0.14
231930_at	ELMOD1	0.43	1.35	7.78	0.00012	0.14
208930_s_at	ILF3	0.44	1.36	7.65	0.00013	0.14
205552_s_at	OAS1	0.46	1.38	7.52	0.00005	0.13
219463_at	C20orf103	0.46	1.38	7.12	0.00014	0.14
242629_at	<NA>	0.47	1.39	5.02	0.00013	0.14
218857_s_at	ASRGL1	0.48	1.39	9.14	0.00003	0.11
229886_at	C5orf34	0.48	1.39	7	0.00011	0.14
203819_s_at	C7orf30	0.49	1.40	8.68	0.00014	0.14
230058_at	SDCCAG3	0.50	1.41	5.31	0.00005	0.13
200841_s_at	EPRS	0.50	1.41	8	0.00013	0.14
1559840_s_at	TBX18	0.51	1.42	7.01	0.00002	0.11
213979_s_at	CTBP1	0.52	1.43	9.71	0.00006	0.13
207601_at	SULT1B1	0.55	1.46	8.49	0.00003	0.11
237062_at	RNF10	0.56	1.47	6.87	0.00006	0.13
230256_at	C1orf104	0.61	1.53	5.83	0.00005	0.13
215509_s_at	BUB1	0.62	1.54	7.35	0.00009	0.14
206715_at	TFEC	0.85	1.80	4.74	0.00003	0.11

Appendix Table A1 Top 50 probes de-regulated in the presence of the KSHV miRNA cluster. The top 50 de-regulated probes are identified by the affymetrix probe id and gene symbol. Probes down-regulated in LEC expressing the Cluster compared to empty lentiviral vector are shown in black, those up-regulated are in blue.

Appendix Table A2 PITA prediction results Top 205 KSHV miRNA targets as predicted by PITA. The target and targeting miRNA are listed as is the location of the target site in the 3'UTR The degree of seed complementation is indicated under the Seed heading, 8 refers to the size of the seed, a 1 in the second column indicates a G:U wobble in the seed whereas a 1 in the third column indicates a single mismatch. The PITA score is explained in Figure 3.12 and Section 3.6.1.

Ensemble ID	Gene	microRNA	Start	End	Seed	PITA score
ENSG00000196715	VKORC1L1	kshv-miR-K12-2	3232	3224	08:00:00	-16.41
ENSG00000065060	C6orf107	kshv-miR-K12-6-5p	2290	2282	08:00:00	-16.42
ENSG00000198417	MT1F	kshv-miR-K12-1	105	97	08:00:01	-16.42
ENSG00000161960	SNORA67	kshv-miR-K12-10b	2070	2062	08:01:00	-16.42
ENSG00000132128	LRRC41	kshv-miR-K12-4-3p	68	60	08:01:00	-16.43
ENSG00000088888	MAVS_HUMAN	kshv-miR-K12-10b	1703	1695	08:00:01	-16.45
ENSG00000087263	OGFOD1	kshv-miR-K12-4-3p	1041	1033	08:01:00	-16.45
ENSG00000185432	METTL7A	kshv-miR-K12-4-3p	1852	1844	08:01:00	-16.47
ENSG00000169504	CLIC4	kshv-miR-K12-11	1903	1895	08:00:01	-16.48
ENSG00000163808	KIF15	kshv-miR-K12-6-5p	130	122	08:00:00	-16.48
ENSG00000183853	KIRREL	kshv-miR-K12-10b	3429	3421	08:01:00	-16.48
ENSG00000047188	YTHDC2	kshv-miR-K12-10b	480	472	08:01:00	-16.48
ENSG00000140464	PML	kshv-miR-K12-1	286	278	08:01:00	-16.49
ENSG00000182319	SG223_HUMAN	kshv-miR-K12-8	62	54	08:01:00	-16.5
ENSG00000174903	RAB1C	kshv-miR-K12-10b	84	76	08:00:01	-16.51
ENSG00000170442	KRT86	kshv-miR-K12-8	64	56	08:01:00	-16.52
ENSG00000066322	ELOVL1	kshv-miR-K12-11	702	694	08:00:01	-16.53
ENSG00000108946	PRKAR1A	kshv-miR-K12-6-5p	1006	998	08:01:00	-16.54
ENSG00000135999	EPC2	kshv-miR-K12-2	121	113	08:00:01	-16.55
ENSG00000069509	FUNDC1	kshv-miR-K12-10a	127	119	08:00:01	-16.56
ENSG00000184863	RBM33	kshv-miR-K12-6-3p	2376	2368	08:01:00	-16.57
ENSG00000120314	WDR55	kshv-miR-K12-2	1023	1015	08:01:00	-16.57
ENSG00000116148	CCNL2	kshv-miR-K12-2	2947	2939	08:01:00	-16.58
ENSG00000174371	EXO1	kshv-miR-K12-10b	217	209	08:00:01	-16.59
ENSG00000025800	KPNA6	kshv-miR-K12-6-3p	3378	3370	08:00:01	-16.6
ENSG00000183155	RABIF	kshv-miR-K12-11	1562	1554	08:01:00	-16.62
ENSG00000072364	AFF4	kshv-miR-K12-6-5p	2326	2318	08:01:00	-16.64
ENSG00000183856	IQGAP3	kshv-miR-K12-1	1041	1033	08:01:00	-16.65
ENSG00000038382	TRIO	kshv-miR-K12-6-3p	1656	1648	08:00:01	-16.65
ENSG00000088832	FKBP1A	kshv-miR-K12-11	334	326	08:00:01	-16.66
ENSG00000048740	CUGBP2	kshv-miR-K12-4-3p	245	237	08:01:00	-16.67
ENSG00000166224	SGPL1	kshv-miR-K12-4-3p	149	141	08:01:00	-16.69
ENSG00000165219	GAPVD1	kshv-miR-K12-6-3p	1369	1361	08:00:00	-16.71
ENSG00000165219	GAPVD1	kshv-miR-K12-6-3p	2136	2128	08:00:00	-16.71
ENSG00000163171	CDC42EP3	kshv-miR-K12-11	613	605	08:00:01	-16.72
ENSG00000112773	FAM46A	kshv-miR-K12-6-3p	1861	1853	08:01:00	-16.74
ENSG00000138685	FGF2	kshv-miR-K12-2	5290	5282	08:00:01	-16.75
ENSG00000069493	CLEC2D	kshv-miR-K12-10b	796	788	08:00:01	-16.77
ENSG00000069493	CLEC2D	kshv-miR-K12-10b	869	861	08:00:01	-16.77
ENSG00000141720	PIP4K2B	kshv-miR-K12-10a	3381	3373	08:00:00	-16.77
ENSG00000141720	PIP4K2B	kshv-miR-K12-10b	3381	3373	08:00:01	-16.77
ENSG00000162300	ZFPL1	kshv-miR-K12-8	442	434	08:01:00	-16.77
ENSG00000187720	THSD4	kshv-miR-K12-6-5p	799	791	08:01:00	-16.79
ENSG00000129194	SOX15	kshv-miR-K12-2	105	97	08:00:00	-16.82
ENSG00000167658	EEF2	kshv-miR-K12-10a	276	268	08:01:00	-16.84
ENSG00000124164	VAPB	kshv-miR-K12-6-5p	814	806	08:00:00	-16.85
ENSG00000124164	VAPB	kshv-miR-K12-6-5p	884	876	08:00:00	-16.85
ENSG00000124422	USP22	kshv-miR-K12-6-3p	1752	1744	08:00:01	-16.86
ENSG00000173418	NAT5	kshv-miR-K12-4-3p	269	261	08:01:00	-16.87

ENSG00000173418	NAT5	kshv-miR-K12-4-3p	324	316	08:01:00	-16.87
ENSG00000108175	ZMIZ1	kshv-miR-K12-6-3p	3473	3465	08:00:00	-16.87
ENSG00000197622	CDC42SE1	kshv-miR-K12-6-3p	272	264	08:01:00	-16.89
ENSG00000075420	FNDC3B	kshv-miR-K12-6-5p	2337	2329	08:01:00	-16.91
ENSG00000170915	PAQR8	kshv-miR-K12-2	844	836	08:01:00	-16.92
ENSG00000189306	ZG14_HUMAN	kshv-miR-K12-10b	1249	1241	08:00:01	-16.94
ENSG00000150712	MTMR12	kshv-miR-K12-1	543	535	08:01:00	-16.95
ENSG00000170348	TMED10	kshv-miR-K12-6-3p	3057	3049	08:00:01	-16.95
ENSG00000182180	MRPS16	kshv-miR-K12-4-3p	1548	1540	08:01:00	-16.97
ENSG00000125266	EFNB2	kshv-miR-K12-10b	1688	1680	08:00:01	-16.98
ENSG00000054523	KIF1B	kshv-miR-K12-6-3p	1092	1084	08:00:01	-16.98
ENSG00000054523	KIF1B	kshv-miR-K12-6-3p	2907	2899	08:00:01	-16.98
ENSG00000198205	ZXDA	kshv-miR-K12-4-3p	676	668	08:01:00	-16.99
ENSG00000185896	LAMP1	kshv-miR-K12-10a	632	624	08:01:00	-17
ENSG00000185896	LAMP1	kshv-miR-K12-10a	2162	2154	08:01:00	-17
ENSG00000043143	PHF15	kshv-miR-K12-6-3p	1749	1741	08:00:01	-17.03
ENSG00000158352	SHROOM4	kshv-miR-K12-6-5p	1421	1413	08:00:00	-17.05
ENSG00000112159	MDN1	kshv-miR-K12-10b	3084	3076	08:00:01	-17.06
ENSG00000178075	GRAMD1C	kshv-miR-K12-6-3p	704	696	08:00:01	-17.08
ENSG00000108406	DHX40	kshv-miR-K12-10a	912	904	08:00:00	-17.11
ENSG00000108406	DHX40	kshv-miR-K12-10b	912	904	08:00:01	-17.11
ENSG00000088766	CRLS1	kshv-miR-K12-2	2559	2551	08:00:01	-17.13
ENSG00000088766	CRLS1	kshv-miR-K12-2	2761	2753	08:00:01	-17.13
ENSG00000152767	FARP1	kshv-miR-K12-10b	613	605	08:01:00	-17.13
ENSG00000159140	SON	kshv-miR-K12-6-5p	462	454	08:01:00	-17.13
ENSG00000125834	STK35	kshv-miR-K12-10b	2979	2971	08:01:00	-17.14
ENSG00000204420	G6B_HUMAN	kshv-miR-K12-1	1348	1340	08:01:00	-17.15
ENSG00000175866	BAIAP2	kshv-miR-K12-4-5p	1176	1168	08:00:01	-17.17
ENSG00000132740	IGHMBP2	kshv-miR-K12-8	644	636	08:00:01	-17.19
ENSG00000135677	GNS	kshv-miR-K12-10a	2919	2911	08:00:00	-17.24
ENSG00000135677	GNS	kshv-miR-K12-10b	2919	2911	08:00:01	-17.24
ENSG00000143157	POGK	kshv-miR-K12-6-3p	386	378	08:00:01	-17.24
ENSG00000103423	DNAJA3	kshv-miR-K12-10a	132	124	08:01:00	-17.25
ENSG00000103423	DNAJA3	kshv-miR-K12-10a	168	160	08:01:00	-17.25
ENSG00000114383	TUSC2	kshv-miR-K12-10b	871	863	08:00:00	-17.26
ENSG00000186638	Q5T7B8-2	kshv-miR-K12-6-3p	969	961	08:01:00	-17.31
ENSG00000076356	PLXNA2	kshv-miR-K12-8	1253	1245	08:00:01	-17.32
ENSG00000130147	SH3BP4	kshv-miR-K12-6-3p	1678	1670	08:00:01	-17.32
ENSG00000105993	DNAJB6	kshv-miR-K12-10b	770	762	08:01:00	-17.35
ENSG00000174371	EXO1	kshv-miR-K12-2	400	392	08:01:00	-17.36
ENSG00000120549	KIAA1217	kshv-miR-K12-6-3p	876	868	08:00:00	-17.4
ENSG00000084090	STARD7	kshv-miR-K12-1	722	714	08:00:01	-17.43
ENSG00000182667	NTRI_HUMAN	kshv-miR-K12-10b	62	54	08:01:00	-17.44
ENSG00000168734	PKIG	kshv-miR-K12-10b	371	363	08:01:00	-17.45
ENSG00000112339	HBS1L	kshv-miR-K12-2	3810	3802	08:00:01	-17.46
ENSG00000132256	TRIM5	kshv-miR-K12-6-3p	734	726	08:01:00	-17.46
ENSG00000132256	TRIM5	kshv-miR-K12-6-3p	91	83	08:01:00	-17.49
ENSG00000123933	MXD4	kshv-miR-K12-1	1170	1162	08:01:00	-17.51
ENSG00000173269	MMRN2	kshv-miR-K12-4-3p	305	297	08:01:00	-17.52
ENSG00000165757	KIAA1462	kshv-miR-K12-6-3p	212	204	08:00:00	-17.56

ENSG00000170906	NDUFA3	kshv-miR-K12-6-3p	61	53	08:01:00	-17.57
ENSG00000132716	WDR42A	kshv-miR-K12-6-3p	556	548	08:01:00	-17.58
ENSG00000092140	KIAA1333	kshv-miR-K12-10b	1232	1224	08:00:01	-17.6
ENSG00000100288	CHKB	kshv-miR-K12-10b	1150	1142	08:00:01	-17.61
ENSG00000085832	EPS15	kshv-miR-K12-10b	2405	2397	08:00:01	-17.62
ENSG00000099219	ERMP1	kshv-miR-K12-6-3p	393	385	08:00:01	-17.65
ENSG00000099219	ERMP1	kshv-miR-K12-6-3p	631	623	08:00:01	-17.65
ENSG00000102471	NDFIP2	kshv-miR-K12-4-3p	2889	2881	08:00:01	-17.66
ENSG00000118689	FOXO3	kshv-miR-K12-10b	280	272	08:00:01	-17.69
ENSG00000101849	TBL1X	kshv-miR-K12-10b	2694	2686	08:00:00	-17.72
ENSG00000132912	DCTN4	kshv-miR-K12-10b	774	766	08:00:01	-17.73
ENSG00000125968	ID1	kshv-miR-K12-8	86	78	08:01:00	-17.73
ENSG00000178202	KDELC2	kshv-miR-K12-6-3p	1393	1385	08:01:00	-17.74
ENSG00000169184	MN1	kshv-miR-K12-6-5p	1401	1393	08:00:00	-17.76
ENSG00000198960	ARMCX6	kshv-miR-K12-8	469	461	08:01:00	-17.77
ENSG00000148335	C9orf32	kshv-miR-K12-6-5p	192	184	08:00:00	-17.77
ENSG00000066583	ISOC1	kshv-miR-K12-8	132	124	08:00:01	-17.77
ENSG00000139211	AMIGO2	kshv-miR-K12-4-5p	1516	1508	08:00:00	-17.78
ENSG00000132912	DCTN4	kshv-miR-K12-1	1272	1264	08:00:01	-17.78
ENSG00000165879	FRAT1	kshv-miR-K12-6-3p	508	500	08:00:00	-17.82
ENSG00000134882	UBAC2	kshv-miR-K12-10b	694	686	08:01:00	-17.87
ENSG00000134882	UBAC2	kshv-miR-K12-10b	1073	1065	08:01:00	-17.87
ENSG00000111530	CAND1	kshv-miR-K12-6-3p	149	141	08:00:01	-17.89
ENSG00000066117	SMARCD1	kshv-miR-K12-10a	130	122	08:01:00	-17.9
ENSG00000146757	ZNF92	kshv-miR-K12-6-3p	567	559	08:01:00	-17.94
ENSG00000125534	C20orf149	kshv-miR-K12-1	123	115	08:01:00	-17.97
ENSG00000185070	FLRT2	kshv-miR-K12-10b	3457	3449	08:00:01	-17.99
ENSG00000075790	BCAP29	kshv-miR-K12-10b	1070	1062	08:00:00	-18.01
ENSG00000075790	BCAP29	kshv-miR-K12-10b	1312	1304	08:00:00	-18.01
ENSG00000102309	PIN4	kshv-miR-K12-6-3p	322	314	08:00:00	-18.01
ENSG00000102309	PIN4	kshv-miR-K12-6-3p	920	912	08:00:00	-18.01
ENSG00000127603	MACF1	kshv-miR-K12-6-5p	5856	5848	08:00:00	-18.02
ENSG00000182356	POM121L1	kshv-miR-K12-10a	103	95	08:01:00	-18.03
ENSG00000123130	ACOT9	kshv-miR-K12-10a	1089	1081	08:01:00	-18.04
ENSG00000129667	RHBDF2	kshv-miR-K12-10a	587	579	08:00:01	-18.05
ENSG00000129667	RHBDF2	kshv-miR-K12-10a	1478	1470	08:00:01	-18.05
ENSG00000134531	EMP1	kshv-miR-K12-6-3p	442	434	08:00:01	-18.17
ENSG00000160209	PDXK	kshv-miR-K12-10b	4534	4526	08:00:01	-18.25
ENSG00000123146	CD97	kshv-miR-K12-6-3p	67	59	08:00:01	-18.33
ENSG00000145833	DDX46	kshv-miR-K12-10b	1184	1176	08:00:01	-18.38
ENSG00000197969	VPS13A	kshv-miR-K12-4-3p	89	81	08:00:01	-18.47
ENSG00000173531	MST1	kshv-miR-K12-10a	401	393	08:01:00	-18.48
ENSG00000166025	AMOTL1	kshv-miR-K12-10a	1067	1059	08:00:01	-18.49
ENSG00000166025	AMOTL1	kshv-miR-K12-10a	2118	2110	08:00:01	-18.49
ENSG00000007168	PAFAH1B1	kshv-miR-K12-10b	373	365	08:01:00	-18.51
ENSG00000063587	ZNF275	kshv-miR-K12-1	3404	3396	08:01:00	-18.51
ENSG00000119986	AVPI1	kshv-miR-K12-6-3p	392	384	08:01:00	-18.52
ENSG00000168522	FNTA	kshv-miR-K12-6-5p	158	150	08:00:00	-18.52
ENSG00000158062	UBXD5	kshv-miR-K12-10b	360	352	08:01:00	-18.53
ENSG00000172534	HCFC1	kshv-miR-K12-8	1666	1658	08:01:00	-18.55

ENSG00000143324	XPR1	kshv-miR-K12-6-3p	1457	1449	08:01:00	-18.62
ENSG00000165219	GAPVD1	kshv-miR-K12-2	623	615	08:01:00	-18.7
ENSG00000165219	GAPVD1	kshv-miR-K12-2	1390	1382	08:01:00	-18.7
ENSG00000163960	UBXD7	kshv-miR-K12-1	52	44	08:00:01	-18.71
ENSG00000114554	PLXNA1	kshv-miR-K12-8	2841	2833	08:01:00	-18.73
ENSG00000182197	EXT1	kshv-miR-K12-10a	722	714	08:01:00	-18.78
ENSG00000115649	C2orf24	kshv-miR-K12-6-5p	445	437	08:01:00	-18.79
ENSG00000105281	SLC1A5	kshv-miR-K12-10b	371	363	08:00:00	-18.82
ENSG00000153558	FBXL2	kshv-miR-K12-6-3p	342	334	08:00:01	-18.83
ENSG00000159256	MORC3	kshv-miR-K12-6-3p	112	104	08:01:00	-18.84
ENSG00000095951	HIVEP1	kshv-miR-K12-6-3p	610	602	08:00:01	-18.91
ENSG00000163820	FYCO1	kshv-miR-K12-6-3p	103	95	08:00:01	-18.92
ENSG00000188529	FUSIP1	kshv-miR-K12-1	148	140	08:01:00	-19.01
ENSG00000163960	UBXD7	kshv-miR-K12-10a	1196	1188	08:00:01	-19.04
ENSG00000125430	HS3ST3B1	kshv-miR-K12-6-3p	2084	2076	08:00:00	-19.15
ENSG00000197119	SLC25A29	kshv-miR-K12-4-3p	184	176	08:00:01	-19.19
ENSG00000116641	DOCK7	kshv-miR-K12-10b	661	653	08:00:00	-19.2
ENSG00000116016	EPAS1	kshv-miR-K12-10b	1536	1528	08:00:01	-19.28
ENSG00000128989	ARP19_HUMAN	kshv-miR-K12-4-3p	4376	4368	08:00:01	-19.37
ENSG00000198198	KIAA0467	kshv-miR-K12-10a	428	420	08:01:00	-19.41
ENSG00000105245	NUMBL	kshv-miR-K12-10b	118	110	08:01:00	-19.43
ENSG00000197373	NP_001091084.1	kshv-miR-K12-6-3p	192	184	08:01:00	-19.53
ENSG00000205236	NP_116581.3	kshv-miR-K12-6-3p	192	184	08:01:00	-19.53
ENSG00000157106	SMG1_HUMAN	kshv-miR-K12-4-3p	1952	1944	08:01:00	-19.7
ENSG00000136758	YME1L1	kshv-miR-K12-10a	855	847	08:01:00	-19.93
ENSG00000136758	YME1L1	kshv-miR-K12-10a	945	937	08:01:00	-19.93
ENSG00000168264	IRF2BP2	kshv-miR-K12-6-5p	627	619	08:00:00	-20.03
ENSG00000213699	C2orf18	kshv-miR-K12-11	732	724	08:00:00	-20.09
ENSG00000212870	MT-ND5	kshv-miR-K12-6-3p	338	330	08:01:00	-20.09
ENSG00000114861	FOXP1	kshv-miR-K12-1	1641	1633	08:01:00	-20.2
ENSG00000114861	FOXP1	kshv-miR-K12-1	2296	2288	08:01:00	-20.2
ENSG00000136933	RABEPK	kshv-miR-K12-6-3p	61	53	08:01:00	-20.26
ENSG00000162971	C2orf60	kshv-miR-K12-6-5p	3562	3554	08:00:00	-20.44
ENSG00000103423	DNAJA3	kshv-miR-K12-10b	132	124	08:00:00	-20.75
ENSG00000160094	ZNF362	kshv-miR-K12-10a	1590	1582	08:01:00	-20.84
ENSG00000182356	POM121L1	kshv-miR-K12-10b	103	95	08:00:00	-21.13
ENSG00000181634	TNFSF15	kshv-miR-K12-10b	331	323	08:01:00	-21.17
ENSG00000173436	C1orf151	kshv-miR-K12-1	961	953	08:00:00	-21.2
ENSG00000164754	RAD21	kshv-miR-K12-1	1041	1033	08:00:00	-21.31
ENSG00000104643	MTMR9	kshv-miR-K12-4-3p	3847	3839	08:00:00	-21.4
ENSG00000177469	PTRF	kshv-miR-K12-10b	344	336	08:01:00	-21.59
ENSG00000112031	MTRF1L	kshv-miR-K12-1	2029	2021	08:01:00	-21.68
ENSG00000164151	NP_056140.1	kshv-miR-K12-10a	52	44	08:00:01	-21.82
ENSG00000168461	RAB31	kshv-miR-K12-4-3p	3129	3121	08:01:00	-21.86
ENSG00000066117	SMARCD1	kshv-miR-K12-10b	130	122	08:00:00	-21.9
ENSG00000149257	SERPINH1	kshv-miR-K12-10b	387	379	08:01:00	-21.93
ENSG00000155016	CYP2U1	kshv-miR-K12-6-5p	2576	2568	08:01:00	-22.07
ENSG00000204218	RGL2	kshv-miR-K12-10a	416	408	08:00:00	-22.37
ENSG00000204218	RGL2	kshv-miR-K12-10b	416	408	08:00:01	-22.37
ENSG00000138468	SENP7	kshv-miR-K12-4-3p	1330	1322	08:00:00	-22.62
ENSG00000172757	CFL1	kshv-miR-K12-10b	304	296	08:00:01	-22.69